SCIENTIFIC REPORT 2001-2002

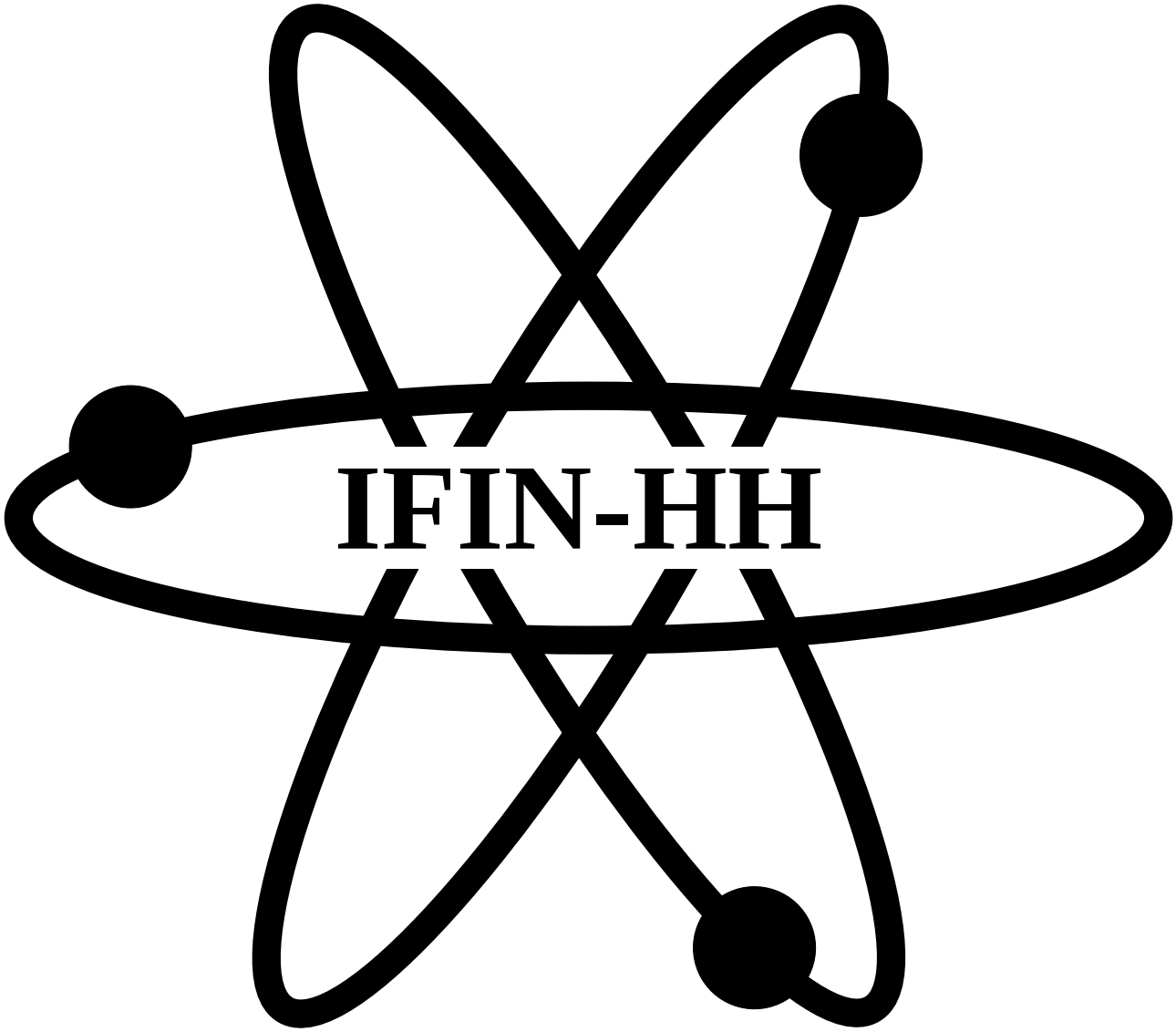

Bucharest, Romania, 2003

ISSN 1454-2714
IFIN-HH-AR–2003

Publisher: "Horia Hulubei" National Institute for Physics and Nuclear Engineering
Str. Atomistilor no. 407
P.O. Box MG-6
RO-77125 Bucharest-Măgurele
Romania
Telephone: +40 21 404 23 00
Fax: +40 21 404 23 11
E-mail: anuar@ifin.nipne.ro
WWW home page: http://www.nipne.ro

Editors: Margareta Oancea, Claudiu Schiaua, Dan Grecu, Marinela Dumitriu

Printed by: Gelu Chisnăr

Cover: Adrian Socolov

The editors have not modified the text of the contributions, not even for spelling or grammar. Changes were only made in the title of some contributions by converting some capital-case letters to lower-case for case uniformity, in the placement of some pictures, and in the spelling of some author's names to assure the correct building of the author index.

FOREWORD

The year 2001 was marked by the startup of the European center of excellence IDRANAP (Inter-Disciplinary Research and Applications based on Nuclear and Atomic Physics). Its 18 work packages are structured into 5 topical areas: determining environmental pollution; nuclear methods in biology and medicine; radionuclide metrology; analysis and characterization of materials; and nuclei far from stability, decay modes, cosmic rays, and facilities. During the first 18 months, 39 young researchers and specialists from 15 European countries visited the facility and 37 Romanian researchers traveled abroad. Three international meetings organized by IDRANAP— Biological Effects of Ionizing Radiation, Electromagnetic Fields, and Chemical Toxic Agents – Sinaia, October 2001; the 3rd International Balkan Workshop on Applied Physics – Târgovişte, June 2002; and the International Conference on Applications of High Precision Atomic and Nuclear Methods – Neptun, September 2002—attracted a large number of participants. The scientific work of the center materialized into nearly 200 articles appearing in leading international journals and internal reports. Further details on the IDRANAP activity can be found on the center's web page, `http://idranap.nipne.ro`.

Cooperation with CERN was a primary concern of the Institute and major strides were reported in every experiment in which our researchers were involved, including ATLAS, ALICE, LHC-B, DIRAC, and NA50. A landmark accord of cooperation between the Romanian Government and CERN was signed in Geneva in March 2002 and ratified by a Government Decision in November 2002, paving the way to a regulated participation of Romanian researchers in the CERN activity. The first steps were thus made towards Romania's pre-accession to this outstanding scientific institution. The Institute's potential of making a significant contribution to the CERN scientific program was underscored as a CERN group, including LHC program director Professor Roger Cashmore, toured the Măgurele Campus in June 2002.

Romania's early steps towards integration into the global GRID communication project were marked by an international seminar that brought together distinguished personalities in April 2002. The project is poised to become increasingly necessary, given the huge amount of complex data that will have to be processed once the LHC is put into operation at CERN. This has made our Institute all the more interested in the implementation of the GRID technology in Romania and all the more actively involved in every stage of the process, as the following short chronology will prove: (i) A ROGRID National Consortium was established in May 2002, with IFIN-HH and six other institutions as its founding members. (ii) IFIN-HH took the initiative of setting up MAGGI (Măgurele Grid Initiative) Consortium, consisting of twelve institutions located on the Măgurele Campus. (iii) A fiber optic connection allowing data transfers of up to 2.5GB/s was installed in November 2002 between IFIN-HH and the academic communication network RoEduNet. (iv) Romania's first GRID application was conducted as part of the Institute's cooperation to ALICE. (v) IFIN-HH took part in the elaboration by ROGRID of an implementation strategy for the GRID project in Romania.

IRASM Multipurpose Irradiation Facility, the upshot of a technical co-operation project between IAEA and the Romanian Government, went into operation in early 2001. Chiefly designed for industrial irradiation services such as sterilizing medical devices and treating food against microbes, its tasks expanded and diversified as its microbiological laboratory opened in June 2002. Two months later, IRASM was ISO accredited and earned several other major international certifications.

A watershed Government Decision of April 2002 provided for the permanent shutdown for decommissioning of the Institute's VVR-S research reactor. Over four decades since its startup in 1957, the reactor supplied neutron fluxes that were used in scientific research and the production of radioisotopes applied in medicine and industry. The decommissioning task will chiefly rest upon the IFIN-HH specialists that will however also draw on the experience and support of other organizations, including the IAEA, Argonne National Laboratory of the U.S., and several local units.

The switch to a project-based financing of research also occurred during this period and IFIN-HH learned from experience both the benefits and the difficulties the new financing scheme involved. We would like to thank everyone that took an active part in working out and winning projects in the National Program contests, which helped to keep alive the Institute's high-level research in rather arduous conditions.

This report summarizes the main scientific results our scientists delivered in 2001 and 2002. The published paper list, though incomplete, proves that our research work matches the highest international standards. The part that our researchers took in international scientific events as well as in organizing the annual National Physics Conferences (Târgu Mureş, 2001, 2002) and the 1st National Conference on Theoretical Physics (Bucharest, September 2002) provide a glimpse of the vibrant activity that took place at Romania's most representative research organization.

Dr. Emilian Drăgulescu
Director General

Dr. Florin D. Buzatu
Scientific Director

Contents

Results included in the following are progress reports of research projects and therefore should be considered as preliminary communications.

Theoretical Physics

Nuclear, Atomic and Molecular Physics

Jump phenomenon induced by potential strength variation and the influence of exotic resonant states.

N. Grama[1], C. Grama[1], I. Zamfirescu[1]

[1] IFIN-HH

We consider the non-relativistic scattering of a spinless particle by a central potential $gV(r)$, $g \in \mathbf{C}$. In a scattering problem the potential $gV(r)$ represents a mean potential. For example, in atomic physics it represents the mean intermolecular potential averaged over internal states. Consequently the potential strength g could undergo small changes and we may ask which is the effect of these changes.

An adequate quantum mechanical description of the bound and resonant states is through the S-matrix poles. The pole function $k = k^{(l)}(g)$ is a multi-valued function. In [1] an approach to bound and resonant states, based on the construction of the Riemann surface over the g-plane $R_g^{(l)}$, on which the pole function is single-valued and analytic, has been presented. If the potential strength g takes a value on a given sheet $\Sigma_n^{(l)}$ of $R_g^{(l)}$, then the function $k = k^{(l)}(g)$ takes only one value on the k-plane image $\Sigma_n^{\prime(l)}$ of the sheet, i.e. there is only a single pole on each sheet image. In this way the sheet $\Sigma_n^{(l)}$ of the Riemann surface $R_g^{(l)}$ and its k-plane image $\Sigma_n^{\prime(l)}$ have been associated to a given state with quantum numbers (l, n).

Let us suppose that the potential strength has a small variation around a branch point of the function $k = k^{(l)}(g)$. This small potential strength variation can either determine a small change of the pole function $k = k^{(l)}(g)$, or it may induce a large variation of the function $k = k^{(l)}(g)$ by the transition from one branch of the function to another branch. As jump phenomena, ubiquitous in science, are characterized by large dynamic responses of the system to small amplitude disturbances, it is justified to call "jump" the transition of the system from the state (l, n) to the state (l, m) as a result of a small potential strength variation. The rules governing the jump phenomenon are important in the study of the pole trajectories, avoiding the accidental jumps from one pole to other pole when one calculates the pole trajectories. In this way we are sure that the same pole is followed.

The aim of this paper is to establish the conditions for the system to undergo a jump from one state (l, n) to other state (l, m) as a consequence of a small potential strength variation. Let the parameter g follow a prescribed contour starting from a value $g \in \Sigma_n^{(l)}$. The choice of the contour can induce quite distinct effects : a) if g describes a closed curve on $\Sigma_n^{(l)}$ not enclosing a branch point where $\Sigma_n^{(l)}$ is joined to other sheet then its image $k = k^{(l)}(g)$ takes values on a continuous path on the Riemann sheet image $\Sigma_n^{\prime(l)}$, i.e. the potential strength variation does not change the state (l, n); b) on the contrary, if g describes a closed contour which starts from a point on the sheet $\Sigma_n^{(l)}$ and encloses the branch point joining the sheets $\Sigma_n^{(l)}$ and $\Sigma_m^{(l)}$ and no other branch points, then the variable g is transferred from the sheet $\Sigma_n^{(l)}$ to the sheet $\Sigma_m^{(l)}$. As a consequence the pole $k = k^{(l)}(g)$ is transferred from the sheet image $\Sigma_n^{\prime(l)}$ to the sheet image $\Sigma_m^{\prime(l)}$. In other words the potential strength variation induces a jump from the state (l, n) to the state (l, m).

In [1] it was shown that in the case of a potential well followed by a barrier there were exotic poles situated on certain Riemann sheet images, having extraordinary properties. An exotic resonant state pole does not become a bound or virtual state pole as the depth of the potential well increases to infinity, but it remains a resonant state pole situated in the neighborhood of an attractor in the k-plane. The wave function of the exotic resonant state corresponding to an exotic resonant pole situated near the attractor is almost completely localized inside the potential barrier. The influence of the exotic resonant state poles on the rules governing the jumps is discussed.

References

[1] C. Grama, N. Grama and I. Zamfirescu, Phys. Rev. A **61** (2000) 032716.

[2] C. Grama, N. Grama and I. Zamfirescu, Ann. Phys. (NY) **232** (1994) 243.

Critical view on double-beta decay matrix elements within quasi random phase approximation-based methods

S. Stoica [1], H.V. Klapdor Kleingrothaus [2]

[1] Institute of Physics and Nuclear Engineering, Department of Theoretical Physics, POBox MG - 6, Bucharest, Romania

[2] Max-Planck-Institut für Kernphysik, W-6900 Heidelberg, Germany

Abstract

A systematic study of the two-neutrino and neutrinoless double-beta decay matrix elements (ME) for the nuclei with A=76, 82, 96, 100, 116, 128, 130 and 136 is done.the calculations are performed with four different quasi random phase approximation (QRPA) based methods. i.e. the proton-neutron QRPA (pnQRPA), the renormalized proton-neutron QRPA (pnQRPA), the full-RQRPA and the second-QRPA (SQRPA).First we checked the conservation of the Ikeda sum rule (ISR) and found that it is fulfilled with a good accuracy for the SQRPA, while for the pnRQRPA and full-RQRPA the deviations are up to 17 %.Then we studied the dependence of the ME on thesingle-partical (s.p.) basis.For that we performed the calculations using the same set of parameters and two different s.p. basis.For the two-neutrino decay mode the ME manifest generally the largest sesitivity to the choice of the basiswhen they are calculated with the pnQRPA, while the smallest sensitivity is got with the SQRPA.For all the methods the largest differences between the results were found for $^{128,130}Te$ and ^{136}Xe. For the neutrinoless decay mode the ME display generally a stronger dependence on the basis than for two-neutrino decay mode, when they are calculated with the pnQRPA, RQRPA and full-RQRPA, while for SQRPA differences in the results are within 30%. A better stability against the change of the s.p. basis used and a good fulfillment of the ISR allow to reduce the uncertainties in the values of the neutrinoless ME predicted by theQRPA-based methods to about 50% from their magnitude.Further, we fixed the values of g_{pp} from the two-neutrino calculations and according to recent experimental data, and then we used them to compute the ME for the neutrinoless decay mode.Taking the most recent experimental limits for the neutrinoless half-lives, we deduce new upper limits for the neutrino mass parameter. Finally, there are estimated, for each nucleus, scales for the neutrinoless double-beta decay half-lives that the experiments should reach for exploring neutrino masses around o.1 eV. This might guide the experimentalists in planning their setups.

Nuclear Physics A **694**, 269-294, 2001

PACS:21.60.Jz; 23.40.Hc;23.40.Bw

Test of the proton-neutron random-phase approximation method within an extended Lipkin-type model

S. Stoica [1], I. Mihut [1], J. Suhonen [2]

[1] Institute of Physics and Nuclear Engineering, Department of Theoretical Physics, POBox MG - 6, Bucharest, Romania

[2] Departament of Physics, University of Jyväskyä, P.O. Box 35, FIN-40351 Jyväskyä, Finland

Abstract

An extended Lipkin-Meshkov-Glick model for testing the proton-neutron random-phase approximation (pnRPA) method is developed, taking into account explicitly proton and neutron degrees of freedom.Besides the proton and neutron single-particle terms two types of residual proton-proton interactions, one simulating a particle-particle and other a particle hole interaction, are including in the model Hamiltonian so that the model is exactly solvable in an isospin SU(2)$\bigotimes$SU(2) basis.The behavior of the first excited (collective)state obtained by (i) exact diagonalization of the Hamiltonian matrix and(ii) with the pnRPA is studied as a function of the model parameters and the two results are compared with each other. Furthermore, charge-changing operators simulating nuclear beta decay and their action on eigenfunctions of the model Hamilto-

nian are defined and transition amplitudes of them are calculated using exact, the Tamm-Dancoff, and pn-RPA eigenfunctions.

PHYSICAL REVIEW C **64**, 017303, 2001
DOI:10.1103/ PhysRevC.64.017303
PACS number(s): 21.60.Fw, 21.30.Fe, 21.60.Jz

Neutrinoless double-β-decay matrix elements within the second quasirandom phase approximation method

S. Stoica [1], H.V. Klapdor Kleingrothaus [2]

[1] Institute of Physics and Nuclear Engineering, Department of Theoretical Physics, POBox MG - 6, Bucharest, Romania
[2] Max-Planck-Institut für Kernphysik, W-6900 Heidelberg, Germany

Abstract

A computation of the neutrinoless double-β-decay matrix elements is performed with the second quasirandom phase approximation (QRPA) method [A.A.Raduta, A.Faessler, S.Stoica and W.A.Kaminski, Phys.Lett.B 254, 7 (1991); A.A.Raduta, A.Faessler and S.Stoica, Nucl. Phys. A 534, 149 (1991); S.Stoica and W.A.Kaminski, Phys. Rev. C 47, 867 (1993); S.Stoica, ibid. 49, 787 (1994); Phys. Lett. B 350, 152 (1995); S.Stoica and I.Mihut, Nucl. Phys. A 602, 197 (1996)] for the nuclei with A=76, 82, 96, 100, 116, 128, 130 and 136. It was found that the Ikeda sum rule is fulfilled with a good accuracy and the results display a weak dependence on the single particle basis used. Comparing our calculations with similar ones performed with other quasirandom phase approximation-based methods we estimate more precisely the accuracy of these methods in the predictions in the neutrinoless matrix elements and neutrino mass parameter, which is settled to about 50% from their calculated values. Taking the most recent experimental limits for the neutrinoless half-lives, we also deduced new upper limits for the neutrino mass parameter.

Physical Review C **63**, 064304, 2001

PACS:21.60.Jz; 23.40.Hc;23.40.Bw

Nuclear effects on bremsstrahlung neutrino rates of astrophysical interest

S. Stoica [1], J.E. Horvath [2]

[1] Institute of Physics and Nuclear Engineering, Department of Theoretical Physics, POBox MG - 6, Bucharest, Romania
[2] IAG/USP, Avenue M. Stéfano 4200, Agua Funda, 04301-904 São Paulo, SP, Brazil

We calculate in this work the rates for the neutrino pair production by nucleon-nucleon bremsstrahlung taking into account the full contribution from a nuclear one-pion-exchange-potential.It is shown that if the temperatures are low enough (T=< 20 MeV), the integration over the nuclear part can be done for the general case, ranging for the completely degenerate (D) to the nondegenerate (ND) regime. We find that the inclusion of the full nuclear contribution enhances the neutrino pair production by nn and pp bremsstrahlung by a factor of about 2 in both the D and ND limits when compared with previous calculations.This result may be relevant for the physical conditions of interest in the semitransparent regions near the neutrinosphere in type II supernovae, cooling of neutron stars, and other astrophysical situations.

Physical Review C **65**, 028801, 2002

DOI:10.1103/PhysRevC.65.028801

PHACS number(s):26.65.+t, 95.30.-k

Microscopic structure of four body resonances

D.S. Delion[1], J. Suhonen[2]

[1] National Institute of Physics and Nuclear Engineering, Bucharest-Măgurele, POB MG-6, Romania
[2] Department of Physics, University of Jyväskylä, POB 35, FIN-40351, Jyväskylä, Finland

A microscopic approach of four body states, seen as decaying states or scattering resonances, is given. The equations of motion describing cluster-like states are derived within the multi-step shell-model approach. The lowest collective two-particle eigenmodes are used as building blocks for the α-like states. A good agreement with the low-lying states in ^{212}Po is obtained. The spectroscopic factor of the α-decay between ground states is reproduced. It is shown that only by including the continuum part of the single particle spectrum the decay width for α and cluster-decay processes is reproduced. The α-like structure of the lowest states in ^{212}Po is analyzed and strong high-lying resonances are predicted. A good agreement with experimental quasimolecular states in ^{40}Ca is obtained.

Published in *Romanian Journal of Physics* **47** (2002) 177-188

Towards a microscopic description of an α-condensate in nuclei

G.G Dussel[1], D.S. Delion[2], R.J. Liotta[3]

[1] Institute of Physics and Nuclear Engineering, Bucharest Măgurele, POB MG-6, Romania
[2] Departamento de Física "Juan Jose Giambiaggi", Facultad de Ciencias Exactas y Naturales, Universidad de Buenos Aires, Pabellón 1, Ciudad Universitaria, (1428) Buenos Aires, Argentina
[3] KTH, Stockholm Center for Physics, Astronomy and Biotechnics SE-10691, Stockholm, Sweden

A theory to describe α-condensates in nuclei is presented. The corresponding quasiparticles consist of fermions as well as bosons. The fermions are a combination of one-particle and three-hole states, while the bosons are combinations of pair-particles and pair-holes. A relation between the fermionic and bosonic gap parameters is predicted and confirmed by experimental data.

Published in *Romanian Journal of Physics* **47** (2002) 97-106

Anisotropic α-decay

D.S. Delion[1], A. Insolia[2], R.J. Liotta[3]

[1] National Institute of Physics and Nuclear Engineering, Bucharest-Măgurele, POB MG-6, Romania
[2] Department of Physics and Astronomy, University of Catania and INFN, I-95129 Catania Italy
[3] Center of Physics, Astronomy and Biotechnics, S-10405, Stockholm, Sweden

A microscopic approach to the aqnisotropic α-decay problem in deformed nuclei is presented. Nuclear wave functions are calculated within the BCS approach, while WKB semicvlassical approximation is used for the penetration through the deformed Coulomb barrier. Results are compared with recent experimental data obtained at CERN by the ISOLDE and NICOLE Collaborations. The redictions of the model for well deformed nuclei are in very good agreement with the experimental findings.

Published in *Yadernaia Physika* **65** (2002) 685; *Phys. Atomic Nuclei* **65** (2002) 653

Influence of the continuum on cluster decay processes

D.S. Delion[1], J. Suhonen[2]

[1] National Institute of Physics and Nuclear Engineering, Bucharest-Măgurele, POB MG-6, Romania
[2] Department of Physics, University of Jyväskylä, POB 35, FIN-40351, Jyväskylä, Finland

A microscopic approach of cluster decay including single-particle states in continuum is given. The equations of motion describing cluster-like states are derived within the multi-step shell-model approach. The lowest collective two-particle eigenmodes are used as building blocks for the α-like states. A good agreement with the low-lying states in ^{212}Po is obtained. The spectroscopic factor of the α-decay between ground states is reproduced. It is shown that only by including the continuum part of the single particle spectrum the decay width for α and cluster-decay processes is reproduced. The α-like structure of the lowest states in ^{212}Po is analyzed and strong high-lying resonances are predicted.

Published in *Yadernaia Physika* **65** (2002) 653; *Phys. Atomic Nuclei* **65** (2002) 621

Self-consistent description of the ternary cold fission: tri-rotor mode

D.S. Delion[1], A. Săndulescu[1], W. Greiner[2]

[1] National Institute of Physics and Nuclear Engineering, Bucharest Măgurele, POB MG-6, Romania
[2] Institut für Theoretische Physik der Universität, Frankfurt/Main, Robert Mayer straβe 8-10, Germany

We give a quantum description of the ternary cold fission process within a stationary scattering formalism. The dynamics of the light particle and heavy fragments is described by a self-consistent system of equations for radial wave functions. We consider the spontaneous cold ternary fission of ^{252}Cf accompanied by ^{4}He and ^{10}Be. The light cluster decays from some resonant eigenstate in the Coulomb plus nuclear potential. It turns out that for the angular momentum projection K=0 the light cluster emission is concentrated in the polar direction. By increasing K the maximum of the angular distribution moves towards the equator, as measured in experiment. For ^{4}He we predict short living decaying states. Due to a large repulsive core, proportional to K^2, such states are hindered in the case of ^{10}Be. The motion of the two heavy fragments with $-K$ compensates the rotation of the light fragment. We call this collective motion tri-rotor mode and it should be detected in the fragment yields by magnetic transitions.

Published in *Journal of Physics* **G 28** (2002) 2921-2938

Towards a self-consistent microscopic α-decay theory

D.S. Delion[1], A. Săndulescu[2]

[1] National Institute of Physics and Nuclear Engineering, POB MG-6, R-76900 Bucharest-Măugurele, Romania
[2] Institut für Theoretische Physik der J W Goethe Universität, Robert-Mayer Straβe 8-10, D-60054 Frankfurt/Main, Germany

We show that for osmium, platinium and mercury isotopes the α-particle preformation factors given by the standard shell model are not consistent with the barrier penetrabilities. The internal cluster formation amplitude and the outgoing Coulomb wave function should have the same logarithmic derivatives for the experimental Q-value. The usual shell model wave functions are not able to satisfy this condition along any isotopic chain. In order to correct this deficiency we use an effective procedure. We diagonalize the mean field using a single particle basis with two harmonic oscillator parameters, proposed in a previous

paper. In order to obtain correct tails of the wave functions the second harmonic oscillator parameter should increase with the mass number. This is consistent with the suppression of the α-clustering by increasing the proton-neutron asymmetry. A parabolic fit of this parameter versus the mass number is able to ensure a consistency with experimental Q-values within a mean deviation of 300 keV.

Published in *Journal of Physics* **G 28** (2002) 617-625

Double fine structure in the binary cold fission

D.S. Delion[1], A. Săndulescu[1], S. Mişicu[2], F. Carstoiu[1], W. Greiner[2]

[1] National Institute of Physics and Nuclear Engineering, Bucharest-Măgurele, POB MG-6, Romania
[2] Institut für Theoretische Physik, J.W.v.-Goethe Universität, Robert-Mayer-Str. 8-10, 60325 Frankfurt am Main, Germany

We give a description of the binary cold fission process of ^{252}Cf within the stationary scattering formalism. The decay of the dinuclear system (quasi-molecule) consists in the tunneling of a metastable state from an internal region, where the nucleus-nucleus potential has a quasi-molecular pocket, to the asymptotic region which is governed solely by the Coulomb repulsion. As a transversal internal motion we suppose angular oscillations of the fragments up to the scission point. In the external region these vibrations transform into rotations. The nuclear interaction is given by a double folding procedure using M3Y forces plus a repulsive contact potential. For the experimental Q-value we find several resonant states of the binary system, depending on the repulsive strength. We predict a strong dependence of decay widths upon the internal structure of the considered resonant state. Therefore the measured yields of the two fragments with given angular momenta in coincidence are able to provide more insight on the internal molecular dynamics of the decaying dinuclear system.

Published in *Journal of Physics* **G 28** (2002) 289-306

Equal-time formulation for off-shell transport theory

R.A. Ionescu[1], H.H. Wolter[2]

[1] Department of Nuclear Physics, IFIN-HH
[2] Sektion Physik, Universitaet Muenchen

The conventional approach to the description of heavy ion collisions is based on the Boltzmann equation with a self-consistent mean field and a collision term of the Uehling-Uhlenbeck form. The main improvements were the formulation in terms of a relativistic hadronic field theory some non-equilibrium effects in a Local (phase space) Configuration Approximation [1]. Only recently there has been an increasing interest in the inclusion of further quantum effects in the description of heavy ion collisions, in particular in the inclusion of the off-shell propagation of the baryons. In these formulations the Kadanoff-Baym equations are solved with test particles in 8-dimensional phase space. This leads to certain problems with the initial conditions and the persistence of the off-shellness.

We have developed an alternative method by a systematic energy moment expansion of the spectral functions of finite width by formulating an equal-time theory for the one-particle Green functions. These energy moments measure the spreading of the Green function in energy, e.g. the second order energy moment is a measure of the width of the spectral function. From the Kadanoff-Baym equations we obtain two hierarchies of equations for each of the two independent components of the one-particle Green function, spectral and kinetic. We discuss the compatibility of the two hierarchies of equations and the possibility of their systematic truncation. The hierarchies for the spectral Green function truncate by themselves. The lowest order truncation of the hierarchies for the kinetic Green function is a Bolzmann-like equation. We have tested this scheme using a nonrelativistic self-interacting fermionic field. Our formulation in prin-

ciple keeps all the terms in the gradients for space coordinates. We investigated the effects of higher order terms in a gradient expansion. These terms represent quantum effects and we investigated them numerically in a simple model of one-dimensional slab-on-slab collisions. The contour plots of the results of various approximations are shown in Fig.1. We find that the gradient corrections to the drift term result in a much smoother behaviour of the phase-space distribution function.

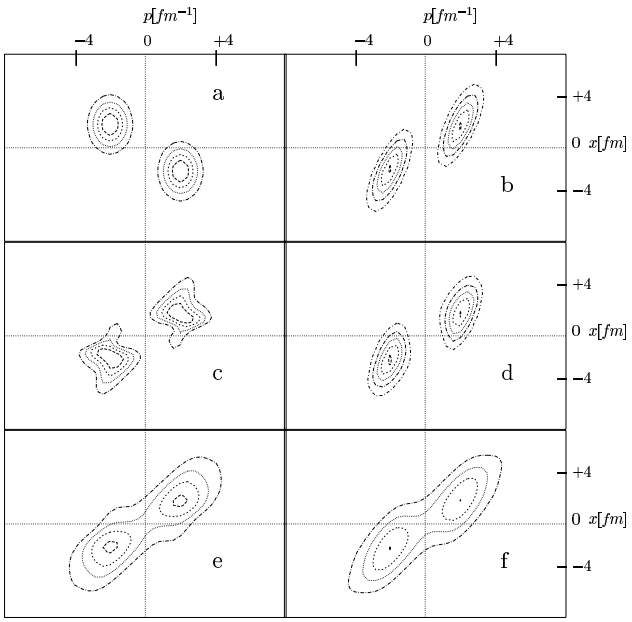

Figure 1: Contour plots of the phase space distribution of slab-on-slab collisions at 80 MeV per nucleon. Panel (a) initial distribution. Other panels distributions (at 10 fm/c) in the following approximations: (b) free motion; (c) Vlasov approximation; (d) Vlasov plus next order gradient terms; (e) Vlasov plus collision term (i.e. BUU approximation); (f) Vlasov plus next order gradient plus collision terms.

The time evolution of the width of the spectral function is presented in Fig.2. We found that it increases from the initially nonequilibrated momentum configuration, being largest for the maximum overlap of the two slabs. The width goes to zero outside of the range of the system. We derived, in the gradient approximation, the modification in the Boltzmann equation in the next order truncation of the hierarchies with improved approximations for the collision integral, including memory effects. These are found to be controlled by a parameter related to the width of the spectral function. The equations could be applied to a realistic description of heavy ion collisions using nonrelativistic or relativistic formulations.

References

[1] T. Gaitanos, C. Fuchs, H.H. Wolter, Nucl. Phys. **A650**(1999) 97

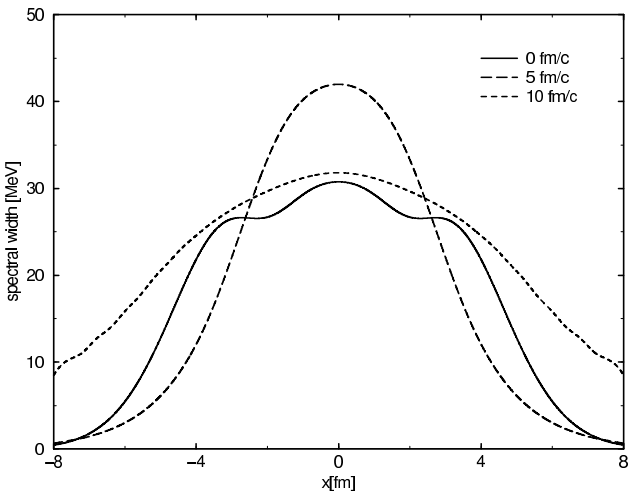

Figure 2: Width (i.e. second order energy moment) of the spectral function at different times as a function of the coordinate of the one-dimensional model.

Evaluation of bonding energies by quantum mechanical methods

Cristian Postolache[1], Lidia Matei[1]

[1] National Institute of Research and Development for Physics and Nuclear Engineering "Horia Hulubei", Magurele, Bucharest, Romania, e-mail: cristianpostolache@yahoo.com

In this paper we proposed a quantum mechanical evaluation model for bonding energies in organic compounds. Values of bonding energies were determined as homolytic dissociation energies.

The molecular structures were built and geometry optimized in first stage using MM2, MM+, AMBER molecular mechanic. Energetically minimizations were refined using semiempirical methods. In concordance with choose molecular structure we used, methods like CNDO, INDO, PM3, AM1.

Binding energies were evaluated by simulation of homolytic dissociation processes. Using cuanto–mechanical methods we characterized molecular structures and fragments resulted from dissociation of chemical bond. Were determinated and analyzed total binding energies (TBE) of unoptimized fragments, those geometrical minimized post-fragmentation, transitional state and initial molecular structures. Enthalpy of reaction (ΔH) were determined from difference between fragments TBE and TBE of system. The values of activation energy (Ea) is indicated by the difference between transitional state TBE and TBE of system. ΔH and Ea are correlated with binding energy.

Method accuracy and application fields of different evaluation modalities (optimized, non-optimized, transition states) were achieved by intercomparison of obtained values with those experimental found in literature.

More than 74 organic and inorganic compounds (alkans, alkenes, alkynes, aromatic structures, halogenated compounds, alcohols, peroxides, aldehydes and ketones, carboxylic acids, ammines, nitro derivatives, nitrates, nitrites, thyols, thyoethers, water, hydrogen peroxide, ammonium, hydrazine etc.) were analyzed.

Mathematical Physics, Field Theory and Elementary Particles

Uniform asymptotic approximation of 3-D Coulomb scattering wave function

N. Grama[1], C. Grama[1], I. Zamfirescu[1]

[1] IFIN-HH

The regular solution $\Psi_c(\mathbf{r})$ of the Schrödinger equation which describes the scattering by a pure Coulomb potential acting between two charged particles has been obtained by Gordon [1].

$$\Psi_c(\mathbf{r}) = \mathrm{e}^{-\pi\eta/2}\Gamma(1+\mathrm{i}\eta)\mathrm{e}^{\frac{\mathrm{i}}{2}\mathrm{k}(\zeta-\xi)}{}_1\mathrm{F}_1(-\mathrm{i}\eta;1;-\mathrm{ik}\xi) \quad (1)$$

where ${}_1F_1$ is the confluent hypergeometric function. $\Psi_c(\mathbf{r})$ depends on two parabolic variables, $\xi = r - z$ and $\zeta = r + z$, where z is the axis along the incident beam, and on the Sommerfeld parameter $\eta = Z_1 Z_2 e^2 m/\hbar^2 k$. The solution (1) is an important result in quantum mechanics, but it is not sufficiently simple for practical applications (e.g. Coulomb excitation) and it is not suitable for the obtainment of a 3-D WKB approximation or an uniform asymptotic approximation for large η of $\Psi_c(\mathbf{r})$. It is well known that even for problems which have been solved exactly it often happens that only the asymptotic approximation of the solution is sufficiently simple to be useful in practical applications and stresses the functional de-

pendence of the solution on the parameters. As far as we know there is no uniform asymptotic approximation reported for the solutions of a 3-D Schrödinger equation.

In the present work a closed form expression of Ψ_c in terms of the regular Coulomb wave function $F_0(\eta, \frac{1}{2}k\xi)$ and its derivative is obtained:

$$\Psi_c(\mathbf{r}) = \mathrm{e}^{\mathrm{i}\sigma_0}\ \mathrm{e}^{\mathrm{i}\frac{\mathrm{k}}{2}\zeta}\left[F_0'(\eta, \tfrac{1}{2}k\xi) - \mathrm{iF}_0(\eta, \tfrac{1}{2}\mathrm{k}\xi)\right] \qquad (2)$$

where $\sigma_0 = \arg\Gamma(1 + \mathrm{i}\eta)$ is the Coulomb phase shift for the orbital angular momentum $l = 0$.

The WKB approximation of the 3-D Coulomb scattering wave function $\Psi_c(\mathbf{r})$ fails at the caustic (the paraboloid defined by the equation $\xi = \frac{4\eta}{k}$ which separates the classically forbidden region $\left(0 < \xi < \frac{4\eta}{k}\right)$ from the classically allowed region $\left(\xi > \frac{4\eta}{k}\right)$). An uniform asymptotic approximation, valid near and away from the caustic is necessary. The uniform asymptotic approximation reduces to the WKB approximation away from the caustic and remains finite at the caustic. By using the exact closed form (2) of the wave function Ψ_c derived above we obtain an uniform asymptotic approximation for large η

$$\begin{aligned}\Psi_c \quad \sim \quad & -\mathrm{i}\pi^{1/2}(2\eta)^{1/6}\mathrm{e}^{\mathrm{i}(\sigma_0+\frac{\mathrm{k}}{2}\zeta)}\left\{\mathrm{q}(\tfrac{1}{2}\mathrm{k}\xi) - \right. \\ & \left. -\mathrm{i}(2\eta)^{-1/3}\tilde{\mathrm{q}}(\tfrac{1}{2}\mathrm{k}\xi)\right\}, \end{aligned} \qquad (3)$$

where q, and $\tilde{q}$ are given by

$$q(\rho) = [\phi'(x)]^{-1/2}\ \mathrm{Ai}[-(2\eta)^{2/3}\phi(x)] \qquad (4)$$

$$\tilde{q}(\rho) = [\phi'(x)]^{1/2}\ \mathrm{Ai}'[-(2\eta)^{2/3}\phi(x)] \qquad (5)$$

with the notation

$$\frac{2}{3}[-\phi(x)]^{3/2} = \begin{cases} -\mathrm{i}\ f(x)\ , & \text{for} \quad x > 0, \\ -\chi(x) + \frac{\pi}{2}, & \text{for} \quad -1 < x \leq 0, \end{cases}$$

where

$$f(x) = [x(1+x)]^{1/2} - \log[(1+x)^{1/2} + x^{1/2}],$$

$$\chi(x) = [-x(1+x)]^{1/2} - \frac{\cos^{-1}(2x+1) + \pi}{2},$$

and $x = (\rho - 2\eta)/2\eta$. One can see that in both the classically allowed region and forbidden region the uniform asymptotic approximation for large η of $\Psi_c(\mathbf{r})$ is expressed in terms of the Airy function Ai and its derivative. The wave function Ψ_c changes from an oscillatory behaviour on one side of the caustic (classically allowed region) to an exponential behaviour on the other side of the caustic (classically forbidden region).

[1] Gordon W., Z. Physik 48 (1928) 180.

The causal approach in quantum field theory

D. R. Grigore[1]

[1] NIPNE-HH, Department of Theoretical Physics

The mathematical formulation of perturbative renormalization theory starts from Bogoliubov axioms imposed on the S-matrix (or equivalently on the chronological products). The S-matrix is formal series of operator valued distributions: these distributions are denoted by $T(x_1, \cdots, x_n)$ and one supposes that they act in the Fock space of some collection of free fields. These operator-valued distributions are called *chronological products*. The expression $T(x)$ is called the *interaction Lagrangian*. It is convenient to construct more general objects namely the operator-valued distributions $T(W_1(x_1), \ldots, W_n(x_n))$ where W_j are arbitrary Wick monomials. These objects verify some properties (following from Bogoliubov axioms) and expressing the following properties: the initial condition, skew-symmetry in all arguments, Poincaré invariance, causality and unitarity (see for instance [2]). The existence of solutions follows from the analysis of Epstein and Glaser [1] as a recursive procedure using in an essential way the causality axiom.

Sometimes it is possible to supplement these axioms by other invariance properties with respect to space-time symmetries (inversions and/or scale invariance), charge conjugation, global symmetry with respect to some internal symmetry group, supersymmetric invariance, etc. if they are valid for the interaction Lagrangian.

In [6] the invariance properties of the chronological products with respect to scale invariance was analyzed in detail. The scale invariance operators $\mathcal{U}_\lambda$ are transforming field operators corresponding to particles of masses m_j in fields corresponding to scaled masses $\lambda^{-1}m_j$. One can prove that if all masses are positive the chronological products can be normalized such that they are scale invariant. On the contrary, if all masses of the model are zero then the scale invariance of the chronological products can be implemented only up to some logarithmic terms in λ.

For models describing higher spin particles unphysical degrees of freedom are necessary and the factor-

ization of the chronological products to the physical Hilbert space follows from a new axiom: the gauge invariance condition. The gauge invariance condition on the chronological products can be expressed in such a way that infrared divergences are not considered [3]:

$$[Q, T(x_1, \ldots, x_n)] = i \sum_{l=1}^{n} \frac{\partial}{\partial x_l^\mu} T_l^\mu(x_1, \ldots, x_n) \quad (1)$$

for some chronological products $T(X)$, $T_l^\mu(X)$. Here Q is the *gauge charge*; it is formally the linear part of the well-known BRST operator. The obstructions to such a factorization process are the well-known *anomalies*.

For some simple models as it is quantum electrodynamics one can provide rather elementary proofs that gauge invariance can be implemented in every order of perturbation theory [9], [4] i.e. there are no anomalies. For more general gauge models as the Standard Model of the elementary particles the analysis is more complicated. One can prove that the condition (1) for $n = 1, 2, 3$ gives the usual expression for the Yang-Mills interaction Lagrangian and for the axial anomaly [5]. For arbitrary orders one can re-express (1) in terms of vacuum averages of chronological products and obtains the so-called Ward (or C-g identities) [8]. This combinatorial argument is very involved and uses some ideas from differential geometry: jet-bundle extensions techniques. It is conjectured the Ward identities are valid in all orders of perturbation theory if they are valid for $n \leq 5$; this conjecture seems extremely difficult to prove in full generality.

References

[1] H. Epstein, V. Glaser, Ann. Inst. H. Poincaré **19 A** (1973) 211-295

[2] M. Dütsch, K. Fredenhagen, Commun. Math. Phys. **203** (1999) 71-105

[3] M. Dütsch, T. Hurth, F. Krahe, G. Scharf, Il Nuovo Cimento **A 106** (1993) 1029-1041

[4] D. R. Grigore, Ann. Phys. (Leipzig) **10** (2001) 439-471

[5] D. R. Grigore, Journ. Phys. **A 34** (2001) 5420-5462

[6] D. R. Grigore, Ann. Phys. (Leipzig) **10** (2001) 473-496

[7] D. R. Grigore, European Phys. Journ. **C 21** (Particles and Fields) (2001) 732-734

[8] D. R. Grigore, hep-th/0108083

[9] G. Scharf, "*Finite Quantum Electrodynamics: The Causal Approach*", (second edition) Springer, 1995

Renormalization scheme dependence of modified QCD perturbative expansions

I. Caprini [1], J. Chyla [2], J. Fischer [2]

[1] NIPNE-HH, Theoretical Physics Department

[2] Institute of Physics, Academy of Sciences of the Czech Republic, 182 21 Prague 8, Czech Republic

In the standard perturbation theory the finite order approximations of physical quantities are renormalization scale (μ) and scheme (RS) dependent. The quest for in some sense "optimal" scale and scheme is vital for meaningful applications. There are several recipes for scale and scheme fixing [1, 2, 3], but so far there is no generally accepted solution. We consider a physical quantity $\mathcal{R}(Q)$ depending on one external kinematical variable Q and admitting the perturbative expansion of the form

$$\mathcal{R}(Q) = a(1 + r_1 a + r_2 a^2 + \ldots), \quad (1)$$

where the couplant $a \equiv \alpha_s/\pi = a(\mu, \mathrm{RS})$ and the coefficients $r_i = r_i(Q, \mu, \mathrm{RS})$ depend on the scale and scheme. The scheme can be labeled by the set of free parameters $c_k, k \geq 2$, defining the r.h.s. of the renormalization group equation for the couplant a

$$\frac{\partial a(\mu, \mathrm{RS})}{\partial \ln \mu} = \beta(a) = -ba^2(1 + ca + c_2 a^2 + \ldots), \quad (2)$$

together with a parameter $\tilde{\Lambda}$ specifying the boundary condition on the solution.

By imposing at each order the formal (*i.e.* to the order considered) scale and scheme independence of the physical quantity $\mathcal{R}(Q)$, a set of scale and scheme invariants quantities ρ_i can be defined [1], [4]. By expressing the perturbative coefficients r_i in terms of the invariants, the scale dependence of the truncated QCD

expansions can be investigated in a systematic way. In [4] this study was done for the conventional perturbative expansion (1). In the present work we perform a similar analysis for the modified QCD expansion proposed recently in [5]. Instead of the powers a^n, the QCD correaltors are expanded in terms of some functions $W_n(a)$, which include the available knowledge of the large order behaviour of standard perturbative expansions. For instance, for the hadronic τ decay rate R_τ the expansion functions are

$$W_n = \frac{1}{n!}\left(\frac{8}{3}\right)^n \left(\frac{2}{b}\right)^n \frac{2}{ab}\int_C \mathrm{e}^{-\frac{2u}{ab}} F(u) w^n(u) \mathrm{d}u, \quad (3)$$

where

$$F(u) = \frac{-12\sin(\pi u)}{\pi u(u-1)(u-3)(u-4)} \quad (4)$$

and

$$w(u) = \frac{\sqrt{1+u}-\sqrt{1-u/2}}{\sqrt{1+u}+\sqrt{1-u/2}}. \quad (5)$$

We consider also a set of "weighted" functions $\tilde{W}_n(a)$, which exploit the known leading singularities in the Borel plane [5].

The preliminary results show that the scale dependence of the new expansion is very different from that of the conventional perturbation series. We show as an example in Figure 1 the scale dependence of the expansions of R_τ in terms of the'weighted functions $\tilde{W}_n(a)$ at the LO, NLO and NNLO. Similar analyses of other non-power expansions introduced in Refs. [6] and [7] are currently under study.

References

[1] P.M. Stevenson, Phys.Rev. **23**, 2916 (1981)

[2] G. Grunberg, Phys. Rev. **D29**, 2315 (1984)

[3] S. Brodsky, P. Lepage and P. Mackenzie, Phys. Rev. **D28**, 228 (1983)

[4] J. Chyla, A. Kataev and S. Larin, Phys.Lett. **267**, 269 (1991).

[5] I. Caprini and J. Fischer, Phys.Rev D**60**, 054014 (1999); Phys. Rev. D**62**, 054007 (2000); Eur. Phys. J. C**24**, 127 (2002)

[6] D.V. Shirkov, I.L. Solovtsov, Phys.Rev.Lett. **79** 1209 (1997).

[7] G. Cvetic, C. Dib, T. Lee and I. Schmidt, Phys.Rev. **D64**, 093016 (2001)

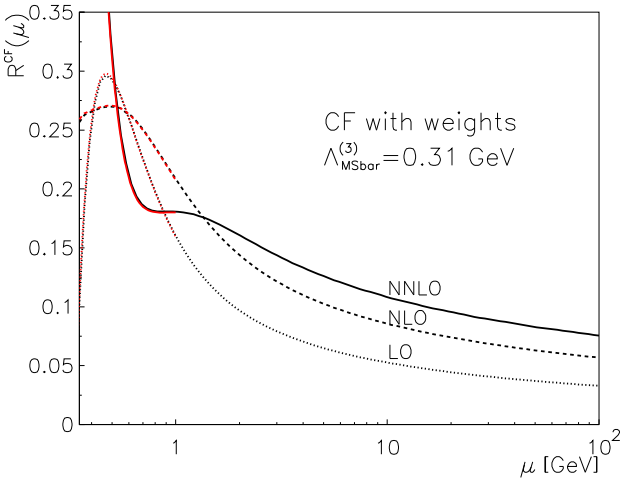

Figure 1: Scale dependence of the modified expansion of R_τ at the first three orders.

Omnès representations for $K \to \pi\pi$ amplitudes

I. Caprini [1], L. Micu [1], C. Bourrely [2]

[1] NIPNE-HH, Theoretical Physics Department

[2] Centre de Physique Théorique, CNRS-Luminy, Marseille, France

The weak decay $K \to \pi\pi$ has been a continuous challenge for the theoretical investigations. In chiral perturbation theory (ChPT) beyond the leading order [1], the appearance of many unknown counterterms and renormalization constants render the numerical predictions difficult. Most lattice calculations [2] simulate matrix elements of the type $\langle\pi|O_i|K\rangle$, related to the physical matrix elements $\langle\pi\pi|O_i|K\rangle$ by lowest order ChPT. In this procedure the higher order final state interactions are completely missing, while it is expected that these interactions play an important role for the $\Delta I = 1/2$ rule and the CP-violating ratio ϵ'/ϵ.

In a combined approach proposed recently, the results obtained by lattice simulations at unphysical points are extrapolated to the physical configuration by using calculations to NLO in ChPT [1].

An alternative way to connect the on-shell amplitude to lattice or ChPT results at unphysical points and to spectral functions measured experimentally is based on dispersion relations. This formalism was used some time ago for the CP conserving amplitudes in order to explain the $\Delta I = 1/2$ rule [3]) and more recently to evaluate the effects of final state interactions upon ϵ'/ϵ [4]- [5]. These dispersion relations were written down by analogy with the familiar cases of the electromagnetic form factors [4] or πK scattering amplitudes [5]. However, while these functions depend on a physical energy used as dispersive variable, in the weak decay the external momenta are fixed by the mass shell condition. Therefore, an analytic continuation of these momenta is necessary in order to obtain a dispersion relation. In the present work we perform the continuation using the Lehmann-Symanzik-Zimmermann (LSZ) formalism and hadronic unitarity. We follow the dispersive treatment of $B \to \pi\pi$ decay considered in [6]. However, the difference in scale between the two processes requires specific treatments. More exactly, using Watson theorem we derive for the $K \to \pi\pi$ amplitude a generalized Omnès representation, with contributions from both the direct and the crossed channels.

We treat decay amplitudes A_I of definite isopin

$$A_I = \langle (\pi(k_1)\,\pi(k_2))_I\,;\mathrm{out}\,|\mathcal{H}_w(0)|K(p)\,;\mathrm{in}\rangle\,, \qquad (1)$$

where $\mathcal{H}_w$ is the $\Delta S = 1$, $\Delta B = 0$ weak hamiltonian density. We shall consider the amplitude as function of the momentum variables $s = p^2 = (k_1 + k_2)^2$ and $t = k_1^2 = (p - k_2)^2$. The physical amplitude corresponds to the on-shell values $s = m_K^2$, $t = m_\pi^2$. It can be shown that $A_I(s,t)$ can be decomposed as a sum of two functions, each depending on a single variable

$$A_I(s,t) = A_s(s) + A_t(t)\,. \qquad (2)$$

We consider first the amplitude $A_I(s, m_\pi^2)$. Denoting $A_\pm = A_I(s \pm i\epsilon, m_\pi^2)$, we write the unitarity relation in the s-channel as

$$A_+(1 - 2iM_I^*) - A_- = 2i\,\theta(s - s_{in})\,\sigma_{in}(s), \qquad (3)$$

where $M_I(s)$ is the S-wave $\pi\pi$ scattering amplitude of isospin I, σ_{in} denotes the sum of the inelastic final state and initial state interactions and $s_{in} = 4m_K^2$. Eq. (3) is an inhomogeneous Hilbert equation, which has the solution

$$A_I(s, m_\pi^2) = \Omega\left[P + \frac{1}{\pi}\int\limits_{s_{in}}^{\infty}\frac{\sigma_{in}(s')\mathrm{d}s'}{\Omega^*(s'-s)}\right], \qquad (4)$$

where P is a polynomial and

$$\Omega = \exp\left[-\frac{s-s_0}{2\pi i}\int\limits_{4m_\pi^2}^{\infty}\frac{\ln[1-2iM_I^*]}{(s'-s_0)(s'-s)}\mathrm{d}s'\right]. \qquad (5)$$

Using the decomposition (2) we treat in a similar way the amplitude $A_I(s,t)$. The result is an Omnès representation which incorporates the $\pi\pi$ and πK S-wave phase shifts and inelastic contributions from the direct and the crossed channel. The result is useful for making the analytic continuation of the ChPT and lattice calculations from unphysical momenta to the physical point.

References

[1] P. Boucaud et al. (The SPQ(CD)R Collaboration, Nucl. Phys. Proc. Suppl. 106, 329 (2002).

[2] C. T. Sachrajda, hep-ph/0110304; G. Martinelli, hep-ph/0110023.

[3] T. N. Truong, Phys. Lett. B**207**, 495 (1988).

[4] E. Pallante and A. Pich, Phys. Rev. Lett. **84** (2000) 2568; Nucl. Phys. B **592**, 294 (2000)

[5] M. Bücher, G. Colangelo, J. Kambor and F. Orellana, Phys. Lett. B**521**, 29 (2001).

[6] I. Caprini, L. Micu and C. Bourrely, Phys. Rev. D **60**, 074016 (1999); Phys. Rev. D**62**, 034016 (2000); Eur.Phys. J.C**21**, 145-153 (2001).

Low energy contributions of hadronic vacuum polarization

I. Caprini [1]

[1] NIPNE-HH, Theoretical Physics Department

Thorough tests of the Standard Model have been made possible recently by a number of very high precision measurements. In particular, the extremely accurate value of the muon magnetic moment determined by the "Muon $g-2$ Collaboration" [1] imposed severe constraints on the hadronic physics at low energies. A quantity which received much interest in connection with the low energy limit of QCD is the hadronic vacuum polarization dressing the photon. Numerically, the contribution of the vacuum hadronic polarization to the magnetic moment of the muon is about $a_\mu^{VP} \approx 700 \times 10^{-10}$, which is a small fraction of the total $a_\mu \approx 11659202(8) \times 10^{-10}$ [1]. However, tomatch the experimental precision requires a determination of a_μ^{VP} to about 1%. Since the most important contribution of the vacuum polarization (around 70%) is brought by pairs of two-pions, a determination of the electromagnetic form factor of the pion to an accuracy of about half a percent is required. A dispersive analysis was performed to this end [2], based on Watson theorem and the description of $\pi\pi$ scattering by Roy equations, combined with the technique of conformal mapping [3] to parametrize the inelastic singularities.

A subtle problem which became relevant for a precision prediction of the muon anomaly is the proper treatment of the radiative corrections in the experimental data. The contribution to a_μ of the hadronic vacuum polarization up to two loops is given by

$$\delta a_\mu^{1+2,VP} = -\frac{\alpha}{\pi} \int_0^1 dx (1-x)[\Pi_h(\xi) - \Pi_h^2(\xi)] \,, \quad (1)$$

where $\xi = -x^2 m_\mu^2/(1-x)$ and the hadronic vacuum polarization amplitude $\Pi_h(s)$ satisfies the dispersion relation

$$\Pi_h(s) = \frac{s\alpha}{3\pi} \int_{4m_\pi^2}^\infty \mathrm{d}s' \frac{R(s')}{s'(s'-s)} \,. \quad (2)$$

Here $R(s)$ is defined in terms of the "undressed" cross section $\sigma_h(s)$ of the annihilation $e^+e^- \to \gamma^* \to$ hadrons as

$$R(s) = \sigma_h(s) \frac{3s}{4\pi\alpha^2} \,. \quad (3)$$

The measured cross section σ_h^{exp} includes however the vacuum polarization dressing the photon, so that

$$R^{exp}(s) = R(s)/|1+\Pi(s)|^2 \,. \quad (4)$$

In order to obtain $R(s)$ one must remove from R^{exp} the contribution of the vacuum polarization. Most experimental groups correct their data for the leptonic vacuum polarization, which is exactly calculable in QED, but do not remove the effect of the hadronic vacuum polarization. We show below that using this partially corrected data in the one loop hadronic contribution to a_μ (the first term in (1)), is equivalent to using theone+ two-loop contribution calculated with corrected data.

By replacing in Eq.(1) each Π_h in the product $\Pi_h\Pi_h$ by a dispersion relation of the form (2), one obtains easily

$$\delta a_\mu^{2,VP} = \frac{\alpha^3}{9\pi^3} \int_{4m_\pi^2}^\infty \frac{\mathrm{d}s}{s} \int_{4m_\pi^2}^\infty \frac{\mathrm{d}s'}{s'} R(s) R(s') K^{(2c)}(s,s') \,, \quad (5)$$

where $K^{(2c)}(s,s')$ is given in Eq. (14) of [4].

Alternatively, we can insert in (1) the dispersion relation

$$\Pi_h(s) - \Pi_h^2(s) = \frac{s}{\pi} \int_{4m_\pi^2}^\infty \mathrm{d}s' \frac{\mathrm{Im}[\Pi_h(s') - \Pi_h^2(s')]}{s'(s'-s)} \,, \quad (6)$$

with the spectral function

$$\mathrm{Im}[\Pi_h(s) - \Pi_h^2(s)] \approx \frac{\alpha}{3} \frac{R(s)}{|1+\Pi_h(s)|^2} \,. \quad (7)$$

This gives after a straightforward calculation

$$\delta a_\mu^{1+2,VP} = \frac{\alpha^2}{3\pi^2} \int_{4\,m_\pi^2}^\infty \mathrm{d}s\, K(s) \frac{R(s)}{|1+\Pi_h(s)|^2} \,, \quad (8)$$

which coincides with the one loop expression which follows from (1), with a hadronic cross section including the dressing of the photon by the hadronic vacuum polarization. Therefore, using as input experimental data not corrected for the hadronic vacuum polarization and adding the contribution to a_μ of the two hadronic loops, given in [4], represents a double counting.

References

[1] H. N. Brown et al., (Muon $g-2$ Collaboration), Phys. Rev. Lett. **86**, 2227 (2001).

[2] I. Caprini, G. Colangelo. J. Gasser, H. Leutwyler, F. Jegerlehner, S. Eidelman, work in progress

[3] M. F. Heyn, C.B. Lang, Zeit. Phys. C**7**, 169 (1981); I. Caprini, Eur. Phys. J. C.**13**, 431 (2000).

[4] B. Krause, Phys.Lett.B390, 392-400 (1997).

Solitonic model for energy transport in quasi-1-D biological systems

D. Grecu[1], Anca Vişinescu[1], A.S. Cârstea[1]

[1] IFIN-HH, Department of Theoretical Physics; E-mail: dgrecu@theor1.theory.nipne.ro

The classical equation of motion of a Davydov model in a coherent state approximation is analyzed using the multiple scales method. In the first order, the dominant amplitude has to be a solution of the well known nonlinear Schrödinger equation (NLS). In the next order the second amplitude satisfies an inhomogeneous linearized NLS equation, the inhomogeneous term depending only on the dominant amplitude. In order to eliminate possible secular behaviour the dominant amplitude has to satisfy also the next equation in the NLS hierarchy (a complex modified KdV equation). When the second order derivative of the dispersion relation vanishes (ZDP case) the scaling of the slow space variable has to be changed, and the equation verified by the dominant amplitude is found.

One of the basic mechanism for producing biological energy is the hydrolysis of the ATP in ADP

$$ATP^{4-} + H_2O \rightarrow ADP^{3-} + HPO_4^2 + H^+$$

The problem of energy transport in proteins is confronted with a main difficulty: in a linear dynamic analysis, the mean lifetime of such an excitation is unacceptable short. The "crisis" was avoided by nonlinear models. An attractive model was proposed by Davydov [1] for storage and transport of energy in proteins in the context of α-helix structure.

One considers a linear chain of aminoacids connected between them by hydrogen bonds and only the $C = O$ group vibrations are taken into account. A dipole-dipole interaction occurs. If $B_n^+(B_n$ is the creation (annihilation) operator of the intra-molecular excitation in the n-th cell, the vibronic Hamiltonian can be written as

$$H_{ex} = E_0 \sum_n B_n^+ B_n - \frac{1}{2} \sum_{mn} J_{mn} B_n^+ B_m, \qquad (1)$$

where J_{mn} term takes into account the interaction between vibrons.

A coherent state approximation was used by Davydov. His ansatz for the state vector is

$$|\Psi(t)> \;=\; \sum_n a_n(t) B_n^+ exp\left(-\frac{i}{\hbar}\sum_j(\beta_j(t)\hat{p}_j - \right.$$
$$\left. -\pi_j(t)\hat{u}_j)\right)|0>, \qquad (2)$$

$|0>$ being the vacuum state both for vibrons and phonons. Using the average value of $\hat{H}$ as Hamiltonian in the classical equations of motion and through a combined Laplace-Fourier transform one gets

$$i\hbar\dot{a_n} = Ea_n - \sum J_p(a_{n+p} + a_{n-p}) - \frac{\chi^2}{w}|a_n|^2 a_n. \qquad (3)$$

a typical self-trapping equation. The solution is written as an asymptotic expansion in a small parameter ϵ.

$$a_n = e^{i(kln-\omega t)} \sum_j \epsilon^j A_j(\xi, t_2, t_3, ...) \qquad (4)$$

where the amplitudes A_j depend on some slow variables $\xi, t_2, t_3, ...$

$$\xi = \epsilon(ln - v_g t), \quad t_j = \epsilon^j t, \quad j = 2, 3... \qquad (5)$$

In order ϵ^3 the first amplitude A_1 has to satisfy the well known nonlinear Schrödinger equation [2]

$$\frac{\partial A_1}{\partial t_2} + \omega_2 \left(\frac{\partial^2 A_1}{\partial \xi^2} + 2c|A_1|^2 A_1\right) = 0 \qquad (6)$$

where $c = \frac{\chi^2}{2\omega_2 \hbar w}$. This represents a complete integrable equation, solvable by IST method (Inverse Scattering Transform). One can eliminate the secularity by imposing that the dependence of the dominant amplitude A_1 on the slow temporal variable t_3 to be determined by

$$-\frac{\partial A_1}{\partial t_3} + \omega_3 \left(\frac{\partial^3 A_1}{\partial \xi^3} + 6c|A_1|^2 \frac{\partial A_1}{\partial \xi}\right) = 0. \qquad (7)$$

This is the complex mKdV equation, the second in the NLS hierarchy.

References

[1] A.S. Davydov, J. Theor. Biol. **38**, 559 (1993)

[2] D. Grecu, Anca Vişinescu, A.S. Cârstea, Journal of Nonlinear Mathematical Physics, **8**, 139 (2001)

Modulational instability in some nonlinear one-dimensional lattices and soliton generation

D. Grecu [1], Anca Vişinescu [1]

[1] IFIN-HH, Department of Theoretical Physics; E-mail: dgrecu@theor1.theory.nipne.ro

The modulational instability (MI), also known as the Benjamin-Feir instability [1] is a generic phenomenon in continuum and discrete nonlinear physical systems. The phenomenon is generally believed to be responsible for the formation of robust localized coherent structures.

$$i\frac{\partial A}{\partial \tau} + \omega_2 \frac{\partial^2 A}{\partial \xi^2} - \lambda P A = 0$$
$$\frac{\partial P}{\partial \tau} + \mu \frac{\partial}{\partial \xi}|A|^2 = 0 \qquad (1)$$

The systems of equations (1) have been obtained for the first time by Zakharov [3] in plasma physics (coupling between Langmuir oscillations and ion sound) and by Benney [3] in a hydrodynamic context (coupling between gravity and capillary modes of surface waves) and are known as the Zakharov-Benney equations. In the 1-D case it was proved to be an integrable system. One consider the basic solution

$$A = a e^{-i\lambda P_0 \tau}, \quad P = P_0 \qquad (2)$$

and a slightly perturbed solution around it

$$A = a[1 + \epsilon \tilde{A}(\xi, \tau)] e^{-i\lambda P_0 \tau}$$
$$P = P_0 + \epsilon \tilde{P}(\xi, \tau) \qquad (3)$$

The linearized equations for $\tilde{A}$ and $\tilde{P}$ write

$$i\frac{\partial \tilde{A}}{\partial \tau} + \omega_2 \frac{\partial^2 \tilde{A}}{\partial \xi^2} - \lambda \tilde{P} = 0 \qquad (4)$$

$$\frac{\partial \tilde{P}}{\partial \tau} + \mu |a|^2 \frac{\partial}{\partial \xi}(A + \tilde{A}^*) = o \qquad (5)$$

Considering plane wave solutions

$$\tilde{A} = \alpha e^{i(q\xi - \Omega\tau)} + \beta e^{-i(q\xi - \Omega^*\tau)}$$
$$\tilde{P} = \gamma e^{i(q\xi - \Omega\tau)} + \gamma^* e^{-i(q\xi - \Omega^*\tau)} \qquad (6)$$

we get

$$(\Omega - \omega_2 q^2)\alpha = \lambda\gamma$$
$$-(\Omega + \omega_2 q^2)\beta^* = \lambda\gamma \qquad (7)$$
$$\Omega\gamma = \mu|a|^2 q(\alpha + \beta^*)$$

The compatibility condition is a third order algebraic equation

$$\Omega^3 + p\Omega + q = 0 \qquad (8)$$

where

$$p = -\omega_2^2 q^4 < 0 \qquad q = -2\omega_2 \mu\lambda |a|^2 q^3$$

If the discriminant of this equation is positive we have one real root and two complex ones and consequently the system is unstable at small modulations of the amplitudes. Using the above expressions for p and q the condition $D > 0$ gives

$$3\sqrt{3}\frac{\mu\lambda|a|^2}{\omega_2^2} > q^3 \qquad (9)$$

which is fulfilled for enough small values of q.

The main results of this paper are the following:

One shows that a Stokes wave solution of the ST-DNEE is unstable at small modulation of the amplitude if $\omega_2 > 0$, $\omega(k)$ being the dispersion relation and ω_2 its second derivative. A multiple scales analysis of this model leads to the NLS equation for the dominant amplitude and $\omega_2 > 0$ corresponds to the focusing case when NLS equation admits solitonic solutions. The instability is related to the generation of sidebands around the principal wave and their resonant interaction.

The problem of MI for the NLS equation is discussed also from a statistical point of view, when the amplitude is considered as a random variable. A kinetic equation for the Fourier transform of the two-point correlation function (with respect to the relative coordinate) is deduced. The linear stability analysis gives a stability equation similar to the dispersion relation obtained in the treatment of linearized Vlasov equation in plasma physics. The equation is solved both for a Gaussian and a Lorentzian form of the initial condition $F_0(k)$. Again the instability is present if $\omega_2 > 0$.

The coupled system of the DNEE was discussed when a long-wave-short wave resonance takes place. The multiple scales method leads in this case to the Zakharov-Benney equations, which in 1-D are completely integrable. The MI for ZB equations is discussed from the deterministic point of view.

References

[1] T.B. Benjamin, J.E. Feir, J. Fluid Mechanics, **27**, 417 (1967)

[2] D.J. Benney, Stud. Appl. Math. **56**, 81 (1977)

[3] V.E. Zakharov, Sov.Fiz. JETP **72**, 908 (1972)

Coherent amplification of dual-frequency optical solitons in a doped fiber

I. V. Melnikov [1,4], D. Mihalache [2], N.-C. Panoiu [2,3], F. Ginovart [4], A. Zamudio Lara [1]

[1] Centro de Investigaciones en Ingenieria y Ciencias Aplicadas, Universidad Autonoma del Estado de Morelos, 62210 Cuernavaca, Morelos, Mexico

[2] Department of Theoretical Physics, Institute of Atomic Physics, National Institute of Physics and Nuclear Engineering, P.O. Box MG-6, Bucharest, Romania

[3] Department of Physics, New York University, 4 Washington Place, New York, NY 10003, USA

[4] Laboratoire ENSSAT, B.P. 447, 22305 Lannion Cedex, France

It is found that the temporal behavior of sub-picosecond optical soliton-like pulses propagating through a fiber amplifier exhibits large deviations from the predictions based on standard soliton interaction theories. Both cases of adiabatic and pure coherent amplification of these dual-frequency solitons are studied. We show that it is possible to generate either a dual-frequency bound state or a soliton train. The structure of the emerging optical state depends on the balance between the retarded coherent response introduced by an inverted two-level medium, nonresonant cubic nonlinearity, group-velocity dispersion, and Raman self-scattering.

Published in:

Optics Communications v. 191, pp. 133-140 (2001)

Limits for interchannel frequency separation in a soliton wavelength-division multiplexing system

C. Etrich [1], N.-C. Panoiu [2,3], D. Mihalache [1,3], F. Lederer [1]

[1] Institute of Solid State Theory and Theoretical Optics, Friedrich Schiller University Jena, Max-Wien-Platz 1, Jena, D-07743, Germany

[2] Department of Physics, New York University, 4 Washington Place, New York, NY 10003, USA

[3] Department of Theoretical Physics, Institute of Atomic Physics, National Institute of Physics and Nuclear Engineering, P.O. Box MG-6, Bucharest, Romania

We identify the required interchannel frequency separation of the input field for a soliton wavelength-division multiplexing (WDM) system. It is found that the critical frequency separation above which WDM with solitons is feasible increases with the number of transmission channels. Moreover, it is shown that a combination of time- and wavelength-division multiplexing yields the largest transmission capacity. Finally, the structure of the soliton spectra which correspond to the frequency separation smaller than the critical frequency is discussed.

Published in:

Physical Review E, v. 63, 016609 (2001).

Spinning solitons in cubic-quintic nonlinear media

L.-C. Crasovan[1], B.A. Malomed[2], D. Mihalache[1]

[1] Department of Theoretical Physics, Institute of Atomic Physics, National Institute of Physics and Nuclear Engineering, P.O. Box MG-6, Bucharest, Romania
[2] Faculty of Engineering, Tel Aviv University, Tel Aviv 69978, Israel

We review recent theoretical results concerning the existence, stability and unique features of families of bright vortex solitons (doughnuts, or "spinning" solitons) in both conservative and dissipative cubic-quintic nonlinear media.

Published in:
Pramana Journal of Physics, v. 57, pp. 1041-1059 (2001)

Spinning optical spatiotemporal solitons in quadratic media

D. Mihalache[1]

[1] Department of Theoretical Physics, Institute of Atomic Physics, National Institute of Physics and Nuclear Engineering, P.O. Box MG-6, Bucharest, Romania

The unique features of the families of bright spinning spatiotemporal solitons (doughnuts or vortex light bullets) in dispersive quadratic media, including their stability are presented. Both analytical results, obtained by means of a simple variational approximation, and numerical simulations are presented and compared. It was found that though the variational approximation is not very accurate, it correctly describes the qualitative features of the spinning spatiotemporal solitons. The spinning light bullets are subject to a strong azimuthal instability, which leads to the break-up of the spinning soliton into a set of fragments, each being a *stable* nonspinning spatiotemporal soliton.

Published in:
Acta Physica Polonica A, v. 99, pp. 47-56 (2001).

Stable vortex solitons in the two-dimensional Ginzburg-Landau equation

L.-C. Crasovan[1], B.A. Malomed[2], D. Mihalache[1]

[1] Department of Theoretical Physics, Institute of Atomic Physics, National Institute of Physics and Nuclear Engineering, P.O. Box MG-6, Bucharest, Romania
[2] Department of Interdisciplinary Sciences, Faculty of Engineering, Tel Aviv University, Tel Aviv 69978, Israel

In the framework of the complex cubic-quintic Ginzburg-Landau equation, we perform a systematic analysis of two-dimensional axisymmetric doughnut-shaped localized pulses with the inner phase field in the form of a rotating spiral. We put forward a qualitative argument which suggests that, on the contrary to the known fundamental azimuthal instability of spinning doughnut-shaped solitons in the cubic-quintic NLS equation, their GL counterparts may be stable. This is confirmed by massive direct simulations, and, in a more rigorous way, by calculating the growth rate of the dominant perturbation eigenmode. It is shown that very robust spiral solitons with (at least) the values of the vorticity $S = 0$, 1, and 2 can be easily generated from a large variety of initial pulses having the same values of intrinsic vorticity S. In a large domain of the parameter space, it is found that all the stable solitons coexist, each one being a strong attractor inside its own class of localized two-dimensional pulses distinguished by their vorticity. In a smaller region of the parameter space, stable solitons with $S = 1$ and 2 coexist, while the one with $S = 0$ is absent. Stable

breathers, i.e., both nonspiraling and spiraling solitons demonstrating persistent quasiperiodic internal vibrations, are found too.

Published in:

Physical Review E, v. 63, 016605.

Erupting, flat-top, and composite spiral solitons in the two-dimensional Ginzburg-Landau equation

L.-C. Crasovan[1], B.A. Malomed[2], D. Mihalache[1]

[1] Department of Theoretical Physics, Institute of Atomic Physics, National Institute of Physics and Nuclear Engineering, P.O. Box MG-6, Bucharest, Romania
[2] Department of Interdisciplinary Sciences, Faculty of Engineering, Tel Aviv University, Tel Aviv 69978, Israel

We present three novel varieties of spiraling and nonspiraling axisymmetric solitons in the complex cubic-quintic Ginzburg-Landau equation. These are irregularly "erupting" pulses, and two diferent types of very broad stationary ones, found near a border between ordinary pulses and expanding fronts. The region of existence of each pulse is identified numerically. We test their stability and compare their features with those of their counterparts in the one-dimensional and conservative two-dimensional models.

Published in:
Physics Letters A, v. 289, pp.59-65 (2001).

Stability of spinning ring solitons of the cubic-quintic nonlinear Schrödinger equation

I. Towers[1], A.V. Buryak[1], R.A. Sammut[1], B.A. Malomed[2], L.-C. Crasovan[3], D. Mihalache[3]

[1] School of Mathematics and Statistics, Australian Defense Force Academy, Canberra, ACT 2600, Australia
[2] Department of Interdisciplinary Sciences, Faculty of Engineering, Tel Aviv University, Tel Aviv 69978, Israel
[3] Department of Theoretical Physics, Institute of Atomic Physics, National Institute of Physics and Nuclear Engineering, P.O. Box MG-6, Bucharest, Romania

We investigate stability of (2+1)-dimensional ring solitons (localized vortices) of the nonlinear Schrödinger equation with focusing cubic and defocusing quintic nonlinearities. Computing eigenvalues of the linearised equation, we show that rings with the spin (topological charge) $s = 1$ and $s = 2$ are linearly stable, provided that they are very broad. The stability regions occupy, respectively, 9% and 8% of the corresponding existence regions. These results finally resolve a controversial stability issue for this class of models.

Published in:

Physics Letters A, v. 288, pp. 292-298.

Tandem light bullets

L. Torner[1], S. Carrasco[1], J.P. Torres[1], L.-C. Crasovan[2], D. Mihalache[2]

[1] Laboratory of Photonics, Department of Signal Theory and Communications, Universitat Politecnica de Catalunya, Barcelona ES 08034, Spain
[2] Department of Theoretical Physics, Institute of Atomic Physics, National Institute of Physics and Nuclear Engineering, P.O. Box MG-6, Bucharest, Romania

We put forward a novel strategy to achieve formation of fully three-dimensional light bullets. The new scheme is based on tandem structures where nonlinearity and group-velocity dispersion required for the self-trapping of light are spatially distributed, opening the door for the possibility that they are not necessarily contributed by the same crystal. We show that multicolor light bullets do exist for a wide variety of tandems with feasible domain lengths.

Published in:

Optics Communications, v.199 , pp.277-281 (2001).

Amphiphile-rich phase in a model ternary solution on the honeycomb lattice

Dale A. Huckaby[1], Andrzej Pękalski[2], Daniela Buzatu[3], Florin D. Buzatu[4]

[1] Department of Chemistry, Texas Christian University, Fort Worth, Texas 76129
[2] Institute of Theoretical Physics, University of Wrocław, 50-204 Wrocław, Poland
[3] Physics Department, Politehnica University, Bucharest, 77206, Romania
[4] Department of Theoretical Physics, National Institute for Physics and Nuclear Engineering "Horia Hulubei", Bucharest-Măgurele, 76900, Romania

A model three-component system is considered in which the bonds of a honeycomb lattice are covered by bifunctional molecules of types AA, BB, and AB. The AB type molecule represents an amphiphile. An accurate approximation to the boundary in temperature-composition space of an ordered amphiphile-rich phase is calculated by transforming an accurate closed-form approximation of the critical frontier of an antiferromagnetic phase in an equivalent Ising model. This Ising model has coupling constants and a magnetic field that are temperature dependent.

Published in *Journal of Chemical Physics* 115 no.14 (2001) 6775-6779.

An exactly solvable model ternary solution with strong three-body interactions

Florin D. Buzatu[1], Dale A. Huckaby[2]

[1] Department of Theoretical Physics, National Institute for Physics and Nuclear Engineering "Horia Hulubei", Bucharest-Măgurele, 76900, Romania
[2] Department of Chemistry, Texas Christian University, Fort Worth, TX 76129, USA

We consider a three-component model of rodlike molecules AA, BB, and AB, confined to the bonds of the honeycomb or three-coordinated Bethe lattice, and with three-body interactions between the molecular ends near a common lattice site. The model can be mapped onto the standard Ising model through a star-triangle transformation followed by a double-decoration transformation, and the exact coexistence curves have been previously determined for weak three-body interactions. We investigate the

strong three-body coupling regime using the same procedure, but extended to the more general case when the Ising model on the intermediate lattice may have complex parameters. The exact coexistence curves are drawn for different values of the two independent model parameters, the reduced three-body coupling constant and the reduced temperature. The particular case of a binary solution is also illustrated.

Published in *Physica A* 299 (2001) 427-440.

Spinodal curve of a model ternary solution

Florin D. Buzatu [1,3], Daniela Buzatu [2,3], John G. Albright [3]

[1] Department of Theoretical Physics, National Institute for Physics and Nuclear Engineering "Horia Hulubei", Bucharest-Măgurele, 76900, Romania
[2] Physics Department, Politehnica University, Bucharest, 77206, Romania
[3] Department of Chemistry, Texas Christian University, Fort Worth, TX 76129, USA

We consider a lattice model for ternary solutions in which the lattice bonds are covered by molecules of type AA, BB, and AB, and the only interactions are between the molecular ends of a common lattice site. Using its equivalence with the standard Ising model for magnets, we derive the spinodal curve of the three-component model on the honeycomb lattice in the mean-field and Bethe-lattice approximations. The spinodal and the coexistence curves of the ternary solution are drawn at different values of the reduced temperature, the only parameter of the model. The particular case of a binary solution is also illustrated.

Published in *Journal of Solution Chemistry* 30, no.11, (2001), 969-983.

Dirac operators on Taub-NUT space: relationship and discrete transformations

I. I. Cotăescu [1], M. Vişinescu [2]

[1] West University of Timişoara, 1900-Timişoara, Romania; E-mail: cota@physics.uvt.ro
[2] IFIN-HH, Department of Theoretical Physics; E-mail: mvisin@theor1.theory.nipne.ro

The theory of the usual or hidden symmetries of the Lagrangian quantum field theory on curved space-times, give rise to interesting mathematical problems concerning the properties of the physical observables. It is known that one of the largest algebras of conserved operators is produced by the Euclidean Taub-NUT geometry since beside usual isometries this has a hidden symmetry of the Kepler type [1].

When discussing the geodesic equations in the Taub-NUT metric the existence of extra conserved quantities was noticed. These reflect a symmetry of the phase space of the system and enable the Schrödinger [1, 2] and Dirac equations [3] to be separated in a special coordinate system. This is related to the existence of a Stäckel-Killing tensor of rank 2 in Taub-NUT space.

The theory of the Dirac equation in the Kaluza-Klein monopole field was studied in the mid eighties . We have continued these studies showing that the Dirac equation is analytically solvable [3] and determining the energy eigenspinors of the central modes. Moreover, we derived all the conserved observables of this theory, including those associated with the hidden symmetries of the Taub-NUT geometry. Thus we obtained the Runge-Lenz vector-operator of the Dirac theory, pointing out its specific properties [4]. The consequences of the existence of this operator were studied in [5] showing that the dynamical algebras of the Dirac theory corresponding to different spectral domains are the same as in the scalar case but involving other irreducible representations.

In the Taub-NUT geometry four Killing-Yano tensors are known to exist. Three of these are special because they are covariantly constant and define the complex structures of the manifold. Using these covariantly constant Killing-Yano tensors it is possible to construct new Dirac-type operators [6] which anticommute with the standard Dirac operator. The aim

of this paper is to prove explicitly that these operators and the standard Dirac one are equivalent among themselves.

We show that the representation of the whole theory can be changed using the $U(2)$ transformations among them the $SU(2)$ ones are generated just by the spin-like operators constructed using the above mentioned three Killing-Yano tensors [3].

The Taub-NUT space also possesses a Killing-Yano tensor which is not covariantly constant. The corresponding non-standard operator, constructed with the general rule [6] anticommutes with the standard Dirac operator but is not equivalent to it. This non-standard Dirac operator is connected with the hidden symmetries of the space allowing the construction of a conserved vector operator analogous to the Runge-Lenz vector of the Kepler problem [4]. The final objective here is to discuss the behavior of this operator under discrete transformations pointing out that the hidden symmetries are in some sense decoupled from the discrete symmetries studied here. The explanation of this distinction is that the standard $N = 4$ supersymmetry are linked to the hyper-Kähler structure of the Taub-NUT space [7]. The corresponding supercharges close on the Hamiltonian of the theory. The quantal anticommutator of the Dirac-type operators closes on the square of the Hamiltonian operator. On the other hand, the non-standard supercharge involving the non-covariant constant Killing-Yano tensor does not close on the Hamiltonian. The appearance of the non-covariant constant Killing-Yano tensor in this context is not surprising since it also plays an essential role in the existence of hidden symmetries. Its existence requires the Weyl tensor to be of Petrov type D. The quantal anticommutator of the non-standard Dirac operator does not close on the square of the Hamiltonian, as would Dirac-type operators, rather on a combination of different conserved operators of the theory.

References

[1] G. W. Gibbons and N. S. Manton, *Nucl. Phys.* **B274** (1986) 183.

[2] I. I. Cotăescu and M. Visinescu, `hep-th/9911014`; *Mod. Phys. Lett. A***15** (2000) 145.

[3] I. I. Cotăescu and M. Visinescu, `hep-th/0008181`; *Int. J. Mod. Phys. A* **16** (2001) 1743.

[4] I. I. Cotăescu and M. Visinescu, `hep-th/0101163`; *Phys. Lett.* **B502** (2001) 229.

[5] I. I. Cotăescu and M. Visinescu, `hep-th/0102083`; *Class. Quantum Grav.* **18** (2001) 3383.

[6] B. Carter and R. G. McLenaghan, *Phys. Rev.* **D19** (1979) 1093.

[7] I. I. Cotăescu and M. Visinescu, `hep-th/0107205`; *J. Math. Phys.* **43** (2002) 2978.

Some applications of Riemannian submersions in physics

Maria Laura Falcitelli [1], S. Ianuş [2], Ana Maria Pastore [3], M. Vişinescu [4]

[1] Dipartimento di Matematica, Universitádi Bari, Bari 70125, Italy; E-mail: falci@dm.uniba.it
[2] Department of Mathematics, Univ. Bucharest, Bucharest, Romania; E-mail: ianus@gta.math.inibuc.ro
[3] Dipartimento di Matematica, Universitádi Bari, Bari 70125, Italy; E-mail: pastore@dm.uniba.it
[4] IFIN-HH, Department of Theoretical Physics; E-mail: mvisin@theor1.theory.nipne.ro

Many results on the Riemannian submersions are relevant in various areas of mathematical physics as Kaluza-Klein theories, Yang-Mills equations, strings, supergravity. Interest in higher dimensional theories has been ignited once again in recent years due largely to the discovery that the underlying symmetry of the fundamental interactions is geometrical, local and gauged.

A current trend in modern physics is the search for a theory which provides a unification of gravity with the other fundamental forces of nature. One of the early possibilities for such a unification was suggested by Kaluza [1] and later expanded upon by Klein [2]. It was shown within a five dimensional extension of Einstein's theory of general relativity how both gravity and electromagnetism could be treated on a similar footing. Both interactions were described as part of the five dimensional metric. The fifth coordinate was made invisible through a "cylindrical condition": it was assumed that in the fifth direction, the world curled up into a cylinder of very small radius (10^{-33} cm, Planck's length).

A natural generalization of the original Kaluza-Klein idea which incorporates non-Abelian gauge fields is to consider a higher than five dimensional theory in which the gauge fields become part of the metric in the same way as the electromagnetic field did in Kaluza's theory.

We describe a compactification scheme for the Kaluza-Klein theory triggered by a scalar sector in the form of a non-linear sigma model [3, 4, 5].

The final part of the paper is devoted to the Kaluza-Klein monopole in connection with the Hopf maps [6]. In physics, the Hopf maps represent systems with nontrivial topological properties, e.g. the Z_2 kink or sine-Gordon soliton, $U(1)$ magnetic monopole or vortex in a superconducting sheet, $SU(2)$ instanton, etc. Other physical realizations of the Hopf maps are possible.

After a brief presentation of the formalism of the magnetic charges, the Dirac monopole is described in terms of Hopf maps. Finally the Kaluza-Klein monopole is constructed by embedding the Taub-NUT gravitational instanton into five-dimensional Kaluza-Klein theory. Let us note also that the same object has re-emerged in the study of monopole scattering. In the long-distance limit, neglecting radiation, the relative motion of two monopoles is described by the geodesics of the Taub-NUT space [7].

References

[1] T. Kaluza, *Zum Unitätsproblem der Physik.* Sitzber. Preuss. Akad. Wiss. Kl. **2** (1921), 966-970.

[2] O. Klein, *Quantentheorie und fünf-dimensionale Relativitätstheorie.* Z. Phys. **37** (1929), 895-901.

[3] S. Ianus and M. Visinescu, *Spontaneous compactification induced by non-linear scalar dynamics, gauge fields and submersions.* Class. Quantum Gravity **3** (1986), 889-896.

[4] S. Ianus and M. Visinescu, *Kaluza-Klein theory with scalar fields and generalised Hopf manifolds.* Class. Quantum Gravity **4** (1987), 1317-1325.

[5] S. Ianus and M. Visinescu, *Space-time compactification and Riemannian submersions.* in *The Mathematical Heritage of C. F. Gauss* Ed. G. M. Rassias, World Scientific Publ. Co. Singapore (1990), 358-371.

[6] S. Ianus, A. M. Pastore and M. Visinescu, *Recent results relevant to mathematical physics.* Theor., Math. and Comp. Phys. (1998), 1-14.

[7] M. F. Atiyah and N. J. Hitchin, *The Geometry and Dynamics of Magnetic Monopoles*, Princeton University Press, Princeton (1988).

Spinning particles on curved spaces

M. Vişinescu [1]

[1] IFIN-HH, Department of Theoretical Physics; E-mail: mvisin@theor1.theory.nipne.ro

The aim of this paper is to investigate the quantum objects, namely spin one half particles, in curved spaces. Having in mind the lack of a satisfactory quantum theory for gravitational interaction, this study is justified and not at all trivial.

We review the geodesic motion of pseudo-classical spinning particles in curved spaces. Investigating the generalized Killing equations for spinning spaces, we express the constants of motion in terms of Killing-Yano tensors. Passing from the spinning spaces to the Dirac equation in curved backgrounds we point out the role of the Killing-Yano tensors in the construction of the Dirac-type operators. The general results are applied to the case of the four-dimensional Euclidean Taub-Newman-Unti-Tamburino space. From the covariantly constant Killing-Yano tensors of this space we construct three new Dirac-type operators which are equivalent with the standard Dirac operator. Finally the Runge-Lenz operator for the Dirac equation in this background is expressed in terms of the forth Killing-Yano tensor which is not covariantly constant.

The models of relativistic particles with spin have been proposed for a long time starting with the paper by Frenkel which appeared in 1926 [1]. After that the literature on the particle with spin grew vast. The models involving only conventional coordinates are called classical models while the models involving anticommuting coordinates are generally called pseudo-classical.

In the beginning of this paper we discuss the relativistic spin one half particle models involving anticommuting vectorial degrees of freedom which are

usually called the spinning particles. Spinning particles are in some sense the classical limit of the Dirac particles. The action of spin one half relativistic particle with spinning degrees of freedom described by Grassmannian (odd) variables was first proposed by Berezin and Marinov [2].

The generalized Killing equations for the configuration space of spinning particles (spinning space) are analyzed and the solutions are expressed in terms of Killing-Yano tensors [3, 4, 5, 6]. We mention that the existence of a Killing-Yano tensor is both a necessary and a sufficient condition for the existence of a new supersymmetry for the spinning space [7, 8].

Passing from the pseudo-classical approach to the Dirac equation in curved spaces, we point out the role of the Killing-Yano tensors in the construction of new Dirac-type operators. The Dirac-type operators constructed with the aid of covariantly constant Killing-Yano tensors are equivalent with the standard Dirac operator. The non-covariantly constant Killing-Yano tensors generates non-standard Dirac operators which are not equivalent to the standard Dirac operator and they are associated with the hidden symmetries of the space [9, 10, 11, 12, 13].

References

[1] J.Frenkel, *Z.für Physik* **37**, 243 (1926).

[2] F. A. Berezin and M. S. Marinov, *Ann. Phys.* **104**, 336 (1977).

[3] M. Visinescu, *Phys. Lett.* **B339**, 28 (1994).

[4] D. Vaman and M. Visinescu, *Phys. Rev.* **D54**, 1398 (1996).

[5] D. Vaman and M. Visinescu, *Phys. Rev.* **D57**, 3790 (1998).

[6] D. Vaman and M. Visinescu, *Fortschr. Phys.* **47**, 493 (1999).

[7] G. W. Gibbons, R. H. Rietdijk and J. W. van Holten, *Nucl. Phys.* **B404**, 42 (1993).

[8] M. Visinescu, *Fortschr. Phys.* **B48**, 229 (2000).

[9] I. I. Cotăescu and M. Visinescu, *Phys. Lett.* **B502**, 229 (2001).

[10] I. I. Cotăescu and M. Visinescu, *J.Math.Phys* **43**, 2978 (2002).

[11] M. Visinescu, *J. Phys. A: Math. Gen.* **33**, 4383 (2000).

[12] I. I. Cotăescu and M. Visinescu, *J. Phys. A: Math. Gen.* **34**, 6459 (2001).

[13] M. Visinescu, *Int. J. Mod. Phys.* **A17**, 1049 (2002).

Statistical approach of the modulational instability of a discrete self-trapping equation

Anca Vişinescu[1], D. Grecu[1]

[1] IFIN-HH, Department of Theoretical Physics; E-mail: dgrecu@theor1.theory.nipne.ro

Abstract

The discrete self-trapping equation (DST) represents an useful model for several properties of one-dimensional nonlinear molecular crystals. The modulational instability of DST equation is discussed from a statistical point of view, considering the oscillator amplitude as a random variable. A kinetic equation for the two-point correlation function is written down, and its linear stability is studied. Both a Gaussian and a Lorentzian form for the initial unperturbed wave spectrum are discussed. Comparison with the continuum limit (NLS equation) is done.

The discrete self-trapping (DST) equation

$$i\frac{da_n}{dt} - \omega_0 a_n + \lambda(a_{n+1} + a_{n-1}) + \mu|a_n|^2 a_n = 0 \quad (1)$$

is a typical equation for a system of harmonically coupled nonlinear oscillations [1], [2] relevant for several physical problems. We mention here only Davydov's model of energy transport in α-helix structures in proteins [2], where (1) appears as a certain approximation of the model. In (1) a_n is the complex classical dimensionless amplitude of the oscillator of frequency

ω_0 in the n-th molecule, and λ, μ (of dimension of frequency) are the coupling constants between nearest neighbour oscillators and the one-site nonlinearity respectively. It is well known that depending upon of the parameters and the chosen initial condition the equation (1) can lead either to self-trapping (i.e. local modes or solitons), or to chaos, or to a mixture of the above two behaviours [1], [2]. Instead of (1) we shall consider the equation

$$i\frac{da_n}{dt} + \lambda(a_{n+1} + a_{n-1}) + \mu|a_n|^2 a_n = 0 \qquad (2)$$

which is obtained if $a_n \to a_n e^{-i\omega_0 t}$. This equation admits plane wave solutions with constant amplitude

$$a_n = ae^{i(kn-\omega t)}$$

(the lattice constant is taken equal with unity) but with an amplitude depending dispersion relation

$$\omega(k) = -2\lambda\cos k - \mu|a|^2$$

This is a Stokes wave solution and it is well known to be unstable at small modulation of the amplitude (Benjamin-Feir or modulational instability) [4]. The aim of this note is to study the modulational instability of equation (2) from a statistical point of view, considering a_n as a random variable. In doing this we shall follow the procedure used by several authors to discuss the effects of randomness on the stability of weakly nonlinear waves, especially in hydrodynamics [5].

In the next section a kinetic equation for a two-point correlation function will be obtained. Using a Wigner-Moyal transform the equation is written in a mixed configuration-wave vector space. The linear stability around a homogeneous basic solution is discussed in section 3. An integral stability equation is derived, very similar with the dispersion relation of the linearized Vlasov equation in ionized plasmas. Two forms for the spectrum of the initial unperturbed condition will be considered, namely a Gaussian and a Lorentzian form and in the limit of vanishingly small bands widths the increment of the modulational instability is calculated. Comparison with the continuum limit, when (1) transforms into the nonlinear Schrödinger equation is done. Few concluding remarks are also presented.

References

[1] J.C. Eilbeck, P.S. Lomdahl, A.C. Scott, Physica D **16**, 318 (1985)

[2] *Davydov's Soliton Revisited. Self Trapping of Vibrational Energy in Proteins*, edited by P.L. Christiansen, A.C. Scott, NATO ASI Series B **243** (Plenum Press, New York, 1990)

[3] L. Cruzeiro-Hansson, H. Feddersen, R. Flesch, P.L. Christiansen, M. Salerno, A.C. Scott, Phys. Rev. B **42**, 522 (1990)

[4] D. Grecu, Anca Vişinescu, "Modulational instability in some nonlinear one-dimensional lattices and soliton generation" *Ann.Univ. Craiova* **12**, 129-149 (2002)

[5] M. Onorato, A. Osborne, M. Serio, R. Fedele, nlin.CD/0202026.

Influence of third order dispersion on the bound state of two solitons of the NLS equation

D. Grecu[1], Anca Vişinescu[1]

[1] IFIN-HH, Department of Theoretical Physics; E-mail: dgrecu@theor1.theory.nipne.ro

Using Karpman-Soloviev perturbation procedure the influence of the third order dispersion on the bound state of two solitons of the NLS equation is investigated. The problem has two small parameters (supposed to be of the same order): the small overlap of the two well separated solitons, and the amplitude of the third order dispersion. If the velocities of the two solitons are the same, a bound state is formed, with an oscillating expression for the distance between solitons. When the third order dispersion is introduced a slow monotonous increasing function of time is superposed over this oscillatory behaviour.

References

[1] A. Hasegawa, Y. Kodama, "Solitons in Optical Communicationa" (Oxford Univ. Press, Oxford 1995)

[2] V.I. Karpman, V.V. Solov'ev, Physica D **3**, 487 (1981)

[3] J.M. Arnold, J. Opt. Soc. **21**, 31 (1996)

[4] V.S. Gerdjikov, E.G. Evstatiev, D.J. Kaup, G.L. Diankov, I.M. Uzunov, Phys. Lett. **241**, 323 (1998)

[5] V.S. Shechesovich, Phys. Rev. E **65**, 46614 (2002)

Multiwavelength pulse transmission in an optical fibre-amplifier system

N.-C. Panoiu [1], I. V. Melnikov [2], D. Mihalache [3], C. Etrich [4], F. Lederer [4]

[1] Department of Applied Physics and Applied Mathematics, Columbia University, New York, New York 10027
[2] A. M. Prokhorov General Physics Institute of the Russian Academy of Sciences, ul. Vavilova 38, Moscow 117942, Russian Federation
[3] Department of Theoretical Physics, Institute of Atomic Physics, P.O. Box MG-6, Bucharest, Romania
[4] Institute of Solid State Theory and Theoretical Optics, Friedrich Schiller University Jena, Max-Wien-Platz 1, Jena, D-07743, Germany

The structure and dynamics of solitary waves created by interaction of multiwavelength pulses in a monomode optical fiber with amplification, filtering, and amplitude modulation is analyzed.

It is shown that there is a critical wavelength separation between channels above which wavelength–division multiplexing with solitons is feasible and that this separation increases with the number of channels.

Published in: *Quantum Electronics, v. 32, pp. 1009-1016 (2002)*

Soliton generation from a multi-frequency optical signal

N.-C. Panoiu [1], I. V. Melnikov [2], D. Mihalache [3], C. Etrich [4], F. Lederer [4]

[1] Department of Applied Physics and Applied Mathematics, Columbia University, New York, New York 10027
[2] A. M. Prokhorov General Physics Institute of the Russian Academy of Sciences, ul. Vavilova 38, Moscow 117942, Russian Federation
[3] Department of Theoretical Physics, Institute of Atomic Physics, P.O. Box MG-6, Bucharest, Romania
[4] Institute of Solid State Theory and Theoretical Optics, Friedrich Schiller University Jena, Max-Wien-Platz 1, Jena, D-07743, Germany

We present a comprehensive analysis of the generation of optical solitons in a monomode optical fiber from a superposition of solitonlike optical pulses at different frequencies. It is demonstrated that the structure of the emerging optical field is highly dependent on the number of input channels, the inter-channel frequency separation, the time shift between the pulses belonging to adjacent channels, and the polarization of the pulses. Also, it is found that there exists a critical frequency separation above which wavelength-division multiplexing with solitons is feasible and that this critical frequency increases with the number of transmission channels. Moreover, for the case in which only two channels are considered, we analyze the propagation of the emerging two-soliton solutions in the presence of several perturbations important for optical networks: bandwidth-limited amplification, nonlinear amplification, and amplitude and phase modulation. Finally, the influence of the birefringence of the fiber on the structure of the emerging optical field is discussed.

Published in: *Journal of Optics B: Quantum and Semiclassical Optics, v. 4, pp. R53-R68 (2002)*

Globally-linked vortex clusters in trapped wave fields

L.-C. Crasovan[1], G. Molina-Terriza[2], J.P. Torres[2], L. Torner[2], V.M. Perez-Garcia[3], D. Mihalache[1]

[1] Department of Theoretical Physics, Institute of Atomic Physics, National Institute of Physics and Nuclear Engineering, P.O. Box MG-6, Bucharest, Romania

[2] Laboratory of Photonics, Universitat Politecnica de Catalunya, Gran Capitan UPC-D3, 08034 Barcelona, Spain.

[3] Departamento de Matemáticas, E.T.S.I. Industriales, Universidad de Castilla-La Mancha, 13071 Ciudad Real, Spain

We introduce the existence of stationary vortex entities nested in paraxial wave fields confined by trapping potentials, and discover that: (i) A rich variety of fully stationary vortex structures, termed H-clusters, made of an increasing number of vortices can be built. (ii) The constituent vortices are globally linked, rather than products of independent vortices. (iii) These stationary clusters can exhibit, in the simplest cases, matrix or array geometries, and they feature a monopolar global wave front. (iv) Clusters with multipolar global wave fronts tend to be non-stationary, when the number of vortices and their location is not constant, or flipping, when the vortices periodically flip their topological charges through extremely sharp Berry trajectories.

Published in: *Physical Review E , v. 66, 036612 (2002)*

Stability of vortex solitons in the cubic-quintic model

B.A. Malomed[1], L.-C. Crasovan[2], D. Mihalache[2]

[1] Department of Interdisciplinary Studies, Faculty of Engineering, Tel Aviv University, Tel Aviv 69978, Israel

[2] Department of Theoretical Physics, Institute of Atomic Physics, National Institute of Physics and Nuclear Engineering, P.O. Box MG-6, Bucharest, Romania

We investigate one-parameter families of two-dimensional bright spinning solitons (ring vortices) in dispersive media combining cubic self-focusing and quintic self-defocusing nonlienarities. In direct simulations, the spinning solitons display a symmetry-breaking azimuthal instability, which leads to breakup of a soliton into a set of fragments, each being a stable nonspinning soliton. The fragments fly out tangentially to the circular crest of the original vortex ring. If the soliton's energy is large enough, the instability develops so slowly that the spinning solitons may be regarded as virtually stable ones, in accord with earlier published results. Growth rates of perturbation eigenmodes with different azimuthal "quantum numbers" are calculated as a function of the soliton's propagation constant κ from a numerical solution of the linearized equations. As a result, a narrow (in terms of κ) *stability window* is found for extremely broad solitons with values of the "spin" $s = 1$ and $s = 2$. However, analytical consideration of a special perturbation mode in the form of a spontaneous shift of the soliton's central "bubble" (core of the vortex embedded in a broad soliton) demonstrates that even extremely broad solitons are subject to an exponentially weak instability against this mode. In actual simulations, a manifestation of this instability is found in a three-dimensional soliton with $s = 1$. In the case when the two-dimensional spinning solitons are subject to tangible azimuthal instability, the number of the nonspinning fragments into which the soliton splits is usually, but not always, equal to the azimuthal number of the instability eigenmode with the largest growth rate.

Published in: *Physica D, v. 161, 187-201 (2002).*

Stable two-dimensional spinning solitons in a bimodal cubic-quintic model with four-wave mixing

D. Mihalache[1], D. Mazilu[1], I. Towers[2], B. A. Malomed[2], F. Lederer[3]

[1] Department of Theoretical Physics, Institute of Atomic Physics, National Institute of Physics and Nuclear Engineering, P.O. Box MG-6, Bucharest, Romania

[2] Department of Interdisciplinary Sciences, Faculty of Engineering, Tel Aviv University, Tel Aviv 69978, Israel

[3] Institute of Solid State Theory and Theoretical Optics, Friedrich-Schiller Universität Jena, Max-Wien-Platz 1, D-07743, Jena, Germany

We show the formation of stable two-dimensional spinning solitons in a bimodal system described by coupled cubic-quintic nonlinear Schrödinger equations. The cubic part of the model includes the self-phase modulation, cross-phase modulation, and four-wave mixing. Thresholds for the formation of both spinning and non-spinning solitons are found. Instability growth rates of perturbation eigenmodes with different azimuthal indices are calculated as functions of the solitons' propagation constant. As a result, existence and stability domains are identified for the solitons with vorticity $s = 0$, 1, and 2 in the model's parameter plane. The vortex solitons are found to be stable if their energy flux exceeds a certain critical value, so that, in typical cases, the stability domain of the $s = 1$ solitons occupies about 18% of their existence region, whereas that of the $s = 2$ solitons occupies 10% of the corresponding existence region. Direct simulations of the full nonlinear system are in perfect agreement with the linear stability analysis: stable solitons easily self-trap from arbitrary initial pulses with embedded vorticity, while unstable vortex solitons split into a set of separating zero-spin fragments whose number is exactly equal to the azimuthal index of the strongest unstable perturbation eigenmode.

Published in: *Journal of Optics A: Pure and Applied Optics, v. 4, pp. 615-623 (2002).*

Robust propagation of two-color soliton clusters supported by competing nonlinearities

Y.V. Kartashov[1,2], L.-C. Crasovan[1,3], D. Mihalache[1,3], L. Torner[1]

[1] Institute of Photonic Sciences and Department of Signal Theory and Communications, Universitat Politecnica de Catalunya, 08034, Barcelona, Spain

[2] Physics Department, M.V. Lomonosov Moscow State University, 119899, Moscow, Russia

[3] Department of Theoretical Physics, Institute of Atomic Physics, National Institute of Physics and Nuclear Engineering, P.O. Box MG-6, Bucharest, Romania

We reveal numerically the remarkably robust propagation of quasistationary two-color soliton clusters in media with competing quadratic and cubic nonlinearities. We predict that such clusters carrying nonzero angular momentum can propagatate over any practically feasible crystal length before they can decay, even in the presence of input random perturbations.

Published in: *Physical Review Letters, v. 89, 273902 (2002).*

Stable spinning solitons in three dimensions

D. Mihalache [1,2,5], D. Mazilu [1,2], L.-C. Crasovan [1,5], I. Towers [3,4], A.V. Buryak [3], B.A. Malomed [4], L. Torner [5], J.P. Torres [5], F. Lederer [2]

[1] Department of Theoretical Physics, Institute of Atomic Physics, National Institute of Physics and Nuclear Engineering, P.O. Box MG-6, Bucharest, Romania
[2] Institute of Solid State Theory and Theoretical Optics, Friedrich-Schiller Universität Jena, Max-Wien-Platz 1, D-07743, Jena, Germany
[3] School of Mathematics and Statistics, Australian Defense Force Academy, Canberra, ACT 2600, Australia
[4] Department of Interdisciplinary Sciences, Faculty of Engineering, Tel Aviv University, Tel Aviv 69978, Israel
[5] Institute of Photonic Sciences and Department of Signal Theory and Communications, Universitat Politeccnica de Catalunya, 08034, Barcelona, Spain

We introduce spatiotemporal spinning solitons (vortex tori) of the three-dimensional nonlinear Schrödinger equation with focusing cubic and defocusing quintic nonlinearities. The first ever found completely stable spatiotemporal vortex solitons are demonstrated. A general conclusion is that stable spinning solitons are possible as a result of competition between focusing and defocusing nonlinearities.

Published in: *Physical Review Letters, v. 88, 073902 (2002).*

Stable three-dimensional spinning optical solitons supported by competing quadratic and cubic nonlinearities

D. Mihalache [1,2,5], D. Mazilu [1,2], L.-C. Crasovan [1,5], I. Towers [3], B.A. Malomed [3], A. V. Buryak [4], L. Torner [5], F. Lederer [2]

[1] Department of Theoretical Physics, Institute of Atomic Physics, National Institute of Physics and Nuclear Engineering, P.O. Box MG-6, Bucharest, Romania
[2] Institute of Solid State Theory and Theoretical Optics, Friedrich-Schiller Universität Jena, Max-Wien-Platz 1, D-07743, Jena, Germany
[3] Department of Interdisciplinary Sciences, Faculty of Engineering, Tel Aviv University, Tel Aviv 69978, Israel
[4] School of Mathematics and Statistics, Australian Defense Force Academy, Canberra, ACT 2600, Australia
[5] Institute of Photonic Sciences and Department of Signal Theory and Communications, Universitat Politeccnica de Catalunya, 08034, Barcelona, Spain

We show that the quadratic interaction of fundamental and second harmonics in a bulk dispersive medium, combined with self-defocusing cubic nonlinearity, gives rise to stable completely localized spatiotemporal solitons (vortex tori) with intrinsic vorticity $s = 1$. The soliton is stable if its energy exceeds a certain critical value, so that the stability domain occupies about 10 % of the existence region of the solitons. On the contrary to spatial vortex solitons in the same model, the spatiotemporal ones with $s = 2$ are never stable. These results might open the way for experimental observation of spinning three-dimensional solitons in optical media.

Published in: *Physical Review E, v. 66, 016613 (2002).*

Method for generating solitons sustained by competing nonlinearities by use of optical rectification

J.P. Torres[1], S.L. Palacios[1], L. Torner[1], L.-C. Crasovan[2], D. Mihalache[2], I. Biaggio[3]

[1] Laboratory of Photonics, Department of Signal Theory and Communications, Universitat Politecnica de Catalunya, Barcelona ES 08034, Spain

[2] Department of Theoretical Physics, Institute of Atomic Physics, National Institute of Physics and Nuclear Engineering, P.O. Box MG-6, Bucharest, Romania

[3] Institute of Quantum Electronics, Swiss Federal Institute of Technology, ETH H "onggerberg, CH-8093, Z "urich, Switzerland

We put forward a method to generate engineerable competing quadratic and cubic nonlinearities in suitable settings where frequency generation is accompanied by optical rectification. The novel scheme is based on the full exploitation of the geometrical conditions that determine the magnitude of the rectified fields, and translates the different orientations of an elliptical pump beam into tunable nonlinearities which can be used to act on the spectral composition and overall features of optical solitons.

Published in: *Optics Letters, v. 27, pp. 1631-1633 (2002).*

Multichannel soliton transmission and pulse shepherding in bit-parallel-wavelength optical fiber links

E.A. Ostrovskaya[1], Y.S. Kivshar[1], D. Mihalache[2], L.-C. Crasovan[2]

[1] Nonlinear Physics Group, Research School of Physical Sciences and Enginnering, the Australian National University, Canberra, Australia

[2] Department of Theoretical Physics, Institute of Atomic Physics, National Institute of Physics and Nuclear Engineering, P.O. Box MG-6, Bucharest, Romania

We study basic principles of the bit-parallel-wavelength (BPW) pulse transmission in multichannel single-mode optical fiber links for high-performance computer networks. We develop a theory of the pulse shepherding effect that allows simultaneous propagation of pulses in patrallel bit slots by binding them into a multicomponent BPW soliton. We describe families of the BPW solitons and bifurcation cascades in a system on N incoherently coupled nonlinear Schrödinger equations that model the multichannel multiwavelength transmission in a single-mode optical fiber. We demonstrate high robustness of the composite BPW solitons, due to their underlying linear stability, to a moderate pulse walkoff.

Published in: *IEEE Journal of Selected Topics in Quantum Electronics, v. 8, pp. 591-596 (2002).*

Properties of 3-dimensional cosexponential functions

Silviu Olariu[1]

[1] NIPNE-HH, Department of Nuclear Physics

The functions cx, mx, px, which will be called 3-dimensional cosexponential functions, are defined by the series

$$\mathrm{cx}\, y = 1 + y^3/3! + y^6/6! + \cdots \tag{1}$$

$$\mathrm{mx}\, y = y + y^4/4! + y^7/7! + \cdots \tag{2}$$

$$\mathrm{px}\, y = y^2/2! + y^5/5! + y^8/8! + \cdots. \tag{3}$$

From the series definitions it can be seen that $\mathrm{cx}\, 0 = 1$, $\mathrm{mx}\, 0 = 0$, $\mathrm{px}\, 0 = 0$. The tridimensional polar co-

sexponential functions belong to the class of the polar n-dimensional cosexponential functions g_{nk}, and $\mathrm{cx} = g_{30}$, $\mathrm{mx} = g_{31}$, $\mathrm{px} = g_{32}$. [1], [2]

It can be checked that

$$\mathrm{cx}\, y + \mathrm{px}\, y + \mathrm{mx}\, y = \exp y. \tag{4}$$

The following addition theorems can be obtained

$$\mathrm{cx}\,(y+z) = \mathrm{cx}\, y\ \mathrm{cx}\, z + \mathrm{mx}\, y\ \mathrm{px}\, z + \mathrm{px}\, y\ \mathrm{mx}\, z, \tag{5}$$

$$\mathrm{mx}\,(y+z) = \mathrm{px}\, y\ \mathrm{px}\, z + \mathrm{cx}\, y\ \mathrm{mx}\, z + \mathrm{mx}\, y\ \mathrm{cx}\, z, \tag{6}$$

$$\mathrm{px}\,(y+z) = \mathrm{mx}\, y\ \mathrm{mx}\, z + \mathrm{cx}\, y\ \mathrm{px}\, z + \mathrm{px}\, y\ \mathrm{cx}\, z. \tag{7}$$

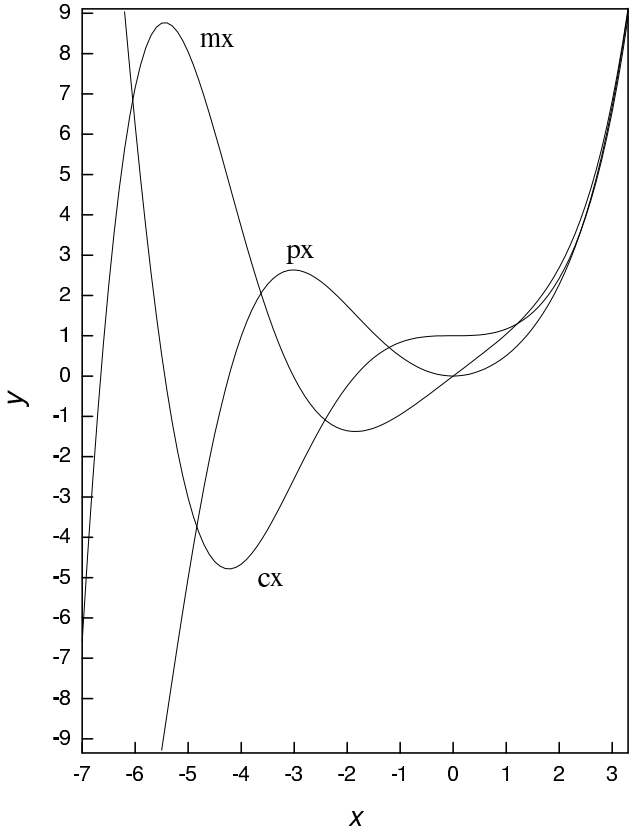

Figure 1: Graphs of 3-dimensional cosexponential functions.

The following identities can be obtained,

$$\mathrm{cx}^2\, y + \mathrm{mx}^2\, y + \mathrm{px}^2\, y = \frac{2}{3}e^{-y} + \frac{1}{3}e^{2y}, \tag{8}$$

$$\mathrm{cx}\, y\ \mathrm{mx}\, y + \mathrm{cx}\, y\ \mathrm{px}\, y + \mathrm{mx}\, y\ \mathrm{px}\, y = -\frac{1}{3}e^{-y} + \frac{1}{3}e^{2y}. \tag{9}$$

From Eqs. (8) and (9) it results that

$$\mathrm{cx}^2\, y + \mathrm{mx}^2\, y + \mathrm{px}^2\, y - \mathrm{cx}\, y\ \mathrm{mx}\, y - \mathrm{cx}\, y\ \mathrm{px}\, y - \mathrm{mx}\, y\ \mathrm{px}\, y = \exp(-y). \tag{10}$$

It can be shown that the 3-dimensional cosexponential functions cx, mx, px fulfil the interesting identity

$$\mathrm{cx}^3\, y + \mathrm{mx}^3\, y + \mathrm{px}^3\, y - 3\,\mathrm{cx}\, y\ \mathrm{mx}\, y\ \mathrm{px}\, y = 1. \tag{11}$$

Expressions of the 3-dimensional cosexponential functions cx, mx, px, in terms of the regular exponential and cosine functions can be obtained as

$$\mathrm{cx}\, y = \frac{1}{3}\, e^{y} + \frac{2}{3}\cos\left(\frac{\sqrt{3}}{2}y\right)\, e^{-y/2}, \tag{12}$$

$$\mathrm{mx}\, y = \frac{1}{3}\, e^{y} + \frac{2}{3}\cos\left(\frac{\sqrt{3}}{2}y - \frac{2\pi}{3}\right)\, e^{-y/2}, \tag{13}$$

$$\mathrm{px}\, y = \frac{1}{3}\, e^{y} + \frac{2}{3}\cos\left(\frac{\sqrt{3}}{2}y + \frac{2\pi}{3}\right)\, e^{-y/2}. \tag{14}$$

It is remarkable that the series in Eqs. (1)-(3), in which the terms are either of the form y^{3m}, or y^{3m+1}, or y^{3m+2}, can be expressed in terms of elementary functions whose power series are not subject to such restrictions. The cosexponential functions differ by the phase of the cosine function in their expression, and the designation of the functions in Eqs. (13), (14) as mx and px refers respectively to the minus or plus sign of the phase term $2\pi/3$. The graphs of the functions cx, mx, px are shown in Fig. 1.

References

[1] S. Olariu, Int. J. Math. and Math. Sciences **25**, 429-450 (2001).

[2] S. Olariu, Complex Numbers in n Dimensions, Elsevier, 2002.

Commutative hypercomplex numbers in n dimensions

Silviu Olariu [1]

[1] NIPNE-HH, Department of Nuclear Physics

Two distinct systems of hypercomplex numbers in n dimensions have been studied, for which the multiplication is associative and commutative, and which are rich enough in properties such that exponential and trigonometric forms exist and the concepts of analytic n-complex function, contour integration and residue can be defined. [1], [2] The n-complex numbers described in this work have the form $u = x_0 + h_1 x_1 + \cdots + h_{n-1} x_{n-1}$, where $h_1, ..., h_{n-1}$ are the hypercomplex bases and the variables $x_0, ..., x_{n-1}$ are real numbers, unless otherwise stated. If the n-complex number u is represented by the point A of coordinates $x_0, x_1, ..., x_{n-1}$, the position of the point A can be described with the aid of the modulus $d = (x_0^2 + x_1^2 + \cdots + x_{n-1}^2)^{1/2}$ and of $n-1$ angular variables.

The first type of hypercomplex numbers is characterized by the presence, in an even number of dimensions $n \geq 4$, of two polar axes, and by the presence, in an odd number of dimensions, of one polar axis. Therefore, these numbers will be called polar hypercomplex numbers in n dimensions. One polar axis is the normal through the origin O to the hyperplane $v_+ = 0$, where $v_+ = x_0 + x_1 + \cdots + x_{n-1}$. In an even number n of dimensions, the second polar axis is the normal through the origin O to the hyperplane $v_- = 0$, where $v_- = x_0 - x_1 + \cdots + x_{n-2} - x_{n-1}$. Thus, in addition to the distance d, the position of the point A can be specified, in an even number of dimensions, by 2 polar angles θ_+, θ_-, by $n/2-2$ planar angles ψ_k, and by $n/2-1$ azimuthal angles ϕ_k. In an odd number of dimensions, the position of the point A is specified by d, by 1 polar angle θ_+, by $(n-3)/2$ planar angles ψ_{k-1}, and by $(n-1)/2$ azimuthal angles ϕ_k. The multiplication rules for the polar hypercomplex bases $h_1, ..., h_{n-1}$ are $h_j h_k = h_{j+k}$ if $0 \leq j+k \leq n-1$, and $h_j h_k = h_{j+k-n}$ if $n \leq j+k \leq 2n-2$, where $h_0 = 1$.

The other type of hypercomplex numbers exists as a distinct entity only when the number of dimensions n of the space is even. The position of the point A is specified, in addition to the distance d, by $n/2-1$ planar angles ψ_k and by $n/2$ azimuthal angles ϕ_k. These numbers will be called planar hypercomplex numbers. The multiplication rules for the planar hypercomplex bases $h_1, ..., h_{n-1}$ are $h_j h_k = h_{j+k}$ if $0 \leq j+k \leq n-1$, and $h_j h_k = -h_{j+k-n}$ if $n \leq j+k \leq 2n-2$, where $h_0 = 1$. For $n = 2$, the planar hypercomplex numbers become the usual 2-dimensional complex numbers $x + iy$.

The development of analytic functions of hypercomplex variables was rendered possible by the existence of an exponential form of the n-complex numbers. The azimuthal angles ϕ_k, which are cyclic variables, appear in these forms at the exponent, and lead to the concept of n-dimensional hypercomplex residue. Expressions are given for the elementary functions of n-complex variable. In particular, the exponential function of an n-complex number is expanded in terms of functions called in this work n-dimensional cosexponential functions of the polar and respectively planar type. The polar cosexponential functions are a generalization to n dimensions of the hyperbolic functions $\cosh y, \sinh y$, and the planar cosexponential functions are a generalization to n dimensions of the trigonometric functions $\cos y, \sin y$. Addition theorems and other relations are obtained for the n-dimensional cosexponential functions.

Many of the properties of 2-dimensional complex functions can be extended to hypercomplex numbers in n dimensions. Thus, the functions $f(u)$ of an n-complex variable which are defined by power series have derivatives independent of the direction of approach to the point under consideration. If the n-complex function $f(u)$ of the n-complex variable u is written in terms of the real functions $P_k(x_0, ..., x_{n-1})$, $k = 0, ..., n-1$, then relations of equality exist between the partial derivatives of the functions P_k. The integral $\int_A^B f(u)du$ of an n-complex function between two points A, B is independent of the path connecting A, B, in regions where f is regular. If $f(u)$ is an analytic n-complex function, then $\oint_\Gamma f(u)du/(u-u_0)$ is expressed in this work in terms of the n-dimensional hypercomplex residue $f(u_0)$.

In the case of polar complex numbers, a polynomial can be written as a product of linear or quadratic factors, although several factorizations are in general possible. In the case of planar hypercomplex numbers, a polynomial can always be written as a product of linear factors, although, again, several factorizations are in general possible.

References

[1] S. Olariu, Int. J. Math. and Math. Sciences **25**, 429-450 (2001).

[2] S. Olariu, Complex Numbers in n Dimensions, Elsevier, 2002.

Supersymmetries in the causal approach

D. R. Grigore[1]

[1] NIPNE-HH, Department of Theoretical Physics

The scattering matrix is formal series of operator valued distributions $T(x_1, \cdots, x_n)$ which act in the Fock space of some collection of free fields. The expression $T(x)$ is the *interaction Lagrangian*. It is convenient to construct more general objects namely the operator-valued distributions $T(W_1(x_1), \ldots, W_n(x_n))$ where W_j are arbitrary Wick monomials; they are called *chronological products* and verify the so-called Bogoliubov axioms expressing the following properties: the initial condition, skew-symmetry in all arguments, Poincaré invariance, causality and unitarity (see for instance [3]). The existence of solutions is rigorously established in [1] using a recursive procedure based on the causality axiom. Sometimes it is possible to supplement these axioms by other invariance properties. In this way supersymmetric invariance can be treated also in this formalism.

A quantum supersymmetric theory is a collection of quantum relativistic free fields b_j (resp. f_A) which are bosonic (resp. fermionic) acting in the Hilbert space $\mathcal{H}$ together with the operators $Q_a, \quad a = 1, 2$ such that the following properties are valid:

$$\begin{aligned} Q_a\Omega = 0, \quad \bar{Q}_{\bar{a}}\Omega = 0 \\ \{Q_a, Q_b\} = 0 \quad \{Q_a, \bar{Q}_{\bar{b}}\} = 2\sigma^{\mu}_{a\bar{b}}P_\mu \\ [Q_a, P_\mu] = 0 \quad U^{-1}_{a,A}Q_bU_{a,A} = A_b{}^cQ_c \\ i[Q_a, b] = f, \qquad \{Q_a, f\} = b; \end{aligned} \tag{1}$$

here $P_\mu = -i\,\partial_\mu$ are the infinitesimal generators of the translation group, σ^μ are the usual Pauli matrices and $\bar{Q}_{\bar{b}} \equiv (Q_b)^\dagger$ We have denote generically by b (resp. f) arbitrary linear combinations of the Bose (resp. Fermi) fields and their partial derivatives. These relations express the definition of a supersymmetric algebra (without central extensions) and the tensor properties of the fields with respect to (infinitesimal) supersymmetry transformations. If these conditions are true we say that Q_a are *super-charges* and b_j, f_A are forming a *quantum supersymmetric multiplet.*

Then supersymmetric invariance of the model can be expressed in an infinitesimal form analogue with gauge invariance [4]:

$$[Q_a, T(x_1, \ldots, x_n)] = i\sum_{l=1}^{n}\frac{\partial}{\partial x_l^\mu}T^\mu_{a;l}(x_1, \ldots, x_n) \tag{2}$$

for some chronological products $T(X)$, $T^\mu_{a;l}(X)$.

One can establish by a direct analysis that the chronological products can be normalized such that these identities are true in all orders for toy models as it is Wess-Zumino model [5].

For general supersymmetric theories one finds necessary to generalize the preceding framework introducing *superfields*. We consider the space $\mathcal{H}_G \equiv \mathcal{G} \otimes \mathcal{H}$ where $\mathcal{G}$ is a Grassmann algebra generated by Weyl anticommuting spinors θ_a and their complex conjugates $\bar{\theta}_{\bar{a}} = (\theta_a)^*$ and perform a Klein transform such that the Grassmann parameters θ_a are anti-commuting with all fermionic fields. The operators acting in $\mathcal{H}_G$ are called *superfields*. Of special interest are the *supersymmetric Wick monomials* constructed as in [2] according to the formula:

$$W(X) \equiv e^{iS}w(x)e^{-iS} \tag{3}$$

where $X = (x, \theta, \bar{\theta})$ are the superspace coordinates, $S \equiv \theta^aQ_a - i\bar{\theta}^{\bar{a}}\bar{Q}_{\bar{a}}$, w is a Wick monomial in $\mathcal{H}$ and we interpret the exponential as a (finite) Taylor series.

Then one can generalize the Bogoliubov axioms in a purely supersymmetric context [6] by considering chronological products $T(W_1(X_1), \ldots, W_n(X_n))$. The condition (2) can be proved to be true in all orders of perturbation theory if it is true for the interaction Lagrangian. In [7] we show that the starting point of the analysis is not trivial. The construction of a quantum multiplet is very difficult task because of the condition of positivity of the scalar product. This condition is not imposed in the standard literature where it is assumed that it follows automatically from the path-integral quantization procedure..

References

[1] H. Epstein, V. Glaser, Ann. Inst. H. Poincaré **19 A** (1973) 211-295

[2] F. Constantinescu, M. Gut, G. Scharf, Ann. Phys. (Leipzig) **11** (2002) 335-356

[3] M. Dütsch, K. Fredenhagen, Commun. Math. Phys. **203** (1999) 71-105

[4] M. Dütsch, T. Hurth, F. Krahe, G. Scharf, Il Nuovo Cimento **A 106** (1993) 1029-1041

[5] D. R. Grigore, European Phys. Journ. **C 21** (Particles and Fields) (2001) 732-734

[6] D. R. Grigore, G. Scharf, hep-th/0204105, to appear in Annalen der Physik

[7] D. R. Grigore, G. Scharf, hep-th/0212026

Supersymmetric soliton equations

A.S. Cârstea [1]

[1] IFIN-HH, Department of Theoretical Physics; E-mail: acarst@theor1.theory.nipne.ro

The description of particles through the appropriate solutions of nonlinear evolution equations is an ongoing quest.A new turn in this approach was registered when it was discovered (through the pioneering work of Kruskal and Zabusky [1]) that integrable nonlinear evolution equations possess solutions that present coherent structures.Prominent among these solutions are the solitons which are localised solutions that retain their identity even through interaction with other solutions (localised or not) of the nonlinear equations. Thus the solitons are the *par excellence* candidates for the description ofparticle-like behaviour. One important datum of nature is that elementary particles appear in two distinct varieties: bosons and fermions, depending on the value of their spin. In the recent decades, mathematical techniques have been proposed which allow fermions and bosons to be treated on an equal footing [2]. One considers anticommuting variables of Grassmann type (for the description of fermions) together with the usual commuting variables (which are adequate for the description of bosons [3]) and introduces some transformation relating them, leading to the notion of supersymmetry. It thus became natural to ask various questions. First, can one extend the usual (bosonic) nonlinear integrable equations to a supersymmetric setting while preserving integrability? In what we have done the answer is affirmative. As a matter of fact, this extension can be obtained in various ways. In some cases the resulting equation does indeed possess a supersymmetry invariance. In some other cases, the resulting equations just incorporate some fermionic degrees of freedom,coupled to the bosonic ones, but without boson-fermion symmetry. Given the existence of integrable supersymmetric(or fermionic-extended) evolution equations, the second important question is how one can construct their multisoliton solutions. It turns out that the Hirota bilinear approach [4], which has been (and still is) the life saver of all true solitonists, can be extended to the supersymmetric domain. Supersymmetric bilinear operators can indeed be introduced [5], following the infallible guide of gauge invariance, and integrable nonlinear supersymmetric equations can be bilinearised. Using this we construct the general supersymmetric solitonic solutions for various equations[6,7]. An important finding is that, contrary to the standard (bosonic) case, in a supersymmetric setting the solitons get "dressed" through their mutual interaction. However, just as the interaction term, the dressing is also completely determined at the level of the two-soliton solution. Another interesting aspect of integrable nonlinear equations is the fact that they possess reductions through similarity transformations, to equations which have the Painlevé property [8] and, whenever they are of the second order, belong to the Painlevé/Gambier classification. Since the similarity reduction procedure can be applied to fermionic equations it is straightforward to use it in order to construct supersymmetric (or just fermionic) extensions of the Painlevé equations. We have used this procedure in order to obtain supersymmetric forms for the P_I and P_{II} equations [9].The striking parallel that exists between the properties of supersymmetricintegrable nonlinear evolutions equations and their standard, bosonic, counterparts has suggested the study of similarity reductions. We were thus able to produce the supersymmetric analogues of Painlevé equations. Several open problems exist at this point. Although many supersymmetric integrable nonlinear evolution equations do exist their bilinearisation is known only in very few cases and the same applies *a fortiori* to their multisoliton solutions. Moreover the domain of supersymmetric Painlevé equations is far from having been explored. Given the results obtained already for the simplest Painlevé equations wecan surmise the existence of a treasure of new integrable systems awaiting the Indiana Jones and/or LaraCroft of integrability.

References

[1] N. J. Zabusky, M. D. Kruskal, Phys. Rev. Lett. 15, (1965), 240.

[2] J. Wess, B. Zumino, Nucl. Phys. B70, (1974), 39.

[3] F. A. Berezin, *Introduction to Super-Analysis*, Reidel,Dodrecht, (1987).

[4] R. Hirota, in *Solitons*, R. Bullough and P. Caudrey eds.Springer, (1980), 157.

[5] A. S. Carstea, Nonlinearity 13, 5, (2000), 1645.

[6] A. S. Carstea, A. Ramani and B. Grammaticos, Nonlinearity 14,(2001), 1419.

[7] B. Grammaticos, A. Ramani and A. S. Carstea, J. Phys. A 34(2001) 4881.

[8] M.J. Ablowitz, A. Ramani and H. Segur, Lett. Nuov. Cim. 23(1978) 333.

[9] A. Ramani, A. S. Carstea and B. Grammaticos, Phys. Lett. A. 292, (2001), 115

Geometrical phases on hermitian symmetric spaces

Stefan Berceanu [1]

[1] NIPNE-HH, Department of Theoretical Physics

Six questions referring to coherent states and geometry have been presented in [1]. In the same context, reference [2] was devoted to the following question: find a geometric significance of the phase of the scalar product of two coherent states. An explicit answer to this question for the Riemann sphere was given by Perelomov. Earlier, S. Pancharatnam [3] showed that the phase difference between the initial and final state is $< A|A' >= \exp(-i\Omega_{ABC}/2)$, where Ω_{ABC} is the solid angle subtended by the geodesic triangle ABC on the Poincaré sphere. The holonomy of a loop in the projective Hilbert space is twice the symplectic area of any two-dimensional submanifold whose boundary is the given loop (cf. Aharonov & Anandan).

A general answer to the question of the geometric significance of the phase of the scalar product of two coherent state vectors using the coherent state embedding and the so called "Cauchy formulas" was given in [2] and [4]. In reference [2] it was proved that for compact hermitian symmetric spaces the phase of the scalar product of two coherent states is twice the symplectic area of a geodesic triangle determined by the corresponding points on the manifold and the origin of the system of coordinates. Lately, we learned that the formula for the symplectic area on the noncompact Grassmann manifold was found out earlier [5]. Also there are other references on two-cocycles on real simple Lie groups, which are related to the symplectic area of geodesic triangles [6, 7].

A. Guichardet and D. Wigner [6] have proved that a simple Lie group has non-trivial continuous 2-cohomology group $H^2(G, \mathbf{R})$ if and only if G/K admits a G-invariant complex structure, where K is a maximal compact subgroup of G. In this context, let us remained some well known facts: If $\mathbf{g}$ is the Lie algebra of the compact and connected Lie group G, then $H^q(\mathbf{g})$ is isomorphic with the q^{th} cohomology group $H^q(G)$ with real coefficients and the ring $H(\mathbf{g})$ is isomorphic with the cohomology ring $H(G)$ of G. If $\mathbf{g}$ is a semi-simple Lie algebra over a field of characteristic 0, then $H^1(\mathbf{g}) = \{\mathbf{0}\}$, $H^2(\mathbf{g}) = \{\mathbf{0}\}$ and $H^3(\mathbf{g}) \neq \{\mathbf{0}\}$. Moreover, for a simply connected Lie group G, not only $H^1(G) = \{0\}$, but also $H^2(G) = \{0\}$.

We can give an explicit calculation of the two-cocycle for the complex Grassmann manifold, which, when expressed in Pontrjagin's coordinates, it is shown to be identical with that considered by A. Guichardet and D. Wigner. The notation and technique for manipulating the Grassmann manifold is that from references [8].

The geometric significance of the 2-cocycle as a symplectic area of a geodesic triangle was found by J.-L. Dupont and A. Guichardet [7]. Using the results of [6, 7] and our results in [2] it follows that: *If G is a simple Lie group, then the only coherent state manifolds G/K for which the phase of the scalar product of two coherent state vectors is twice the symplectic area of a geodesic triangle are the hermitian symmetric spaces.* This remark is a completion of our assertions in [2].

In this context, the following question naturally arise: *For which Lie groups G, which admits coherent state representations* (cf. [9], [10]), *the assertion "the phase of the scalar product of two coherent states is twice the symplectic area of geodesic triangles" is still true?*

References

[1] S. Berceanu, hep-th/9408008;

[2] S. Berceanu Math. DG/9903190

[3] S. Pancharatnam, *Proc. Indian. Acad. Sci.* **XLIV, 5 A** (1956) 247-262

[4] S. Berceanu and M. Schlichenmaier, *J. Geom. Phys.* **34** (2000)

[5] A. Domic and D. Toledo *Math. Ann.* **276** (1987) 425-432

[6] A. Guichardet et D. Wigner, *Ann. scient. Éc. Norm. Sup.*4^e série, t. **11** (1978) 277-292

[7] J.-L. Dupont et A. Guichardet, *Ann. scient. Éc. Norm. Sup.* 4^e série 4, t. **11**, (1978) 293-296

[8] S. Berceanu and L. Boutet de Monvel, *J. Math. Phys.* **34** (1993) 2353-2371; S. Berceanu, *Bull. Belg. Math. Soc. Simon Stevin* **4** (1997) 205-243

[9] W. Lisiecki, *Ann. Ins. Henri Poincarè*, **53** (1990) 245-258; — *Bull. Amer. Math. Soc.* **25** (1991) 37-43 ; — *Rep. Math. Phys.*, **35** (1995) 327-358

[10] K-H. Neeb, *Holomorphy and convexity in Lie theory*, Walter de Gruyter, (2000), de Gruyter Expositions in Mathematics 28

Computational Physics (Physics of Information)

Numerical operations on oscillatory functions

L. Gr. Ixaru [1]

[1] Institute of Physics and Nuclear Engineering, Department of Theoretical Physics, POBox MG - 6, Bucharest, Romania, Email : ixaru@theor1.theory.nipne.ro

We consider some typical numerical operations on functions (differentiation, integration, solving differential equations, interpolation) and show how the standard algorithms can be modified to become efficient when the functions are oscillatory, of the form $y(x) = f_1(x)\sin(\omega x) + f_2(x)\cos(\omega x)$ where $f_1(x)$ and $f_2(x)$ are smooth functions. The expressions of the parameters of the new formulae are written in a way which makes them tuned also for functions of form $y(x) = f_1(x)\sinh(\lambda x) + f_2(x)\cosh(\lambda x)$. Our formulae only require the values of y at some points and those of ω or λ and they tend to the classical formulae when ω or λ tends to zero.

For the derivation we follow the exponential fitting technique introduced in a previous paper (L. Gr. Ixaru, Comput. Phys. Commun. **105** (1997), 1–19). We list the tuned expressions for the first and the second derivative, for the Simpson quadrature formula and for the Numerov algorithm to solve differential equations. We also show how the Gauss quadrature formulae can be adapted and finally give a few tuned formulae for the interpolation. Numerical illustrations are presented for each case. Some open problems are also mentioned.
(Computers and Chemistry **25**, 39 – 53, 2001 (invited paper))

A Gauss quadrature rule for oscillatory integrands

L. Gr. Ixaru [1], B. Paternoster [2]

[1] Institute of Physics and Nuclear Engineering, Department of Theoretical Physics, POBox MG - 6, Bucharest, Romania

[2] Dipartimento di Informatica e Applicazioni, Universitá di Salerno, Italy

We consider the Gauss formula for an integral, $\int_{-1}^{1} y(x)dx \approx \sum_{k=1}^{N} w_k y(x_k)$, and introduce a procedure for calculating the weights w_k and the abscissa points $x_k, k = 1, 2, \ldots, N$, such that the formula becomes best tuned on oscillatory functions of the form $y(x) = f_1(x)\sin(\omega x) + f_2(x)\cos(\omega x)$ where $f_1(x)$ and $f_2(x)$ are smooth. The weights and the abscissas of the new formula depend of ω and, by the very construction, the formula is exact for any ω provided $f_1(x)$ and $f_2(x)$ are polynomials of class $\mathcal{P}_{N-1}$. Numerical illustrations are given for N between one and six.
(Comput. Phys. Commun. **133**, 177 – 188, 2001)

A comment on "Reliable operations on oscillatory functions"

L. Gr. Ixaru [1]

[1] Institute of Physics and Nuclear Engineering, Department of Theoretical Physics, P. O. Box MG - 6, Bucharest, Romania

This is a short comment on a recently published paper [Gh. Adam, S. Adam, Comput. Phys. Commun. 125 (2000) 127].
(Comput. Phys. Commun. **134**, 267 – 268, 2001)

Frequency determination and step-length control for exponentially-fitted Runge-Kutta methods

G. Vanden Berghe [1], L. Gr. Ixaru [2], H. De Meyer [1]

[1] Department of Applied Mathematics and Computer Science, Universiteit Gent, Krijgslaan 281–S9, B–9000 Gent, Belgium

[2] Institute of Physics and Nuclear Engineering, Department of Theoretical Physics, POBox MG - 6, Bucharest, Romania

An exponentially–fitted Runge–Kutta (EFRK) fifth-order method with six stages is constructed, which exactly integrates first–order differential initial–value problems whose solutions are linear combinations of functions of the form $\{\exp(\omega x), \exp(-\omega x)\}$, $\omega \in \mathcal{R}$ or $i\mathcal{R}$. By combining this EFRK method with an equivalent classical embedded (4,5) Runge–Kutta method, a technique is developed for the estimation of the occuring ω–values. Error and step–length control is carried out by using the Richardson extrapolation procedure. Some numerical experiments show the efficiency of the introduced methods.
(Journal Comp. and Appl. Math. **132**, 95 – 106, 2001)

Optimal implicit exponentially–fitted Runge–Kutta methods

G. Vanden Berghe [1], L. Gr. Ixaru [2], M. Van Daele [1]

[1] Department of Applied Mathematics and Computer Science, Universiteit Gent, Krijgslaan 281–S9, B–9000 Gent, Belgium

[2] Institute of Physics and Nuclear Engineering, Department of Theoretical Physics, POBox MG - 6, Bucharest, Romania

Implicit Runge–Kutta methods for first–order ODEs are considered and the problem of how frequencies should be tuned in order to obtain the maximal benefit from the exponential fitted versions of such algorithms are examined. The key to the answer lies in the analysis of the behaviour of the error. A two–stage Runge–Kutts method is particularly investigated. Formulae for optimal frequencies are produced; in that case the order of the method is increased by one unit.
(Comput. Phys. Commun. **140**, 346–357, 2001)

Emission of electromagnetic radiation in α - decay

S. Mişicu[1], M. Rizea[2], W. Greiner[1]

[1] Institut für Theoretische Physik, Frankfurt am Main, Germany
[2] Institute of Physics and Nuclear Engineering, Department of Theoretical Physics, POBox MG - 6, Bucharest, Romania

The electromagnetic radiation during the non-uniform motion of the fragments resulting from the α - decay of a heavy nucleus is computed in a time-dependent quantum formalism. The dynamical characteristics of the α - particle such as position, velocity and acceleration are computed by taking average values of the position and momentum operators and next the bremsstrahlung emission is determined by resorting to the classical formula for the radiation power. The contribution of the α - particle intra-barrier motion to the total bremsstrahlung yield is evaluated and some hints are given for the case when one considers α - decay from the ground state.

Enhancing reliability of interpolatory quadrature rules

Gh. Adam[1], S. Adam[1]

[1] NIPNE-HH, Department of Theoretical Physics

We investigate ways of enhancing the reliability of interpolatory quadrature rules which derive their local error estimates from specific pairs $\{Q_n,\ Q_{2n+1}\}$ of quadrature sums involving n and $2n+1$ knots respectively. Towards this end, a validating scheme of the computed local error estimates is derived from the study of parametric elementary integrals. According to this scheme, a local error estimate is unconditionally rejected as unreliable if its magnitude exceeds a given fraction of $|Q_{2n+1}|$. Moreover, it is only conditionally accepted iff: (i) the average value $\bar{f}$ of the integrand does not belong to one or more of the ranges of variation of the integrand f over its monotonicity subranges defined over the $2n+1$-knot sampling of Q_{2n+1} and/or (ii) the isolated fixed points of the quadrature mesh, defined as the common extremal points of f over the corresponding n and $2n+1$-knot samplings such that they are not consecutive extrema inside the n-knot sampling, result in smaller stability regions around the $2n+1$-knot extrema as compared to those arising from the n-knot extrema.

Finally, the procedure is illustrated on the archetypal Gauss-Kronrod 10-21 quadrature rule.

To be published in Romanian Journal of Physics, vol. 47, No. 3-4 (2002)

Efficient and reliable subdivision strategy in automatic adaptive quadrature

Gh. Adam[1], S. Adam[1]

[1] NIPNE-HH, Department of Theoretical Physics

A scrutiny of the standard approach to the class conscious automatic adaptive quadrature allows us to propose an improved general control based on three elements: (i) direct access of the general control routine to the integrand sampling; (ii) modified priority keys to the instantiations of the heaps T_H associated to the current stages of the subrange subdivision tree T_D; (iii) hierarchical ordering of the status of the generated subranges, allowing clearly defined decisions in each of the following possible cases: insufficiently resolved integrand profile,occurrence of integrand singularities solvable by an acceleration procedure, occur-

rence of an ill-conditioned integrand structure which cannot be solved by means of convergence acceleration algorithms, well conditioned integrands.

The procedure increases the output reliability by at least three orders of magnitude.

Invited talk at The 2nd International Colloquium "Mathematics in Engineering and Numerical Physics", *University 'Politehnica' of Bucharest, ROMANIA, April 22–27, 2002*

Robust automatic adaptive quadrature

Gh. Adam[1], S. Adam[1]

[1] NIPNE-HH, Department of Theoretical Physics

The paper describes a code developed by the authors for automatic adaptive quadrature of integrals which may include oscillatory or hyperbolic weight functions, accelerated at multiple entries (`EAQWOM`). Ways of enhancing code qualities like reliability, robustness, efficiency, user friendliness, structuredness, portability, are discussed.

Communication at 1st Annual Communication Session of the Theoretical Physics Department, *in memory of Aretin Corciovei (1930 - 1992), January 24–25, 2002;*
To be published in Romanian Journal of Physics, vol. 47, No. 1–2 (2002)

Frequency evaluation in exponential fitting multistep methods for ODEs

L. Gr. Ixaru[1], G. Vanden Berghe[2], H. De Meyer[2]

[1] Institute of Physics and Nuclear Engineering, Department of Theoretical Physics, POBox MG - 6, Bucharest, Romania

[2] Department of Applied Mathematics and Computer Science, Ghent University, Krijgslaan 281 (S9), B-9000 Gent, Belgium

We consider the linear multistep algorithms for first order ODEs and examine the problem of how the λ–frequencies should be tuned in order to obtain the maximal benefit from the exponential fitting versions of such algorithms. We find out that the key of the answer consists in analysing the behaviour of the error. On further investigating the simple case of two-step bdf algorithms we produce formulae for the optimal λ-s and show that, if the optimal λ-s are used, the order of the method is increased by one unit. The reported numerical illustrations suggest that further investigations along these lines deserve a real attention.
(Journal Comp. and Appl. Math. **140**, 423–435, 2002)

Quadrature rules using first derivatives for oscillatory integrands

Kyung Joong Kim [1], Ronald Cools [1], L. Gr. Ixaru [2]

[1] Department of Computer Science, Katholieke Universiteit Leuven, Celestijnenlaan 200A, B-3001, Heverlee, Belgium

[2] Institute of Physics and Nuclear Engineering, Department of Theoretical Physics, POBox MG - 6, Bucharest, Romania

We consider the integral of a function $y(x)$, $I(y(x)) = \int_{-1}^{1} y(x)dx$ and its approximation by a quadrature rule of the form

$$Q_N(y(x)) = \sum_{k=1}^{N} w_k y(x_k) + \sum_{k=1}^{N} \alpha_k y'(x_k),$$

i.e., by a rule which uses the values of both y and its derivative at nodes of the quadrature rule. We examine the cases when the integrand is either a smooth function or an ω dependent function of the form $y(x) = f_1(x)\sin(\omega x) + f_1(x)\cos(\omega x)$ with smoothly varying f_1 and f_2. In the latter case the weights w_k and α_k are ω dependent. We establish some general properties of the weights and present some numerical illustrations.

(Journal Comp. and Appl. Math. **140**, 479–498, 2002)

LILIX – a package for the solution of the coupled channel Schrödinger equation

L. Gr. Ixaru [1]

[1] Institute of Physics and Nuclear Engineering, Department of Theoretical Physics, POBox MG - 6, Bucharest, Romania

The code `LILIX` is based on a CP method for solving systems of coupled Schrödinger equations. The method is of the sixth order, highly stable and with uniform accuracy with respect to the energy. The package contains three main subroutines to be accessed directly by the user. Subroutine `LI` generates the partition consistent with the desired accuracy while subroutine `LIX` helps propagating the solution and its derivative with respect to the momentum k in both directions (forwards and backwards) along the mesh points of the partition. Subroutine `RENORM` helps conserving the linear independence of various vectors in the solution matrix whenever this may be of concern.

(Comput. Phys. Commun. **147**, 834–852, 2002)

PERSYS - a program for the solution near the origin of coupled channel Schrödinger equation with singular potential

M. Rizea [1]

[1] Institute of Physics and Nuclear Engineering, Department of Theoretical Physics, POBox MG - 6, Bucharest, Romania

The code `PERSYS` produces the regular solution of a system of coupled Schrödinger equations near the origin, where the potential exhibits a singularity, due to the centrifugal, spin-orbit and Coulomb components. The solution is calculated by means of a highly accurate method, which consists of a perturbative technique in which the centrifugal term is taken as the reference potential while the rest of terms are seen as a perturbation.

(Comput. Phys. Commun. **143**, 83–99, 2002)

Enhancing reliability of interpolatory quadrature rules

Gh. Adam[1], S. Adam[1]

[1] NIPNE-HH, Department of Theoretical Physics

The detection of insufficiently resolved or ill conditioned integrand structures is critical for the reliability assessment of the quadrature rule outputs. We discuss a method of analysis of the *profile of the integrand at the quadrature knots* which allows inferences approaching the theoretical 100% rate of success, under error estimate sharpening. The proposed procedure is of the highest interest for the solution of parametric integrals arising in complex physical models.

To be published in Computer Physics Communications, (2003)

Solid State Physics

Obmennyi i spin-fluktuatsionnyi mehanizmy sverhprovodimosti v kupratah [Exchange and spin-fluctuation mechanisms of superconductivity in cuprates]

N.M. Plakida[2], L. Anton[3], S. Adam[1], Gh. Adam[1]

[1] NIPNE-HH, Department of Theoretical Physics
[2] BLTF, OIYaI- Dubna, Russia
[3] INFLPR

We propose a microscopical theory of superconductivity in CuO_2 layer within the effective two-band Hubbard model in the strong correlation limit. By applying a projection technique for the matrix Green function in terms of the Hubbard operators, the Dyson equation is derived. It is proved that in the mean-field approximation d-wave superconducting pairing mediated by the conventional exchange interaction occurs. Allowing for the self-energy corrections due to kinematic interaction, a spin-fluctuation d-wave pairing is also obtained. T_c dependence on the hole concentration and $\mathbf{k}$-dependence of the gap function are derived. The results show that the exchange interaction (which stems from the interband hopping) prevails over the kinematic interaction (which stems from the intraband hopping).

To be published in Jurnal Eksperimental'noi i Teoretichescoi Fiziki, JETF, (in Russian) (2003)

Nuclear Physics

Nuclear Structure

Excitation of nuclear states by synchrotron radiation

Albert Olariu [1]

[1] NIPNE-HH, Department of Nuclear Physics

We study the excitation of nuclear states by gamma ray beams of energy up to 200 keV, produced as synchrotron radiation. We consider the possibility to populate an excited state $|i\rangle$ in two steps: from the ground state $|g\rangle$ to an intermediary state $|n\rangle$, which decays by gamma emission or internal conversion to a lower state $|i\rangle$. The aim of this study is to establish if it is possible that the propability P_2 of the two-step transition $|g\rangle \rightarrow |n\rangle \rightarrow |i\rangle$ should be grater than the probability P_1 of the direct tranzition $|g\rangle \rightarrow |i\rangle$ (Fig. 1). The probabilities P_1 and P_2 correspond to a radiation pulse of duration equal to the the half-time of the state $|i\rangle$.

We have written a computer program in C++ which computes the probability P_2, the ratio P_2/P_1 and the rate C_2 of the two-step transitions, for all nuclei and different configurations of states. The program uses a database from [1] which contains information on the the energy levels, half-lives, spins ant parities of nuclear states, and on the relative intensities of the nuclear transitions [2]. If the half-lives or the relative intensities are not known, the program uses the Weisskopf estimates for the transition half-lives. An interpolation program of internal conversion coefficients obtained from [1] has also been used.

In the table below we listed the values obtained for P_2 , P_2/P_1 and C_2 in a number of cases for which P_2 is significant, from the 2900 considered cases. The states $|i\rangle$ and $|n\rangle$ have the energies E_i and E_n, the corresponding half-lives being t_i and t_n. The spectral density of the synchrotron radiation has been considered to be 10^{12} photons cm^{-2} s^{-1} eV^{-1}.

In the table we listed only cases for which the relative intensities of the transitions from levels $|n\rangle$ and $|i\rangle$ to lower states are known.

The calculations done in this study allowed us to identify nuclei for which P_2 has relatively great values. In the listed cases $P_2/P_1 \gg 1$, so the two-step excitation whith synchrotron radiation is more efficient than the direct excitation $|g\rangle \rightarrow |i\rangle$. For a sample having 10^{19} nuclei the probability $P_2 = 2.4 \times 10^{-11}$, obtained for ^{144}Pr, would give a number of $2.4{\times}10^8$ excited nuclei in that sample. The activity of these excited nuclei would be of $3.8{\times}10^5$ Bq, being measurable.

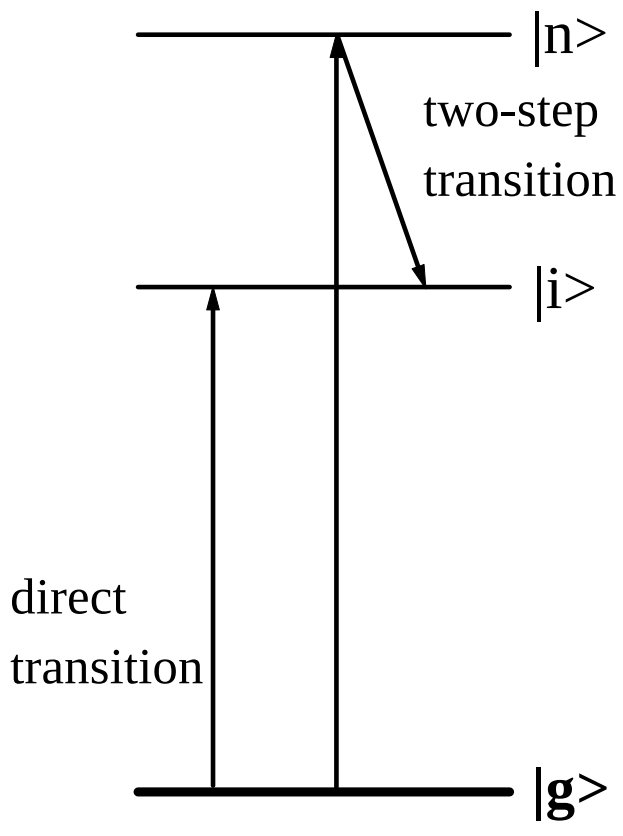

Figure 1: Direct transition and two-step transition

Nucleus	E_i, keV	E_n, keV	t_i	t_n	P_2	P_2/P_1	C_2, s^{-1}
^{144}Pr	59	100	430 s	0.66 ns	2.4×10^{-11}	2.2×10^{12}	3.8×10^{-14}
^{79}Kr	129.8	147.1	50 s	79 ns	2.9×10^{-14}	1.6×10^{7}	4×10^{-16}
^{169}Yb	24.2	191.2	46 s	3.3 ns	5.3×10^{-16}	2.7×10^{10}	8.1×10^{-18}
^{67}Zn	93.3	184.6	9.2 μs	1 ns	5×10^{-20}	440	3.8×10^{-15}
^{65}Zn	53.9	115.1	1.6 μs	0.44 ns	7.1×10^{-20}	760	3.1×10^{-14}
^{151}Sm	4.8	168.4	35 ns	39 ps	1.1×10^{-20}	26	2.2×10^{-13}
^{127}Cs	66.1	139	26 ns	0.12 ns	5.3×10^{-21}	13	1.4×10^{-13}

References

[1] Brookhaven National Laboratory, National Nuclear Data Center, http://www.nndc.bnl.gov

[2] Richard B. Firestone, Table of Isotopes - Eigth Edition, Whiley, New York, 1996

An approach for cross-talk rejection in halo neutron coincidence measurements

M. Petrascu[1], A. Constantinescu[2], I. Cruceru[1], M. Giurgiu[3], A. Isbasescu[1], M. Isbasescu[1], H. Petrascu[1], C. Bordeanu[1], I. Tanihata[4], T. Kobayashi[4], K. Morimoto[4], K. Katori[4], M. Chiba[4], Y. Nishi[4], S. Nishimura[4], A. Ozawa[4], T. Suda[4], K. Yoshida[4]

[1] Horia Hulubei National Institute for Physics and Nuclear Engineering, POB MG-6, Bucharest, Romania
[2] Faculty of Physics, Bucharest University
[3] Technical University, Bucharest
[4] RIKEN, Wako-shi, Saitama, Japan

Recently, an experiment with a new array detector aiming the investigation of halo neutron pair preemission in Si(^{11}Li, fusion) has been performed [1]. The ultimate goal of a neutron coincidence experiment is the obtaining of the nn correlation function which represents an unique means to map the valence neutrons within a halo nucleus. In this aim it is very important to have adecuate criteria for cross-talk (c.t.) rejection. In this paper, the criterion [2] for selecting the true coincidences against cross-talk (c.t.) was adopted. Cross-talk is a spurious effect in which the same neutron is registered by two or more detectors. A coincidence between two detectors is rejected whenever the following condition is fulfilled:

$$E_1 > E_{min} = \frac{1}{2} m \frac{d_{min}^2}{\Delta t^2} \qquad (1)$$

Here E_1 is the energy of the first neutron. E_{min} is the minimum energy required by the neutron scattered from the first detector to travel the minimum distance d_{min} to the second detector, in the time interval Δt. For the first rejection we took d_{min} equal to the distance between the detector centers. For example, by applying this criterion to the first order coincidences, a number of 118 true coincidences were found. For further rejection we consider that it is more appropriate to use the d_{min} parameter instead of time of flight, because the distance between the adjacent detector centers is close to the detector dimension. By taking d_{min}=1.8 cm as it is specified in Fig.4, the number of first order true coincidences is reduced from 118 to 46. From geometrical considerations, assuming an uniform distribution of the neutrons coming from the target over the surface of detector #1, in the 5 mm slice are about 12% of the incoming neutrons. Assuming also that these neutrons are scattered toward detector #2, it follows that the remaining c.t. is less than 1.5%. We tested the consistency of such estimation by the MENATE program. The author of MENATE, Pierre Desesquelles [3], has adapted the program [3] for calculation of c.t. rejection in the case when d_{min} is used as rejection parameter. In one of the used configurations, detector #1 surrounded by detectors #2 to #9 (see Fig. 2) is uniformly fired by neutrons of given energy. The c.t. rejection, and diaphony are calculated as a function of the incoming neutron energy, the detector number and the distance d_{min} . For example in the case 100,000, 15 MeV neutrons are fired uniformly

on detector #1, 32900 neutrons are detected by this detector, for a threshold of 0.3 MeVEE. The total induced c.t. on detectors 2-9 are 2815 counts of which 2814 are rejected for d_{min}=1.8 cm. This means that in about 3000 counts only one c.t. can pass as a true coincidence. In the case d_{min}=4.8 cm about 7% of c.t. could pass as true coincidences. Thus the upper estimation is confirmed by the Menate program. More relaxed c.t. conditions appear in the case of second and higher order coincidences.

References

[1] M.Petrascu, Proc.Int.Symp. on Exotic Nuclei, Baikal Lake, Russia, July 1991, World.Sci.2002, p256.

[2] R.Ghetti et al.,Nucl.Instr.Meth.**A421**,542 (1999)

[3] P.Desesquelles, The Monte Carlo Program Menate

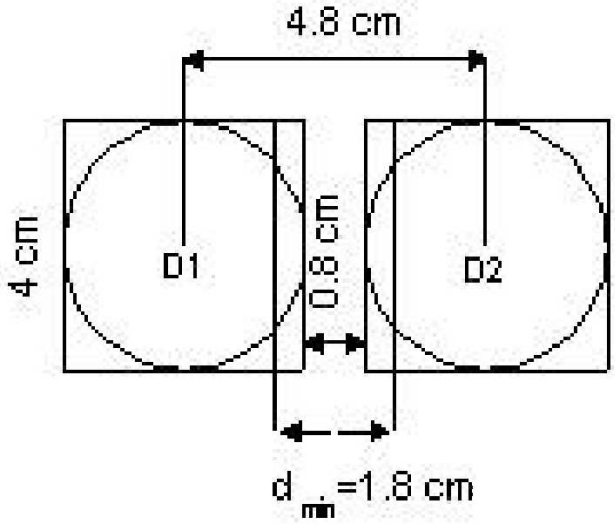

Figure 1: The principle of c.t. rejection by using d_{min} parameter for first order coincidences is shown.

Nuclear Reactions

The correlation function of the halo neutrons pre-emitted in the fusion of ^{11}Li radioactive nuclei with Si targets

M. Petrascu[1], A. Constantinescu[2], I. Cruceru[1], M. Giurgiu[3], A. Isbasescu[1], M. Isbasescu[1], H. Petrascu[1], C. Bordeanu[1], I. Tanihata[4], T. Kobayashi[4], K. Morimoto[4], K. Katori[4], M. Chiba[4], Y. Nishi[4], S. Nishimura[4], A. Ozawa[4], T. Suda[4], K. Yoshida[4]

[1] Horia Hulubei National Institute for Physics and Nuclear Engineering, POB MG-6, Bucharest, Romania
[2] Faculty of Physics, Bucharest University
[3] Technical University, Bucharest
[4] RIKEN, Wako-shi, Saitama, Japan

The problem of the correlation function denominator building, was presented in a previous contribution to this volume [1]. In the following, the preliminary results concerning the nn correlation function will be presented. The two-neutron correlation function is given by [2]:

$$C(q) = k\frac{N_c(q)}{N_{nc}(q)} \qquad (1)$$

In (1) $N_c(q)$ represents the yield of coincidence events and $N_{nc}(q)$ the yield of uncorrelated events. The normalization constant k is obtained from the condition that $C(q)$=1 at large relative momenta. The relative momentum q is given by: q=1/2mod($\mathbf{p_1} - \mathbf{p_2}$), $\mathbf{p_1}$ and $\mathbf{p_2}$ being the momenta of the two coincident neutrons. In Fig.1, the correlation functions obtained by using denominators A and B are represented. The normalization was done in the range q=30-40 MeV/c, far away from the c.t range. The points with error bars represent the correlation function constructed by using condition B. The solid line showing good agreement with the experimental points was calculated according [3] for r_0=4.2 fm. Here r_0 represents the variance of

Gaussian source assumed in the model of ref. [3]. The n-n separation r_{nn} is then a Gaussian function with the variance=$2^{0.5}r_0$, and $r_{nn}^{rms}=6^{0.5}r_0$. The lower dotted line in Fig. 1, in good agreement with the correlation function obtained with denominator A, was calculated for r_0=5 fm. This value is close to the one (5.3 fm) obtained in ref. [4]. This means that in [4] a denominator similar to A was used. The upper dotted line calculated for r_0=3.4 fm illustrates a correlation function in agreement with r_{nn}^{rms}= 8.3 fm predicted by COSMA$_I$ model [5]. The small anomalies in denominator B could account probably for the difference between the solid line and the upper dotted line in Fig.1. The other value r_{nn}^{rms}=6.7 fm predicted by COSMA$_{II}$ [5] is however too far from the solid line to be accounted by denominator B. It follows that the present data are likely to favor the r_{nn}^{rms} value predicted by COSMA$_I$. One has to mention that in [6] almost the double number of iterations were necessary for ^{11}Li in comparison with ^{14}Be and ^{6}He to obtain a stable solution nearer to COSMA$_{II}$. A definite answer to this question will be an experiment aiming to determine the intrinsic correlation function by using ^{11}Li and ^{11}Be halo nuclei. The nucleus ^{11}Be will be an ideal uncorrelated background source, since it contains only one halo neutron.

References

[1] M.Petrascu et al., contribution in this volume.

[2] G.I.Kopylov, Phys.Lett**50b**,472 (1974)

[3] R.Lednicki, L.Lyuboshits, Sov. J. Nucl. Phys. **35**,770 (1982)

[4] K.Ieki et al.,Phys. Rev.Lett.**70**,730 (1993)

[5] M.V.Zhukov et al.,Phys.Rep.**231**,151 (1993).

[6] F.Marques et al.,Phys.Lett. **B476**,219(2000)

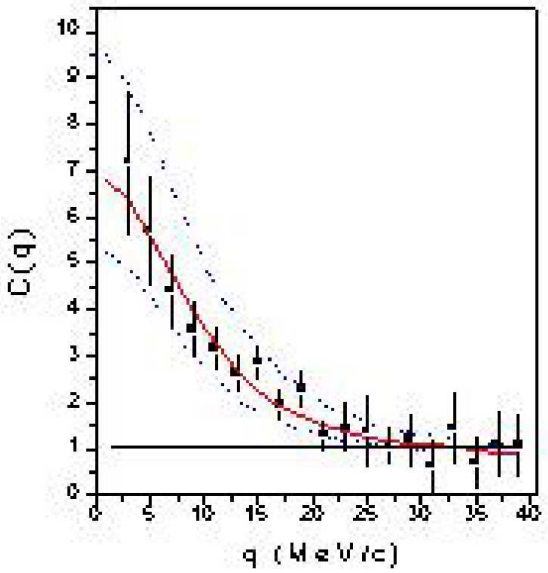

Figure 1: The correlation function C(q) (points with error bars) was obtained using formula (1). The used denominator was of type B (see text). The solid line was calculated according [3] for respectively r_0=4.2 fm. For the meaning of upper and lower dotted lines see text

Experimental evidence for residual correlation of the halo neutrons pre-emitted in the fusion of ^{11}Li radioactive nuclei with Si targets

M. Petrascu[1], A. Constantinescu[2], I. Cruceru[1], M. Giurgiu[3], A. Isbasescu[1], M. Isbasescu[1], H. Petrascu[1], C. Bordeanu[1], I. Tanihata[4], T. Kobayashi[4], K. Morimoto[4], K. Katori[4], M. Chiba[4], Y. Nishi[4], S. Nishimura[4], A. Ozawa[4], T. Suda[4], K. Yoshida[4]

[1] Horia Hulubei National Institute for Physics and Nuclear Engineering, POB MG-6, Bucharest, Romania
[2] Faculty of Physics, Bucharest University
[3] Technical University, Bucharest
[4] RIKEN, Wako-shi, Saitama, Japan

The halo nuclei discovered by Tanihata and coworkers [1] are characterized by very large matter radii, small separation energies, and small internal momenta of valence neutrons. Recently it was predicted [2] that, due to the very large dimension of ^{11}Li, one may expect that in a fusion process on a light target, the valence neutrons may not be absorbed together with the ^{9}Li core, but may be emitted in the early stage of the reaction. Indeed, the experimental investigations of neutron pre-emission in the fusion of ^{11}Li halo nuclei with Si targets [3], have shown that a fair amount of fusions (40±12)% are preceded by one

or two halo neutron pre-emission. It was also found that in the position distribution of the pre-emitted neutrons, a very narrow neutron forward peak, leading to transverse momentum distribution much narrower than that predicted by COSMA model [4], is present. Recently, an experiment with a new array detector aiming the investigation of halo neutron pair pre-emission in Si(^{11}Li, fusion) has been performed [5] [6]. This new experiment confirms the presence of the forward peak with an aperture of 9 msrad. It was found also that this peak is due predominantly to the pre-emission of neutron pairs. In the aim to obtain the n-n correlation function, the critical problem of the denominator construction was carefully analyzed. It was found that the single product denominator A, built by a random coupling of single detected neutrons, followed by cross-talk rejection [7], exceeds by up to 70% the denominator B constructed by replacing with single neutrons, the neutrons in the coincidence sample. We consider this feature of denominator A, together with the large fluctuations revealed when represented in small steps of relative momentum q (Fig. 1), as an experimental evidence for residual correlation [8] of single detected halo neutrons. As one can see in Fig. 1, denominator A is much larger than denominator B. In the case denominators A and B are represented in larger steps of q, (2 MeV/c), the fluctuations seen in Fig.1 disappear, but denominator A remains still significantly larger than B. The correlation functions obtained with A and B denominators will be given elsewhere [9].

References

[1] I.Tanihata et al.,Phys.Lett.**160B**,380(1985).

[2] M.Petrascu et al.,Balk.Phys.Lett.**3**, **4**,214 (1995).

[3] M.Petrascu et al.,Phys.Lett.**B405**,245,(1997).

[4] M.V.Zhukov et al.,Phys.Rep.**231**,151 (1993).

[5] M.Petrascu et al.,*Prep.RIKEN – 395*,April 2001.

[6] M.Petrascu, Proc.Int.Symp. on Exotic Nuclei, Baikal Lake, Russia, July 1991, World.Sci.2002, p256.

[7] R.Ghetti et al.,Nucl.Instr.Meth.**A421**,542 (1999)

[8] F.Marques et al.,Phys.Lett. **B476**,219(2000)

[9] M.Petrascu et al., contribution in this volume.

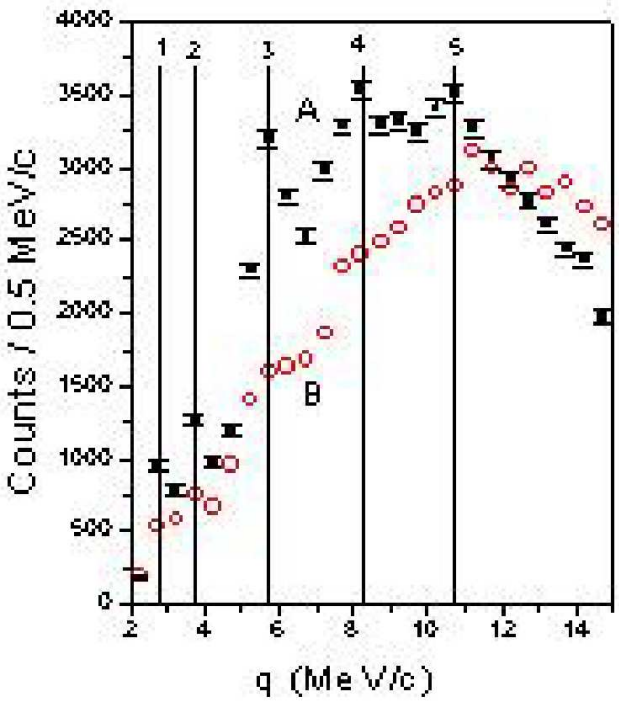

Figure 1: The denominators A and B of the correlation function represented as a function of q in steps of 0.5 MeV/c.

Atomic Physics

PIXE (Particle Induced X rays Emission) and ICP (Inductive Coupled Plasma) applied in biology and environmental

Ion V. Popescu[1,2], M. Iordan[1], Teodor Badica[2], Agata Olariu[2], G. Dima[1], C. Stihi[1], Olga Guguianu[2]

[1] Applied Physics Department, Science Faculty, University "Valahia" of Targoviste
[2] National Institute for Nuclear Physics and Engineering, Bucharest, Romania

Particle Induced X-ray Emission (PIXE) and Inductive Coupled Plasma (ICP) are sensitive and reliable techniques for the determination of elements with atomic number greater than 13 in biological materials in the case of PIXE and greater than 10 in the case of ICP. One of the research direction of our department is the application of those methods in biology: the elemental analysis of leaves from different Basella plants cultivated in Variety Testing Centre and in Green Houses of Targoviste and the microelemental analysis of blood serum samples collected from healthy and ill cows (downer cow syndrome (DCS)) hosted in animal farms in the neighbourhood of Targoviste city. Another research direction is the environmental study, especially air samples from Romanian cities.

The PIXE quantitative method applicable to Basella plants, is described in this work, along with the results obtained from the. The target samples were bombarded with 3 MeV protons beam obtained at Tandem Accelerator of IFIN-HH Bucharest. The X-rays were detected with Ge hiperpur detector with 160 eV at 5.9 KeV energy resolution and the characteristic X-ray spectra were recorded using an acquisition system with a PC computer. The concentration obtained for the chemical elements who give a great nourishment value of Basella plants : P, Ca, Mg, K, Na, Fe, Mn, Zn, Cu, have an estimated precision of less than 12%.

Another part of our research work is dedicated to the microelemental analysis of blood serum samples collected from healthy and ill cows (downer cow syndrome (DCS)). Until today the origin of DCS is uncertain. At the beginning of our work, we assume some connections among the diminution of some nutritive elements from food, the activity of some enzymes and the origin of DCS. The samples were collected from cows at some animal farms on the neighborhood of Targoviste city. To obtain a microelemental monitoring of these samples, we used a nuclear analysis method PIXE (Particle Induced X-Rays Emission) and a spectrometric one ICP (Inductive Coupled Plasma). For Ca and P content of the analyzed samples, we used PIXE based on the internal standard method. The ICP analysis method was used for Mg content determination. The determinations of phosphatase alkaline enzyme of analyzed blood serum samples were made by a spectrometric analysis using Bessey-Lowry method. In studying diseases, a significant variation in Ca, P, Mg and enzyme contents was observed. Those changes correlate with age, season of alimentation and type of disease.

The environmental studies consists in the analysis of air samples from 10 Romanian cities, of different industrial levels. The samples were collected using air sampler by sucking the air through filter papers. For the analysis of the trace elements included in the air. Particle Indiced X Rays Emission (PIXE) was used. It was identified the the traces of S, K, Ca, Ti, V, Cr, Mn, Fe, Co, Ni, Cu, Zn, As, Hg and Pb. The gradient of pollution for different cities is directly proportional to the industrial levels.

References

[1] S.A.E. Johansson, J.L. Campbell, PIXE: A Novel Technique for Elemental Analysis, Wiley, 1988

[2] O. M. Radostils, D.C. Blood, C.C. Gay: Veterinary medicine, Bailliere Tindall, Eighth edition, London, 1994

[3] S. Ghergariu: The basis of medical pathology of animals, All Pub, 1995

[4] D. Mihai: Nutrition and metabolic diseases of animals, Ceres Pub, 1996

[5] H. Barza: The synoptic presentation of downer cow syndrome, Rev. Roum. Of Veterinary Med., vol.4(1), 68-69.

[6] R. Walter: Chaire de nutrition et alimentation, E.N.V., Lyon Cedex, 1975

[7] D. Mihai: The differential clinical diagnosis on internal diseases of animals, Ceres Pub, 1990

[8] W.E. Glassegen, J.W. Metzger, S. Heuer, Phytochemistry, Vol. 33, No.6, pp 1525-1527, 1993

Proton Induced X-rays Excitations (PIXE) and Atomic Absorption Spectrometry (AAS) applied in the environmental samples analysis

Ion V. Popescu[1,3], V. Ciupina[2], M. Iordan[1], Teodor Badica[3], C. Stihi[1], M. Belc[2], A. Bancuta[1], G. Dima[1], G. Busuioc[1]

[1] Physics Department, Valahia University of Targoviste, 0200, Targoviste, Romania
[2] Physics Department, Ovidius University of Constanta, Constanta, 8700, Romania
[3] National Institute for Nuclear Engineerging Horia Hulubei", Bucharest, Romania

The aim of this work is to determine the elemental composition of tree leaves using Proton Induced X-Rays Excitation (PIXE) and Atomic Absorption Spectrophotometry (AAS) methods. By PIXE Spectrometry we identified and determined the concentration of: S, Cl, K, Ca, Ti, Cr, Mn, Fe, Co, Ni, Cu Zn, As, Br, Sr and by AAS method the concentration of elements: Cr, Mn, Fe, Co, Cu, Zn, Se, Cd. Pb was identified in only 2 samples from 29. For leaves trees samples collected from a grather distance to pollution source the Sr concentration decreased and the Mg, Ca, Se, Zn and Fe concentrations increased. Also we can observe a small afinity of these leaves for the environmental Pb which are detected for two samples from a small distance to pollution source.

Status of the 14 GHz ECR ion source RECRIS

S. Dobrescu[1], L. Schachter[1]

[1] IFIN-HH, Department of Nuclear Physics

The Romanian 14 GHz ECR Ion Source (RECRIS) was developed as a stand-alone facility in the Department of Nuclear Physics of IFIN-HH for atomic physics and materials studies. The researches in these fields take advantage of the highly charged ion beams delivered by ECRIS due to the fact that the large Coulomb potential of these ions induce various interactions on atoms and surfaces even at relative small ion kinetic energies (tens or hundreds of keV). The extremely diversified species of ions with different charge states available from ECRIS open thus a large field of research without an accelerator.

The 14 GHz ECR source able to deliver intense beams of highly charged ions of many elements was previously described [1]. The first ECR plasma was ignited in 1999. In 2001, the facility has been completed with a 90^o analyzing magnet, with beam diagnosis boxes (horizontal and vertical adjustable slits and faraday cups) in the object and image points of the magnet and with a magnetic steerer of the ion beam. A schematic drawing of the completed facility is given in the figure below. The base vacuum in the installation is in the range $8 \times 10^{-8} \div 2 \times 10^{-7}$ mbar. Different experimental set-ups can be coupled to this facility.

Argon and oxygen ion beams of tens of microamperes have been experimentally obtained so far. The performances may be improved by further optimizing the source operation, by using different methods as a biased disk and an MD liner [2] and by modifying the analyzing magnet which is actually limiting the beam currents.

References

[1] S. Dobrescu et. al., Proceedings 14th International Workshop on ECR Sources "ECRIS'99", CERN, Geneva, Switzerland, May 1999, p. 124.

[2] L. Schachter et. al., Rev. Sci. Instrum., **71**, 918 (2000).

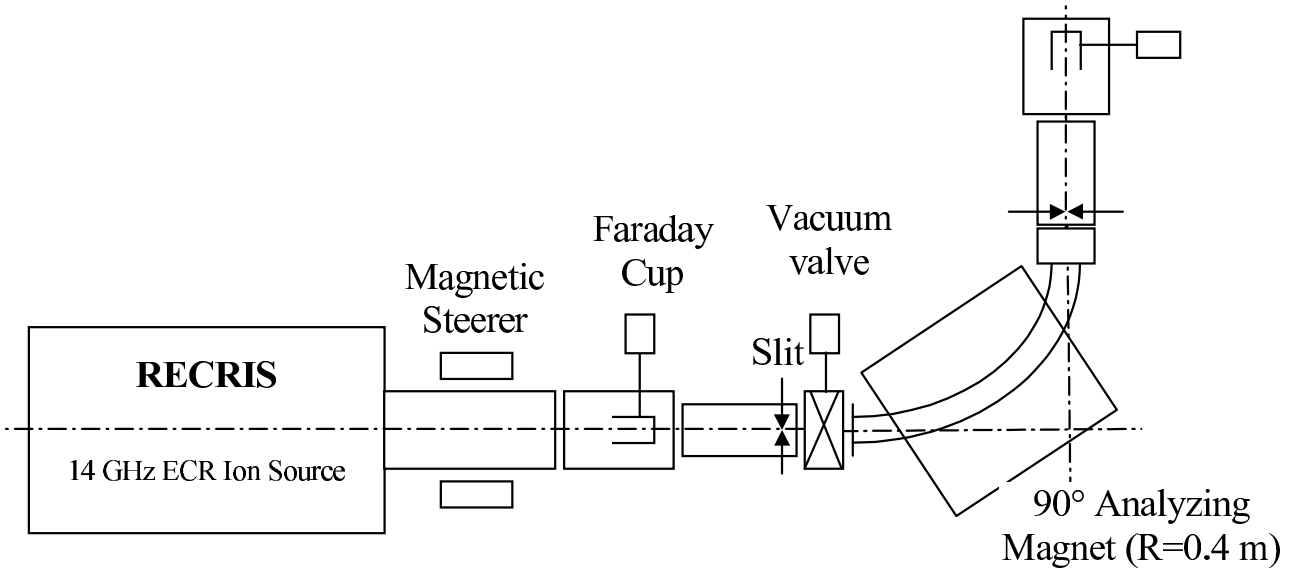

Figure 1: General layout of the RECRIS facility

The role of cold electrons in the increase of the electron cyclotron resonance ion sources performances

L. Schachter[1], S. Dobrescu[1], K. E. Stiebing[2], A. Drentje[3]

[1] National Institute of Physics and Nuclear Engineering, Nuclear Physics Department, P.O.Box MG-6, Bucharest, Romania

[2] Institut fr Kernphysik der J. W. Goethe Universitt, August Euler Strasse 6, D-60486, Frankfurt/Main, Germany

[3] Kernfysisch Versneller Instituut, 9747AA Groningen, The Netherlands

A new aproach of the possibility to significantly increase the high charge state ion beams delivered by the ECR ion sources was tested in experiments at the Institut fur Kernphysic (IKF) der J. W. Goethe Universitat, Frankfurt/Main, Germany and Kernphysich Versneller Instituut (KVI), Groningen, The Netherland. The intensities of argon beams extracted from the 14 GHz ECR ion sources were measured in the standard mode of operation, that means without any supply of supplementary cold electrons and respectively by using the new method consisting in the introduction of a cold electron emitter in the plasma chamber of the sources.

In both experiments very high enhancements of the high charge states of argon ions beam were obtained indicating this method as a very efficient method to increase the ECR ion sources performances.

The cold electron emitter is a special cylindrical metal-dielectric (MD) structure able to sustain the ECR plasma conditions and that is introduced in the plasma chamber of the ECR ion source. Under the impact of electrons and ions escaping from the ECR plasma the metal-dielectric structure emitts a high number of secondary cold electrons.

The goal of the experiments was to measure and compare the charge state distribution of the extracted ion beams in the standard conditions and when the special MD cylindrical stucture is used. The main results obtained at the IKF 14 GHz and at the KVI 14 GHz ECR ion sources are represented in the figure below. 1 It can be observed a similar trend. Both sources were much more productive in argon ions with charge states higher than 9+ when the cold electron supplly was used (light columns) than in the case of the standard mode of operation.

The experiments carried out at the IKF and KVI ECR ion sources led to similar results, clearly demonstrating the higher capability of the cold electron emitting MD structure, introduced in the plasma chamber of the source, to strong enhace the output of the highest charge states. The sources were very stable in operation in the presence of the MD structures. A more

detailed analysis of the influence of a MD structure on the physical processes which occur in the ECR plasma is in view and new experiments are planned.

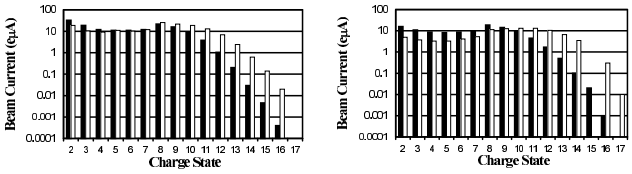

Figure 1: Charge state distribution of the argon beam in standard conditions (no MD - dark columns) and respectively with the MD structure inserted (light columns) at the IKF ECRIS (left diagram) and at KVI ECRIS (right diagram).

Mössbauer data acquisition system for Rayleigh scattering of Mössbauer radiation

A. Kluger[1], S.E. Enescu[1], I. Bibicu[2], C. Ciortea[1], A. Enulescu[1]

[1] NIPNE-HH, Nuclear Physics Department, Bucharest, Romania
[2] NIMP, Bucharest, Romania

A new data acquisition system integrating on a common board the Mössbauer drive signal generator, the analog-to-digital converter (ADC), the internal single channel analyzer (SCA) and the 32kB RAM for data storage is reported. The system (Fig. 1) was successfully tested in Rayleigh scattering of Mössbauer radiation (RSMR) measurements on pyrolytic graphite single crystal. The main functions of the data acquisition system are: to generate the driving signal for the relative source-absorber motion, to convert the analog output from the detector, the multichannel analyzer function and the storage of current data.

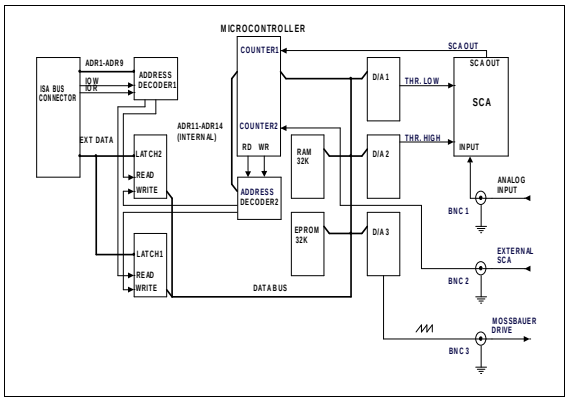

Figure 1: Schematic diagram of the acquisition system hardware.

In the usual systems these functions are performed by different external modules possibly giving rise to data corruption by electronic noise and counts loosing. An Intel 80C52 type microcontroller is used for communication, data processing and command signals generation.

A special software protocol was developed for the timing and handshaking process. The software is running under WINDOWS operating system. The software ensures presettable number of channels, dwell time, acquire time, SCA modes and thresholds. An application path permits to do any other PC work concurrently without stopping the acquisition system.

RSMR was chosen for testing the system performances because this kind of experiments reacquire additional experimental features with respect to the Mössbauer transmission experiments. In order to test the energy resolution a natural iron absorber was placed between the Mössbauer source containing ^{57}Co isotope in rhodium matrix and the proportional counter was used as detector. The resonances lines were fitted with Lorentzian functions assuming that their dips and linewidth are equal. The resulted common linewidth was $\Delta E = 1.210 \cdot 10^{-8}$eV (0.252±0.007 mm/s). For an infinitely narrow instrumental function the measured linewidth should be twice the natural linewidth of the Mössbauer transition $\Gamma = 4{,}665 \cdot 10^{-9}$eV (0.097mm/s). Thus, the difference between the actual linewidth and this ideal value characterize the system energy resolution. The model scatterer was the pyrolytic graphite. The incident Mössbauer radiation of 14.4 keV diffracted on the (002) crystallographic plane gives a first diffraction maximum at θ^1_{BRAGG} = 7.381°. The nuclear absorption spectrum obtained when the absorber is placed between the scatterer and the detector is not very different with respect to the spectrum obtained in the direct transmission configuration. In fact, the dip amplitude measured in the scattering configuration decreases when the fraction of the inelastically scattered radiation is significant. Even in the case of pyrolytic graphite for which this fraction is very small (about 1.5%) due to the small

yield of the inelastic scattering process the difference is detectable [1]. It is worth noting the scatterer induces no alteration in the shape, position and width of incident line. This proves that the acquisition system works correctly and is suitable for RSMR experiments.

References

[1] Enescu S. E., Bibicu I, Zoran V., Kluger A., Stoica A. D. and Tripadus V., Eur.Phys.J.AP **3**, 119 (1998)

Trace element and cutaneous cancer

C. Ciortea[1], A. Pantelică[1], O. Constantinescu[1], I. Cata Danil[1], D. Flueraşu[1], D.E. Dumitriu[1], A. Enulescu[1], I. Piticu[1], M.M. Gugiu[1], A.T. Dumitrescu[1], K. Gasparova[1], M. Ciortea[2], A. Popa[2], Ganea A. Sauteanu[3], B. Burghelea[4], E. Popescu[2], D. Donciu[2], A. Moldovan[2], L. Popescu[2], D.J. Diaconu[3]

[1] "Horia Hulubei" National Institute of Physics and Nuclear Engineering, P.O. Box MG-6, RO 76900 Bucharest, Romania

[2] "Carol Davila" Medicine and Pharmacy University,"Prof. Dr. Ovidiu Marina" Clinical Hospital, Sf. Dumitru 2, Bucharest, Romania

[3] "Carol Davila" Medicine and Pharmacy University, "Prof. Dr. Scarlat Longhin" National Center for Dermal-Venereal Diseases, Calea Serban Voda 216, Bucharest, Romania

[4] Cantacuzino Institute, Splaiul Independentei 103, P.O. Box 1-525, RO 70100 Bucharest, Romania

The mineral macro- and micro-elements are playing essential biological roles, as for example: some are co-factors of enzymes, or act as organizers of the molecular structures of the cell, or have an important role in ionic transport; some could be even beneficial as anti-tumor agents. Their concentration status in the organism is closely linked to: the long-term dietary intake, the environmental exposure, e.g. cumulative exposure to chemicals from industrial sources could increase the incidence of skin cancer, the health profile of the concerned subject. The research objective consisted in the examination of the content levels of some micro- and macro-elements found in the tumor tissue of patients having skin cancer disease, namely basal cell carcinoma (BCC), squamous cell carcinoma (SCC), malignant melanoma (MM), as well as benign tumor nevi. The analytical method of proton induced X-ray emission (PIXE) was used. Sample preparation and PIXE measurements The skin samples were collected from 22 cancer patients, aged 32-88 years, 11 males and 11 females. Controls were health skin samples (histopathological diagnose) from patients having skin cancer. The samples were freeze-dried and then mineralized for PIXE analysis, using nitric acid at 1200 temperature. The internal standard (Yttrium) technique was used for quantitative determination. Thin targets were measured in vacuum using a 3 MeV proton beam delivered by the Van de Graaff Tandem accelerator of the Institute of Physics and Nuclear Engineering in Bucharest - Magurele. A collimated beam (of 3 mm diameter) bombarded the target oriented at an angle of 450 with respect to the beam direction. The beam current entering the scattering chamber was maintained at several nAs. The samples were typically irradiated for a collected charge of 10 ?C. The emitted X-rays have been detected by a Canberra Ge(HP) detector with energy resolution of 180 eV / 5.9 keV placed perpendicular to the beam direction. Data manipulation and storage were performed with a Canberra S100 counting system, based on an IBM personal computer. For efficiency calibration, samples of known concentrations prepared in our laboratory were used. To calculate elemental concentrations, the ratios of element/standard (Yttrium) peak areas, detector efficiency, and X-ray attenuation in Be windows (reaction chamber and detector) as well as in air were taken into account. The results obtained for tumor samples were compared with those for normal samples (histopathological diagnose) from patients having skin cancer (control group). In spite of large standard deviations, the present results put in evidence the following: - a large significant increase (within the error bars) of P, S and K concentrations in all tumor samples (ratios between 2.3 ± 0.7 and 9.1 ± 6.6); - a large increase of Ca and Zn concentrations in nevi (6.1 ± 3.3 and 2.3 ± 1.6, respectively), and of Fe concentrations in BCC, MM and nevi (6.2 ± 5.7, 3.3 ± 2.5 and 4.0 ± 1.6, respectively); some of these elevated concentrations have been found previously, e.g. Zn in skin carcinoma [1] - levels of Cl, Ti, Cr, Mn and Cu not significantly different (in the limits of rather large standard deviations of present results) in the tumor compared

to control samples. The present preliminary results obtained for only a limited number of samples should be confirmed in more cases before we could definitely conclude. If higher concentration levels of P, S, K, Fe and possible Zn in tumor compared to normal tissue will be confirmed by future analyses, then this result is similar to that found for Mg [2] The element capture by the tumor is due to a greater need of it in the growing tumor tissue. As a result, a depletion of these elements in the healthy tissue is possibly occurring.

References

[1] Allen R.O., Steinnes E., Baker M.D., *Proc. Int. Symp. on Nuclear Activation Techniques in the Life Sciences, 1978* -IAEA, Vienna, 1979, 447

[2] Collery P., Anghileri L. J., Coudoux P., Durlach J., *Magnesium Bull.* **3**, (1981) 11-20

Data processing and inter-comparison of analytical results obtained by INAA, PIXE and ICP-MS

C.L. Dinescu[1], C. Ciortea[1], E. Steinnes[2], T. Sjobakk Eidhammer[2], O.G. Duliu[3], D.E. Dumitriu[1], M.M. Gugiu[1], D. Fluerașu[1], M. Haralambie[1], N.GH. Mihailescu[4]

[1] Horia Hulubei National Institute of Physics and Nuclear Engineering, Magurele, P.O. Box MG-6, RO-76900 Bucharest, Romania

[2] Norwegian University of Science and Technology Department of Chemistry, N-7491 Trondheim, Norway

[3] University of Bucharest, Department of Atomic and NuclearPhysics, Magurele, P.O. Box MG-11, RO-76900 Bucharest, Romania

[4] Geological Survey of Romania, Caransebes St. 1, RO-78344 Bucharest, Romania

Expanding industrial activity over recent decades has regularly introduced heavy and toxic metals, fertilizers or pesticides in any ecosystem [1]. At the same time, nuclear weapon tests or nuclear power station accidents discharged significant amounts of radioactive material into the environment. Once released, these pollutants enter atmospheric and hydrological circulation and are finally deposited on river beds, in reservoirs, deltas and in the marine environment where both lacustrine and marine sediments, continuously enriched by all kinds of pollutants, become a sui generis archive for the past history of contamination processes. Therefore, the investigation of the distribution of pollutants in sedimentary cores can furnish useful information concerning these processes. The Danube Delta represents a flat region, with a surface of 5,640 km^2. More than 150 lakes and bogs are spread over the entire Delta. Both morphologically and by taking into account recent history (the last 10 000 years), the Danube Delta can be divided into two regions: Fluvial (western part) and Fluvial-marine (eastern part and the Razelm-Sinoe lacustrine complex). The bottom sediments of almost all lakes of Danube delta are intensively bio-disturbed by the living activity of various invertebrates which spend their life cycle buried in the mud [2] This fact also contributes to the dissemination of pollutants within the sediments. Two sediment cores collected in the lakes Mester and Furtuna, in an active sedimentation zone, one core from channel Sontea and three soil samples, all located in Danube Delta, have been analyzed by using Instrumental Neutron Activation Analysis (INAA), Thick Target Proton Induced X-ray Emission (TTPIXE) and Induced Coupled Plasma Mass Spectrometry (ICP-MS) methods. Continuously increasing number of multi-partner projects involving different countries made date exchange inevitable which in turn needs much more care in comparing data from various laboratories. One criterion for establishing whether an element represents a pollutant is the analysis of its vertical profile in the soil or sediment under investigation. In the absence of any noticeable mixing or revoking of the sediments, the presumed pollutants present increased concentrations in the upper, more recent, layers of the sediments [3] Concentrations of 25 elements by using INAA, 13 elements by TTPIXE and 36 elements by ICP-MS have been determined. The vertical distribution of these elements in the three analyzed cores was obtained. In addition to the elements identified previously by INAA (Zn, As, Sb, Br) and TTPIXE and ICP-MS (Cu, Pb, Zn) as potential pollutants (by taking into consideration their vertical distribution), other elements were put in evidence as potential pollutants by using ICP-MS: Cd, Hg, Tl. The vertical distribution of V and Al do not show significant variation with depth, while Ni concentrations show increased values with depth. The top layer concentrations for Zn, Cu, As, Sb, Br, Pb and Tl are 1.5 to 3 times larger than in the lower part of the core, while the concentrations of Cd and Hg are 5-7 times larger,

but according to the Romanian Regulations, the sediments can not be considered as polluted. The vertical profiles of the other elements are characterized by a relatively uniform distribution along the cores. The element concentrations determined in the soil samples are generally much lower than those in the lacustrine sediments. They do not show significantly increased values at surface as compared to the 30 cm depth, arguments favoring the conclusion that, within the limits stated by Romanian Regulations, no pollution of the measured soil samples from Danube Delta was found.

References

[1] Steinnes E.: *Lead, mercury, cadmium and arsenic in the environment*, eds. T.C. Hutchinson and K.M.Meema, J.Wiley & Sons, NY 107-117

[2] Duliu O.G. and Mihailescu N.G., *Acta Geologica Hungarica* **41** (1998), 121

[3] Mahaney W.C. and Hancock R.G.V., *J. Radioanal.Nucl.Chem.Articles* **148** (1991) 91

Inner-shell vacancy production and multiple ionization effects in 0.1-1.75 MeV/U Mn, Fe, Co, Ni, Cu + Au, Bi collisions

C. Ciortea[1], I. Piticu[1], D.E. Dumitriu[1], D. Fluerașu[1], A. Enulescu[1], S.E. Enescu[1], M.M. Gugiu[1], A.T. Dumitrescu[1]

[1] National Institute of Physics and Nuclear Engineering "Horia Hulubei", 76900 Bucharest, Romania

Vacancy production in 0.1-1.75 MeV/u Mn, Fe, Co, Ni, Cu + Au, Bi collisions has been studied by measuring integral inner-shell ionization cross sections and mean outer-shell ionization probabilitie. X-ray spectra induced by ion beams of Mn, Fe, Co, Ni and Cu impinging on thin solid-foil targets of Au and Bi have been measured. Total ionization cross sections for the K-shell of the projectile and L_3-subshell of the target, as well as vacancy sharing probabilities, corrected for the effect of multiple ionization, are reported. The experimental results are discussed in terms of two model calculations. In slow, moderately asymmetric collisions, the general tendency of inner shell ionization cross sections can be understood within the concept of electron promotion and vacancy sharing [1]. In particular, for collision partners with matching of their K and L energy levels, the dominant process of inner shell vacancy production is the ionization of the highly promoted $3d\sigma$ molecular orbital (MO) at small inter-nuclear distances followed by the sharing of the primary vacancy among the K- and L- shells of the partners [2]. The ionization of the $3d\sigma$ MO has been successfully interpreted within Briggs model [3]. Studies of the impact parameter dependence revealed the contribution to the inner shell ionization of other processes as direct excitation of the $2p_{3/2}\sigma$ MO. Due to the the copious production in these collisions of multiple ionization of the outer shells, the extraction of inner shell vacancy production cross sections from the X-ray yields is influenced by the modifications of the fluorescence yields and relative decay widths. We report cross section values corrected for these multiple ionization effects. A model calculation within the Briggs model [3], which uses the SCA-UA computer code of Trautmann and colab. [4], gives a fairly good agreement with the experimental data of $3d\sigma$ MO vacancy production for the collision Ni+Bi as in Fig.1. The vacancy sharing probabilities for one set of the collision systems studied here are given in the Fig 2. For a two-state problem, the sharing probabilities were described by the exponential model of Nikitin [5]. The Nikitin's transition probability at zero impact parameter can be approximated to a few percent by an exponential dependence in function of reciprocal collision velocity. As shown by data, in the measured velocity range, only for the Mn + Bi collisions the sharing probability has the predicted dependence, while for the other cases the better is the K-L level matching, the larger is the difference from an exponential behavior.

References

[1] W.E.Meyerhof, *Phys. Rev. Lett.* **31** (1973) 1341.

[2] W.E.Meyerhof et al., *Phys. Rev.* **A17** (1978) 108.

[3] A. Warczak et al., *J. Phys.* **B16** (1983) 1575.

[4] D. Trautmann et al., *Nucl. Instr. Meth.* **214** (1983) 21

[5] E.E. Nikitin, *Opt. Spektrosk.* **13** (1962) 761

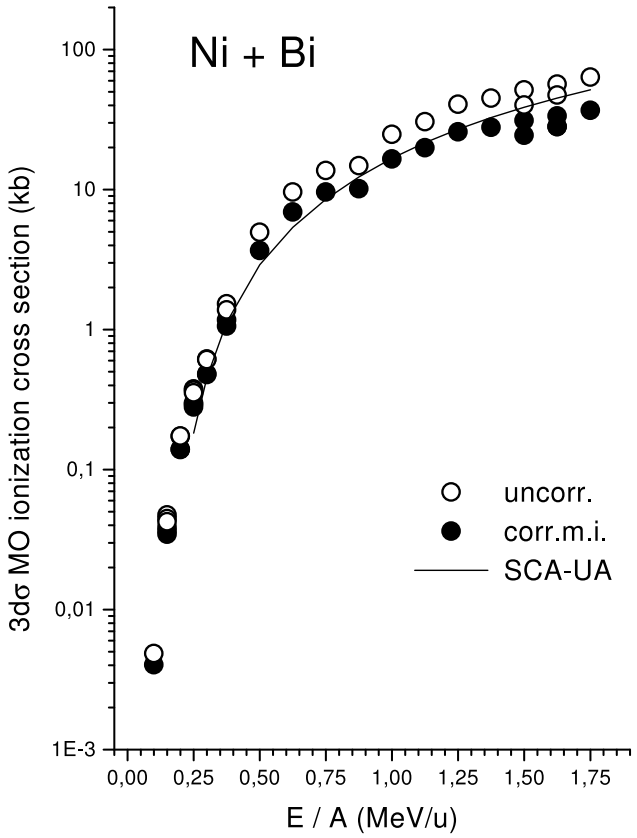

Figure 1: Ionization cross sections of the 3dσ molecular orbital transiently formed during the collision Ni+Bi in dependence of bombarding energy. Values corrected (full symbols) and uncorrected (open symbols) for multiple ionization effects are given. The solid curve gives the predictions of SCA-UA model [4]

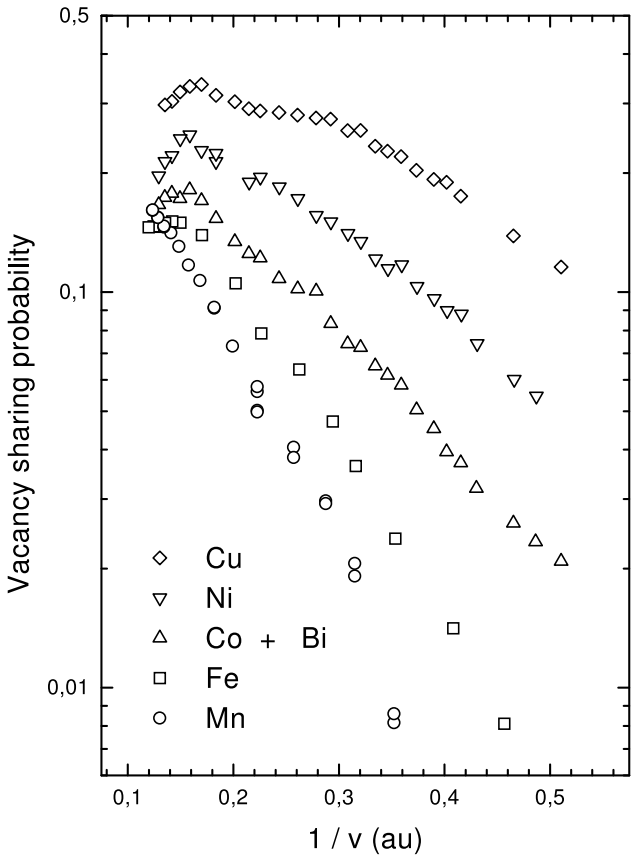

Figure 2: 3dσ-3p$_{3/2}$ σ molecular orbitals vacancy sharing probabilities determined for the collisions Mn, Fe, Co, Ni and Cu + Bi in dependence of reciprocal collision velocity.

Cosmic Rays and Nuclear Astrophysics

The east-west effect of the muon charge ratio at energies relevant to the atmospheric neutrino anomaly

B. Mitrica[1], I.M. Brancus[1], J. Wentz[2], B. Vulpescu[1,3], M. Petcu[1], H. Bozdog[4], H. Mathes[2], H. Rebel[2], F. Badea[1,2], A. Bercuci[1,2], C. Aiftimiei[1], M. Duma[1], G. Toma[1]

[1] National Institute of Physics and Nuclear Engineering - Horia Hulubei
[2] Forschungszentrum Karlsruhe, Institut für Kernphysik
[3] Universität Heidelberg, Physikalisches Institut
[4] Forschungszentrum Karlsruhe, Institut für Reaktorsicherheit

During the propagation of cosmic rays in the atmosphere by the interactions with atmospheric nuclei, pions and kaons are produced, which subsequently decay in muons and neutrinos: Considering the decay chains, it is obviously that the ratio of positive to negative atmospheric muons, called the muon charge ratio: $R_\nu = \mu^+/\mu^-$ maps the neutrino production and carries information on the hadronic interactions, used in the calculations of atmospheric neutrino. Measurements of the charge ratio of atmospheric muons at low energy reveal information of interest for the atmospheric neutrino anomaly [1].

Measurements of EAST-WEST effect of the muon charge ratio, allow to check different models for the hadronic interaction and investigate the influence of the Earth's magnetic field [2].

The WILLI detector (Fig.1), built in IFIN-HH Bucharest measures the charge ratio by the effective life-time of the stopped muons. While positive muons make a free decay with natural life, negative muons built muonic atoms, leading to a shorter life time of negative muons [3].

The measured decay curve of all muons is a superposition of several decay laws [3, 4], containing 3 detector dependent constants, accounting for the stopping power in the materials and the detection efficiencies, which are determined by extensive detector simulations using GEANT.

The investigation of the directional dependence of the muon charge ratio has been started with measurements in the East and West direction at a mean zenithal angle of 35°.

Introducing the azimuthal anisotropy $A_{EW} = (R_W - R_E)/(R_W + R_E)$ with R_W and R_E being the muon charge ratios measured in East and West direction, the preliminary results show a pronounced East-West effect [5].

Direction	$\langle p_\mu \rangle$ [GeV/c]	$\langle \Theta \rangle$ [°]	R(μ^+/μ^-)	ΔR
East	0.32	35	0.87	0.02
	0.36	35	0.88	0.02
	0.49	35	0.88	0.02
West	0.32	35	1.49	0.04
	0.36	35	1.52	0.04
	0.49	35	1.46	0.04

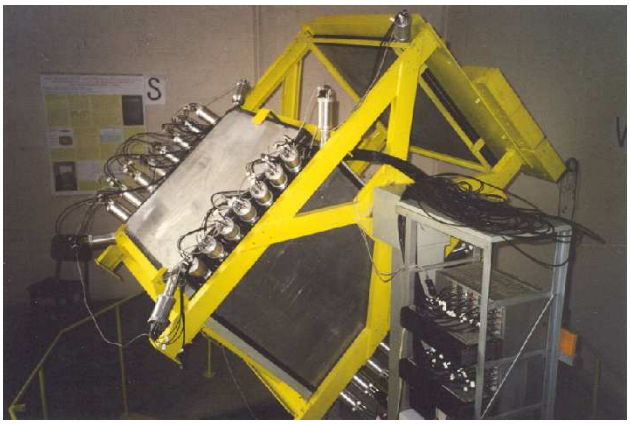

Figure 1: WILLI

References

[1] Y. Fukuda et al., Phys. Rev. Lett. 81 (1998) 1562; Phys. Lett. B436 (1998) 33

[2] J. Wentz et al., J. Phys. G: Nucl. Part. Phys. 27 (2001) 1699

[3] B. Vulpescu et al., Nucl. Instr. Meth. A414 (1998) 205

[4] B. Vulpescu et al., J. Phys. G: Nucl. Part. Phys 27 (2001) 977

[5] B.Mitrică, Diploma Thesis (2002)

Preshower detector and the DIRAC experiment (CERN)

M. Penţia [1], Gh. Caragheorgheopol [2], S. Constantinescu [3], C. Curceanu [4], M. Iliescu [4], T. Ponta [5], D. Pop [6]

[1] NIPNE-HH, Nuclear Physics Department
[2] NIPNE-HH, Applied Nuclear Physics Department
[3] NIPNE-HH, Informatics and Computing Center
[4] NIPNE-HH & INFN - Frascati, Italy
[5] NIPNE-HH, Particle Physics Department
[6] NIPNE-HH & CERN - Geneva, Switzerland

The main goal of the DIRAC Experiment at CERN [1] is to measure the lifetime of $\pi^+\pi^-$ atom (*pionium*), of some $fsec$, with 10% precision. The Preshower Detector (PSh) [2] is a subdetector designed, commissionned and used in DIRAC Experiment by the NIPNE-HH Bucharest group. It is included in the main DIRAC trigger system and along with the Cherenkov Detector, it provides the electron/pion separation.

The *pionium* is produced in proton (24 GeV) interaction with Ni or Ti target. The resulted pion pairs from primary interaction, can form a $\pi^+\pi^-$ bound state by Coulomb interaction in the final state, if the relative distance between π^+ and π^- is of order $\sim fm$. The relativistic pionia, moving in the target, can breakup, giving raise to the so called "atomic pairs". These characteristic $\pi^+\pi^-$ pairs, with low relative momentum ($Q < 2MeV/c$), are the main signals the DIRAC Experiment is looking for. The ratio between the produced "atomic pairs" N_A and Coulomb pairs N_C is a model-independent value.

From the experimental point of view, the "atomic pairs" must be separated off other real pairs (real coincidences) comming either from correlated pairs by Coulomb interaction in the final state or from particle decays. They can be distinguish by specific relative momentum distributions.

To separate such different processes in the presence of a high e^+e^- background, DIRAC uses a multilevel trigger system [3]. The PSh is included both in the fast T0 pretrigger, in the first level trigger T1, and also in the highest neural network triggers DNA and RNA.

In offline data analysis the PSh Detector is using to reject especially the high electron background. This function requires a throughout amplitude analysis. In such a way it has been done the *PSh Detector signal alignment*. This includes the study of amplitude dependence on detector slab inhomogeneities, particle impact position and some external influences, both for pion and electron signals. Finally, we found a linear correction for PSh amplitude: $A = (A_{raw} + a) \times b$, for each ADC channel.

During 2001 runs at the CERN Proton Synchrotron, DIRAC performed about 6 months successfull data taking with fully operating experimental apparatus.

Preliminary analysis of the 2000 and 2001 statistics has lead to the identification of 4920 ± 270 and 1830 ± 160 "atomic pairs" coming from the breakup of pionium atoms in Ni and Ti target, respectively.

From the detected signals a determination of the pionium lifetime was performed. The preliminary results, including only statistical errors, are presented in Fig. 1. A rough estimation of the pionium lifetime gives $\tau = 2.8^{+1.1}_{-0.8} \times 10^{-15}$ sec.

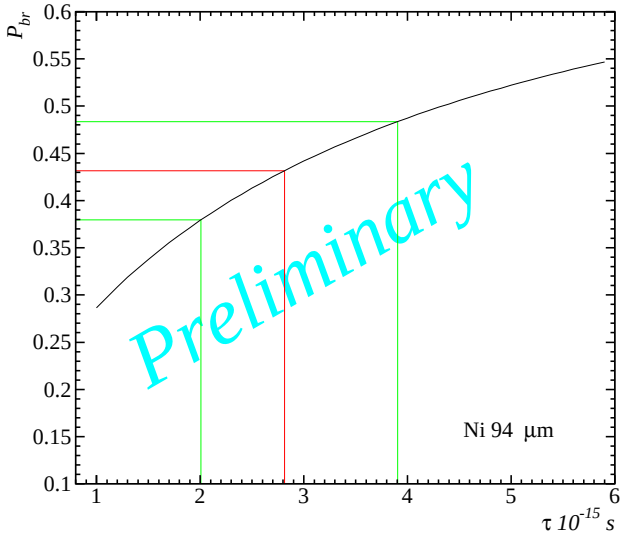

Figure 1: Estimated pionium lifetime

References

[1] B. Adeva et al. - DIRAC Group, Proposal to the SPSLC, *Lifetime measurement of $\pi^+\pi^-$ atoms to test low energy QCD prediction*, CERN/SPSLC 95-1, SPSLC/P 284 (1995).

[2] H. Bozdog, Gh. Caragheorgheopol, M. Penţia, V. Zoran, S. Trusov, *Preshower Scintillation Detector for DIRAC Experiment* (experimental results), DIRAC Note 98-03, 25 Feb. 1998.

[3] L. Afanasyev, et al., *The Multilevel Trigger System of the DIRAC Experiment*, e-print archive: hep-ex/0202045.

[4] P. Kokkas et al. (DIRAC Collaboration), *Dimeson lifetime measurement with DIRAC at CERN*, Proc. Int. Workshop on Chiral Fluctuations in Hadronic Matter, 26-28 September 2001, INP Orsay [France].

Algorithms for reconstruction of shower core and arrival direction of extensive air showers

G. Toma[1], I.M. Brancus[1], J. Wentz[2], B. Mitrica[1], B. Vulpescu[1,3], M. Petcu[1], H. Bozdog[4], H. Mathes[2], H. Rebel[2], F. Badea[1,2], A. Bercuci[1,2], C. Aiftimiei[1], M. Duma[1]

[1] National Institute of Physics and Nuclear Engineering - Horia Hulubei
[2] Forschungszentrum Karlsruhe, Institut für Kernphysik
[3] Universität Heidelberg, Physikalisches Institut
[4] Forschungszentrum Karlsruhe, Institut für Reaktorsicherheit

Two important observables that describe extensive air showers are the center of particle distribution in the shower front(the center of gravity of the particle distribution) and the arrival direction (the zenital and azimuthal angle of the shower axis) [1].

A program was made that, using results given by CORSIKA simulations, reconstructs the center of the EAS front and the arrival direction as well. The program uses different algorithms and also a study of reconstructing efficiency has been done for each algorithm or even for the same algorithm relative to where an extensive air shower hits the detector array. As geometrical model for the detector array, the KASCADE - Grande detector array (Karlsruhe, Germany) has been used [2].

The reconstruction of the center of the shower front has been done by using an algorithm that calculates the center of gravity of particle mass distribution in detectors. A good reconstruction efficiency has been achieved for showers hitting near the center of the array and also an increase in the reconstruction error as the shower front hits the array closer to the border. The arrival direction reconstruction algorithms used as imput data the arival time of particles in detectors and approximated the shower front with a plane, a conic or a spherical surface. Efficiency of these algorithms has also been studied [3].

References

[1] A.F. Badea, Temporal Structure of the Muon Component of Cosmic Rays Extensive Air Showers, march 2001

[2] I.M. Brancus, Phenomenology of Extensive Air Showers, NATO Science Series (2001) 361

[3] G. Toma, Diploma Thesis (2002)

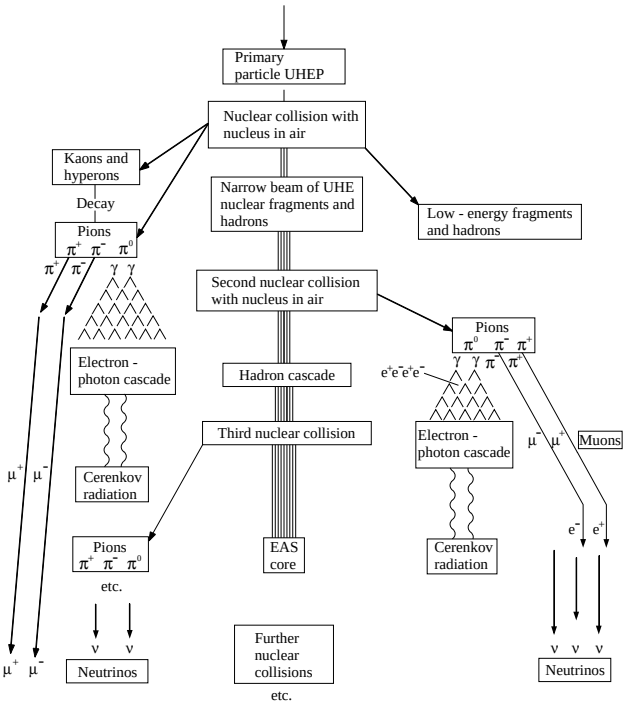

Figure 1: Extensive Air Showers

The charge ratio of the atmospheric muons as probe for azimuthal asymmetry

B. Mitrica[1], I.M. Brancus[1], J. Wentz[2], M. Petcu[1], H. Rebel[2], A. Bercuci[1,2], C. Aiftimiei[1], M. Duma[1], G. Toma[1]

[1] National Institute of Physics and Nuclear Engineering - Horia Hulubei
[2] Forschungszentrum Karlsruhe, Institut für Kernphysik

1. The problem

The charge ratio of the atmospheric muons is a quantity sensitive to hadronic interactions of cosmic rays and to the influence of the geomagnetic field. Experimental information is of current interest for tuning models used for the calculation of atmospheric neutrino fluxes [1]. We are performing measurements of the charge ratio based on the observation of the lifetime of the muons stopped in the absorber layers (aluminum support) of the detector WILLI, mounted in a rotatable frame and installed in IFIN-HH Bucharest (vertical geomagnetic cut-off rigidity of 5.6 GV) [2, 3] .

2. The results

Our method to determine the muon charge ratio by measuring the lifetime of muons stopped in the matter, overcomes the uncertainties appearing in measurements based on magnetic spectrometers, which are affected by systematic effects at low muon energies, due to problems in the particle and trajectory identification. The results obtained with the rotatable WILLI detector, inclined at 45° [4, 5] (i.e. a mean zenith angle of detected muons of 35°) show a pronounced east-west effect, in good agreement with simulation results of CORSIKA. The values of the asymmetry of the charge ratio decreases from 0.25 to 0.20 in the muon momentum range of 0.35-0.50 GeV/c, relevant to the atmospheric neutrino anomaly [6].

References

[1] Wentz J. et al, **2001, J. Phys. G 27, 1699**

[2] Vulpescu B., **1998, Nucl. Instr. Meth. A 414, 205**

[3] Vulpescu b. et al, **2001, J. Phys. G 27, 977**

[4] Mitrica B., **2002, Diploma thesis**

[5] Brancus I.M., **2002, Report WP17 IDRANAP 18-02**

[6] Futagami T., **1999, Phys. Rev. Lett. 82, 5194**

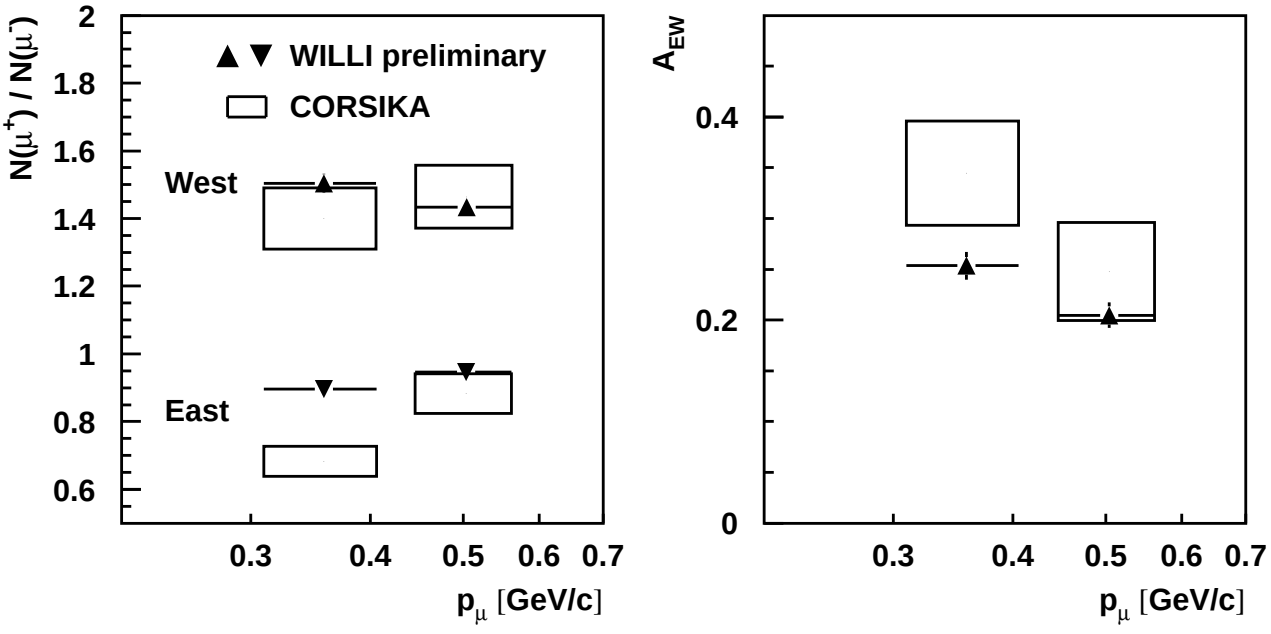

Figure 1: Energy dependence of the east-west effect in the muon charge ratio.

Studies of the lateral distribution of extensive air showers (EAS) particles

G. Toma[1], F. Badea[1,2], A. Haungs[2], H. Rebel[2], I.M. Brancus[1], B. Mitrica[1], T. Thouw[2]

[1] National Institute of Physics and Nuclear Engineering - Horia Hulubei
[2] Forschungszentrum Karlsruhe, Institut für Kernphysik

The lateral distributions of EAS particles has been investigated using CORSIKA simulations for 150 showers initiated by H, C and Fe primaries for the energy 10^{16}eV[1]. In order to express the variation of the lateral density of particles, a generalization of the NKG function has been used [2]:

$$\Delta = \frac{N}{R_0^2} C(\alpha,\eta) \left(\frac{R}{R_0}\right)^{-\alpha} \left(1+\frac{R}{R_0}\right)^{-(\eta-\alpha)}$$
$$C = \Gamma(\eta-\alpha)\left[2\pi\Gamma(2-\alpha)\Gamma(\eta-2)\right]^{-1}$$

and

Δ – the particle density at a distance R from the shower axis
N - the shower size (in our case the total number of electrons and muons)
R_0 - Molliere radius; R_0 has been given a value of 92m for this study
R - radius
α, η - two parameters.

A suitable set of parameters α and η is expected to describe rather accurately the lateral density distribution from distances of a few meters to several kilometers from the shower axis, see Fig.1.

Also the η parameter is expected to be primary mass sensitive, see Fig.2.

References

[1] G. Toma, A. F. Badea, A. Haungs, H. Rebel, T. Thouw, *Study of the Lateral and Temporal Structure of the Shower Front at KASCADE Grande Distances*, Internal report Forschungszentrum Karlsruhe, 2002

[2] J. Linsley, L. Scarsi, B. Rossi, *Energy Spectrum and Structure of Large Air Showers*, Journal of the Physical Society of Japan, Vol.17, Supplement A-III, 1962

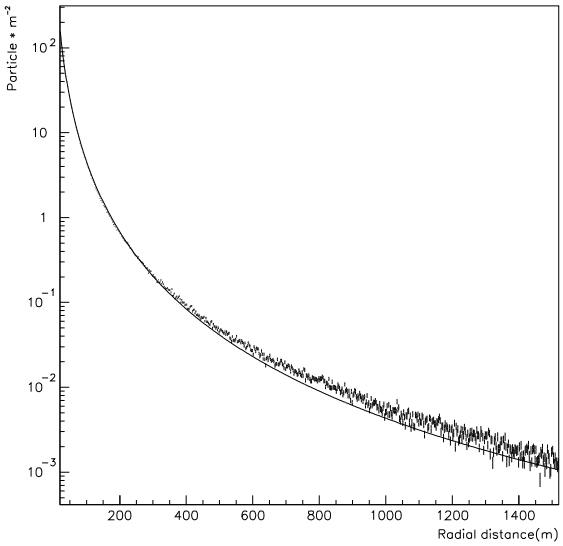

Figure 1: Lateral density distribution fit for a shower initiated by proton.

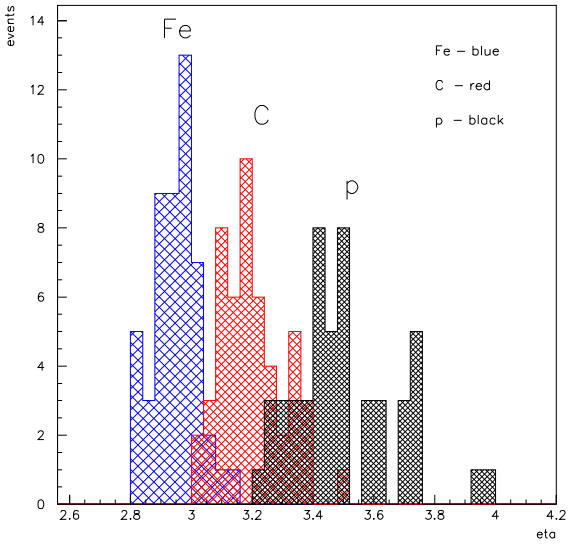

Figure 2: Distribution of η parameter for three different primaries (50 showers for each type of primary).

Inertial Fusion, Physics of Neutrons and Nuclear Transmutations

Influence of the H band modes on the rapid diffusion in Zr hydrides - a combined INS and QENS study

A. Rădulescu[1], R.E. Lechner[2], I. Padureanu[1], C. Postolache[3]

[1] NIPNE-HH, Dept.of Nuclear Physics, RO-76900 Bucharest, Romania
[2] Hahn-Meitner-Institut, BENSC, D-14109 Berlin, Germany
[3] NIPNE-HH, Radioisotope Production Center, RO-76900 Bucharest, Romania

By QENS performed on $ZrH_{0.1}$ the rapid H diffusion was first time observed in Zr hydrides. The model interpretation of the experimental data provided the characteristic parameters of such a process, the mean residence time τ and the jump length l. The dependence of τ plotted on a logarithmic scale against inverse temperature (Fig.1) yields according to

$$\tau = \tau_0 exp(E_a/k_B T) \quad (1)$$

an activation energy E_a=48 meV for the proton jumps between the available positions.

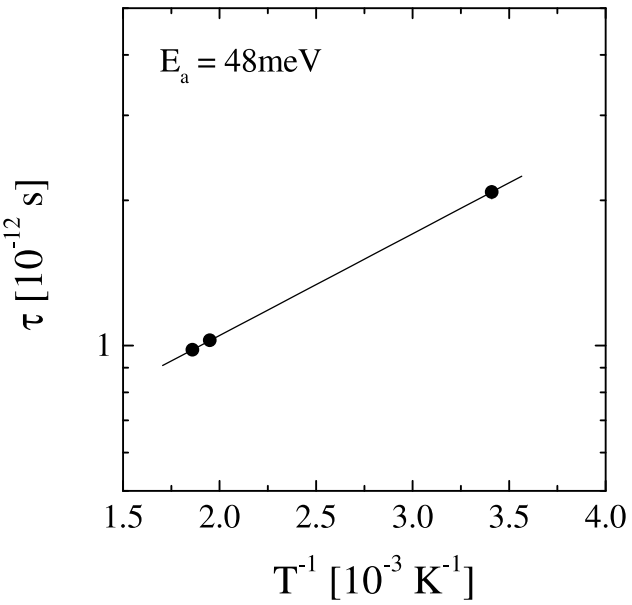

Figure 1: The temperature dependence of the mean residence time for the jump diffusional process of the protons in Zr lattices

Such a very low value for the activation energy of a H diffusional process in a metallic lattice was reported by QENS only for hydrogen in vanadium [1]. Although the rapid H diffusion is usually activated by lower energies than the long-range translational diffusion nevertheless, the typical values stand around 100-200 meV. The rapid H diffusion in Zr was never observed so far and it is worthy to mention that in case of V-H system such a process was also measured by other methods, like 'Gorski' effect (the anelastic relaxation) [2]. Trying to explain this effect in case of Zr-H system we will deal with the Debye-Waller factor $exp\{-Q^2 < u^2 >\}$ that accounts for the form factor given by the vibrational motions of the proton at the interstitial site with the mean square amplitude given by the two kinds of vibrations the proton performs in a metallic lattice, the high-frequency localized modes in the range of the optical phonons and the band-modes within the range of the host lattice acoustic phonons

$$< u^2 >=< u^2 >_{band} + < u^2 >_{local} \quad (2)$$

Generally, assuming that $< u^2 >_{band}=< u^2 >_{host}$ one gets

$$< u^2 >= \hbar/2M_H\omega_{loc} + 3k_B T/M_{host}\omega_D^2 \quad (3)$$

where $\hbar\omega_D$ is the maximum energy (Debye limit) of the lattice vibrations, $\hbar\omega_{loc}$ is the energy of the proton local vibrations and k_B represents the Boltzmann's constant. For this system low-energy vibrations additional to the lattice dynamics were reported by INS [3]. This effect was attributed entirely to the presence of H and from a parallel analysis of the INS and QENS results obtained so far we are inclined to think that it strongly influences the diffusional process. According to [4] the band modes give an important contribution to the thermal mean-square displacement of the H and leads to activation energies for a jump diffusional process distinctly smaller than the excitation energies of the local modes. The $< u^2 >$ experimentaly obtained from the variation of QENS intensity with Q deviates significantly from the calculated one according to Eq.3.

One can conclude that the band modes have a different contribution to the mean square amplitude than the host lattice acoustic modes and implicitly, the ratio $g_{band} < u^2 >_{band} / g_{host} < u^2 >_{host}$ is larger than the unit in case of this Zr-H system. Thus, the extremely low activation energy of the rapid H diffusion is ascribed to the increased thermal mean-square displacement of the proton due to the additional low-energy vibrational effect characteristic to H band modes.

References

[1] J.M.Rowe, K.Sköld, H.E.Flottow and J.J.Rush, J.Phys.Chem.Solids **32**, 41 (1971).

[2] G.Schauman, J.Völkl and G.Alefeld, phys.status solidi **42**, 401 (1970).

[3] A.Radulescu, R.Lechner, I.Padureanu and C.Postolache, Appl.Phys.A (in press 2002).

[4] V.Lottner, H.R.Schober and W.J.Fitzgerald, Phys.Rev.Lett. **42**, 1162 (1979).

Rapid H diffusion in low concentration Zr hydrides observed by quasielastic neutron scattering

A. Rădulescu[1], R.E. Lechner[2], I. Padureanu[1], C. Postolache[3]

[1] NIPNE-HH, Dept.of Nuclear Physics, RO-76900 Bucharest, Romania
[2] Hahn-Meitner-Institut, BENSC, D-14109 Berlin, Germany
[3] NIPNE-HH, Radioisotope Production Center, RO-76900 Bucharest, Romania

Many efforts were dedicated in the past to study the diffusive motions performed by the proton in different Zr host lattices either by NMR, internal friction measurements, ^{15}N nuclear reaction method or mechanical spectroscopy. Nevertheless, the microscopic diffusion mechanism is still not exactly known. No QENS (quasielastic neutron scattering) investigation was reported so far on a low H content Zr hydride. Such a technique offering a powerfull probe for the simultaneuos measurement of both the time and the space development of the elementary step in the diffusion process could bring more usefull information to complete and clarify the H or D diffusion in Zr hydrides and deuterides. Information in this regard is obtained from a study of the detailed shape of the neutron scattering function at small energy transfers and over a range of wave vector transfers. The width of the peak centered at zero energy transfer (the 'quasielastic peak') is proportional to the jump rate. Information about the geometry of the interstitial sites over which diffusing atoms move is obtained from the variation of the width of the quasielastic peak with the wave vector transfer Q. By measuring the variation of the intensity of the quasielastic scattering with wave vector transfer, information is obtained about the spreading out of a proton due to the thermal motions at the equilibrium site. The Chudley-Elliott model [1] applied for polycrystalline samples gives the width of the QENS intensity as

$$\Gamma(Q) = (1/\tau)[1 - \frac{sin(Ql)}{Q}] \qquad (1)$$

where l is the jump length and τ the mean residence time. In the low-Q limit an expansion of this in terms of (Ql) provides the self-diffusion constant D_S by

$$\Gamma(Q) = \frac{Q^2 l^2}{6\tau} = Q^2 D_S \qquad (2)$$

A microscopic study of the diffusive motions was performed by QENS on a $ZrH_{0.1}$ sample prepared in such a manner in order to obtain the γ-hydride as a prevalent phase. The measurements have been carried out at 293, 511 and 538 K by using the NEAT time-of-flight (TOF) spectrometer [2] set-up at the BERII reactor of the Berlin Neutron Scattering Center. Details about the sample preparation and experiments are reported in [3]. The HWHM of the measured quasielastic components were plotted as a function of the squared wavevector transfer (Fig.1) and fitted by Eq.1 assuming a jumping motion performed by protons between the interstitial sites. The fitting procedure gives the characteristic parameters of the diffusional process, the mean residence time τ and the jump length l. From the obtained values the self-diffusion constant D_S was further calculated by using Eq.2.

The very short residence time and accordingly, the very high self-diffusion constant (comparable with those for diffusion in liquids) are typical for the rapid

H diffusion in a metallic lattice. So far, such a process was observed in Pd-H, Nb-H, V-H and Ta-H systems by QENS [4].

References

[1] C.T.Chudley and R.J.Elliott, Proc.Phys.Soc. **77**, 353 (1960).

[2] R.E.Lechner, Physica B **180**, 973 (1992).

[3] A.Radulescu, R.Lechner, I.Padureanu and C.Postolache, Appl.Phys.A (in press 2002).

[4] D.K.Ross in *Topics in Applied Physics*, Vol.73 (ed. H.Wipf), Springer-Verlag Berlin Heidelberg 1997, pp. 153.

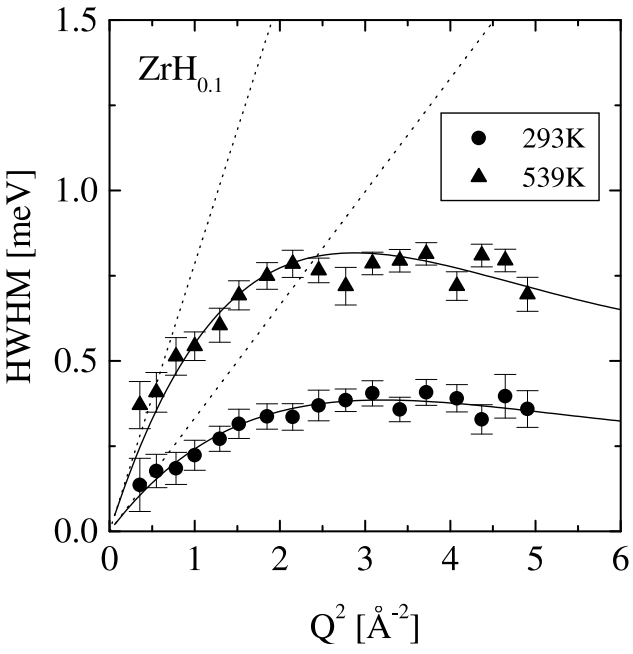

Figure 1: The exeprimental width of QENS line vs. Q^2 at 293 and 539K. The continuous lines represent the fitting of the data according to Eq.1 while the dotted lines denote the $D_S Q^2$ law (Eq.2).

Asymmetric magnetization reversal on exchange biased CoO/Co bilayers

F. Radu[1,2], M. Etzkorn[2], T. Schmitte[2], R. Siebrecht[2,3], K. Westerholt[2], H. Zabel[2]

[1] Departamentul de Fizica Nucleara, Institutul de Fizica si Inginerie Nucleara, 76900 Magurele, Romania
[2] Institut fur Experimentalphysik/Festkorperphysik, Ruhr-Universitaet Bochum, D-44780 Bochum, Germany
[3] Institute Laue-Langevin, 38042 Grenoble cedex 9, France

The exchange bias (EB) phenomenon is associated with an exchange coupling between a ferromagnetic (F) and an antiferromagnetic (AF) layer across their common interface, resulting in an unidirectional magnetic anisotropy and a shift of the magnetic hysteresis by an exchange bias field H_{EB} [1]. A remarkable effect related to the exchange bias is the asymmetry of the magnetization reversal, which is best revealed by neutron scattering [2].

Fig. 5a shows the magnetic hysteresis loop measured by MOKE (Magnetico-Optical Kerr Effect) at T=50 K, after cooling the sample $(CoO(30Å)/Co(200Å)/Ti/Cu/Al_2O_3))$in an applied field of +2000 Oe. Upon descending the field for the first time to negative values, an abrupt magnetization reversal is observed at the coercivity field H_{c1}. Ascending again to positive field values, the magnetization curve at H_{c2} is more rounded. In subsequent cycles the magnetization curves at H_{c1} and H_{c2} are of about the same shape characterised by $H_{EB} = 30$ Oe and $H_c = 200$ Oe. From these measurements we conclude that the first magnetization reversal of the virgin sample after field cooling is conspicuously different from any subsequent 'trained' reversals.

In order to gain more insight into the reversal mechanism in decreasing and increasing magnetic fields, we have performed polarized neutron reflectivity (PNR) measurements on Co/CoO bilayers, using the angle dispersive neutron reflectometer ADAM at the Institut Laue-Langevin, Grenoble with a fixed wavelength of 4.41 Å.

We first discuss the specular spin flip(I_{+-} and I_{-+}) intensities shown by triangles in panels (b) and (c) of Fig. 5. They were measured at the scattering vector

Q corresponding to the neutron resonance peak near the critical edge. The magnetization reversal at H_{c2} exhibits strong spin-flip intensities I_{+-} and I_{-+}. This is always observed for rounded or 'trained' hysteresis loops and is characteristic for a magnetization reversal via rotation. Magnetization reversal by rotation provides a large magnetization component perpendicular to the field or polarization axis, giving rise to neutron spin-flip process. Vice versa, the rather low spin-flip intensities, which are observed during the first magnetization reversal in the virgin state at H_{c1} are indicative of pure 180° domain wall movement. The step like intensity change at H_{c1} =-750 Oe [Fig. 5e] is followed by a steady decrease as the system approaches saturation. From these features it is obvious that domain wall nucleation and propagation let the magnetic spins at the interface canted away from the applied field direction. The non spin-flip (I_{++} and I_{--}) intensities(circles) are measured at another Q, close to the total reflection edge. They provide similar information as MOKE or SQUID. For more details see Ref: [2].

This work is supported by SFB 491.

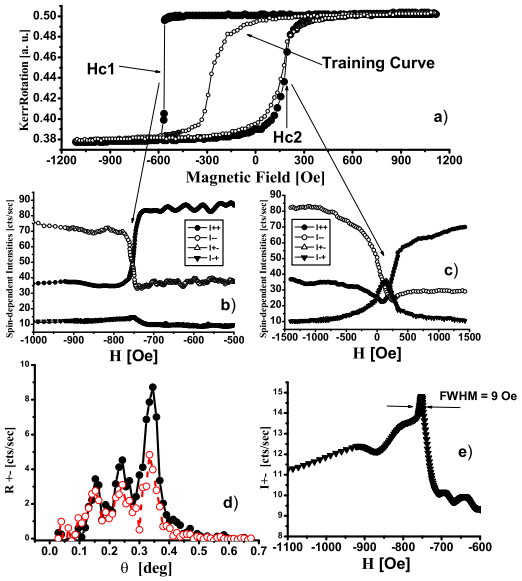

Figure 1: (a) MOKE hysteresis loop of a CoO/Co bilayer after field cooling to 50K in an external field of 2000 Oe. The black dots denote the first hysteresis loop, the open circles the second loop. Any further loops are not significantly different from the second. (b) and (c) Neutron hysteresis loops from the same sample but at 10 K. I ++, I–, I+- and I-+ are non-spin flip and spin-flip intensities as a function of external magnetic field. They are measured at special scattering vector values of the reflectivity curves (see text);(d) Off-specular diffuse spin-flip scattering taken at Hc1=-750 Oe (full dots) and in saturation at -1400 Oe (open dots). (e) Specular spin-flip at Hc1 enlarged from panel (b) for better recognition.

References

[1] W. Meiklejohn and C. P. Bean, Phys. Rev. **102**, 1413 (1956) ; **105**, 904 (1957).

[2] F. Radu, M. Etzkorn, T. Schmitte, R. Siebrecht, A. Schreyer, K. Westerholt, H. Zabel, J. Magn. Magn. Mater., **240**, 251 (2002).

Neutron scattering investigation of the local vibrations in transition metals

I. Pădureanu[1], D. Aranghel[1], Remy Khan[2]

[1] NIPNE-HH, Department of Nuclear Physics, Romania
[2] CEA, Laboratoire Leon Brillouin, Saclay, France

In this paper a study by inelastic slow neutrons scattering (INS) of the local vibrations of hydrogen in titanium based alloys containing vanadium and carbon is presented. The understanding of dynamics of the structure and lattice dynamics of a solid solution of hydrogen in transition metals as well as the rolle of tunnel sppliting have received great attention within the last two decades. At present these are the focus of an important number of experimental and theoretical investigations [1, 2]. It has been found in the earlier studies [3] and references therein that the solubility limit, for instance in niobium increases by substitution alloying with titanium, vanadium, chromium and molybdenum. Another question is whether the type of interstitial site changes in the presence of additional guest or impurity atoms. However it was found that hydrogen in niobium still occupies tetrahedral interstitial sites in the presence of the guest and impurity

atoms mentioned [4]. The exception is substitutional molibdenum. In the present experiment firstly we are following to determine the energies of the local vibrations of hydrogen in the mentioned samples. The INS is suitable for the study of interatomic interactions in solid solutions. The local modes of hydrogen have frequencies above the boundary of the host metal spectrum. In this case the positions of the local modes can give informations about the metal interstitial potentials and site positions. The changes in metal-metal interactions can be derived from the acoustic part of the INS spectrum, while the width of the local modes gives informations about interstitial - interstitial interactions in the solid solutions. Here we report the preliminary results obtained from an INS experiment performed al LLB, Saclay by means of time of flight spectrometer MIBEMOL set up at ORPHEE reactor. In Fig.1 is shown the INS spectrum for a scattering angle $\Theta = 137$ measured with an incident neutron beam on the sample having the energy $E_o = 3.025meV$. The energies corresponding both to the host lattice atomics vibrations and to the hydrogen bount in the host lattice are indicated by arrows in the figure. Now the processing of the data is in progress and the final results we presented in a forthcoming paper.

References

[1] D. Steinbinder et al. Europhys. Lett., 16, 211 (1991)

[2] M. Heene et al., J. Phys.Condens. Matter, 12, 6183 (2000)

[3] D. Richter, Transport Mechanism of Light Interstitials in Metal Muon-Spin-Rotation and Neutron Scattering, Heidelberg-Verlag, Berlin, (1983)

[4] D. Richter et al., Phys. Rev. B 27, 6227 (1983)

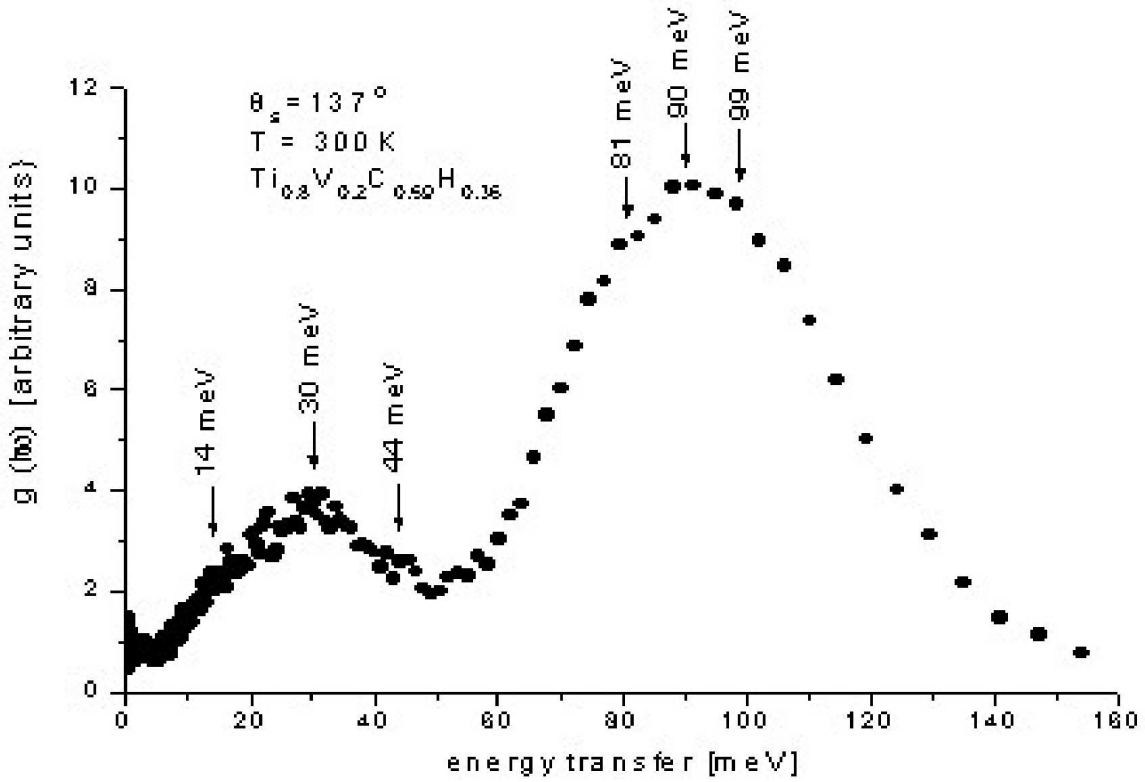

Figure 1: Hydrogen vibration spectrum in TiVC alloy

Neutron scattering investigation of superconducting ceramics Bi1.6Pb0.4Sr1.8Ba0.2Ca2Cu3Ox

I. Pădureanu[1], R. Lechner[2], D. Aranghel[1], A. Rădulescu[1,3], J. Pieper[2]

[1] NIPNE-HH, Department of Nuclear Physics, Romania
[2] Hahn-Meiter-Institut Berlin, BENSC, Germany
[3] Institut fur Festkorperforschung, Forschungszentrum Julich, Germany

The main purpose of this report is to present a short description of the experiment and of the preliminary results obtained from the slow neutron scattering measurements on a high temperature superconducting material taken on the time of flight spectrometer NEAT of BENSC. This spectrometer has been successfully used to obtain the results presented in the papers [1], [2]. In this study we have used cold neutrons with λ =5.1 A and a resolution ΔE=98μeV,(full width at the half maxim of the elastic line of a vanadium sample) The scattering spectra were taken with 140 detectors in a large angular range $15.41° \leq \Theta \leq 134.5°$.

All runs were measured within the temperature range 100K-300K. The final data are obtained at 28 scattering angles as a function of the energy transfer for 4 temperatures (100K,110K,130K and 300K) The preliminary data presented in Fig.1 for 3 temperatures at 300K,110K and 100K corresponding to the normal, transition and respectively to the superconducting state are analysed in terms of the generalised phonon frequency distribution(GFD). The preliminary conclusions could be summarised as follows:

- GFD obtained from an averaging over the final scattering vectors within a large range of scattering angles (Bredov and Oskotskij method) at 3 temperatures are presented in Fig .1 ;

- Well resolved peaks at 5.57meV, 10.43meV, 19.38meV, 29.68meV, 67.42meV and 109.48 meV were observed in GFD at 300K, 5.21meV, 10.39meV, 24.51meV, 45.42meV, 59.5meV, and 69.29meV at 110K and 5.7meV, 10.26meV, 20.46meV and 44.44meV at 100K;

- The presence of the first three excitations including the first soft mode at 5.2 ± 0.5meV for all temperatures during the transition from normal to the superconducting state;

- A strong temperature dependence of the high energy limit of the frequency spectra.

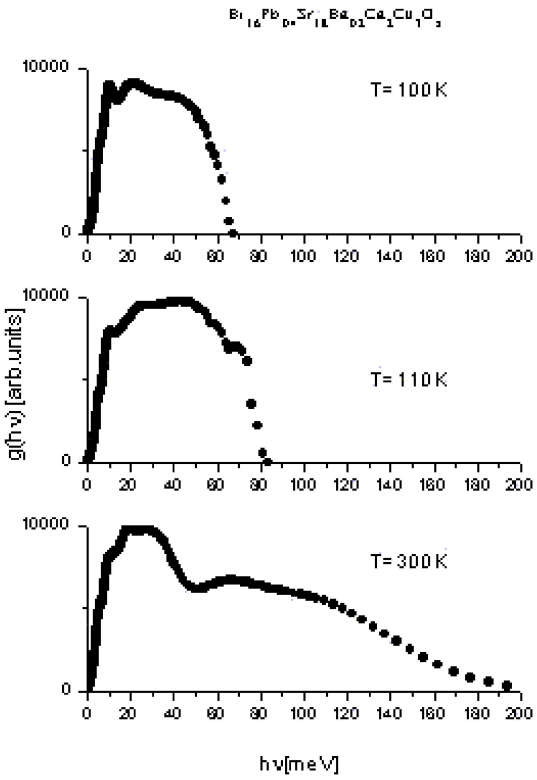

Figure 1: Temperature dependence of the generalized phonon density of states

References

[1] I.Pădureanu, R.E.Lechner, D.Aranghel, A.Rădulescu, J.Pieper, Applied Physics A(2002) in press

[2] A.Rădulescu, R.E.Lechner, I.Pădureanu, C.Postolache, Applied Physics A (2002), in press

Spin-resolved off-specular neutron scattering from magnetic domains using polarized ^3He gas spin filter

F. Radu [1,2], A. Vorobiev [3,4], J. Major [4], H. Humblot [3], K. Westerholt [2], H. Zabel [2]

[1] Departamentul de Fizica Nucleara, Institutul de Fizica si Inginerie Nucleara, 76900 Magurele, Romania
[2] Institut fur Experimentalphysik/Festkorperphysik, Ruhr-Universitaet Bochum, D-44780 Bochum, Germany
[3] Institute Laue-Langevin, 38042 Grenoble cedex 9, France
[4] Max-Planck-Institut für Metallforschung, Heisenbergstr. 1, D-70569 Stuttgart, Germany

The ^{3}He spin filter was recently used for first time [1] to measure diffuse scattering from thin films. The device itself is a cylindrical cell 100 mm in length and 50 mm in diameter, filled with polarized ^{3}He gas. After filling, the polarization is usually 65 % and it decays to about 58 % in 24 hours. The transmission of the neutrons through the filter is spin-dependent with the following cross-sections: $\sigma_{\uparrow\uparrow}$=5 bn and $\sigma_{\uparrow\downarrow}$=3000 bn. In order to record all four (I++, I+-, I-+, I- -) scattering neutron cross-sections the experimental setup includes, as well, two Mezei spin flipper placed before and after the sample. The advantage of using the ^{3}He analyser is that one is able to register spin analysed diffuse scattering for a broad range of exit angles. However, there are drawbacks as well, namely that the intensity is quite reduced and that the flipping ratio seems to be low. We have successfully overcame these difficulties by using an enhancement technique provided by the neutron resonator.

The neutron resonances in thin films [2] can be generated in two different ways: one is in the total reflection region of a neutron resonator and the other way is in a single film, just above its critical edge(in Kissing fringes region). In both cases the neutron density in the system is enhanced for definite incident neutron energies and one uses this phenomenon to increase the measurement sensitivity to magnetic and nonmagnetic inhomogenities, and to noncollinear magnetic spin arrangements at the interface. In our case we used the neutron resonator to study the scattering from magnetic domains in a $CoO(30\AA)/Co(200\AA)$ exchange biased bilayer. The measurements are made at EVA (ILL-Grenoble).

The bilayer was grown on a $Ti/Cu/Al_2O_3$ neutron resonator template. The system is cooled in an applied magnetic field of $H_a = +2000\ Oe$ through the Neel temperature of the ferromagnet to 10 K where the applied magnetic field H_a is swept as to measure the magnetic hysteresis loop. After the the second magnetisation reversal ($H_{c2} = +230\ Oe$), the system is supposed to aproach the original magnetic configuration. In order to proove that this is not the case for our exchange biased bilayer, we have measured four off-specular maps I++, I+-, I-+, I- - [Fig. 5] at $H_a \approx +370\ Oe$, where the magnetic spins were mostly reversed.

These PSD maps show a striking behaviour in the total reflection region: while the nonspin-flip scattering shows no diffuse reflectivity the spin-flip scattering exibits strong diffuse scattering at incident angles which satisfy the resonance conditions [2]. Moreover the spin-flip offspecular part of the reflectivity is asymmetric. The I-+ is scattered at higher exit angles than the specularly reflected neutrons, and the I+- is scattered at lower angles. Their intensity is different and there is a splitting of the resonance positions (α_i), which will be described in details in a fothcoming paper.In saturation the diffuse scattering reduces drastically. Thus, we conclude that the magnetic domains are responsible for the effect we described above.

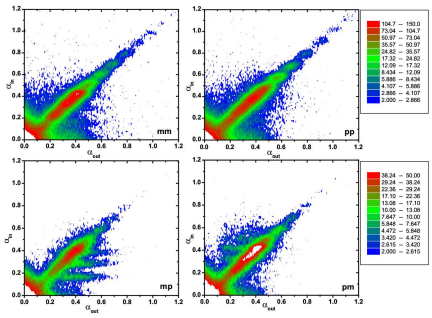

Figure 1: Off-specular scattering maps. The sample was cooled in an applied magnetic field of FC=+ 2000 Oe. At T=10 K the histeresys loop was measured and the sample was set in a field of $H_a = +370\ Oe$, which is close to the second coercive field ($H_{c2} = +230\ Oe$).

This effect opens a door towards the small angle neutron scattering studies of magnetic and nonmagnetic thin films. The sensitivity to clusters, porous media, interface spin misalignment, magnetic domains, vortices, and inhomogenities in general is remarkably high. This work is supported by SFB 491.

References

[1] B. Nickel, A. Rühm, W. Donner, J. Major, H. Dosch, A. Schreyer, H. Zabel, and H. Humblot, Rev. Sci. Instrum. **72**, 163 (2001)

[2] F. Radu, V. K. Ignatovich, Physica B **292**, 160 (2000).

Fusion yield for atomic clusters incident on a fusion target

Silviu Olariu[1]

[1] NIPNE-HH, Department of Nuclear Physics

We studied the fusion gain for the center-of-mass collision of two clusters of radius r, particle concentration n and incident velocity v. We have assumed, as previously, that as a result of the impact of the two clusters a region of hot plasma is created of temperature T, expressed in keV, the radius of the region being $2^{1/3}r$. The gain has been evaluated as $G = n\langle\sigma v\rangle(r/v_T)(E_Q/3T)[1 + (Z_1 + Z_2)/2]^{-1}$, where Z_1 and Z_2 are the charges of the reacting nuclei, and E_Q is the energy released in a fusion process. It will be assumed that the particle concentration n is that corresponding to the normal, uncompressed state of the incident clusters. The gain G has been represented in Fig. 1 for DT processes as a function of the plasma temperature T for several values of the radius r, using $n = 4.5 \times 10^{22}$ particles/cm^3, E_Q=17.6 MeV. Due to the relatively large values of $\langle\sigma v\rangle$ for the DT fusion processes, it can be seen from Fig. 1 that a gain $G = 1$ could be achieved for incident clusters having a radius of the order of r=1 mm, for a plasma temperature of the order of 20 keV. In this model, the gain decreases linearly with the radius r. The gain parameter G has been also calculated for $p^{11}B$ fusion processes, for $n = 3.34 \times 10^{23}$ nuclei/cm^3, which corresponds to B_9H_{15}, and Q_E=8.68 MeV. The $p^{11}B$ fusion process is in principle interesting, and the maximum gain for the $p^{11}B$ processes occurs for a plasma temperature T around 200 keV. We have calculated the radius of the clusters for which the gain is G=1 as a function of the plasma temperature T, for various possible fusion processes. The most suitable process for the production of fusion reactions by cluster impact remains the DT reaction, both as regards the dimensions of the incident clusters and as regards the incident energy per nucleon, with the $p^{11}B$ reaction sensibly far behind, but still interesting. In Fig. 2 we show the incident energy required in the center-of-mass system to obtain a gain G=1 at a plasma temperature T by cluster impact. The requirement on the incident energy for G=1 by uncompressed cluster impact is of about 1 MJ for DT reactions, and is very much larger for the other fusion processes.

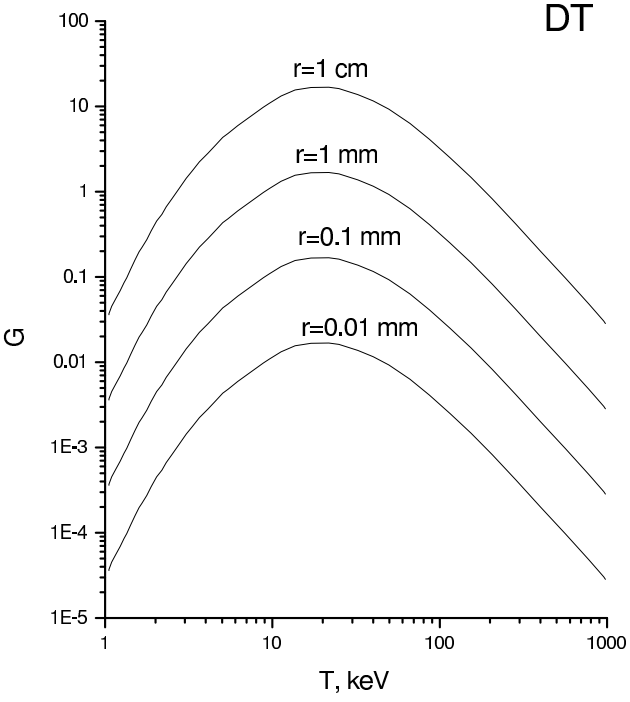

Figure 1: Gain G for DT processes as a function of the plasma temperature T for several values of the radius r, using $n = 4.5 \times 10^{22}$ particles/cm^3, E_Q=17.6 MeV.

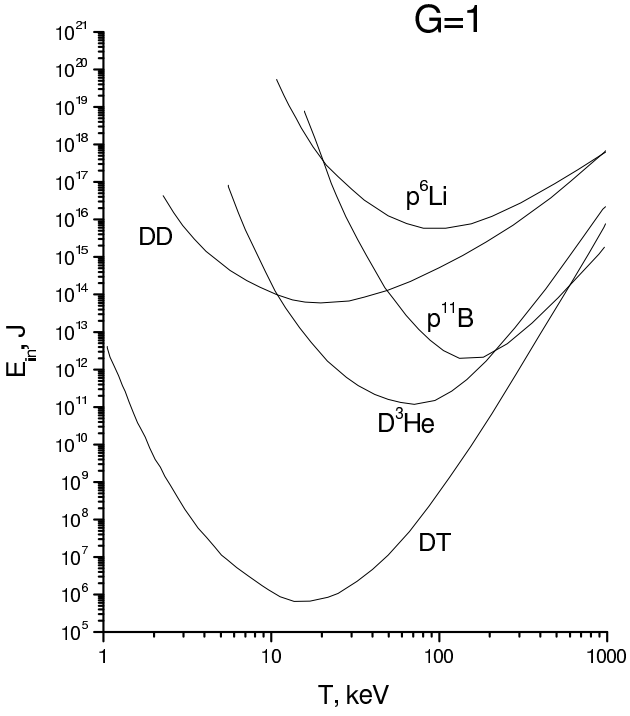

Figure 2: Incident energy required in the center-of-mass system to obtain a gain G=1 at a plasma temperature T by cluster impact.

Nuclear Instruments and Methods

A dedicated beam line for Rutherford back scattering analysis at the IFIN-HH cyclotron

E.A. Ivanov[1], D. Dudu[1], D. Plostinaru[1], D. Catana[1], I. Vata[1]

[1] NIPNE-HH, Cyclotron

Rutherford back-scattering technique (RBS) is an analytical tool that uses elastic scattering of 1-5 MeV charged particles to analyze the surface and the outer few micrometers of solids. IFIN-HH RBS system consist: U-120 Cyclotron, dedicated beam line and scattering chamber with sample manipulators and particle detectors. In our RBS system the samples are bombarded with 2-5 alpha particles accelerated by U-120 Cyclotron (in 3-rd subharmonic regime) and the scattered particles are detected by surface barrier detector. The signal from the detector is processed by common nuclear electronics and the particle energy spectra are stored in a computer based multichannel analyser. The data evaluation is accomplished using standard procedures and computer codes. The necessary vacuum inside chamber is obtained with an oil-free turbo pump. The beam spot dimension on the target is 1x1 mm The standard measurement are done at Θ=165°. The samples are electrical isolated and can be rotate around a vertical axis. The advantage of the RBS technique lies in the quantitative analysis of major and minor constituents lying in the first 0.5 to 2.0 micrometers of a material. Depending on the sample structure and composition, the detection limits vary from 10^{11} to 10^{15} at. cm^{-2} for heavy and light elements respectively. The depth distribution of constituents can be reconstructed with a depth resolution of 10-20 nm. The RBS technique is non-destructive since the erossion and the radiation degradation of the sample material by the particle impact is negligible. The most extensive use of the RBS technique is in the field of electronical and optical materials, special coatings (Fig. 1) and in the study of various physico-chemical processes on the solid surfaces.

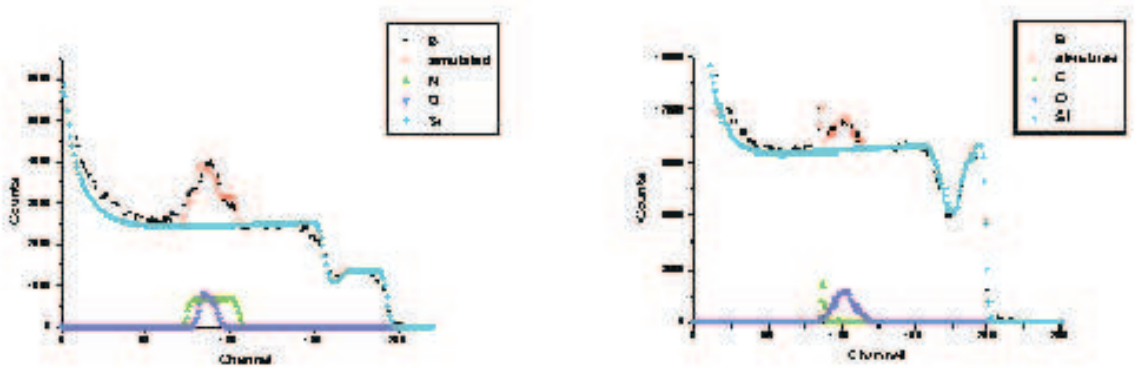

Figure 1: RBS spectra obtained at IFIN-HH Cyclotron (SiON/c-Si and implanted O in c-Si)

Neutron degradation of UV enhanced optical fibers for fusion installations plasma diagnostics

D. Sporea [1], I. Vata [2], D. Dudu [2], E.A. Ivanov [2], A. Danis [2]

[1] National Institute for Lasers, Plasma and Radiation Physics
[2] NIPNE-HH, Cyclotron

The design of ITER and the future operation of DEMO will require high-temperature, high-neutron flux materials to be used in plasma diagnostics, subjected to ITER requirements. A solution for remote plasma diagnostics implies the operation of various optical instruments placed apart from the critical temperature-neutron zones, with the optical signal transmitted over optical channels, for a reduction of radiation effects on the equipment, and a higher immunity to electromagnetic disturbances. Generally, data are available on the radiation effects on optical fibers used in communication applications or for transmission in the visible range. A special problem arises when optical signals have to be transmitted in the UV region (200 nm to 450 nm), where attenuation over the distance is quite high (in the range of several meters), and the UV radiation by itself produces an increase of the attenuation upon several hours of exposure. Until now, practically no data on the radiation effects on optical fibers for fusion plasma diagnostics, operating in UV were published.

In the frame of the EU's funded Fusion Programme, we focused on the evaluation of radiation induced
changes in the optical transmission for different commercially available optical fibers, for their possible use in optical light guides. Pure silica optical fibers with an UV enhanced response, with various cladding/jacket materials, and core diameter of 200 μm and 400 μm were evaluated, as they are subjected to neutron irradiation. The optical fiber core was of a high hydroxyl content type, and the coating was either Polymide or Al. Optical fibers with low (150°C) and high (350°C) temperature jacket materials were investigated.

The optical fiber samples were irradiated at fast neutron facility of the IFIN-HH U-120 Cyclotron. The neutron flux at 0° (i.e. in the beam direction) was found to be equivalent to 2.13 x 10^8 n/cm^2.s. μA, at 10 cm distance from Be target. The neutron energy spectrum shows a mean energy of 5.2 MeV. The neutron and gamma components of the mixed radiation field give rise respectively to 138Gy/C and 2.38 Gy/C at 90 cm distance from Be target. The irradiation steps used correspond to about 6 x 10^{10} n/cm^2.

For the evaluation of the optical transmission degradation in optical fibers we developed a set-up enabling: **a** - the investigation on optical transmission of UV enhanced optical fibers, in the spectral range 200 - 400 nm, with spectral resolution of 1.5 nm, and 12 bits amplitude resolution of the transmission readings; **b** - the evaluation of temperature influence on optical transmission of optical fibers. The set-up is based on a CW stabilized deuterium source, a miniature, multi channels optical fiber spectrometer coupled to a PC via the USB link, and a programmable oven operating under the PC control. As the assessment of the optical transmission in optical fiber for the UV region is very difficult to carry out (source efficiency is very low, UV solarization effects in sampling probes are quite high, detection noise is significant in the CCD array) signal averaging and box-car smoothing were used for data processing. All the measurements were done off-line, at room temperature, between the irradiation steps. Absorption picks were observed for all the optical fibers at about 230 - 250 nm, with an amplitude increasing with the neutron flux. We noticed some absorption related recovery phenomena, induced by the fiber heating, even at 100 - 120°C.

Study of the beam transport from the ion source to the stripper in a Tandem accelerator using Simion

Albert Olariu [1]

[1] NIPNE-HH, Department of Nuclear Physics

We study the beam transport from the ion source to the stripper in a Tandem accelerator using Simion 7.0. Simion is a program which basically calculates electric potentials of elementary points of a volume influenced by different electrodes[1].

The ion source (fig. 3a) is considered point-like, and the beam is considerred to have a divergence of 1 percent. The beam direction makes a 20° angle with the axis of the accelerator tubes and also is perpendicular to the entrance surface of the inflector magnet (fig. 3b). We have taken negative ions of atomic mass 1, charge $-e$ and energy of the order of tens of keV, a tipical preacceleration energy.

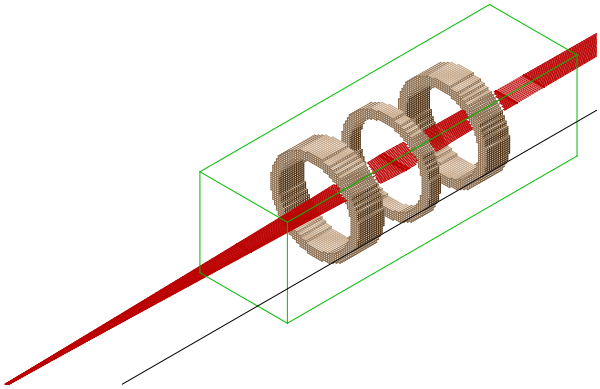

Figure 1: Einzel lens with trajectories.

The inflector magnet is modelled as a region with constant magnetic field. The strength of the field was adjusted to give a 20° deviation of the beam.

Figure 1 shows a 3D view of the Einzel lens. It consists of 3 cillindrical electrodes. The central electrode is at negative potential of the order -10 kV and and the outer electrodes are connected to the ground.

Figure 2 shows a 3D view of the second accelerator tube in the low energy stage. The accelerator tubes are inclined-field tubes, with rectangular plane electrodes having their normal inclined to the tube axis. This inclined-field structure serves to sweep nonbeam charged particles out of the accelerating region soon after their formation and to reduce the probability of regenerative multiplication. Each accelerator tube has 99 electrodes. Electrodes 1,2,3, 13, 32, 56, 84, 99 are straight, while the other electrodes are slightly inclined at +6° or -6° in alternating regions. The distance between 2 neighbouring electrodes is 2,54 cm, the voltage on each electrode is applied with the help of a resistive divider chain.

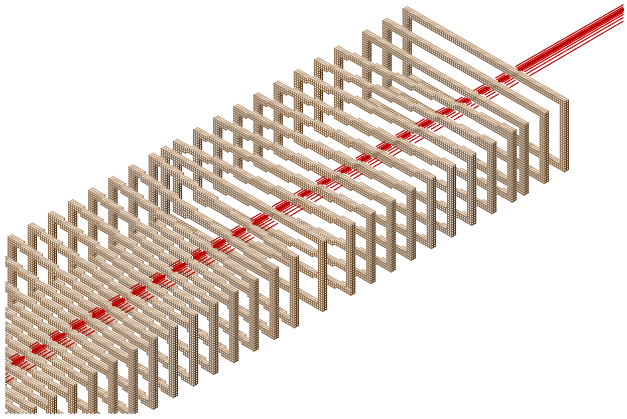

Figure 2: The first electrodes of the second accelerator tube with trajectories.

The stripper (fig. 3f) has a diameter of 5 mm.

The entire workbench is shown in Figure 3. The objective of the study is to maximize the beam current throught the stripper by adjusting the voltage on the Einzel lens.

Acknoledgements. I wish to thank Dr. Sorin Papureanu, Dr. Gh. Cata Danil and Dr. Serban Dobrescu for discussions and support.

[1] SIMION 3D Version 7.0 User's Manual

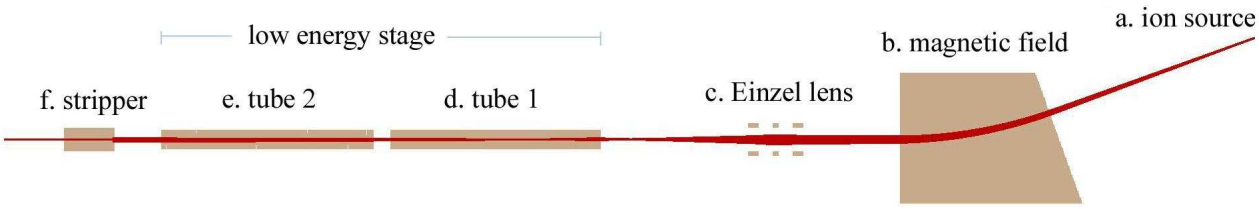

Figure 3: 2D view of the entire workbench.

Complementary techniques based on RBS and UV-Vis reflectance spectroscopy on the characterization of insulated layer deposited on C-Si

D. Dudu[1], M. Bercu[2], R. Muller[3], B.N. Bercu[2], C. Moldovan[3], E.A. Ivanov[1]

[1] NIPNE-HH, Cyclotron
[2] Faculty of Physics, University of Bucharest
[3] National Research Institute on Microtechnology

Abstract.

The insulated layers deposited on c-Si are of great interest for many applications in optoelectronics and in the field of chemical sensors using optical effects. Non-destructive analysis based on complementary techniques as RBS and UV-Vis are used for the characterization of SiO_2, Si_3N_4 and SiON films. This contribution focuses the capability of coupling optical constants determined by UV-Vis with the RBS data related to both the width of the insulated layer and its chemical content. The wave dependency of the real and imaginary part of the refractive index has been determined by an extracting procedure from UV-Vis spectra.

Oral presented at International Conference "ATOM2002 POLITECHNICA University Bucharest"

Total-reflection X-ray fluorescence analysis

E. Cringanu[1], C. Magureanu[1], O. Constantinescu[1]

[1] NIPNE-HH, Department of Applied Nuclear Physics

X-ray flurescence (XRF) is based on the irradiation of a sample by a primary X-ray beam. The individual atoms hereby excited emit secondary X-rays that can be detected and recorded in a spectrum. The spectral lines of this spectrum are characteristic of the individual atoms, so the sample can be analyzed.

Total Reflection X-Ray Fluorescence (TXRF) is a variation of energy-dispersive XRF with, however, one significant difference. In contrast to XRF, where the primary beam strikes the sample at an angle of about 40°, TXRF uses a glancing angle of less than 0.1°, so the primary beam is totally reflected.

TXRF is primarily used for chemical micro and trace analyses. Small quantities of solutions or suspensions are placed on optical flats, quartz glass, serving as sample supports. After evaporation, the residue is excited to fluorescence under the fixed small glancing angle and the characteristic radiation is recorded by a Si(Li) detector as an energy-dispersive spectrum.

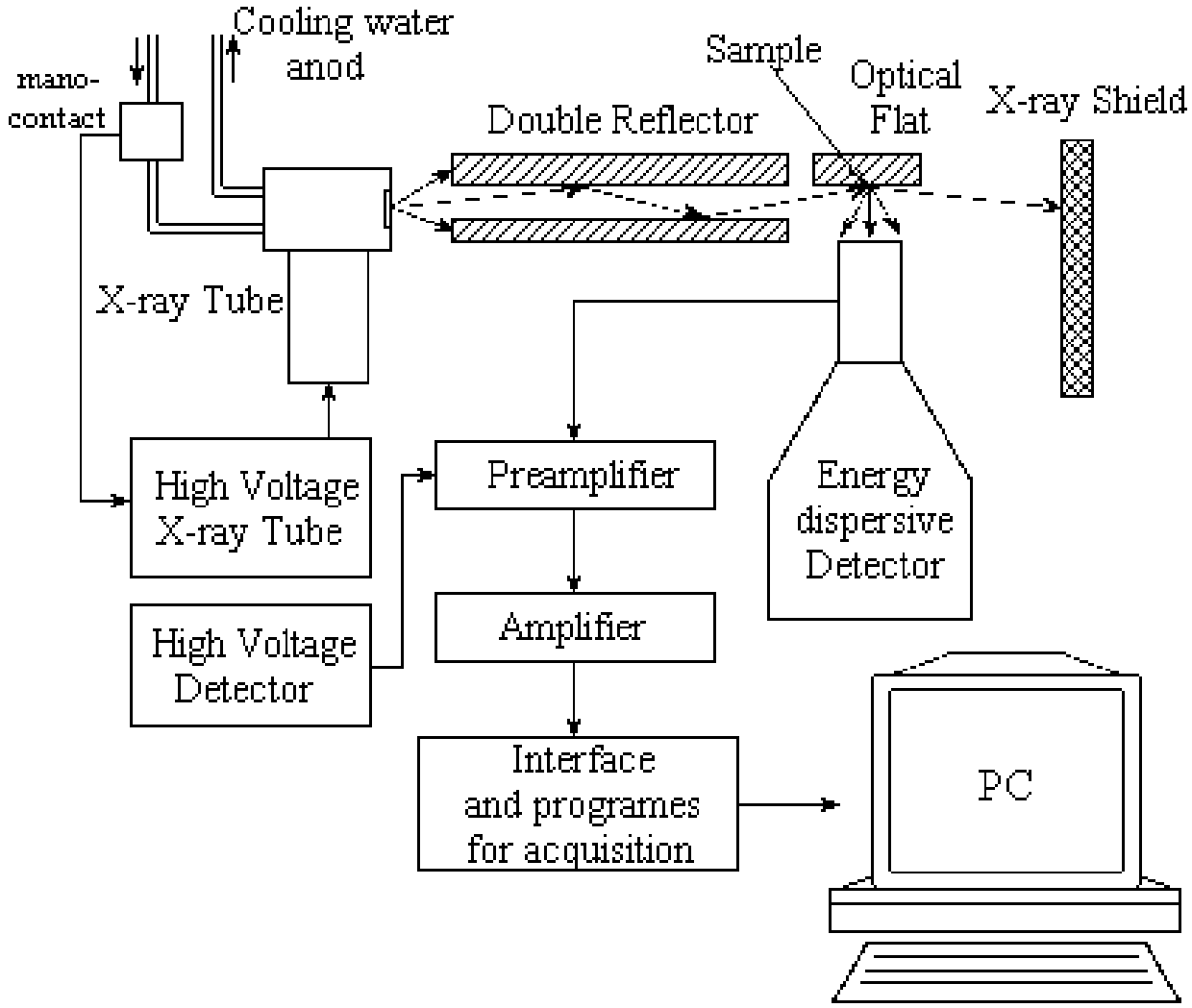

Figure 1: TXRF instrument

The high voltage for X-ray tube is 40 kV and the direct current is 1 mA. This generator of X-ray need to be cooled by a watwr flow.

The linear relationship between the XRF intensity of an analyte element and its concentration will be valid if the analyte is part of a small specimen deposited on a glass carrier. The plot of the measured net intensity vs. The concentration of this element gives a calibration straight line. Its slope is colled absolute sensitivity. For the determination of relative sensitivities were used multielement standards solutions.

There were made measurements on lichens in solutions and the resultes were comparable with the resultes obtained by PIXE methods.

Work performed under contract no.555/2000 in the frame of the ORIZONT Programme supported by the Romanian Ministry of Education and Research.

References

[1] Total Reflection X-Ray Fluorescence Analysis - Reinhold Klockenkamper

[2] The role of total-reflection X-ray fluorescence in atomic spectroscopy - G.Tolg and R. Klockenkamper

Dating of two paleolithic human fossils from Romania by accelerator mass spectrometry

Agata Olariu [1], Emilian Alexandrescu [2], Göran Skog [3], Ragnar Hellborg [4], Kristina Stenström [4], Mikko Faarinen [4], Per Persson [4]

[1] NIPNE-HH, Department of Nuclear Physics
[2] Institute of Archaeology "Vasile Pârvan", Bucharest
[3] Lund University, Radiocaron Dating Laboratory, Department of Quaternary Geology, Lund, Sweden
[4] Lund University, Department of Physics, Division of Nuclear Physics, Lund

In this study we have dated two human fossil remains from Romania, by the method of radiocarbon using the technique of the accelerator mass spectrometry, at the pelletron system of Lund University, Sweden. The two skulls are the most ancient dated fossil remains from our country. 1. Some human remains: the skull, scapulum and tibia were found in Baia de Fier in the Women's Cave, in Gorj county in the province Oltenia, by Constantin Nicolaescu-Plopsor in 1952. 2. Another skull was found in Cioclovina cave, near commune Boşorod, Hunedoara county in Transylvania, found by a worker at the exploitation of phosphate deposits, in the year 1941. The skull arrived at Francisc Rainer, anthropologist, and Ioan Simionescu, geologist, who published a study. [1]. The lack of stratigraphical observations made very difficult the cultural and chronological attribution of this skull. These authors advanced the hypothesis that the skull belongs to the man of the type *Homo sapiens fossilis*. At the same time a number of archaeologists believed that the skull might belong to a modern man and having doubts about this matter. In this condition the dating of the two skulls by the physical analysis is decisive. Samples of bone were taken from the scapulum and tibia from Woman's cave, Baia de Fier and from the skull from Cioclovina cave. The content of Carbon 14 have been determined in the 2 samples by using the technique of accelerator mass spectrometry (AMS), performed at the AMS system of Lund University, in Sweden. Normally, sufficient collagen for AMS measurements can be extracted from bone fragments with masses of 1 g or more providing at least 5 to 10% of the original collagen content. But in the situation of the present studied fossil remains, because of the small quantity of bone samples and at the same time, the bones being very old, the determination of radiocarbon in the skulls was difficult. For the preparation of the bone samples, we have essentially applied the Longin method [2, 3]. The first step concerns the extraction of 'collagen' from the bone structure. We use the word 'collagen' to refer to collagen that has undergone a degree of diagenesis. The next step is the transformation of the 'collagen' into pure carbon in an experimental set-up. The pure carbon, placed in a copper holder is arranged in a wheel, together with 2 standards of oxalic acid and anthracite. The wheel with the samples and standards is put into the ion source of the accelerator. The central part of the Lund AMS system is a Pelletron tandem accelerator. The accelerator is run at a terminal voltage of 2.4 MV during AMS experiments. The particle identification and measuring system consists of a silicon surface barrier detector of diameter of 25 mm. Each sample is measured 7 times. The precision of the measurements is around 1 % . From the processing of the data one obtaineed the follwing results:

Baia de Fier Women's cave	LuA-5228	30150 ±800 years BP
Cioclovina cave	LuA-5229	29000±700 years BP

The analysis of the fossil remains from Baia de Fier and Cioclovina cave by radiocarbon using the AMS technique have demonstrated that the remains are very ancient and could be attributed to the period of upper Paleolithic period, the Aurignacian. On the basis of the dating of the fossil remains presented in this study, a future cultural identification might be possible. In this way the fossil skulls from Baia de Fier and Cioclovina might be associated with other findings of the same type from the Central and Eastern Europe.

References

[1] Fr. Rainer and I. Simionescu, *Sur le premier crâne d'homme paléolithique trouvé en Roumanie*, Analele Academiei Romane, Seria III, Tomul XVII, Bucharest 1942

[2] R. Longin, *New method of collagen extraction for radiocarbon dating*, Nature, **v 230** (1990) p. 241-242

[3] J. S. Vogel, J. R. Southon, D. E. Nelson and T. A. Brown, Nucl. Instr. and Meth. **B5** (1984) p. 289

Particle Physics

Charmonium production in proton-nucleus interactions at CERN SPS

Călin Alexa[1], Venera Boldea[1], Sanda Diţă[1], S. Constantinescu[2], NA50 Collaboration

[1] IFIN-HH, Department of Elementary Particle Physics
[2] IFIN-HH, IT Department

The study of charmonia production in proton-nucleus collisions allows the investigation of the absorption mechanisms of the $c\bar{c}$ state in its path across the nucleus. A considerable theoretical effort has been carried out in the past few years in order to interpret the experimental results available from fixed target experiments at CERN and FNAL energies ($\sqrt{s}$ at 20 - 40 GeV. The results show that the perturbatively produced $c\bar{c}$ pair neutralizes its colour on a time scale which, depending on the kinematical variables of the pair, is of the same order of magnitude, or even larger, than the time needed for the heavy quark pair to escape the nucleus environment. However, a satisfactory quantitative description of the time evolution of the $c\bar{c}$ pair until it becomes a colour-neutral charmonium resonance is not available until now. Therefore, new data, relative to charmonium production, can help in constraining the model parameters and, more generally, in testing the validity of the approach used up to now in the interpretation of p-A data.

Furthermore, the study of the study the J/Ψ in the SPS energy range is interesting as a signature of Quark-Gluon Plasma. A sizable suppression of the J/Ψ yield has been measured in Pb-Pb collisions by the NA50 Collaboration [1, 2], as expected if a phase transition to deconfined partonic matter occurs in those interactions. In particular, analyzing the high statistics J/Ψ data relative to p-p, p-d, and S-U collisions, it has been shown that the observed yield can be reasonably explained in terms of a suppression of this meson exclusively due to hadronic processes. On the contrary, in Pb-Pb collisions there is an extra ("anomalous") suppression that is difficult to explain with conventional mechanisms. Thus, to obtain high statistics p-A data on nuclei heavier than deuterium became a necessity for NA50 Collaboration and justify the present study concerning the production of the charmonium resonances J/Ψ and Ψ' in collisions induced by a 450 GeV/c incident momentum proton beam on various nuclear targets.

The p-A data used in this study have been taken with the standard NA50 dimuon spectrometer described in [3]. The data have been collected with a primary proton beam from the CERN-SPS at 450 GeV incident momentum. The beam intensity was around 2×10^8 protons/s. Five nuclear targets have been used: Be, Al, Cu, Ag, W with thickness ranging from $0.34\lambda_I$ to $0.5\lambda_I$. About 10^6 dimuon events have been collected for each target and analysed with the standard NA50 reconstruction program [3]. In the NA50 kinematical domain, charmonium production occurs essentially through hard gluon scattering. Therefore the production cross sections, in absence of nuclear effects, are expected to scale with the number of nucleon-nucleon collisions, which for p-A interactions is proportional to the target mass number A. Such a scaling can be investigated by considering the production cross section per nucleon-nucleon collisions, expressed through the ratios $B_{\mu\mu}\sigma_{J/\Psi}/A$ and $B'_{\mu\mu}\sigma_{\Psi'}$/A, where $B_{\mu\mu}$ are charmonia branching ratios into muon pairs. In Figure 1 we present our preliminary results on the J/Ψ and Ψ' production cross sections per nucleon-nucleon collision.

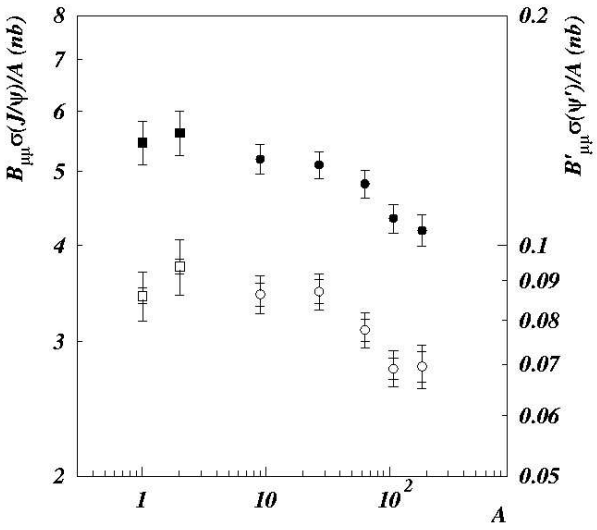

Figure 1: The J/Ψ and Ψ' cross sections per nucleon as a function of A.

References

[1] M.C. Abreu et al. (NA50 Collaboration) Phys. Lett. B450(1999)456.

[2] M.C. Abreu et al. (NA50 Collaboration) Phys. Lett. B477(2000)28.

[3] M.C. Abreu et al. (NA50 Collaboration) Phys. Lett. B410(1997)327.

A measurement of the photonuclear interactions of 180 GeV muons in iron

ATLAS TileCal Collaboration, Călin Alexa[1], Venera Boldea[1], Sanda Diţă[1], S. Constantinescu[2], Dan Pantea[1]

[1] IFIN-HH, Department of Elementary Particle Physics
[2] IFIN-HH, IT Department

Photonuclear interactions of muons $\mu + A \rightarrow \mu' + hadrons + X$ were first observed [1] in 1955. This mechanism of muon energy loss has an increasing impact on the design and the analysis of several type of new experiments, and needs a better understanding.

In Large Hadron Collider (LHC) experiments, high-energy muons are involved in a broad variety of new physics processes. They traverse substantial lengths of dense materials, and their experimental signature must be thoroughly understood in order to identify them, measure their energy and to take the hadronic showers accompanying muon tracks properly into account in the energy flow. In underground experiments, photonuclear interactions of muons must also be taken precisely into account because they may produce backgrounds to rare signals [7].

A measurement of muon photonuclear interactions in iron was performed using 180 GeV/c positive muons incident to a prototype module of the ATLAS Tile Calorimeter [2].

The ATLAS Tile Calorimeter is an iron-scintillator sampling calorimeter equipped with wavelength-shifting fibre readout. The energy spectrum and the cross section of photonuclear interactions of 180 GeV muons in iron were measured at the CERN SPS using prototype modules of the ATLAS hadron calorimeter. The experimental set-up is shown in Fig. 1.

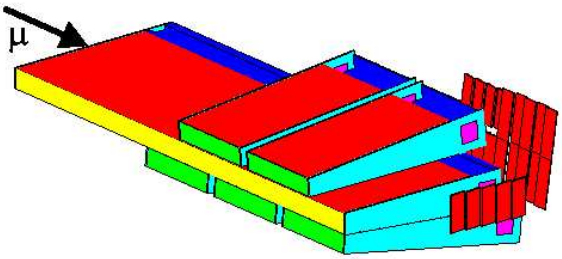

Figure 1: *The experimental set-up.*

As pointed out in Ref. [3], two separate theoretical predictions lead to very different expectations: in particular the more recent prediction of Bezrukov and Bugaev [4] is about an order of magnitude larger than the results based on Refs. [5, 6]. Supported by the results of Ref. [7], the prediction of Ref. [4] is compared to the experimental results.

The differential cross section $(N_A/A)v\mathrm{d}\sigma/\mathrm{d}v$ for a muon fractional energy loss $v = \Delta E_\mu/E_\mu$ was measured in the range $0.1 < v < 1$. The integrated cross section $(N_A/A)\int_{0.1}^{1} v\mathrm{d}\sigma/\mathrm{d}v$ is $(0.26 \pm 0.03_{\mathrm{stat}} \pm 0.03_{\mathrm{syst}}) \cdot 10^{-6}$ cm^{2}g^{-1} is in agreement with the theoretical prediction of $0.267 \cdot 10^{-6}$ cm^{2}g^{-1}. The best adjustment of the data to the theory is achieved for the value of $\sigma_{\gamma N} = (115 \pm 18_{stat} \pm 15_{syst})\mu$b of the photon-nucleon cross section for photons with energies in the range from 18 to 180 GeV. The values of $(N_A/A)v\mathrm{d}\sigma/\mathrm{d}v$ are shown in Fig. 2.

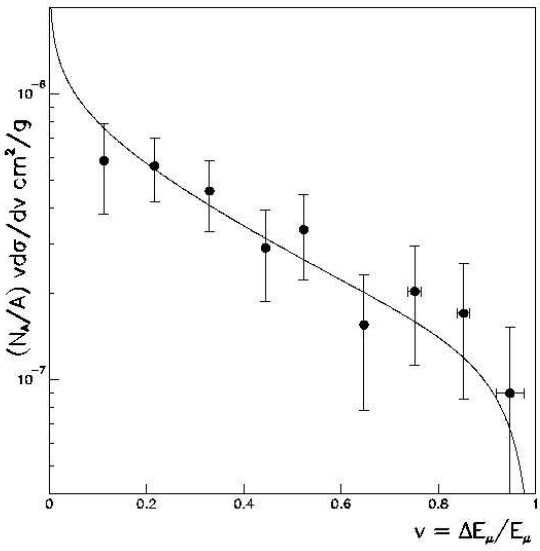

Figure 2: *The full circles show the measured differential energy-loss probability spectrum of 180 GeV muons by photonuclear interactions in iron. The curve is the theoretical prediction of Ref. [4]. The errors shown are statistical only*

References

[1] E.P. George and J. Evans, Proc. Phys. Soc. 68 (1955) 829.

[2] F. Ariztizabal et al., Nucl. Instrum. Methods A349 (1994) 384.

[3] G. Battistoni et al., Nucl. Instrum. Methods A394 (1997) 136.

[4] L.B. Bezrukov and E.V. Bugaev, Sov. J. Nucl. Phys. 33 (1981) 635.

[5] H.Fesefeldt, preprint PITHA 85/02, Aachen 1985.

[6] M.Nagano, preprint INSJ-120, Institute for Nuclear Study, Tokyo University, 1970.

[7] G. Battistoni et al., hep-ex/9809006, 9 Sep 1998.

ATLAS discovery potential study of the charged heavy lepton pair production.

Călin Alexa[1], Sanda Diţă[1]

[1] IFIN-HH, Department of Elementary Particle Physics

The new energy domain, opened by the LHC, will offer in the next future a unique opportunity for the searches of new particles predicted by models beyond SM. The new fermions are playing an important role due to the fact that several gauge groups with various theoretical motivations, containing the $SU_C(3) \times SU_L(2) \times U_Y(1)$ as a subgroup, provide fermion representation with larger dimension (more than 15) and therefore predict the existence of new fermions.

The results we are presenting are referred to the charged heavy lepton pair production by Drell-Yan mechanism as well as by gluon fusion, the later playing a dominant role in the region of the lepton masses higher than 300 GeV. We have assumed Standard Model couplings and the decay of both heavy charged leptons into an electron or muon and a Z boson, with a branching ratio [1] equal to $B.R.(L \to e(\mu)\ Z^0) = 1/3$. The signal and the background processes have been generated with PYTHIA 6.157 [2]. The heavy lepton pair production by gluon fusion was included as a new external process in PYTHIA and the detector response was simulated with the parametrised Monte Carlo program ATLFAST 2.53 [3].

The Drell-Yan processes include $q\bar{q}$ annihilation into (γ^*/Z^0/Z') and their further decay into a pair of charged heavy leptons while for the gluon fusion processes, Z and Z' bosons decay into a pair of heavy charged leptons.

$$\begin{aligned} q\bar{q} &\to (\gamma, Z, Z') \to L^+L^- \\ gg &\to (Z, Z') \to L^+L^- \\ L^+L^- &\to (e,\mu)^+ Z (e,\mu)^- Z \\ &\to (e,\mu)^+ (e,\mu)^- + 4jets \end{aligned}$$

As in many searches for new physics at the TeV scale, the dominant background for our signal processes is $t\bar{t}$ pair production due to its high production cross section. An important signature of dilepton $t\bar{t}$ process is the high value of the E_T^{miss} due to the two escaping neutrinos. The highest values for the signal significance were obtained for $M_{Z'}$ equal to 1 TeV for both decay channels: $L^\pm \to e^\pm + Z^0$ and $L^\pm \to \mu^\pm + Z^0$ (see Fig. 1 and Fig. 2).

Thus, for an integrated luminosity of 30 fb^{-1}, it was found that ATLAS could discover this charged heavy lepton up to 0.9 TeV/c^2 and the discovery limit is pushed up to 1.0 TeV/c^2 for an integrated luminosity of 300 fb^{-1}.

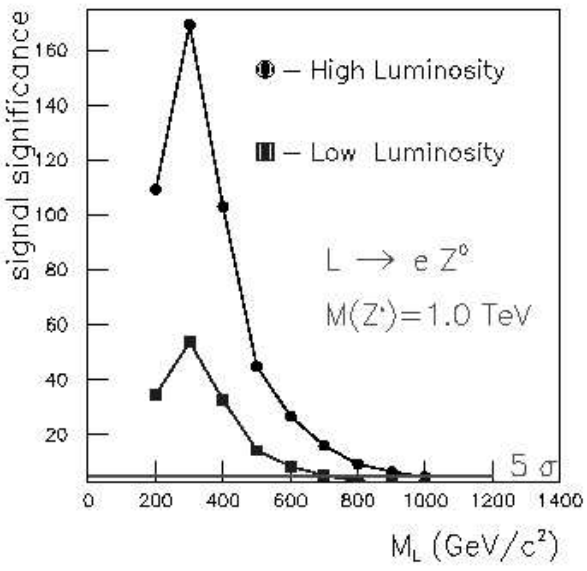

Figure 1: *The signal significance mass (M_L, $M_{Z'}$) dependence for high (300 fb^{-1}) and low (30 fb^{-1}) luminosity for $L^\pm \to e^\pm + Z^0$ decay channel.*

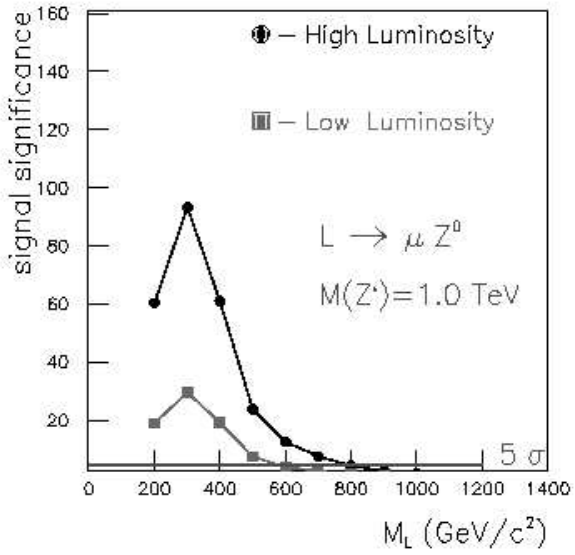

Figure 2: *The signal significance mass* (M_L, $M_{Z'}$) *dependence for high* (300 fb^{-1}) *and low* (30 fb^{-1}) *luminosity for* $L^{\pm} \to \mu^{\pm} + Z^0$ *decay channel.*

References

[1] G. Azuelos and A.Djouadi Z. Phys. C 63(1994)327

[2] T. Sjostrand, Comp. Phys. Comm. 82(1994) 74

[3] A. Richter-Was, D. Froidveaux, L. Poggioli,

An approach for high voltage power supply system for HCAL of LHCb experiment

A. Cimpean[2], C. Coca[1], D. Dumitru[2], A. Kluger[2], C. Magureanu[2], M. Orlandea[1], S. Popescu[1], D. Tarta[2]

[1] Department of Particle Physics, IFIN-HH, Bucharest, Romania

[2] Department of Applied Physics, IFIN-HH, Bucharest, Romania(* presently not at IFIN-HH)

The main aim of the calorimeter system ([1], [2]) of the **LHCb** experiment, a **L**arge **H**adron **C**ollider **B**eauty experiment dedicated for precision measurements of CP violation and rare phenomena, is to provide identification of the electrons, hadrons and photons, for the level-0 trigger and offline analysis with measurements of position and energy. The system consists in scintillator pad/preshower(SPD/PS) detector, electromagnetic(ECAL) and hadron(HCAL) calorimeters, all subdetectors having a similar technology with scintillating tiles as active material that are read out via wavelength-shifting fibers and thus with an identical readout elecronics for ECAL and HCAL and a similar electronics for the PS.

During 1997-1999 a computer controlled High Voltage distribution scheme ([3]) was developed by IFIN-HH group and used to supply the PMTs of half HCAL prototype during the beam tests (1998-2000). This scheme consisted in three parts: 1) a control box which includes low voltage power supply, the RS232 interface to a PC and three modules of high voltage power supply; 2) two types of multichannel HV distributors with an individual voltage setting; 3) a software package to controll all setings and refresh them periodically.

Based on the experience got, a new design for a High Voltage Power Supply ([4]) which satisfys the LHCb requirements has been developed for PMTs of the hadron calorimeter. The demands of this system are simplicity and low cost. This HVPS with multiple outputs (HV for photocathode and D1 - D4 dinodes) is destined to supply, with the same high voltage, groups of PMTs sorted by similar characteristics as gain and sensivity. Because of the high rates (≈40MHz)supported by PMTs there are necessary booster voltage sources to suply current for the last 4 dynodes.

The box has 5 HV power supplies for photocathodes and the last 4 dynodes, each HV power supply being followed by a 4 channel distributor (10mA/channel). The box can independently supply 4 groups of 40 PMTs each. The voltage setting can be made by hand, through keyboard and LCD display located on the front pannel using a μC board which also contains a CAN interpretor, SJA 1000, that makes the serial CAN-bus link from the distance. The connection is bidirectional allowing both the setting of output voltages and the reading of the information on output voltage and current. The power supply has good output features, shortcut protection and special voltages.
The output voltages for a group are:

	Pedestal	HVmax
Photocatode	-1800V	-2150V
D4	-650V(700)	-850V
D3	-500V(550)	-650V(700)
D2	-350V	-500V
D1	-150V	-250V

The box dimensions are: 480x128x525mm

The voltages are transmitted trough HV coaxial cables with SHV connectors. The PMTs of FEU-115m10 type were used. In the following HV system will be adapted to be used to supply PMTs of Hamamatsu type R7899 20 which have been largely investigated by LHCb collaboration. HV Power Supply is going to be integrated in CAN network.

This HVPS with parallel powering groups of fast PMTs has advantages as: a) outside PMTs supply (power dissipation is not inside HCAL modules); b)a very good stability for all HV supplies (photocathode and dinodes); c)a low ripple because of distributors supplementary stabilization with series transistors; d)great reserve of current (it permits high counting rates); f) it does not work in radiation field; g) easy service. The system is dedicated and can be used in any experiments with many fast PMTs.

References

[1] LHCb Technical Proposal, CERN/LHCC 98-4

[2] LHCb Calorimeters, Technical Design Report, CERN/LHCC/2000-0036

[3] M.Bonnet, A.Schopper, C.Coca, D.Dumitru, G.Giolu, C. Magureanu, R.Petrescu, S.Popescu et al., "The hadron calorimeter prototype design and construction", LHCb-2000-035 public note

[4] A.Cimpean, C.Coca, D.D. Dumitru, D.T.Dumitru, C.Magureanu,"A proposal for High Voltage Power Supply system for HCAL of LHCb experiment", LHCb-2000-092 public note (http://weblib.cern.ch)

Inclusive production of antihyperons in nC-interactions

T. Ponta[1], T. Preda[1], EXCHARM Collaboration

[1] IFIN-HH, Department of Elementary Particle Physics

The behavior of the differential cross-sections for inclusive production of antihyperons in nucleon-nucleon interactions is poorly explored. The kinematic region of the validity for existing theoretical models is also uncertain.

Most of the data on antihyperon production have been obtained in charged kaon beams, as cross-sections of antihyperon production by strange particles are higher than those for nucleons. Some measurements have been performed in proton beams [1, 2], and only few in neutron beams [3, 4]. The existing data have very large uncertainties. So, whether total and differential cross-sections of antihyperon production by protons and neutrons are similar is still an open question.

The inclusive production cross-sections of $\overline{\Lambda}^0$, $\overline{\Xi}^+$, and $\overline{\Sigma}(1385)^{\pm}$ in neutron-carbon interactions at ~ 51 GeV mean energy of neutrons have been measured. The parameters n and b of differential cross-section parametrisation $(1 - |x_F|)^n \exp(-bp_t^2)$, where x_F is the Feynman variable, p_t is the transverse momentum, have been obtained. The kinematic region of validity for the parametrisation has been defined. Results are compared with published experimental data.

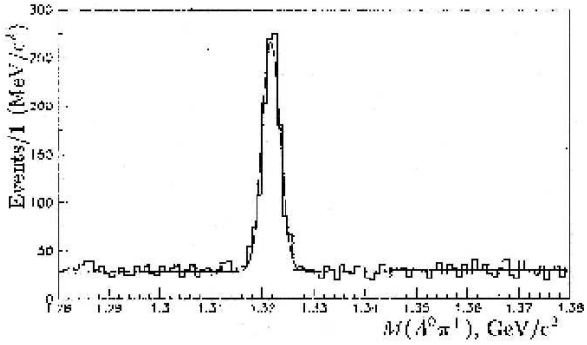

Figure 1: *Effective mass spectrum of* $\overline{\Lambda}^0\pi^+$.

The results have been obtained in the EXCHARM experiment, carried out at the Serpoukhov accelerator.

Antihyperons have been identified by their decays:

$$\begin{aligned} \overline{\Lambda}^0 &\rightarrow \overline{p}\pi^+ \\ \overline{\Xi}^+ &\rightarrow \overline{\Lambda}^0\pi^+ \\ \overline{\Sigma}(1385)^{\pm} &\rightarrow \overline{\Lambda}^0\pi^{\pm} \end{aligned}$$

In Figure 1 and Figure 2 are shown the effective

mass spectrum of $\overline{\Lambda}^0\pi^+$, respectively $\overline{\Lambda}^0\pi^-$, with special selection cuts in order to find the $\overline{\Xi}^+$ and $\Sigma(1385)^-$ particles.

A clear signal of $\overline{\Xi}^+$ decay is seen in the spectrum. The spectrum is approximated by a sum of a Gaussian function describing the signal, and a linear function for the background.

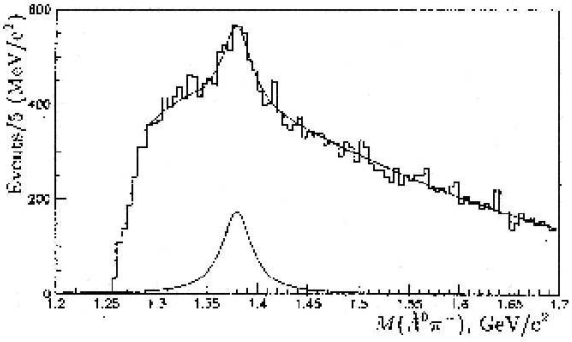

Figure 2: *Effective mass spectrum of* $\overline{\Lambda}^0\pi^-$.

The signal from Figure 2 is approximated by the function

$$\left(\frac{dN}{dM}\right)_- = BG(M) + BW(M)$$

where the signal $BW(M)$ is approximated by the relativistic Breit-Wigner function and the background $BG(M)$ by a product between a power function and an exponential function.

The cross-sections per nucleon are presented in Table 1, where (ext) represents the error, which takes into account a specific extrapolation of the differential cross-section in the region $|x_F| < 0.1$.

State	σ_{nN}, μb
$\overline{\Lambda}^0$	154.4 ± 1.0(stat) ± 7.2 (syst) ± 18.0 (ext)
$\Sigma(1385)^-$	10.2 ± 1.6(stat) ± 0.6 (syst) ± 0.6 (ext)
$\Sigma(1385)^+$	8.2 ± 2.8(stat) ± 0.6 (syst) ± 0.5 (ext)
$\overline{\Xi}^+$	7.9 ± 0.4(stat) ± 0.5 (syst) ± 0.9 (ext)

Table 1: *The total cross-sections per nucleon.*

References

[1] M. Alston et al., Phys. Rev. Lett. **35**, 142 (1975).

[2] R.D. Kass et al., Phys. Rev. D **20**, 605 (1979).

[3] A.N. Aleev et al., *JINR P13-94-312* (Dubna 1994)

[4] M. Zavertyaev, Nucl Phys. Proc. Suppl. B **93**, 62 (2001).

Pionium lifetime measurement to test nonperturbative QCD predictions (DIRAC experiment)

M. Penţia[1], Gh. Caragheorgheopol[2], S. Constantinescu[3], C. Curceanu[4], M. Iliescu[4], T. Ponta[5], D. Pop[6]

[1] IFIN-HH, Nuclear Physics Department
[2] IFIN-HH, Applied Nuclear Physics Department
[3] IFIN-HH, Informatics and Computing Center
[4] IFIN-HH & INFN - Frascati, Italy
[5] IFIN-HH, Particle Physics Department
[6] IFIN-HH & CERN - Geneva, Switzerland

The main goal of the DIRAC Experiment [1] is to measure the pionium ($\pi^+\pi^-$ atom) lifetime with 10% precision. This measurement will provide in a model-independent way the difference between the isoscalar and isotensor S-wave $\pi\pi$ *scattering lengths* $|a_0^0 - a_0^2|$ with 5% precision. Nonperturbative QCD - *Chiral Perturbation Theory* [2] - predicts scattering lengths with very high accuracy $\sim 2\%$.

The pionium atoms are produced by Coulomb interaction in the final state of $\pi^+\pi^-$ pairs, generated in high energy proton-target collisions [3]. If the $\pi^+\pi^-$ pairs are produced at a small distance ($r \sim 10\ fm$), less than the Bohr radius of pionium (387 fm), they can form the $\pi^+\pi^-$ atom.

After production in hadron-nucleus interaction, relativistic pionium atoms ($2\ GeV/c < p_A < 6\ GeV/c$) are moving in the target. They can decay or, due to electromagnetic interaction with the target material, can break up. The resulted "atomic $\pi^+\pi^-$ pairs" are characterised by small relative momenta in c.m. $Q < 3\ MeV/c$. The other pion pairs, free pairs (accidentals, Coulomb and Non-Coulomb pairs), can be separated

by relative momentum distribution.

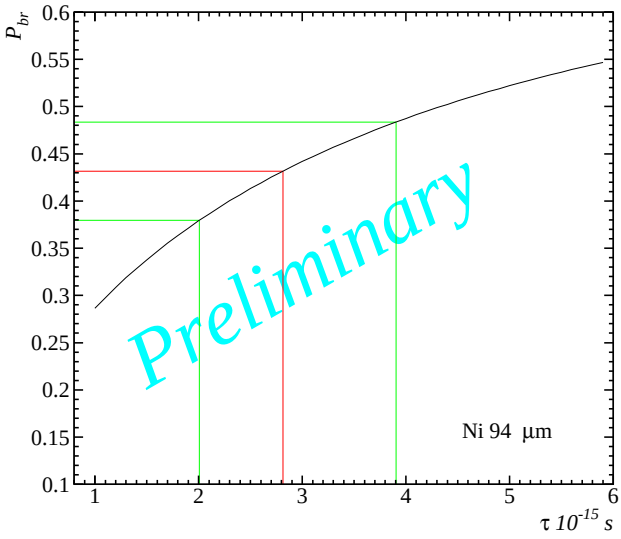

Figure 1: Estimated pionium lifetime (Preliminary).

The aim of DIRAC experiment is to measure the pionium breakup probability $P_{br}(\tau)$. Comparison of the measured break-up probability $P_{br} = n_A/N_A$ (ratio of broken up - n_A and produced - N_A pionia) with the calculated dependence of P_{br} on τ (see Fig. 1) can evaluate the pionium lifetime.

Our main contribution to the hardware part is the construction, commissionning and use of the *Preshower Detector* [4]. It works along with the Trigger System of the setup and also is used in offline data analysis, for electron/pion separation.

The overall statistics of "atomic pairs" is presented in Table 1 for two Q values. The sample of $\sim$ 5000 pionium atoms provides a statistical accuracy for the lifetime measurement at the 20% level. The data analyzed till now for Ni target permit an estimation of the pionium lifetime $\tau = 2.8^{+1.1}_{-0.8} \times 10^{-15}$ sec. For Ti target we get $\tau = 5.4^{+1.5}_{-1.3} \times 10^{-15}$ sec. The combined results, $Ni + Ti$ targets, gives a pionium lifetime estimation $\tau = 3.6^{+0.9}_{-0.7} \times 10^{-15}$ sec.

Table 1: Number of "atomic pairs" detected

Target year	Thick. (μm)	Trigg. 10^6	n_A $Q < 2$ MeV/c	n_A $Q < 3$ MeV/c
Pt 1999	26	55.7	130 ± 43 (3σ)	207 ± 77 (2.7σ)
Ni 2000	94	896	920 ± 170 (5.4σ)	1335 ± 300 (4σ)
Ti 2000+01	244	910	1170 ± 190 (6.2σ)	1495 ± 340 (4.4σ)
Ni 2001	98	647	2686 ± 310 (8.7σ)	3500 ± 510 (6.9σ)
Ni 2002	98	77	400 ± 100 (4σ)	545 ± 170 (3.2σ)

References

[1] B.Adeva et al. - DIRAC Group, Proposal to the SPSLC, *Lifetime measurement of $\pi^+\pi^-$ atoms to test low energy QCD prediction*, CERN/SPSLC 95-1, SPSLC/P 284 (1995)

[2] J.Gasser, H.Leutwyler, *Ann.Phys.*,158,142,(1984)

[3] L.L.Nemenov, *Sov.J.Nucl.Phys.* 41, 629, (1985)

[4] M. Pentia, Gh. Caragheorgheopol, M. Ciobanu, D.Pop, C.Rusu, *DIRAC Note 99-03*, 22 Feb. 1999

Contributions to the integrated graphical user interface

E. Bădescu [1], M. Caprini [1]

[1] NIPNE-HH, Department of Applied Nuclear Physics

The Online Software is a part of the distributed Data Acquisition System (DAQ) for the ATLAS experiment, that will start taking data in 2007 at the Large Hadron Collider at CERN.

The Online Software system [1] is responsible for overall experiment control, including run control, configuration and monitoring of Trigger & Data Acquisition System (TDAQ) and management of data-taking partitions. The system encompasses all the software to do with configuring, controlling and monitoring the data acquisition system, but excludes anyting to do with the management, processing or transportation of physics data. In other words, the Online Software is supposed to act as the "glue" to a quantity of heterogeneous sub-system, providing not only a uniform control interface, but also the possibility of easily abstracting the specificities of those subsystems in order to provide them with control services. The compo-

nents model architecture has been adopted for the system, each component being developed as an individual package. All the hardware and software configurations of the data taking partitions are stored in configuration databases. The Process Manager component [2] performs the basic job control of the software components.

The Integrated Graphical User Interface (IGUI) is one of the integration components of the Online Software, allowing the operator to control and monitor the status of the current data taking run in terms of its main parameters, detector configuration, trigger rate, buffer occupancy and state of the subsystems. Figure 1 presents the context diagram for this component.

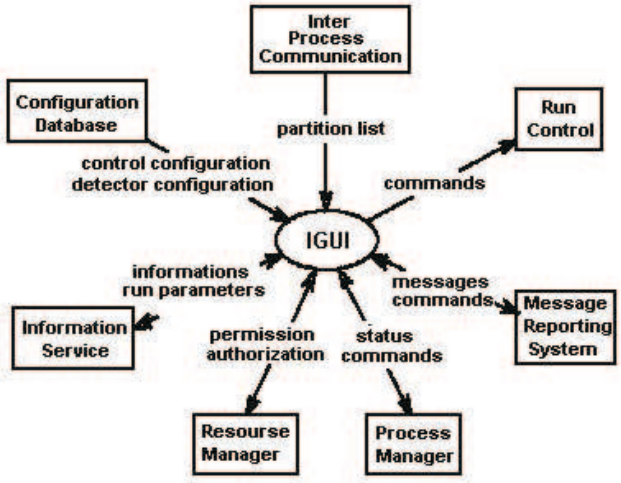

Figure 1: The context diagram of the IGUI component

The component has been designed as a Java application, having defined some specialized panels for allowing the user to send the main DAQ commands and displaying messages, states or run specific parameters of the whole system or related to all the other components (Run Control, Run Parameters, DAQ Supervizor, Process Manager, Message Reporting, Monitoring or Data Flow). The design of this component allows the users to develop their own panel to be displayed.

The Online Software has been deployed for various test beam activities at CERN and in external test setups in laboratories around the world. Several ATLAS detector groups use this software to implement their DAQ system for their test beam activities. The software has also been subject of studies in various large scale test beds [3]. A system with up to two hundred workstations was used to study the scaling behaviour of individual components and of the integrated system. These activities are providing important feedback into the development cycle.

The main functionalities of the Online Software are provided without the need of commercial packages and the software is available for users by download at URL http://atlas-onlsw.web.cern.ch/Atlas-onlsw/download/download.htm

Work performed under contract no. 72 / 2001 in the frame of the CERES Programme supported by the Romanian Ministry of Education and Research.

References

[1] ATLAS High-Level Trigger, DAQ and DCS Technical Proposal-CERN/LHCC/2000-17, 31 March 2000

[2] I. Alexandrov, E. Badescu, M. Caprini et al., - Process Management inside ATLAS DAQ - IEEE Conference 2001, Nuclear Science Symposium, ICALEPCS 2001, 4-10 November 2001, San Diego, California.

[3] I. Alexandrov, E. Badescu, M. Caprini et al., Performance and Scalability of the Back-end subsystem in the ATLAS DAQ/EF Prototype-IEEE Transactions on Nuclear Science, Vol. 47, No. 2, April 2000, pg. 244-249

Strong evidences for nuclear mesonic Cherenkov-like radiation from high energy hadronic collisions

D.B. Ion [1]

[1] IFIN-HH, Bucharest,Magurele

In this paper [1] the esential characteristic features of the *nuclear pionic Cherenkov-like radiation* (NPICR) are discussed and compared with the recent experimental results otained at IUCN-Dubna. The Cherenkov effect for photons is one of the well known collective phenomenon in normal dielectrics which is directly connected with the modification of phase velocity of photons inside the medium. Recently in Refs. [2] we have extended these ideas to the nuclear media where the gamma Cherenkov-like radiation (NGCR)

should be possible to be emitted from charged particles moving through nuclei with a velocity larger than the phase velocity of photons in the nuclear media. The detailed absolute predictions for the spontaneous pion emission as nuclear pionic Cherenkov-like radiation (NPICR) inside the nuclear medium are obtained and published in Refs. [3]. The nuclear pionic Cherenkov-like Radiation (NPICR) was recently (see Ref.[4]) discovered experimentally at Dubna in Mg-Mg central collisons at 4.3 GeV/nucleon by processing the pictures from 2m Streamer Chamber SKM-200. So, after *processing a total of 14218 events*, which were found to meet the centrality criterion, the following experimental results are obtained [4]. The *energy distribution of emitted pions in the central collisions have a significant peak* (4.1 standard deviations) *over the inclusive background.* The *value of the peak energy and its width are* in a good agreement with the predictions [3] on the NPICR-effect.

References

[1] D. B. Ion, Rom. Journ. Phys. **47** (2002) 255.

[2] D. B. Ion and W. Stocker, Phys. Lett. **B 258** (1991) 339; Ann. Phys. (N.Y) **213** (1992) 355; Phys. Lett. **B 311** (1993) 339; Phys. Lett. **B 323** (1994) 446; Astroparticle Physics **2** (1994) 21.

[3] D. B. Ion and W. Stocker, Phys. Lett. **B 273** (1991) 20; Phys. Rev. **48** (1993) 1172; Phys. Lett. **B 346** (1995) 172; Phys Rev. **52** (1995) 3332.

[4] G. L. Gogiberidze, L. K. Gelovani, E. K. Sarkisyan, Phys. Lett. **B 471** (1999) 257.

Optimality, entropy and complexity for nonextensive quantum scattering

D.B. Ion[1], M.L.D. Ion[2]

[1] IFIN-HH, Department of Elementary Particle Physics, Bucharest
[2] University of Bucharest, Faculty of Physics

In this paper [1], by introducing $[S_J(p),\ S_\theta(q)]$ *Tsallis - like entropies [2], the optimality and complexities* as well as the *nonextensive statistical behavior of the* $[J$ *and* $\theta]$*-quantum states* in hadronic scatterings are investigated [2] in an unified manner. A connection between optimal states obtained from the *principle of minimum distance in the space of quantum states* [3] (PMD-SQS) and the most stringent (Max-Ent) entropic bounds on Tsallis-like entropies [2] for quantum scattering is established. A measure of the complexity of quantum scattering in terms of Tsallis-like entropies is proposed. The generalized entropic uncertainty relations as well as a possible correlation between the nonextensivities p and q of the $[J$ *and* $\theta]$-statistics are proved [4]. The results on the experimental tests of *the PMD-SQS-optimality*, as well as on the *optimal entropic bands* and *optimal complexity*, obtained by using the experimental pion-nucleon pion-nucleus phase shifts, are presented [5]. The nonextensivity indices p and q are determined from the experimental entropies by a fit with the optimal entropies $[S_J^{o1}(p),\ S_\theta^{o1}(q)]$ obtained from the *principle of minimum distance in the space of states.* In this way strong experimental evidences for the $p-$nonextensivities in the range $0.5 \leq p \leq 0.6$ with $q = p/(2p-1) > 3$, are obtained with high accuracy ($CL > 99\%$). We conclude that further investigations are needed since this *nonextensive statistical behavior of the quantum scattering* discovered here can be a signature of a *new universal law of the quantum scattering.*

References

[1] D. B. Ion and M. L. Ion, Chaos, Solitons and Fractals, **13** (2002) 547-568.

[2] D. B. Ion and M. L. D. Ion, Phys Rev. Lett. **81** (1998) 5714; Phys. Rev. **E 60** (1999) 5261; Phys Rev. Lett. **83** (1999) 463.

[3] D. B. Ion, Phys. Lett. **B 376** (1996) 282.

[4] D. B. Ion and M. L. D. Ion, Phys. Lett. B **466** (1999) 27; M. L. D. Ion and D. B. Ion, Phys. Lett. B **474** (2000) 395.

[5] D. B. Ion and M. L. D. Ion, Phys. Lett. **B 482** (2000) 57; Phys. Lett. B **503** (2001) 263; Phys. Lett. B **519** (2001) 63;

Dual coherent particle emission as generalized Cherenkov-like effect in high energy particle collision

D.B. Ion [1], E. K. Sarkisyan [2]

[1] IFIN-HH, Department of Elementary Particle Physics, Bucharest
[2] CERN, Geneva, Switzerland

The generalized Cherenkov-like effects based on the four fundamental interactions has been investigated and classified recently by Ion and Stocker in Refs. [1]. This classification includes the nuclear (mesonic, gamma, weak bosonic)-Cherenkov-like radiations as well as the high energy component of the coherent particle emission via (baryonic, leptonic, fermionic)-Cherenkov-like effects. By recent experimental observations of the subthreshold and anomalous Cherenkov radiations it was clarified that some fundamental aspects of the CR can be considered still open and that more theoretical and experimental investigations on the CR are needed. In a recent paper [2] we introduced the *dual coherent particle emission (DCPE)* from which all kind of generalized Cherenkov-like effects can be obtained. The aim of this paper [2] was to obtain a general quantum theory of the *dual coherent particle emission* (DCPE)-*mechanism as two component generalized Cherenkov-like radiation.* Then we proved that recent results on the *anomalous Cherenkov radiation* [3] and those on the *subtreshold Cherenkov-like effects* [4] can be completely interpreted as signatures of this new two component DCPE-effect. The applications of these new results to the development of new kind of particle detectors called DCPE-Cherenkov-like detectors are suggested.

References

[1] D. B. Ion and W. Stocker, Phys Rev. **52** (1995) 3332.

[2] D. B. Ion and E. K. Sarkisyan, **ArXiv hep-ph/0209039 v1 4 Sep 2002**.

[3] A.S. Vodopianov et al., Nucl. Instr. Meth. **B201** (2003) 266.

[4] T. E. Stevens et al. Science **291** (2001) 627; M. Ciljak et al., Nucl. Instr. Meth. **A** (2003) in press.

Health and Environmental Physics

Thorium determination in intercomparison samples and in some romanian building materials by gamma-ray spectrometry

A. Pantelică[1], Em. Cincu, I.I. Georgescu[2], M.D. Murariu-Măgureanu[2], I. Mărgaritescu[2]

[1] NIPNE-HH, Department of Applied Nuclear Physics
[2] "Politehnica" University Bucharest, Faculty of Industrial Chemistry

Thorium content in zircon sand, thorium ore, and a thorium liquid sample, as well as in some Romanian building materials: sand, wood, tufa, asbestos-cement, cement mill dust, fly coal ash, bricks, and tile (28 samples) was determined by gamma-ray spectrometry. For the building materials, ^{226}Ra, ^{40}K and ^{137}Cs specific activities were also measured. All samples were kept tightly closed in the pots for about one month, to permit radioactive equilibrium between the gaseous radionuclides ^{222}Rn (^{238}U series), as well as ^{220}Rn (^{232}Th series) and their decay products be assured.

^{232}Th activity concentration was calculated from its decay products ^{228}Ac, ^{212}Pb, ^{212}Bi, and ^{208}Tl, assuming radioactive equilibrium among all ^{232}Th decay chain isotopes. The activity concentrations of ^{226}Ra was calculated by ^{214}Pb and ^{214}Bi decay products, assuming radioactive equilibrium among all ^{226}Ra decay chain isotopes.

Zircon sand, thorium ore, and a thorium liquid sample were analyzed in the frame of the European Commission Project "Thematic network on the analysis of thorium and its isotopes in workplace materials", coordinated by the Health and Safety Laboratory HSL, Sheffield, United Kingdom. Thorium nitrate solution containing ^{232}Th in equilibrium with its decay products and the two thorium minerals (without any prior treatment) were prepared as test samples by the Centre for Ionizing Radiation Metrology at the UK National Physical Laboratory (NPL), Teddington, England. The obtained ^{232}Th results are in good agreement with those of NPL for the liquid and ore samples (analyst/NPL ratios of 0.97 and 1.05, respectively) and rather good agreement for zircon sand (analyst/NPL ratio of 1.20) [1,2].

Sand, wood, tufa, asbestos-cement, cement mill dust, fly coal ash,tile, red and autoclaved cellular concrete (ACC) bricks collected from building material factories in different zones of Romania were investigated for natural and artificial radioactivity. The results were compared to Romanian standards for maximum permissible ^{232}Th, ^{226}Ra, and 40K activity concentrations in building materials.

References

[1] A.M. Howe, O.T. Butler, *Thematic network on the 2 analysis of thorium and its isotopes in workplace materials: Report on the 3rd intercomparison exercise* HSL (Health and Safety Laboratory, Sheffield S3 7HQ, United Kingdom) Report IEAS/01/01 (2001).

[2] A. Pantelica, I.I. Georgescu, M.D. Murariu-Măgureanu, I. Mărgăritescu, Em. Cincu, Thorium determination in intercomparison samples and in some Romanian building materials by gamma-ray spectrometry, *Radiation Protection Dosimetry*, 97, No.2, 2001, 187-192

Gamma-ray spectrometry on Danube river samples collected in february-march 2000

A. Pantelică[1], I.I. Georgescu[2]

[1] NIPNE-HH, Department of Applied Nuclear Physics
[2] "Politehnica" University Bucharest, Faculty of Industrial Chemistry

The aim of this research was to investigate by gamma-ray spectrometry the contribution of Tisa tributary river to the radionuclides contents of the Danube River in Romania, after the gold mining events at Baia Mare (N-W Romania), in January 2000. It is part of a more extended study concerning aquatic environment pollution with heavy metals and beta radionuclides, too [1].

Fish species *Alburnus alburnus and Carasius auratus* (flesh and scales) were analyzed in relation with

the surface water and bed load sediment samples collected about two months after the mining events. The collection sites were Moldova Noua (km 1073, the river entrance in Romania), Bazias (km 1072.4), Port Corabia (km 633), Corabia (km 629.5), and Giurgiu (km 493).

^{137}Cs, ^{226}Ra (^{238}U series), ^{228}Ra (^{232}Th series) and ^{40}K activity concentrations (in Bq kg^{-1}), measured in sediment, fish (fresh), and water samples are found to be situated at the levels determined in Danube samples during the last years, no radioactive pollution being observed.

References

[1] I.I. Georgescu, Gh.D. Baran, D.T. Breban, V. Cojocaru, M. Ciubotariu, A. Danis, A.I. Pantelică, V.Gh. Stănescu, On the chemical and radioactive content of the Danube river samples collected in February-March 2000, 36^{th} CIESM Congress, 24-28 September 2001, Rapp. Comm. Int. Mer M,dit., 36 (2001) 128.

Elemental analysis of lichen bioaccumulators before exposure as transplants in air pollution monitoring

A. Pantelică [1], V. Cercasov [2]

[1] NIPNE-HH, Department of Applied Nuclear Physics
[2] Institute of Physics, University of Hohenheim, Stuttgart, Germany

Lichen transplants from relatively unpolluted sites are successfully used as heavy metal bioaccumulators for long- term air pollution monitoring. Significant element accumulations are generally revealed after 6 to 12 months of exposure.

The main objective of this interdisciplinary research is to get a low-price survey of the air pollution level in some critical areas of Romania by nuclear and atomic analytical methods, based on the element accumulating property of transplanted lichens.

The lichen species *Evernia prunastri and Pseudevernia furfuracea* collected from the Prealps, northeast Italy, have been selected for this study. Experimental set-up for standardized lichen exposure needs special plastic frames ("little traps": $15 \cdot 15 \cdot 1.5$cm, with 1cm^2 mesh) which are fixed horizontally on stainless steel posts at about 1.5m above the ground. Prior to exposure, the lichen material is cleansed of some vegetal impurities, and then shortly washed using de-ionised water.

The initial (zero-level) contents of lichens were determined by Instrumental Neutron Activation Analysis (INAA) and Energy Dispersive X-Ray Fluorescence Analysis (EDXRFA) methods. INAA was carried out at the Institute of Physics and Nuclear Engineering in Bucharest (IFIN) and Energy Dispersive X-Ray Fluorescence Analysis (EDXRFA) at the University of Hohenheim in Stuttgart.

The investigated elements were: As, Br, Ca, Cd, Co, Cr, Cu, Fe, K, Mn, Ni, Pb, S, Sb, Se, V, and Zn. From among them, Cd, Co, and Sb can be determined only by INAA and ICP- MS, Pb only by EDXRFA and PIXE, and S only by EDXRFA. A statistical intercomparison of the results allowed a good quality control of the used analytical methods for these specific matrices.

This work was supported in part by European Commission Center of Excellence Project ICA1-CT-2000-70023: IDRANAP (Inter-Disciplinary Research and Applications based on Nuclear and Atomic Physics), Work Package 2 (Air pollution monitoring by sampling airborne particulate matter combined with lichen bioaccumulator exposure).

References

[1] Report WP2 IDRANAP 03-01/2001, http://www.nipne.ro/Cenex/cex_eur.

Development of prototypes of advanced systems for nuclear emergency management (NOTEPAD and RODOS)

G. Mateescu[1], D. Galeriu[1], D. Vamanu[1], D. Slavnicu[1], D. Craciunescu[1], A. Gheorghiu[1], C. Turcanu[1], D. Gheorghiu[1], V. Acasandrei[1], A. Melintescu[1]

[1] IFIN-HH, Life and Environmental Physics Department

The project RODOS (Real Time On-line Decision Support System for Off-Site Nuclear Emergencies in Europe) has been carried out under the auspices of EC's "Nuclear Fission Safety Programme". Romania, by IFIN-HH, is a participant to this project, the research and development activities for the RODOS project being performed in the Vth Framework of EC. IFIN-HH has developed also its own system, NOTEPAD, concordant as aim and method with RODOS, both DSS systems being able to offer a quick response to Romanian decision makers by assessing the consequences and countermeasures in case of a nuclear accident.

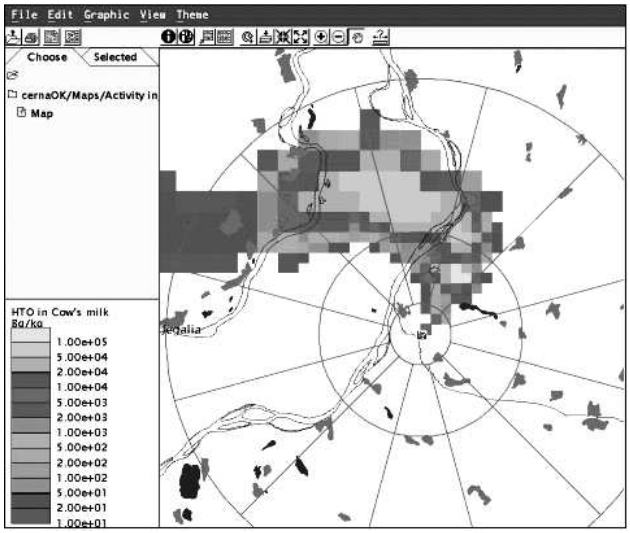

Figure 1: HTO activity in cow's milk.

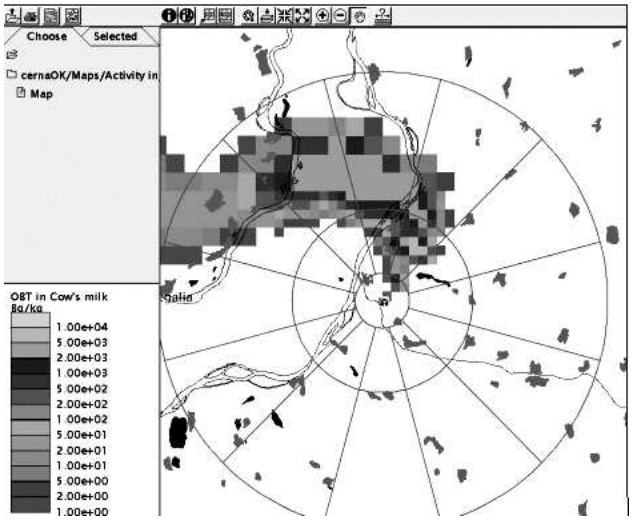

Figure 2: OBT activity in cow's milk.

The main results achieved during 2001 are:
a) Testing of the RODOS-FDMH module, developed in IFIN-HH, using the geographical database for Cernavoda, by simulating a severe CANDU accident scenario with emission of tritium in the form of HTO. Figures 1-2 present applications for HTO and OBT activity distribution in cow's milk.

b) Development of source codes included in the NOTEPAD software package:
1. 'SPILLS TO SURFACE WATERS'
2. 'SPILLS TO GROUND WATERS'.
Fig.3 presents 'SPILLS TO SURFACE WATERS' result for a simulated scenario. For 'SPILLS TO GROUND WATERS' code, a simulated exercise for an illustrative scenario has been made. A tank-car transporting a liquid radioactive solution runs off the rails and overturns with perforation of the tank in the area of Basel-East rail station. The code input-interface for this situation is presented in Fig.4.

Figure 3: Contamination after 100 seconds from the emission.

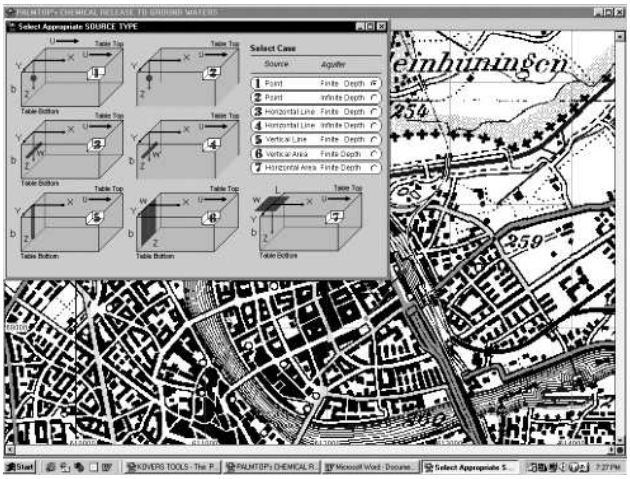

Figure 4: Code input-interface.

Intercomparison exercises between RODOS NOTEPAD were made, for the total effective dose equivalent and thyroid committed dose equivalent, resulting in normalizing factors that make feasible a conversion from one code output to the other and their harmonization.

Routine surveillance of environmental radioactivity in the influence area of the institute during 2001

R. O. Dumitru[1], D. C. Breban[1]

[1] IFIN-HH, Life and Environmental Physics Department

The radioactivity measurements were performed according to the Monitoring Concept for nuclear units in IFIN-HH, which provides the type, the locations and sampling frequency of the environmental factors that were monitored. The radiometric analyses were carried out according to the Working Procedures. The working group was involved in a project supervised by the IAEA "Ouality Assurance and Quality Control for Nuclear Analytical Techniques".

Samples of water, sediment, soil, vegetation and aerosols have been analyzed for both gross beta and gamma activity, as follows: 948 samples of potential radioactive water, surface, drinking and underground water; 24 sediment and 90 soil samples; 24 samples of spontaneous vegetation and samples of milk, cereals and vegetables .

We also analyzed for gross beta and gamma activity 44 samples of radioactive liquid effluents from the nuclear uits CPR, STDR and DCNU.

Airsols samples have been monitored twice a month. The maximum concentration of the artificial total beta activity was of 10 mBq/m3 air (absolute error expressed as 2 standard deviation was 3 mBq/m3).

Gross beta activity for samples of drinking water was always situated bellow the maximum allowed concentration (1 Bq/l).

The maximum value recorded for the total beta activity in sewage water (Reactor Canal) was of 2.1 Bq/l (absolute error expressed as 2 standard deviation was 0.6 Bq/l), but the radioactive concentration of the surface water downstream the spillflow was in this case situated below 0.8 Bq/l. During the whole monitoring period the total beta activity for surface waters did not exceed the Warning Level of 1.85 Bq/l.

Gross beta values for spontaneous, cultivated vegetation and milk samples collected from the living area in Magurele were in the same range to those recorded in the previous years. The working group was also involved in collecting and processing of samples of soil and vegetation from the Fort area.

Distribution of selected artificial and natural radionuclides in samples of soil and sediment from Romania

D. C. Breban[1], J. Morteno-Bermudez[2]

[1] IFIN-HH, Life and Environmental Physics Department
[2] IAEA, Seibersdorf Laboratory, Austria

Amongst the man-made radionuclides, Pu-239+240, Pu-238, Pu-241 and Am-241 are of great concern from radiological point of view because of their high radiotoxicity and long term environment impact.

In 2001, an IAEA fellowship provided the opportunity to analyze these radionuclides in several soil samples collected from an alpine pasture area located in Parang Mountains, offering for the first time information on the accumulation and distribution of these radionuclides in soil samples from Romania.

Sediment samples collected from the Romanian sector of the Danube River and Black Sea were investigated for Am-241, Pb-210, Pu, Th and U radionuclides as well, following up earlier studies in these areas. After radiochemical separation of the radionuclides by sequential combined procedures, based on anion-exchange and extraction chromatography, the alpha-emitters were measured by alpha-spectrometry and the beta Pu-241, Pb-210 by Liquid Scintillation Counting.

In case of sediment, the antropogenic Pu alpha emitting radionuclides were detected only in the samples collected from the Black Sea. The activities concentration ranged between (0.06-1.8) Bq/kg dry mass for Pu-239+240, the maximum values being determined for the deeper layers (20-30) cm of the sediment. Concentration of Am-241 ranged between (0.07-0.5) Bq/kg dry mass.

Pu-241 was detected only in the soil samples, 241Pu, its activities falling within the range of (20-73) Bq/kg dry mass for the upper organic layers. The results showed that 241Pu is the dominat radionuclide amongst the investigated transuranics in the soil samples.

On the basis of activity isotopic ratios Pu-238/Pu-239+240, Am-241/Pu-239+240 in soil and sediment depth profile, the origin of the contamination (Chernobyl accident and nuclear weapon test fallout) was determined.

Pb-210 exhibits concentration between (10 Bq/kg and 90 Bq/kg), the highest values were recorded in the Black Sea sediment.

The concentration of U natural isotopes for sediment samples correspond to those cited in the literature for the Bulgarian and Turkish Black Sea coasts. They were in the range of 30-70 Bq/kg. Activity isotopic ratios U-234/U-238, close to the equilibrium value, showed that no antropogenic contamination has occured.

The radioactive concentration of natural U and Th isotopes in Danube river sediment samples, of (10-30) Bq/kg for U-238 and (15-50) Th-232 are in the same range to those reported for sample collected in previous years from the same sites.

A code comparison exercise for harmonizing domestic and reference tools

D. Vamanu[1], G. Mateescu[1], A. Berinde[1], D. Slavnicu[1], V. Acasandrei[1], E. Slavnicu[2]

[1] IFIN-HH, Life and Environmental Physics Department
[2] Politehnica University of Bucharest,Romania

One lesson drawn from the Chernobyl accident (Ukraine, May 1986) has recognized the importance of an internationally-shared availability of norms, methods and tools to characterize abnormal nuclear events; design prompt response measures commensurate with the potential off-site, including transboundary consequences of such events; monitor the evolvement of the radiological situation over the exposed territories in the medium- and long run; and proportionally adjust and maintain a sound management of the crisis aftermath.

The Comparison Framework: Accident Scenarios

The Source Term

The core inventory was obtained by scaling up to 440 MWe the reference unit inventory of a typical LWR

recommended and taken just before a fresh fuel reload: Λ=2.1x10 ^{9} Ci. All scenario cases assumed a zero-power emission at 30 m height above ground, an effective escape duration of 30 min., and a time interval of cca 0.5 h between the reactor shutdown and the start of the core damage process under a loss of coolant.

The Meteorologic scenario

Comparative code runs have been conducted, for wind velocities of 2.1 m/s and A through F Pasquill stability, with no precipitation and precipitation rate for D stability assumed.

Precipitation rate (mm/h)
0,1
1
5
10

Due to different the terrain roughness of the exposed territory a flat terrain is supposed for Bechet-Kozlodui area and an accidental one for Cernavoda area.

The focus of the in-house exercise was, however, on the comparison of the NOTEPAD and RODOS performance in addressing identical source term and meteo scenarios. To compare NOTEPAD performance against RODOS reference results, the Total Effective Dose Equivalent (TEDE - the sum of cloudshine, groundshine for 7 days and inhalation for 50 years) and the Commited Dose Equivalent of Thyroid (CDE THYR - due to inhalation for 50 years) have been selected in view of their direct relevance in scaling the sheltering, evacuation and iodine administration countermeasures.

One can see that, compared with RODOS, the NOTEPAD results would systematically appear larger. The a priori suspicion that a relatively rigid, rule-based code like NOTEPAD, ignoring the subtleties of a detailed atmospheric dispersion modeling, like the nuclear unit dimensions, the roughness and the noble gas deposition, would generate overconservatism were thus confirmed.

Distance (km)	A class	B class	C class	D class	E class	F class
2	0.247	0.164	0.080	0.029	0.0056	0.0005
10	0.392	0.300	0.251	0.182	0.123	0.057
20	0.292	0.252	0.223	0.142	0.105	0.086
25	0.343	0.268	0.319	0.214	0.180	0.155

Table 1: TEDE , RODOS/NOTEPAD,TEST1,no precipitation

Distance(km)	A class	B class	C class	D class	E class	F class
2	0.125	0.077	0.035	0.012	0.026	0.0002
10	0.351	0.192	0.136	0.079	0.049	0.021
20	0.342	0.196	0.114	0.060	0.041	0.032
25	0.661	0.376	0.220	0.100	0.071	0.055

Table 2: CDE THYR , RODOS/NOTEPAD,TEST1,no precipitation

An intercomparison between JINR - Dubna and NIPNE - Bucharest neutron activation analysis laboratories for major and trace elements in lacustrine sediments

C.L. Dinescu [1], O.A. Culicov [2], O.G. Duliu [3], M.V. Frontasyeva [2], C.D. Oprea [2], M. Haralambie [1]

[1] National Institute for Physics and Nuclear Engineering - Horia Hulubei, P.O. Box MG-06, RO-76900 Bucharest, România

[2] Joint Institute for Nuclear Research, 6, Joliot Curie street, 141980, Dubna, Russia

[3] University of Bucharest, Department of Atomic & Nuclear Physics, P.O. Box Mg-11, RO-76900, Bucharest, România

Neutron Activation Analysis (NAA), one of the best elemental analytical methods, currently used for quantitative analysis, at μg/kg level can be performed by using thermal as well as epithermal neutrons. *The use of thermal neutrons, due to great absorption cross sections has the advantage of a relatively short activation time but in same cases, the resulting gamma-ray spectra are noisy that negatively influence the precision. Alternatively, the cross sections for epithermal neutrons are sensibly smaller that requires longer activation times but, in the case of silicate rocks the epithermal neutrons activation analysis proved to be advantageous in terms of improvement in precision and lowering of detection limits.* In environmental studies, eight REE as well as heavy metal pollutants including Cr, Zn, As or Sb can easily be determined at μg/kg levels by using thermal as well as epithermal neutrons . This fact makes an intercomparison more interesting as two different variants of the same analytical technique are used. Such kind of study has been performed within an intercomparison project between the JINR - Dubna, Russia and the NIPNE in Bucharest, Romania. Within this project, the vertical distribution of 23 major and trace elements (Sc, La, Tb, Yb, Th, Na, Rb, Cs, Ba, As, Sb, Hf, Cr, Fe, Co, Zn, Ce, Sm, Lu, Ca, Br, Ta and Eu) in a 37 cm core fragment (12 different sections) containing recent sediments collected from the Furtuna Lake in the Danube Delta has been determined. In our opinion, this study is more interesting as at Dubna laboratory NAA is performed by using epithermal neutrons (ENAA) produced by a pulsed reactor while Bucharest laboratory uses thermal neutrons (INAA) generated by a continuous flux nuclear reactor.

The technique used in both laboratories has been extensively described in a number of previous papers [?].

In our case, for all samples and all elements we have determined the numerical values of average concentrations, standard deviations as well as relative standard deviations (RSD). Additionally, for each element we calculated the correlation coefficient r^2 between its concentrations as determined in each laboratory. To obtain a global view of our results, we have also calculated for each element its relative concentration to the upper continental crust (UCC). One problem that arises when measuring other than standard samples is the possibility of sample being inhomogeneous. As all investigated samples represent recent sediments, we have checked their homogeneity with respect to some elements by means of three ternary diagrams, *i.e.*, Co-Hf-Th, Sc-La-Th and Rb/10-Yb-Tn. For the same purpose we plotted the La to Th ratio as one of the best indicators of sediment origin. For a better comparison, we plotted the data corresponding to UCC on all these diagrams too.

In the case there are great volumes of experimental data to be processed and interpreted the mathematically methods of multivariate statistics such as factor analysis (FA) or cluster analysis are the most adequate techniques. Accordingly, in our case, to evidence any possible systematic error specific to each laboratory, all the data were checked by means of FA. The main idea of FA is to evidence a minimum number of factors that explain the maximum variance of analyzed data. In our case, we have used the maximum-likelihood FA (varimax normalized rotation) to determine the principal factors. For this purpose, we considered for each element and each sample the ratio between the experimental and the corresponding UCC concentrations. In this way, we avoided any dominant influence of a particular element.

The numerical values of experimentally determined concentrations are, for the majority of elements, close to those corresponding to UCC, which is in good agreement with the nature of the investigated sediments. This feature is confirmed by the resulting ternary diagrams, where almost all the experimental points are grouped around corresponding UCC data, as well as by the La to Th ratio of 3.37 ± 0.29, being close to 2.85 as reported for UCC model.

It must also be pointed out that the result of FA has shows that all the elements form a single relatively homogeneous cluster, within which the variables (elements concentrations) corresponding to the two laboratories could not be separated in any kind of subclusters. This fact can be interpreted as the absence of systematic errors specific to one of the laboratory.

In this way, of the 23 major and trace elements investigated, the best concordance in terms of RSD and correlation coefficient was found for 7 elements, *i.e.*, Cs, Sc, Fe, Na, As, Ba and Ce. For the other elements, we observed discrepancies between the RSD or low values of the correlation coefficient. At the same time, FA indicates that, irrespective of laboratory, all the elements form a single cluster, thus confirming the absence of any significant systematic errors connected to one laboratory.

References

[1] Dinescu, L.C.; Duliu, O.G.; Badea, M.; Mihăilescu, N.G.; Vanghelie, I.M. Investigation of the Vertical Distribution of Major and Trace Elements in Matita Lake (Danube Delta) Sediments by Activation Analysis. J. Radioanal. Nucl. Chem. Articles. **1998**, 248, 75-81.

[2] Dinescu, L.C.; Duliu, O.G. Neutron Activation Analysis Investigation of the Heavy Elements Pollution in Some Lakes of the Danube Delta. Appl. Rad. Isot. **2001**, 54, 853-859.

[3] Frontasyeva, M.V.; Pavlov, S.S. Analytical Investigation at IBR-2 Reactor in Dubna. **2000**, JINR Preprint E-14-2000-177, Dubna, Russia.

Atmospheric deposition of trace metals in Romania studied by the moss biomonitoring technique using NAA and AAS

A. Lucaciu[1], M.V. Frontasyeva[2], C.D. Oprea[2], O.A. Culicov[2], E. Steinnes[3], L. Timofte [1], I. Vata[1]

[1] NIPNE-HH

[2] Joint Institute for Nuclear Research, 141980 Dubna, Moscow Region, Russia

[3] Norwegian University of Science and Technology, Trondheim NO-7491, Norway

To characterize atmospheric deposition of trace elements in Romania, moss samples of *Hylocomium splendens, Pleurozium schreberi and Hypnum cupressiforme* were collected at 272 network sites (20 x 20 km) and in different years between 1995 and 2000. Instrumental neutron activation analysis (INAA) has been used for determination of 37 major, minor and trace elements (e.g. Na, Mg, Al, Cl, K, Ca, Sc, V, Cr, Mn, Fe, Co, Ni, Zn, As, Se, Br, Rb, Sr, Zr, Mo, Ag, Sb, I, Cs, Ba, La, Ce, Sm, Tb, Yb, Hf, Ta, W, Au, Th and U) in moss samples. Copper, cadmium and lead were determined by flame atomic absorption spectrometry (FAAS). In order to identify the sources of air pollution in Romania, the principal component analysis was applied on the overall data set, as well as on each data set. At least 74% of the total variance in data sets could be explained by four to six principal components, including soil dust, general pollution, sea-salt, foliar leaching and local point source categories. The highest concentrations of trace metals related to industrial activities were found in Transylvania Plateau (Cr, Fe, Co, Ni Cu, Zn As, Se, Mo, Ag, Cd, Sb, Ba, W and U) and in the South of Romania (Ni). Crustal enrichment factors, based on scandium, decrease in the order: Cd, Se, Sb, Pb, I, Cl, Br, Au, Ag, Zn, As, Cu, W, Mn, Zr, Hf, Mo, K, Rb, Ba, Cs, Ca, U, Mg, Th, Ce, La, Tb, Sm, Cr, Sr, Al, Ta, V, Yb, Fe, Ni, Co and Na. Comparison of the data from different surveyed regions revealed the differences in concentrations of air toxics related to specific industrial activities concerned. The trace metal levels in Romania were similar to those found by the other East-European countries participating in 2000 European moss survey, but significantly higher compared with Norway.

Clinical evaluation of hTSH IRMA kit developed at IFIN-HH Bucuresti

Virginia Borza[1], Mariana Purice[2], Elena Neacsu[1], Julieta Zaharescu[3], Leonard Dumitriu[2]

[1] "Horia Hulubei" National Institute for Physics and Nuclear Engineering (IFIN-HH Bucharest)
[2] "C.I.Parhon" Institute of Endocrinology, Bd.Aviatorilor 34-36 sector 1, 79600 Bucharest
[3] Universitary Hospital, str.Splaiul Independentei 12, Bucharest

The TSH immunoradiometric assay(IRMA) presents a major interest for the diagnosis of thyroid function state. The hTSH IRMA kit has been developed at IFIN-HH in order to be used for the direct quantitative determination of hTSH in human serum or plasma in the range 0-50μUI/mL. In this paper are presented results obtained at IFIN-HH and Endocrinology Institute in the kit validation: evaluation of performance characteristics, the correlation studies of TSH concentration measured by IFIN kit and by 2 validated commercial kits on patient sample; also, normal range was established. The good results obtained in the validation of the hTSH IRMA kit were the following: the intra-and interassay coefficient of variation were $\leq$10%, recovery: 95-110%, sensitivity $\leq$0, 035μUI/mL, and stability 6 weeks. The TSH concentration measured in clinic samples by the IFIN hTSH IRMA kit and 2 commercial kits correlate very well. Normal range established on 143 untreated euthyroid subjects is: 0.37-3.

References

[1] K.J.Catt, Treager, G.W. - Science , 158 (1967), 1570

[2] R.S.Chapman, - Immunoassay for Clinical Chemistry, 2^{nd} edn (Hunter, W.M., Corrie, J.E.T. Eds) Churchill Livingstone, Edinburg, 1983, 178-190

[3] R.Edwards, H.J.Hope, P.Suprarop - Proceeding of an International Symposium on Radioimmunoassay and Related Procedures, Vienna, aug.1991, pag.177

[4] C.M.Ling, L.R.Overby, - J.Immunol., 109 (1972), 834

[5] L.Wide, Acta Endocrinol.Suppl 142 (1969), 207-218

[6] L.Wide, J.Proath - Biophys.Acta, 130 (1966) 257-262.

Synthesis of testosteron-1, 2-T

Cristian Postolache[1], Lidia Matei[1], Eduard Condac[2]

[1] National Institute of Research and Development for Physics and Nuclear Energy "Horia Hulubei", Măgurele, Atomistilor Street nr. 407, Bucharest
[2] University of Bucharest, Faculty of Biology, Splaiul Independentei, nr. 91-95, Bucharest

Elemental tritium is obtained during the decontamination process of the moderator from Cernavoda Nuclear Power Plant. It might be stocked for its use in controlled fusion, in a relatively far future, or, it might be immediately used as raw material in the synthesis of labelled compounds with important economic value.

Labelling of testosteron with tritium was necessary for the carring out of radiometric and molecular biology studies concerning androgene dependent diseases.

Testosteron was labelled by selective hydrogenation of 1,2 dihydrotestosteron acetate. The forerunner was synthetized in two steps: 1) esterification of testosteron using acetic anhydride, and 2) selective dehydrogenation with 2,6-dichloro-3,5-dicyan-1,4 quinone (DDQ) of the esther formed in the first step. Testosteron acetate was synthetized and purified with yields of 73%, and respectively 80%. The dehydrogenation process was characterized by yields of 82% for synthesis and 33% for purification.

The tritium labelled hormone was obtained in two steps: 1) selective hydrogenation of Δ^1- testosteron acetate in the presence of T_2 gas, at low pressure, and 2) hydrolysis of the esther at basic pH. The raw product obtained was purified by preparative thin layer cromatography. The physical and chemical characterization of labelled testosteron reveals a radiochemical purity higher than 98% and a specific activity of 53.4 Ci/mmol.

Routine monitoring of environmental radioactivity in the influence area of the institute during 2002

D. C. Breban[1], R. O. Dumitru[1]

[1] IFIN-HH, Life and Environmental Physics Department

The radioactivity measurements were performed according to the Monitoring Concept for nuclear units in IFIN-HH, which provides the type, the locations and sampling frequency of the environmental samples.

Samples of water, sediment, soil, vegetation and aerosols have been analyzed for both gross beta and gamma activity, as follows: 930 samples of potential radioactive water, surface, drinking and underground water; 23 sediment and 81 soil samples; 26 samples of spontaneous vegetation and samples of milk, cereals and vegetables.

Atmospheric airsols have been monitored twice a month. The maximum concentration of the artificial total beta activity was of 24 mBq/m^3 air (combined uncertainty expressed as 2 standard deviation was 3 mBq/m^3), below the attention limit of 50 mBq/m^3 air. For the dry and wet atmospheric deposition the total beta activity ranged from 0.02 to 1.2 $Bq/m^2/day$. Cs-137 was the only artificial radionuclide detected by gamma spectrometric analyses of annual composite samples and its specific acitvity was in the range recorded in the last years on the Romanian territory. The radioactive concentration of H-3 in the atmospheric deposition monthly composited was close to the minimum detectable activity (3-6 Bq/l).

Gross beta activity for samples of drinking water was always situated bellow the maximum allowed concentration (1 Bq/l).

For the sewage waters (canal Reactor and canal IFA) the concentration of the total beta was close to the warning limit of 1.85 Bq/l during few days of May, June and July. Co-60 was identified as contaminant in those samples, in the range 2-4 Bq/l (combined uncertainties: 0.2-1.3 Bq/l). In those days the values recorded for total beta activity of the river water collected downstream the spillflow were below 1 Bq/l and Co-60 was not detected. During 2002 the total beta activity of the surface waters varied in the range 0.3-1.6 Bq/l, the higher values being correlated to a higher amount of suspended matter.

In river sediment samples Co-60 was detected only at the sewage spillflow (canal Reactor), the average radioactive concentration, 6.0 Bq/kg dry mass (2.0 Bq/kg combined uncertainty), being much lower than thet recorded in 2001.

Gamma spectrometric analyses performed on annual composite samples showed similar values to those recorded in the previous years for Cs-137 radioactive concentration. Average values were of 40 Bq/kg soil and 8 Bq/kg river sediment (10 and respectively 2 Bq/kg combined standard uncertainties) and below the detection limit for surface and sewage water samples (0.002 Bq/l). These values are characteristic to the post-Chernobyl ones.

Gross beta values for spontaneous, cultivated vegetation and milk samples collected from the living area in Magurele were in the same range to those recorded in the previous years, and similar to the radioactive concentration of K-40. Its concentration varied from 50 Bq/l for milk samples to 140 Bq/kg dry mass for wheat samples. No artificial radionuclide was detected in the analyzed samples of vegetation.

Regarding the monitoring of the Fort area, several soil samples were radiochemically analyzed for Sr-90.

As part of the Quality Assurance and Control system, samples of blanks, spikes and IAEA reference materials were analyzed on regular basis. The working group has also participated in three intercomparison exercises with the IAEA and DOE (USA).

Adaptive response of human lymphocytes exposed to low dose of gamma radiation

D. Savu[1], M. Radu[1], I. Petcu[1]

[1] IFIN-HH, Life and Environmental Physics Department

The main goals of the present work are: (a) to study the induction of radioadaptive response in human lymphocytes and to establish the experimental conditions for which this response is optimized; (b) to evidence the relationship between the observed effect and the phase of the cell cycle.

The radioadaptive response was assessed by the chromosome aberration test. Human lymphocytes were pre-irradiated with 1 cGy or 5 cGy (1 cGy/min) either before stimulation by phytohemaglutinin (for G0 study)) or at 20 h after stimulation by PHA (for G1), followed by 1 Gy (1 Gy/min) at 46 h after stimulation by PHA. After the irradiation with high dose, the cultures were kept for 2 h in the incubator and then the colcemid was added to the cultures (at 48 h). The cultures incubated 2 h with colcemid were exposed to kalium chloride and then fixed in acetic acid:methanol (1:3). The fixed cells were dropped onto wet glass slides and dried. Slides were stained with Giemsa for the scoring of chromatid aberrations. 50 cells were scored from replicate cultures for each treatment. We considered only those metaphases that contained 46 chromosomes.

The following results have been obtained:

- the human lymphocytes pre-exposed in G0 to 1 cGy and 5 cGy exhibit an adaptive response to the subsequent exposure at 1 Gy.
- the evolution of cytogenetic parameter chromosomal aberration in the case of lymphocytes pre-irradiated in G1 is similar with that obtained for lymphocytes pre-irradiated in G0.
- the maximal expression of adaptive response was determined by delivering 1 cGy.
- the time interval between both types of successive irradiation's is optimal for the induction of the repair processes.
- the lymphocytes respond adaptively at low doses of irradiation, regardless the stimulation by phytohemaglutinin.

These results are in accordance with other reported data which prove that human lymphocytes are able to adapt to low dose irradiation so that they undergo less damages at the cytogenetic level (micronuclei, chromosomal aberrations) when exposed to consecutive high dose irradiation.

Adaptive response of yeast cultures (saccharomices cerevisiae) exposed to low dose of gamma radiation

Agnes Kulcsar1[1], D. Savu[2], Raluca Gherasim[3], I. Petcu[2]

[1] Institute of Biophysics, Szeged, Hungary
[2] IFIN-HH, Life and Environmental Physics Department
[3] University of Bucharest, Faculty of Biology, Bucharest, Romania

The present study was planned as follows:

i set-up of standard experimental conditions for investigation of radio-induced adaptive response in lower Eucaryotes.

ii development of a procedure for synchronizing Saccharomyces cerevisiae X 310 D cell cultures and cell cycle stages monitoring.

iii investigation of gamma (Co-60) and UV irradiation effects on the viability of synchronized and non-synchronized cell cultures of Saccharomyces cerevisiae; the effects were correlated with the cell density and cell cycle stage.

iv study of the adaptive response induced by irradiation and set-up of the experimental conditions for which this response is optimized.

The irradiation were performed by using a Co-60 with doses of 10^2-10^4 Gy and dose rates ranging from

2.2 10^2 Gy/h to 8.7 10^3 Gy/h. The study of radioinduced adaptive response was performed applying a pre-irradiation treatment of 100-500 Gy, followed by challenge doses of 2-4 kGy delivered at different time intervals, ranging from 1 h to 4 h.

The survival rate of synchronized and non–synchronized cultures as a function of exposure dose shows an exponential decay shape. No difference in viability of the cells occurred between synchronized and non-synchronized cultures.

The pre-irradiation of cells with 100 and 200 Gy were most efficient to induce an adaptive response for the yeast cells.

In this stage of work we proved the occurrence of the adaptive response in the case of synchronized yeast cultures exposed to gamma radiation. The results will be used in the future to investigate the dependence of this response on the cell cycle and the possibility to induce such a response by a low level electromagnetic field.

Nuclear and atomic techniques in air pollution studies by transplant lichen exposure, bulk deposition, and airborne particulate matter collection after 6 months exposure

A. Pantelică[1], V. Cercasov[2], E. Steinnes[3], P. Bode[4], H.TH. Wolterbeek[4]

[1] NIPNE-HH, Department of Applied Nuclear Physics
[2] Institute of Physics and Meteorology, University of Hohenheim, Stuttgart, Germany
[3] Department of Chemistry, Norwegian University of Science and Technology, Trondheim, Norway
[4] Interlaboratory Reactor Institute, Delft University of Technology (IRI-TUDelft), The Netherlands

This work presents partial results obtained in the study "Air pollution monitoring by sampling airborne particulate matter combined with lichen bioaccumulator exposure", in progress at IDRANAP Center of Excellence EU Project, ICA1-CT-2000-70023, WP2 [1].

Transplants of *Evernia prunastri* and *Pseudevernia furfuracea* lichen species from the Italian Prealps, were exposed for 6 and 12 months at six locations with different degrees and types of industrial activity, as well as on a background site with relatively clean air (Fundata). At each investigated location, bulk deposition was collected for the same periods, while airborne particulate matter was sequentially collected during 2 months, in parallel with those at a reference station (Afumati).

Pollution in the investigated areas is mainly due to the following industrial activities: steel making (Galati); non-ferrous ore processing (Baia Mare); chemicals and non-ferrous industry (Copsa Mica); coal-fired power plant and cement factory (Deva); traffic, coal-fired power plants, inorganic dyes, and galvanic treatment factories (Oradea); agriculture, mixed industry, and traffic (Afumati).

The lichen material was analyzed by INAA, XRFA, and ICP-MS, while the aerosol filters were analyzed by INAA and XRFA, and the bulk deposition only by INAA. XRFA was carried out at Stuttgart, ICP-MS at Trondheim, while INAA at Bucharest (long lifetime radionuclides) and Delft (short lifetime radionuclides, and, in the case of bulk deposition, short and long lifetime radionuclides). The investigated elements having relevant role in environmental studies were: As, Br, Ca, Cd, Co, Cr, Cu, Fe, K, Mn, Ni, Pb, S, Sb, Sc, Se, V, and Zn. From among them, Cd, Co, Sb, and Sc could only be determined by INAA and ICP-MS, while Pb and S only by XRFA and ICP-MS.

After 6-month exposure, both lichen species showed significant enrichment factors (relative to "zero level", before exposure) for all the measured elements, excepting Br, Ca, K, and Mn. Small lichen enrichments in Ca and Mn were determined on the sites with a relatively high atmospheric availability of these elements (Galati, metallurgical industry). *Pseudevernia furfuracea* alone revealed a small enrichment in Br on all the sites excepting Copsa Mica (with a rather high uncertainty).

A strong correlation between "lichen enrichment" and bulk deposition, with similar pattern for each investigated element was observed. The highest enrichment values for As, Ag, Au, Cd, Co, Cu, Pb, S, Sb, Se, and Zn were measured on the sites with non-ferrous industries in Copsa Mica, followed by Baia Mare. Elements such as Fe, Mn, and Cr, originating from the metallurgical industry, showed a significant enrichment in Galati. The highest enrichment values for V, which is especially emitted from oil burning, were found in Afumati (near Bucharest).

The element concentrations in air, as indicated by measurements of the suspended matter collected on filters, were examined relative to Afumati "reference station". High relative enrichments were noted as follows: As and Pb in Deva and Baia Mare; Cr, Fe, Mn,

and Zn in Deva; Cu and Se in Baia Mare; Ca, Ni, and V in Oradea. The high relative contents of Ni and V found on the urban site in Oradea were probably due to industrial oil burning. The ratios of the relative bulk deposition to the relative concentration in air suggested the lowest degree of atmospheric "wash-out" to be found in Deva, especially for Ag, Mn, As, Fe, Cr, Zn, and K.

The accumulating capacity of *Evernia prunastri* and *Pseudevernia furfuracea* corresponding to these specific environmental conditions was compared with those of *Cetraria islandica*, *Evernia prunastri*, and *Ramalina farinacea* used in a previous comparative air pollution study involving exposure sites in Germany, Italy, and Romania [2].

References

[1] Report WP2 IDRANAP WP02 28-02, http://www.nipne.ro/Cenex/cex_eur.htm

[2] V. Cercasov, A. Pantelica, M. Salagean, G. Caniglia, A. Scarlat Comparative study of the suitability of three lichen species to trace-element air monitoringEnvironmental Pollution **119/1**, 129-139 (2002)

Forster resonance energy transfer in the study of membrane rafts

M.A. Acasandrei[1], R. Dale[2], M. vandeVen[3], P. Steels[3], M. Ameloot[3]

[1] IFIN-HH, Life and Environmental Physics Department
[2] King's College London, UK
[3] Limburgs Universitair Centrum, Diepenbeek, Belgium

In biomembranes, glycosphingolipids and cholesterol form very small ($\prec$ 25 nm) assemblies, or "rafts", in which specific proteins are more concentrated than outside them. Forster resonance energy transfer (FRET) between labelled antibody Fab fragments bound to such proteins provides a tool to study these rafts. Two FRET models for rafts have been developed:

i) co-localization of raft components by distribution at random into circular rafts of various sizes; the raft area fraction could be either constant or determined by the expression level. The modelling is based on two simplified hypothesis: a) FRET between raft donors and non-raft acceptors could be neglected and b) every non-raft donor transfers energy to the raft acceptors as they have been homogeneously distributed over the whole membrane surface.

ii) dimer-like cluster model, by including cross-terms that take into account FRET between clusters and monomers; two dimer configurations have been proposed when taking into account the FRET exclusion spaces.

The models include consideration of distributions of donors and acceptors over the surfaces of the respectively labelled antibody fragments, considered as spherical, in the limits of no and infinitely rapid homotransfer between donors due to (a) multiple donors on the Fab surface and (b) high concentration of donor-labelled Fab fragments in the rafts.

Mitochondrial uptake of cytosolic calcium during metabolic inhibition of MDCK cells might be ascribed to the reversal of the mitochondrial Na+/Ca2+ exchanger

I. Smets[5], A. Caplanusi[4], S. Despa[3], Z. Molnar[2], M. Radu[1], M. vandeVen[5], M. Ameloot[5], P. Steels[5]

[1] IFIN-HH, Life and Environmental Physics Department
[2] Dept. of Medical Chemistry, University of Szeged, Szeged, Hungary
[3] Loyola University of Chicago Medical Center, Maywood, IL., 60153 USA
[4] Carol Davila Univeristy of Medicin and Pharmacy, Bucharest, Romania
[5] Limburgs Universitair Centrum, Diepenbeek, Belgium

Objectives. The aim of this study was to investigate the effects of ischemia on the $[Ca^{2+}]$ homeostasis in renal distal tubular cells that are known to be highly resistant towards ischemic conditions. To mimic renal ischemia, metabolic inhibition (MI) with NaCN and 2-deoxyglucose in Madin-Darby canine kidney (MDCK) cells was used as an in vitro model. Intracellular Ca^{2+} ($[Ca^{2+}]_i$) and Na^+ ($[Na^+]_i$) concentrations and the mitochondrial potential ($\Delta\Psi_M$) were monitored at 37°C by fluorescence imaging microscopy.

Methods. MI induced a transient increase in $[Ca^{2+}]_i$ from a resting value of 46±2 nM to a peak value of 632±78 nM (n=12) after 20 min and a subsequent decrease to 118±9 nM during the next 25 min, despite the continuous presence of metabolic inhibitors. Second phase extrusion of Ca^{2+} by Ca^{2+} ATPases in the plasma membrane was ruled out since cellular ATP levels , as determined with a luciferine-luciferase based assay, dropped to 3.2±0.5% (n=6) from control levels in 10 min of MI. Moreover, Ca^{2+} extrusion via the Na^+/Ca^{2+} exchanger (NCE) in the plasma membrane was unlikely since $[Na^+]_i$ increased with a factor 4 in the first 20 min of MI (n=7). Treatment with thapsigargin, a specific blocker of the SERCA pumps, did not modify the biphasic behaviour of [Ca2+]i during MI, excluding the possibility of Ca2+ uptake in the endoplasmic reticulum (ER). Accumulation of Ca^{2+} into the mitochondria after 20 min of MI via the DYM-dependent Ca^{2+} uniporter seemed unlikely since DYM measurements revealed that DYM dropped to 0±2% (n=8) of the control level in the first 20 min of MI. Moreover, in the presence of the mitochondrial uncoupler FCCP, the second phase of the Ca^{2+} transient during MI was still present. When MI was applied under Na^+ free conditions, $[Ca^{2+}]_i$ went up to 565±67 nM (n=7) in 20 min of MI without a subsequent decrease in $[Ca^{2+}]_i$, suggesting a Na+-dependent mechanism for removal of cytosolic Ca^{2+}. To evaluate the Ca^{2+} uptake into the mitochondria via the mitochondrial NCE acting in the reverse mode, CGP37157, a specific inhibitor of the mitochondrial NCE, was used. CGP37157 abolished the drop in $[Ca^{2+}]_i$ when administered from the onset of MI as well as when acutely added just after the start of the decrease in $[Ca^{2+}]_i$. In summary, MI induces a transient increase of $[Ca^{2+}]_i$ in MDCK cells.

Results. MI induced a transient increase in $[Ca^{2+}]_i$ from a resting value of 46±2 nM to a peak value of 632±78 nM (n=12) after about 20 min. A subsequent decrease to 118±9 nM occurred during approximately the next 25 min. Under Na+ free conditions (n=7), or when CGP37157 (CGP), a specific inhibitor of the mitochondrial Na^+/Ca^{2+} exchanger (NCE), was used (n=8), no second phase drop of $[Ca^{2+}]_i$ was seen during MI. Rhod2 spatially relates to the mitochondrial probe MitoTrackerGreen (MTG). Rhod2 intensities increased almost linearly to 434±46% (n=23) from the control value in 60 minutes of MI. In contrast the Rhod2 fluorescence gradually attenuated to 56±8% (n=14) from initial levels in control experiments without MI. In the presence of CGP, the MI-induced increase in mitochondrial Rhod2 fluorescence was nearly abolished (n=8).

Conclusions. Our results suggest that the second phase decrease of $[Ca^{2+}]_i$ is not due to Ca2+ removal out of the cells nor Ca^{2+} storage into the ER, but rather due to Ca^{2+} uptake into the mitochondria via the NCE acting in the reverse mode. The mitochondrial buffering of cytosolic Ca^{2+} might partly underlie the high resistance of MDCK cells towards ischemic conditions.

Applied Physics

Inter-laboratory comparison of thorium content in three reference samples

L. Dinescu [1], A. Danis [1], M. Ciubotariu [1], Em. Cincu [1], D. Matei [1], O. Sima [2]

[1] NIPNE-HH, Department of Applied Nuclear Physics
[2] Bucharest University, Faculty of Physics, Nuclear Physics Department

Three samples, a Thorium solution, a zircon sand and a thorium ore, originating from an EU intercomparison exercise(1) were analyzed by two relative methods: γ-ray spectrometry and alpha track method(2), the last one only applied to the Thorium solution.

In case of the gamma-ray spectrometry, the ^{232}Th activity concentration was determined by analyzing *the decay products* ^{228}Ac (911.2 keV and 969.0 keV), ^{212}Pb (238.6 keV), ^{212}Bi (727.2 keV) and ^{208}Tl (583.2 keV), the radioactive equilibrium of which was considered as already established; the ^{208}Tl activity concentration value was corrected for the branching ratio (0.3594). The reported ^{232}Th activity *concentration was the mean of the concentration values determined for each decay product.*

The detection efficiency calibration was established using an "in-house" standard prepared utilizing a Merck Thorium nitrate solution for the solid samples and the GESPECOR Monte Carlo simulation package(3) for the solution sample.

The analysis of Thorium by the alpha track method was based on the proportionality between the alpha track density obtained in the etched track detector and both the alpha exposure time, when the samples were in intimate contact with the track detector and the ^{232}Th activity concentration in the unknown sample and reference material. A number of 12 samples were analyzed using three "in-house" standards; the final value of the ^{232}Th activity concentration was calculated as the mean of the results obtained for the 12 samples.

The specific "in - house" standard for the alpha track method was prepared by using the same calibrated Thorium nitrate solution.

The obtained results are presented in Table 1 by comparison with the NPL (UK) reference values.

Sample	Reported values [Bq g^{-1}]	NPL values [Bq g^{-1}]	Deviation from NPL VALUE (%)
Th solution*	9.880 ± 0.490	10.716 ± 0.102	- 7.8
Th solution**	10.240 ± 0.614	10.716 ± 0.102	- 4.4
Zr sand**	0.574 ± 0.042	0.551 ± 0.021	+ 4.2
Th ore**	2.502 ± 0.150	2.494 ± 0.032	+ 0.3

* Values determined by the alpha track method.
** Values determined by the γ-ray spectrometry method.

Table 1: Activity concentration of ^{232}Th; comparative results

The relative differences between the ^{232}Th activity concentration values determined in the three intercomparison samples and the values supplied by NPL were found to be less than 5%, when determined by the γ-ray spectrometry method, and less than 8% when determined by the alpha track method. A good agreement was found (3.6 % relative difference) between the results obtained by the two analytical methods in the case of Th solution.

References

[1] A.M. Howe and O.T. Butler, *Thematic network on the analysis ofthorium and its isotopes in workplace materials*, report on the 3^{rd} intercomparison exercise, **IEAS/01/01** Health and Safety Laboratory, UK.

[2] L. Dinescu, O. Sima, A. Danis, M. Ciubotariu, Em. Cincu and D. Matei, *Analysis of Thorium and its Progeny by Gamma-ray Spectrometry and Alpha Track Methods*, Rad. Prot. Dosimetry, **97** (2), 181-186 (2001).

[3] O. Sima, D. Arnold, and C. Dovlete, *GESPECOR: A versatile tool in gamma-ray spectrometry*, J. Radioanal. Nucl. Chem. **248**, 359 (2001).

The study of diffusive motion in bitumen compounds by quasielastic neutron scattering

V. Tripadus [1], M. Popovici [2], M. Peticila [3], L. Craciun [1]

[1] NIPNE-HH, Applied Nuclear Physics Department
[2] Missouri University Research Reactor, Columbia MO, USA
[3] Road Research Institute, Bucharest, Romania

Bitumen is a colloidal system. It contains various types of hydrocarbons of different molecular weights-aromatic or aliphatic hydrocarbons, saturates and other type of molecules. The main component of this compound is asphaltene, a polynucleus aromatic molecule with surfactant characteristics. These macromolecules associate together forming the asphaltene-micelles, that in turn can further aggregate giving rise to a GEL type bitumen. If the micelles can move in the "see" of maltenes, that is the rest of compounds plays the role of a solvent, we deal with a SOL type bitumen. This microscopic picture essentially gives the temperature behavior viscoelastic properties of bitumen. The resin content is also an important parameter. As the resin content is high, the asphaltene-micelles are strong peptized and stabilized.

Many studies were devoted to the study of aggregation properties of asphaltenes extracted from bitumen samples. However it is difficult to connect the classical physical constants -dynamical viscosity, elasticity module- with microscopic model proposed. From this point of view we think that a direct study of internal molecular dynamics of bitumen is a very useful task for a better understanding of this compound. The first measurements were carried out using a NMR experiment on an ESSO bitumen sample. We continued these studies using the quasielastic neutron scattering method on two romanian bitumen samples. Using a focusing crystals method applied to a triple axis neutron spectrometer we obtained the spectra of quasielastic scattered neutrons at five temperature values -between 220 C and 144 0 C and at five momentum transfers.

As we deal with a hydrogenated compound the scattering is an incoherent scattering dominated by the scattering of protons. The reorienational diffusion motions of various molecular groups are responsible for the energy broadening of the incident resolution line. The dependence of this line-broadening of the impulse transfer reflects the type of diffusion performed by the scattering unit. We interpret such curves in terms of two jump-diffusion models developed by Chudley- Elliott (1961) and Hall-Ross (1981). In the first one the protons perform jumps between two equilibrium positions separated by an average length, l. The residence time in this position is to. The Hall-Ross model presumes jump-diffusion a markovian process according to which successive jumps are uncorrelated but governed by a spatial gaussian isotropic distribution. The experimental results are presented in table 1.

	Hall - Ross				Chudley-Elliott			
T ($^\circ C$)	$\tau_0 \times 10^{11}$ (sec)	r_0 (A)	Γ_0 (μeV)	$D_r = l^2/6\tau_0$ ($10^{-6} cm^2 s^{-1}$)	$\tau_0 \times 10^{11}$ (sec)	l (A)	Γ_0 (μeV)	$D_r = l^2/6\tau_0$ ($10^{-6} cm^2 s^{-1}$)
22	6.0	0.65	67.15	0.12	5.8	0.969	70.55	0.27
75	5.2	1.50	80.40	0.72	5.5	2.95	74.88	2.63
105	6.0	2.60	63.31	1.88	5.1	3.44	81.50	3.60
140	5.6	1.41	73.00	2.20	5.1	3.65	81.26	4.35

Table 1: The main results obtained from the fitting the experimental data with the two models. τ_0 - residence time, r_0, l - the lengths of the jumps, Γ_0 - the line broadening, D_r - the rotational diffusion constant

The Chudely- Elliott model apears to be more suited. This jump diffusion model can describe the proton dynamics involved in reorientational motions of various molecular groups. The equilibrium positions of this protons are not randomly distributed but in a molecular quasi-lattice.

Measurement of the production yield for negative Bi-209 ions and compounds

C. Stan-Sion [1], O. Constantinescu [1], M. Enăchescu [1]

[1] NIPNE-HH, Department of Applied Nuclear Physics

In order to perform high sensitivity Accelerator Mass Spectrometry (AMS) measurements of the ratio $^{210}Bi/^{209}Bi$ an important constraint is the to use of a high ion current produced by the ion sputtering source. Until now the information regarding the production of negative Bi ions by sputtering with Cs^+ is rather sparse. The electron affinity (EA) is in some extend proportional to the yield of produced negative ions and can be used as a first approximation in this evaluation. For Bi the EA is 0.95 eV [1].

To obtain reliable information about the production yield of negative ions produced by the sputter process of Cs^+ ions on Bi (in metallic and in other chemical forms) we used the AMS injector deck and performed an experiment in which all produced negative ion species were magnetic analysed. To determine the optimal sputtering yield of negative Bi ions the targets were prepared as Bi_2O_3, $Bi(NO_3)_3$ and metallic Bi. The target material was mixed with Ag and pressed into the source sample holder made of silver. Different fractions of Bi/Ag mixing have been tested to determine the best mechanic resistance and a good electric conductivity. The measurements were performed using the AMS Injector [2]. The negative ions produced in the sputter source are extracted and accelerated up to 15 keV. Then, the negative ions pass through the 90^0 analysing magnet where the selection of the desired ion species is performed and are measured in the second Faraday cup situated at the exit of the analyser.

In the experiment the negative ion current was measured in both Faraday cups placed at the entrance and at the exit of the magnetic analyser. In the first cup, at the entrance of the analyser, we measure the overall ion current accompanied by electrons. The electron current is depending on the ion source operation conditions and in our source this represents about 20% from the total negative current. This fraction can be determined by removing the electrons from the total beam using the deflection produced with a low static magnetic field at the ion source position. In this way it was also possible to determine the transmission through the magnet by integrating over the entire analysed mass spectrum. In our experiments the transmission was T = 70%. Two different energies for the Cs^+ ions were used in the experimental tests to sputter the Bi target: 2.5 keV and 9.2 keV. The extraction energy for negative ions was 15 keV and in one case 25 keV. The current values of negative ions were measured for a Cs^+ sputter beam of 1.2 mA and accelerated at an energy of 2.5 keV. The resume of the obtained results is given in table 1.

Sample	Ag* mixt	U_{sp} (kV)	U_{ext} (kV)	Bi (nA)	BiO (nA)	BiO_2 (nA)	Ag (nA)
Bi_2O_3	1:3	2.5	15	110	480	590	40
	1:5	2.5	15	95	450	580	32
$Bi(NO_3)_3$	1:2	2.5	15	100	500	1000	45
	1:5	9.2	25	78	430	890	16
Bi metal	-	2.5	15	30	95	120	-

* mass ratio of silver to compound

Table 1: Currents of the analysed negative ions produced from sputtering different Bi targets.

It is obviously from the above data in table 1 that $Bi(NO_3)_3$ gives the best negative ion current. For all chemical forms the dioxide BiO_2 gives the best sputtering yield. If we compare the current ratio Bi/Ag we obtain a value which is within the measurement errors close to the ratio of the EA given. The mean sputtering Cs current used was 1.2 mA and averaging over the mass loss of all samples we measured a consumption of Bi sample material of 5±1 mg / h x mA. Thus, at a normal operation of the ion source the sample in the source cathode should be exhausted after about 2 hours. Based on the measured data and on TRIM calculation we have obtained an estimate of the yield of negative Bi ions and compounds (Bi^-, BiO^-, $BiO2^-$) produced by the sputtering of $Bi(NO_3)_3$ with Cs^+ ions of 2.5 kV, at normal incidence. Y^- (Cs/ Bi-nitrate) = 0.8 (2)%. From the TRIM code a total sputtering yield of Cs ions on $Bi(NO_3)_3$ plus Ag (1:2) was calculated to be Y = 2.4 (sputtered ion/ incident ion). This is the only calculated value that was used in the determination of the negative yield of Bi ions and compounds. The TRIM total sputter yield calculation is in agreement with the measured mass loss of target material ($\Delta = 8\%$) giving good support for the obtained results.

References

[1] Ed. R. G. Wilson, F. A. Stevie, Ch. W. Magee, Secondary Ion Mass Spectrometry(1989)

[2] C.Stan-Sion et al., AMS at the National Institute of Nuclear Physics and Engineering in Bucharest, NIM B(172) 806-811(2000).

Radioactivity measurements and control solutions

D Bartos[1], M Ciobanu[1], F Constantin[1], M. Petcu[1], Al Rusu[1]

[1] National Institute for Physics and Nuclear Engineering, Bucharest-Magurele, Romania

In our department, in the last years, a new line of product has been developed concerning the radioactivity measurements (portal monitor, gamma source detector, neutron monitor) Instruments of different design (hand-held, portals or steady-state) are intended for detection and location of radioactive sources. Monitors are intended for detection of radioactive and special nuclear materials in vehicles, pedestrians, luggage, as well as for prevention of illegal traffic of radioactive sources. Monitors provide audio and visual alarms when radioactive and/or special nuclear materials are detected. Neutron dosimeters are designed for dose equivalent rate for use around neutron producing equipment or sources. All devices can be recommended to officers of customs, border guard and emergency services, civil defense, fire brigades, police and military departments or nuclear research or energetic facilities. Incorporating micro controllers and new design, our products span almost all the spectra of radioactivity detection (gamma, beta, X and neutrons). No special knowledge is needed for use of these instruments as all service functions are performed automatically (self-tests, background updating and thresholds calculation).

Portal monitor

The Portal monitor is intended to be a checkpoint in contamination control or in unauthorized pass of radioactive materials. The portal monitor can be installed both in open, unprotected to environmental conditions areas or in enclosed areas. It may be used at pedestrian cross border points; at check points of Nuclear Power Plants, enterprises of nuclear industry, weapons manufacturing and storage plants, nuclear waste disposal and storage sites; at the entrances to steel plants, the post-offices and airports, the governmental offices, banks, private companies etc. The monitor provides audio alarms when radioactive and/or special nuclear materials are detected. The monitor consists in a portal frame, which sustains 5 detectors. Each detector is an assembly of a plastic scintillator, a photo multiplier and the associated electronics, all three elements coated in an aluminum cylindrical capsule. Characteristics:

- Detects at least 1Ci radioactivity spread all over the subject body in a 20 Roentgen/h overall background
- Maximum detectable radioactivity 10Ci.
- Acquisition time between 1 to 10 seconds.

Neutron Monitor

The Neutron Monitor is derived from the Bonner Spectrometer. The Bonner Spectrometer description is quite simple: A proportional counter filled with helium 3 at pressure between 2 and 6 atmospheres ids the detecting element. It is covered with a thick layer of hydrogen-rich material such as polyethylene. The output signal is measured by the current in the conter wire when it is biased to approximately +1000 volts. Our Neutron Monitor is a portable, battery powerd monitor for measurement of dose equivalent rate for use around reactors, accelerators and other neutron producing equipment or sources. The instrument measures the neutron dose equivalent rate in the units of Sv/h. It is important to note that we need to know the neutron energies to be measured so that the appropriate energy response correction factors are coded into the instrument driving calibrations. If these apriori data is not available the Neutron Monitor can only to offer plain counts/second. The appropriate diameter for the polyethylene sphere was chosen to be 5 inches (127 mm). The instrument is equipped with a microprocessor and a 2 x 16 characters display unit along with two push buttons. This simple setup configuration permits to choose the acquisition time base and the display mode (counts or Sv). Characteristics:

- Dose rate 1 Sv/h to 100mSv/h (neutron spectrum information is required before calibration)
- Energy response Thermal to 14 MeV
- Detector He 3 proportional counter surrounded by 127 mm polyethylene sphere(SP9).

Portable gamma sources sniffer

The sniffer consists in NaI(Tl) crystal, a photo multiplier and the associated electronics, all three elements coated in an aluminum cylindrical capsule with a handle and a small 6 x 7 digits read-out. The associated electronics consists in a high voltage supply, a preamplifier, a discriminator and a microprocessor. The device is battery operated with 12 hours autonomy. An acoustic signal proportional with the count rate along the count rate displayed on the display are available. The sniffer incorporate a micro controller which registers the counts, display them and signals a threshold overcome. The main features include:

- Fault alarm probability less than 10^{-3}
- Non detecting probability less than 10^{-2}
- Portable device weighting 2 kg.

Micro-PIXE study of gold archaeological objects

R. Bugoi[1], V. Cojocaru[1], B. Constantinescu[1], D. Grambole[2], F. Herrmann[2]

[1] National Institute for Physics and Nuclear Engineering, PO BOX MG-6, Bucharest-Magurele, Romania
[2] Research Center Rossendorf Inc., Institute for Ion Beam Physics and Materials Research, PO BOX 510119, D-01314 Dresden, Germany

Several fragments of ancient gold objects coming from an Eneolithical hoard and from Pietroasa "Closca cu Puii de Aur" ("The Golden Brood Hen with Its Chickens") hoard, unearthed on Romanian territory, and two Romanian native gold nuggets samples were analyzed using micro-PIXE technique. The purpose of the study was to clarify the metal provenance, establishing if the hypothesis of local gold holds. To reach this goal, trace and minor elements (Cu, Te, Sn, Pb, Ti, Cr, V, Mn, Ta) and PGE (Platinum Group Elements) concentrations were estimated. The presence of inclusions (micrometer size areas of composition different from the surroundings) was also checked. The results obtained by microprobe experiments on gold ancient artifacts, especially the inclusions findings, provided some useful hints regarding the possible provenance of the manufactured metal.

The micro-PIXE elemental mapping and point analyses were made using the Nuclear Microprobe Facility at the Institute of Ion Beam Physics and Materials Research, Forschungszentrum Rossendorf, Germany, in the frame of an European Union Large Scale Facility Access (LSFA) action. This microprobe is based on a 3 MV Tandetron accelerator and a Danfysik magnetic quadrupole triplet for beam focusing. A 3 MeV proton beam was used and the beam current was about 400 pA. The beam was focused down to 6×6 mm^2, rastering an 800×800 mm^2 area (128×128 pixels elemental maps). The X-rays were detected using a Si(Li) detector positioned at 120° with respect to the incident beam, and mylar absorbers of different thickness were employed to reduce the soft X-ray region of the spectra. The total accumulated charge for the scanned areas was of the order of 3 μC. PIXE spectra were analyzed using GUPIX code.

Ta inclusions on two samples from Pietroasa hoard were found. These findings give strong support for the hypothesis of using Ural Mountains gold ore as a source for manufacturing these objects. The investigated Pietroasa hoard artifacts were proved to be of different origins - different composition and even different trace elements were present, confirming the stylistic arguments.

We found some Si and Ca inclusions on two Eneolithic samples. The measurements gave further support to the hypothesis of the use of alluvial gold to manufacture these Eneolithical artifacts.

The lack of Ir in the Romanian gold nuggets is confirmed by the present measurements.

An archaeological work is in progress with respect to these findings, containing the archaeological conclusions of our measurements.

Further analyses on other artifacts belonging to the same hoards are to be done. One must admit that a correct answer to the question of the native metal provenance used for each artifact will be a difficult task as long as a comprehensive data bank for the composition of Euro-Asian native gold will not be available.

Contributios to large scale and performance tests of the ATLAS online software

E. Bădescu[1], M. Caprini[1]

[1] NIPNE-HH, Department of Applied Nuclear Physics

One of the sub-system of the Trigger/DAQ system of the future ATLAS experiment is the Online Software system. It encompasses the functionality needed to configure, control and monitor the DAQ. Its architecture is based on a component structure described in the ATLAS Trigger/DAQ technical proposal [1].

Online Software is responsible for control, supervision and internal communication, excluding the event data flow. For the final Atlas experiment in 2006 it is expected that it will have to control up to 1000 processors. The core components are the run control, process manager, configuration database, inter process communication, message reporting system and information exchange system. The auxiliary components

are resource manager, online bookkeeper and the integrated graphical user interface were in use for tests.

All the components are unit tested for functionality, fault tolerance, performance and scalability. Extended functionality tests are performed at CERN and remote institutes before each official release. The test objective was the verification of the scalability of the system to a configuration containing a large number of nodes. The aim was to study the interaction between the components, to identify critical areas and to investigate the variation and optimization of online system parameters. The timing of the data acquisition transition phases were recorded and analysed.

The information on all processes and their relationships the run control hierarchy in the online system as well as startup and shutdown dependencies are defined in the configuration database data file.

Timing measurements were performed for the transitions shown in Figure 1 and defined as follows: **Setup**: start online server infrastructure. **Close**: remove online infrastructure. **Boot**: start all supervised processes. **Shutdown**: stop all supervised processes. **Cold start**: start the supervised processes and go to the *Running* state. **Cold stop**: reverse of the cold start phase. **Luke warm start**: once all processes are started and the controllers are in the *Initial* state, go to *Running* state. **Luke warm stop**: reverse of the luke warm start phase. **Warm start**: once all processes are alive and all controllers are the *Configured* state, go to the *Running* state. **Warm stop**: Reverse of the warm start phase.

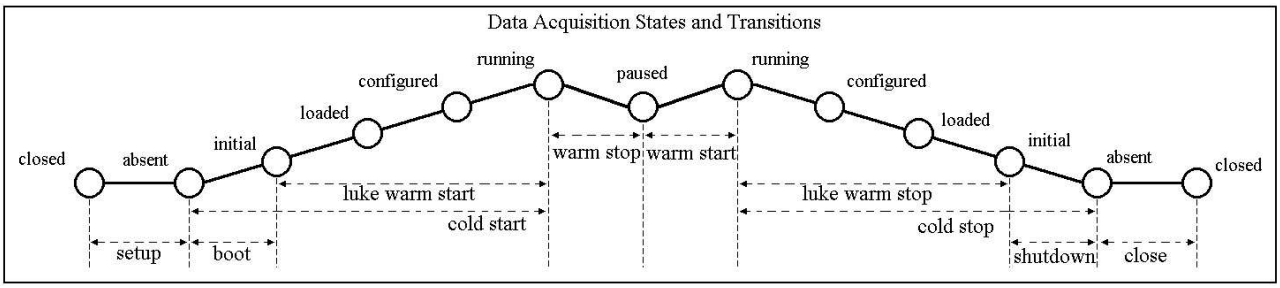

Figure 1: Graphical view of data acquisition timing intervals

It was shown that the online system is capable of running on 111 PCs controlling a 3 or 4 level hierarchy of up to 111 run controllers. Furthermore parallel partitions with a 2 level hierarchy of 11 run controllers were run successfully demonstrating the principle of partition independence.

The set of incremental configurations was run sequentially to study the system behaviour with increasing numbers of controllers and PCs. Aspects of interoperability and correct system behaviour for a large scale was verified with the partition containing 111 controllers which represent more than a factor 10 in size compared to its current use in test beam [2].

In order to start studies of the online system for the next order of magnitude, the 4-level super partitions with 300 and 1000 crate controllers were exercised. Limits were found on the level of communication and state transition coordination which will be investigated further.

References

[1] ATLAS High-Level Triggers, DAQ and DCS Technical Proposal, CERN/LHCC/2000-17 (2000)

[2] I. Alexandrov, E. Badescu, M. Caprini et al. "The Performance and Scalability of the back-end DAQ sub-system", CHEP-2000, Padova

Gamma and proton degradation studies in optical transmission materials

B. Constantinescu [1], R. Bugoi [1], P. Ioan [1], M. Dragusin [1], M. Brasoveanu [2], M. Nemtanu [2]

[1] National Institute for Physics and Nuclear Engineering, Department of Applied Nuclear Physics, Bucharest-Magurele

[2] National Institute for Laser, Plasma and Radiation Physics, Electron Accelerator Department, Bucharest-Magurele

In 2002, studies on gamma and high-energy proton irradiation-induced modifications in ultraviolet transmission properties on KU1 quartz glass samples were performed. The optical transmission components of the future thermonuclear reactor will be expected to maintain their transmission properties under high levels of ionizing radiations (~5 Gy/h) during hundreds of hours. For such applications, radiation-induced optical absorption imposes a severe limitation. It is therefore necessary to study the optical degradation of suitable candidate materials, to assess the system lifetimes. KU1 quartz glass is known to be radiation-resistant. This type of silica glass, presently examined within the ITER diagnostics program, has been studied under ^{60}Co gamma and 3 MeV proton irradiation at room temperature. For this, 0,8 mm thick samples provided by IAE Kurchatov (Moscow) in the frame of ITER programme have been gamma irradiated with 0.2 to 2 Mrad doses at a 20 kCi ^{60}Co irradiator and implanted using the Bucharest HVEC Tandem accelerator with 8×10^{13} and $1{,}5\times10^{14}$ protons, respectively. The implantation was performed with a small intensity ($\leq$1 nA) beam, in order to keep the sample heating as low as possible (RT conditions). The proton irradiated area on the sample was around 2 mm^2. The optical transmission properties (absorption, transmission and reflectivity) in the UV region have been measured with a Cary 4 VARIAN spectrophotometer. For gamma irradiated samples two main absorption peaks were observed: 215 nm (produced by E' type defects) and 240 nm (ODC II - oxygen-deficient center type defects). There is a clear dose dependence of these peaks intensity. As concerning the proton implanted samples, for the lower dose, absorption peaks at 215 nm and 240 nm, similar in shape, but smaller in intensity to gamma irradiation case, can be observed. For higher dose, a supplementary 202 nm peak appeared, splitting the 215 nm peak. In the upper region of UV spectrum ($\geq$ 350 nm), same small peaks are also presented, possibly due to defects as OH^- produced by the implanted hydrogen. The 3 MeV protons produce considerable ionization, which is the main cause of the energy loss at such low energies. The knock-on ions displaced by the protons also produce ionization. The result of the overall ionization is the 215 nm band. As concerning the number of induced defects, our doses, equivalent to 4×10^{15} p/cm^2 and $7{,}5\times10^{15}$ p/cm^{2}produced 4×10^{-6} and $7{,}5\times10^{-6}$ dpa, respectively, in the 3 MeV protons range in quartz (80 μm), equivalent to 5×10^{-4} and 9×10^{-4} dpa for 1 cm. At that damage level, we have considerably defects formation, which gives an undefined general absorption. This is the explanation for the aspect of our absorption curves in the region above 450 nm. We intend to continue our KU1 studies using 14 MeV proton irradiation, because of the following advantages: at this energy, the displacement damages simulate quite well the 14 MeV high energy neutrons damages; and since we are using a thin sample, the damage is more uniform throughout the thickness. However, we must be careful that at 14 MeV protons, a certain amount of radioactivity will be induced in the samples.

A cyclotron neutron irradiation facility at IFIN-HH

I. Vata[1], A. Danis[1], D. Dudu[1], E.A. Ivanov[1], D. Plostinaru[1], D. Catana[1], D. Sporea[2]

[1] NIPNE-HH, Cyclotron
[2] National Institute for Lasers, Plasma and Radiation Physics

U-120 Cyclotron facility is used for fast neutrons fields generation. The nuclear reaction produced by deuterons on Be is the best neutron source, due to the high yield and angular distribution strongly peaked forward and low gamma ray production.

A maximum 10μA beam of 13MeV deuterons, when incident on the thick Be target (165 mg/cm^2), produces a high neutron flux by stripping reactions.

A dosimetric characterization of the neutron fields were performed prior to the radiation-damage studies. The threshold detectors (^{115}In, ^{197}Au), mica track detectors (Th and U), ^{6}LiF and ^{7}LiF dosimeters were used to determine the neutron fluence and photon doses, and to measure the total absorbed dose angular distribution. The neutron flux at 0° (i.e. in the beam direction) was found to be equivalent to 2.13 10^8 neutrons/cm^2.s. μA , at 10cm distance from Be target. The higher part of the energy spectrum was derived by time of flight (TOF) spectrometer. The neutron energy spectrum shows a mean energy of 5.2MeV. The neutron and gamma components of the mixed radiation field give rise respectively to 138Gy/C and 2.38 Gy/C at 90cm distance from Be target. In practice, a neutron fluence up to 10^{13} n/cm^2 can be obtained in about two days, over an area 100 cm^2 [1].

The beam power (maximum 100W) released in the Be target is removed by a flow of cooling water. At full beam power, the highest temperature on the target does not exceed 50°C. Some precautions have been taken to maintain the Be disk electrically insulated, thus permitting on-line monitoring of the beam current on the target .

During irradiations the neutron fluences were monitored by activated foil dosimetry (^{58}Ni (n,p) ^{58}Co reaction) and mica track detectors. The absolute accuracy is ~15% due to uncertainty in activation cross-sections, but results are typically reproducible to within a few percent. The measured uniformity of neutron field in the region of irradiation (20cm x 8cm) is beter than 25%.

By measuring the integrated beam current, the time-stability of the neutron source was checked at 30 minute intervals during the irradiation; the current was roughly constant over the irradiation period .

References

[1] Energy spectrum of neutrons produced by deuterons on thick Be Target Fl.Tancu et all. Rev. Roum. Phys, Tome 28, no:10 p 857-865 (1983)

^{22}Na positron source for annihilation positron spectroscopy

C. Cimpeanu[1], L. Craciun[1], E. Dragulescu[1], D. Dudu[1], N. Miron[2], P.M. Racolta[1], Dana Voiculescu[1]

[1] National Institute for Physics and Nuclear Engineering "Horia Hulubei", Bucharest, Romania
[2] Institute for Applied Physics, Chisinau, Moldova Republic

To extend the nuclear physics applications and to perform the study of vacancy – type defects in metals, semiconductors, polymers etc., we decide to promote positron annihilation techniques. In order to this goal we started a project of dedicated positron sources produced at the IFIN-HH U-120 Cyclotron. We have used the nuclear reaction: ^{24}Mg(d, α)^{22}Na and deuterons of 13 MeV energy. The paper present the main steps of this procedure like as: general conditions asked for ^{22}NaCl sources, reactive chamber and characteristics of Mg target, parameters for the irradiation, radiochemical procedures to separate Na from Mg after the irradiation and geometrical or mechanical requirements for dedicated NaCl source for positron annihilation spectrometry. In the e^+ lifetime measurements the e^+ death- start signals may be obtained from prompt γ -quanta emitted from the NaCl source (1,275 MeV photons).The ^{22}NaCl stock solution obtained by radiochemical separation will keeping in the quartz sealed ampoules in dry places and will be dropped between the study materials before used by positron spectrometry.

* International Conference on Applications of High Precission Atomic & Nuclear Methods, Neptun Romania 2-6 sept. 2002 HIPAN

Dedicated NaCl source for annihilation positron spectrometry

C. Cimpeanu[1], D. Dudu[1], N. Miron[2], P.M. Racolta[1], Dana Voiculescu[1]

[1] National Institute for Physics and Nuclear Engineering "Horia Hulubei", Bucharest, Romania
[2] Institute for Applied Physics, Chisinau, Moldova Republic

To extend the nuclear physics applications and to perform the study of vacancy – type defects in metals, semiconductors, polymers etc., we decide to promote positron annihilation techniques. In order to this goal we started a project of dedicated positron sources produced at the IFIN-HH U-120 Cyclotron. We have used the nuclear reaction: ^{24}Mg(d, α)^{22}Na and deuterons of 13 MeV energy. The paper present the main steps of this procedure like as: general conditions asked for ^{22}NaCl sources, reactive chamber and characteristics of Mg target, parameters for the irradiation, radiochemical procedures to separate Na from Mg after the irradiation and geometrical or mechanical requirements for dedicated NaCl source for positron annihilation spectrometry. In the e^+ lifetime measurements the e^+ death- start signals may be obtained from prompt γ -quanta emitted from the NaCl source (1,275 MeV photons).The ^{22}NaCl stock solution obtained by radiochemical separation will keeping in the quartz sealed ampoules in dry places and will be dropped between the study materials before used by positron spectrometry.

1. 5-th International Topical Meeting on Industrial Radiation and Radioisotope Measurement Applications, Bologna, Italia, 9-14 iunie, 2002

Influence of the background approximation methods on the analysis of gamma-rays spectra

A. Luca[1], Jean Morel[2]

[1] National Institute of R&D in Physics and Nuclear Engineering "Horia Hulubei" (IFIN-HH), 407 Atomistilor Street, PO Box MG-6, Com. Magurele, Jud. Ilfov, 76900 Romania
[2] Commissariat à l'Énergie Atomique, Bureau National de Metrologie, Laboratoire National "Henri Becquerel" (LNHB), CEA-Saclay, 91191 Gif sur Yvette Cedex, France

In any X- or gamma-rays spectrometry measurement, the approximation of the continuum background is important, because it influences strongly the net area values and the associated uncertainties of the total absorption peaks and consequently, the activity determination.

Two mathematical methods to describe the background situated under the peaks are tested: the first using a step function and the second orthogonal polynomials. These methods were applied to different spectral regions having multiple peaks. The results obtained from this work and the main conclusions are presented here.

Radon measurement with a radiation detector of ionization chamber type in pulse mode

M.R. Călin[1], N. Vâlcov[1]
[1] NIPNE-HH, DFVM

Abstract: Measuring atmospheric radon is a highly interesting area of environmental radiation protection. As it is well known, the radon penetrates the human organism by breathing the atmospheric air. The radioactive element is produced from the earth due to processes involved in a chain nuclear disintegrations and can also be produced or accumulated by other sources such as building materials, which are part of the buildings, underground stations, coal pits, salt mines, quarries, etc. In various circumstances, it is quite important that the volumic activity of the radon and its progeny be checked, which justifies the wide diversity of methods that have been developed for this purpose.

One of the most widespread method is based on the measurement of the average ionization current produced by the radon circulation through an ionization-chamber detector. This paper presents the development of a lab device for monitoring the radon volumic activity, using a radiation detector of ionization chamber type (in 3 different variants). It is a pulsed mode device, in which the measurement of the average value of the ionization current is replaced by a measurement of the ionization current pulses generated by alpha disintegrations within the sensitive volume of the detector. The ionization chamber thus operates as a 4p counter, in which the radon and its progeny are the alpha sources. The paper provides a mathematical evaluation of the efficiency of the method and of the measuring device, based on a data acquisition system and a special computing program, which makes possible to study the time and amplitude distributions of the pulses produced by alpha radiation in the ionization chamber. Preliminary results have indicated that the volumic activity of the radon and its progeny can be measured with a 5%-6% uncertainty.

Tracers, Radiopharmaceuticals and Radiometry

Homologated procedure to obtain an uniform atom distribution of the calibrated radionuclide in the solidified state of liquid reference materials

A. Danis[1], E. Iliescu[2]

[1] NIPNE-HH, Nuclear Engineering and Vacuum Department
[2] NIPNE-HH, Standardization, Metrology and Quality Laboratory

Any physical and radiochemical relative analysis methods used for content measurements imply the use of reference materials calibrated in the analyzed element. In this case, especially for the analysis methods based on it the track detection, the following requirements must be met both for the unknown samples and the reference materials: i) the same or similar elemental matrix, ii) an uniform atom distribution of the analyzed radionuclide, iii) the analyzed element concentration value of the same order of magnitude and iv) the same physical state and, for the powdered samples, the same powder grain.

For the liquid samples, the uniformity of radionuclide atoms in the matrix is a real problem due to the radiocolloidal and/or pseudoradiocolloidal states, which, in time, can be naturally installed earlier or later depending on different factors such as: the elemental composition of the matrix, the type and quantity of impurities, the pH of the liquid samples, the investigated element concentrations and the duration from the preparation moment of the calibrated solutions up to their use as reference materials.

A new procedure to obtain an uniform atom distribution of the calibrated radionuclide in it the solidified state of the liquid reference materials, was carried out by it the Track Detection Group in the NIPNE-HH. By this procedure, a well determined volume of standard solution calibrated in the analyzed element is transformed into a plastic foil by dissolving of a well determined quantity of Rhodoviol in the respective standard solution and applying special thermal and dry treatments. The obtained foil is the it solidified stateof the liquid reference material, which consists of the calibrated element in the quantity equal with the calibrated element content in the determined standard solution volume transformed. The new solid state of the reference material assures a stable physical state, a uniform atom distribution for an unlimited time period as well as an easier handling. This procedure can be applied to the unknown samples,too. In such way, a similar matrix can be obtained both to reference materials and unknown samples.

Foils calibrated in U, Th, U and Th, and Ra were obtained by authors by the proposed procedure.

The checking out of the homogeneity of the atom distribution was performed using it the alpha track micromapping technique. All the alpha track micromappings obtained for the plastic foils with U, Th, U and Th, and Ra presented a uniform track distribution. Therefore a uniform distribution of investigated element atoms in the respective foils was assumed.

The alpha track density values, obtained by two observers, for the same area in different measure places of the track micromappings corresponding to the two surfaces of the Th foil were not found different for more than 4.7 %.

Th internal contamination of animals

M. Ciubotariu[1], A. Danis[1]

[1] NIPNE-HH, Nuclear Engineering and Vacuum Department

Since 1999, using the fission and alpha track micromapping technique for analysis of Th, the biodistribution, retention and elimination of this element in the internal contamination of animals have been studied. At present, it the internal contamination by ingestion was investigated and the other two internal contamination ways it by inhalation and through wounds are in progress under the CERES Program, Project no. 71/2001.

As any internal contamination study, these contamination ways imply: i) animal contaminations in pre-established conditions (contaminant amount, number of administration doses, the time interval of dose administration), as well as ii) establishing when, which and how many samples will be collected from the contaminated subjects during contamination and

at their sacrificing.

The two internal contaminations, i.e. containation by inhalation and through wounds, were already performed in the following conditions.

Four Wistar-London breed rats, used as experiment animals, were contaminated it by inhalation using an airtight device, designed and realized in our laboratory, in which a fog, consisting in a fine powdered state of dehydrated Thorium nitrate, was permanently generated by pulverizing. The animal bodies were shielded from contamination, except their nose. They were kept in these conditions during an hour.

Also, three rats were contaminated it through wounds. Their wounds were applied behind their necks by cutting out 1.5 - 2 square centimeters of hide. Using identical aliquot parts of the calibrated Th solution of (51.516 ± 0.412) gTh/l concentration, corresponding to the a Th Annual Limit Intake, the wounds of the rats were moistened at different time interval and with a different administration number of Th solution doses.

After contamination the animals were kept in separate cages, in normal life conditions and under permanent surveillance up to their sacrificing.

In both internal contamination cases the animals were sacrificed at different time intervals after their last administrated dose and their vital organs were sampled. These organ samples as well as their eliminations sampled every 24 hours, urine sparred from excrements, were weighted, calcined, re-weighted and then analyzed by the alpha/fission fragments track micromapping technique.

The micromappings obtained in etched track detectors, representing the replicas by tracks of the Th atom distributions in the analyzed samples, are studied by optical microscopy for qualitative and quantitative determinations of the biodistribution, retention and elimination of Th element. At present, these studies are in progress.

Evaluation of absorbed doses at the interface: solid surfaces - tritiated water solutions

Cristian Postolache[1], Lidia Matei[1]

[1] National Institute of Research and Development for Physics and Nuclear Engineering "Horia Hulubei", Magurele, Bucharest, Romania, e-mail cristianpostolache@yahoo.com

Studies concerning the isotopic exchange H/D/T in the system: elemental hydrogen – water and in the presence of platinic metals on hydrophobic supports as catalyst were carried out at ICSI Rm. Valcea Romania. Due to the very low energy of β-radiation emitted by tritium, the direct measurements of dose absorbed by the isotopic exchange catalyst using classical methods is practically impossible.

For this purpose an evaluation model was developed. The volume of tritiated water which can irradiate the catalyst was represented by a semi sphere with the radius equal to the maximal rate of β-radiation emitted by tritium. The catalyst surface is represented by a circle with a 0.2 μm radius and the same centre as the circle of the semisphere secant plane. Flow rate of absorbed dose is computed with the relation: $d = (1/100)(\Phi \cdot Em/m)$, where d = dose flow rate, expressed in rad/s; Φ = total radiation flux which interacts with the catalyst surface, expressed in erg; m = catalyst weight, in grams. Total flux of available radiation, Φ, was determined as a function of three parameters: a) total flow of tritium β-radiation emitted in the semi sphere of tritiated water, dependent on the volume and radioactive concentration; b) emission coefficient on the direction of the catalyst surface; c) attenuation coefficient (due to self-absorption) of the tritium β-radiation in the tritiated water body.

Studies of radiolytical and self-radiolytical processes in polyacrylic hydrogels using RES spectrometry

Cristian Postolache[1], Lidia Matei[2], Rodica Georgescu[3], Corneliu C. Ponta[2]

[1] National Institute of Research and Development for Physics and Nuclear Engineering "Horia Hulubei", Magurele, Bucharest, Romania, e-mail cristianpostolache@yahoo.com

Due to remarkable capacity of water retain, polyacrylic (PAA) hydrogels represent an interesting alternative for tritium (tritiated water-HTO) liquid wastes trapping. The study was developed on radiolytical processes in PAA:HTO systems derivated from irradiaton of polymeric network by disintegration of tritium atoms from HTO. The aim of these studies is the identification of polymeric structures and optimal storage conditions.

RES studies of radiolytical processes were realized on dry polyacrylic acid (PAA) and polyacrylic based hydrogels irradiated and determined at 77 K.

In the study we observed the effect of swelling capacity of hydrogel on the formation of free radicals. In RES spectres of irradiated PAA were identified a signal with quintet structure attributed, in conformity with literature, to radical from α position referred to carboxylic group. We also identified a triplet attributed to a radical resulted by fragmentation of polymeric main chain. In case of PAA hydrogels were identified signals attributed to HO radical resulted form water radiolysis, R-OO radicals resulted from the presence of atmospheric O_2 in samples and a signal with quintet structure more less splited like dry polymer. The signal is attributed to a radical from the polymeric main chain in α position referred to carboxylic group. The decrease of split parameter is determined by tension of main chain as result of swelling, associated with increase of θ angle between p_x axis of C_α radical and the C_α C_β H_β plane. RES analysis of labelled hydrogels indicate the presence of HO and COO radicals resulted from internal primary effect . RES analysis of PAA:HTO samples indicate the preponderant role of the internal primary effect in selfradiolytical effects in concordance with the role of secondary effects stopped in RES study due to freeze material.

Tritium labelled colesterol its synthesis and stability studies

Cristian Postolache[1], Lidia Matei[1]

[1] National Institute of Research and Development for Physics and Nuclear Energy "Horia Hulubei", Măgurele

By the detritiation of contaminated moderator from Cernavoda Nuclear Power Plant a raw material is obtained, with an economic value of $\sim$ 3 USD/Ci . It might be stocked for long-term in order to be used in controlled fusion or, it might be immediately used in the synthesis of labelled compounds with an economic value up to 5 orders of magnitude higher than the raw material.

Cholesterol-T-G was synthetized using the isotopic exchange technic in heterogeneous catalysis. Two labelling methods were tested: (a) labelling at neutral pH, and b) labelling at acidic pH. Higher specific activities (54 Ci/mmol) were obtained when the second method was applied, similar to those obtained in the case of labelling through chemical synthesis.

The stability test of the labelled synthetized compound consisted in two steps: one of theoretical analysis and quantum chemistry modelling of the decomposing processes, and the second one of identification of critical stocking parameters of the labelled compound.

The quantum chemistry modelling of radiolytic processes made it possible the highlightining of radiolytic interaction zone (LUMO orbital) and of labile chemical bonds in the radiolytic process.

The chromatographic analysis of colesterol-T-G samples confirmed the major role of the secondary radiolytic processes. Due to this reason, the critical stocking parameter of labelled colesterol is the radiochemical purity and working temperature.

Synthesis and stability studies of acyclovir labelled with tritium

Lidia Matei[1], Cristian Postolache[1], Nicolae Negoiţa[1]

[1] National Institute of Research and Development for Physics and Nuclear Engineering"Horia Hulubei", Magurele, Bucharest, Romania, e-mail: lidiamatei@personal.ro

Acyclovir, $C_8H_{11}N_5O_3$ is a biologically active compound, with antiviral properties. The use of the radioisotopic labelled compound, accompanied by radiometric measurements in biological samples is recommended in pharmacokinetical and pharmacodynamical studies for promoting pharmaceutical products.

The labelled Acyclovir was obtained by isotopic exchange reaction in heterogenous catalysis, using Acyclovir as substrate and T_2 as labelling agent. Pd/C and $Pd/BaSO_4$ were used as catalyst and the mixtures dioxane-water-acetic acid or dimethylformamide-phosphate buffer as solvents. Reaction time was 20-25 hours. The raw labelled compound was purified by preparative thin layer chromatography, using the system: silicagel GF 254 activated at $110^o$for one hour and n-buthylic alcohol: acetic acid: water (4:1:1v/v/v).

The labelled compound was conditioned as aqueous solution. Characterization of labelled compound was accomplished by determination of chemical and radioactive concentrations and purities.

Radiolytical processes were evaluated by cuanto chemical methods. Were analyzed the primary and secondary radiolytical effects. For energetically minimized molecular structure with charge +1 and multiplicity 1 was evaluated the primary effect by analysis of binding energies and LUMO orbital distribution. Secondary effects were evaluated by analysis of radical HO attack over neutral molecular structure.

The values of binding energies associated with LUMO orbital distribution indicate a radiolytical fragmentation especially for guanidic C-N bond.

Secondary effects study was developed by analysis of reactions between acyclovir (in fundamental, excitated, ionized states) water and active species from radiolytical act. We analyzed the reaction enthalpies and activation energies.

The results also indicate the radio sensibility of guanidic C-N bond. The experimental results sustain the results obtained from radiolytical simulation

Biosynthesis of dihydrotestosterone-1, 2-T

Lidia Matei[1], Eduard Condac[2], Cristian Postolache[1]

[1] National Institute of Research and Development for Physics and Nuclear Engineering "Horia Hulubei", Magurele, Bucharest, Romania

[2] Faculty of Biology, University of Bucharest, Romania; e-mail adin@bio.bio.unibuc.ro

Dihydrotestosterone-1,2-T was obtained by biosynthesis using as substrate Testosterone-1,2-T. Labelled testosterone was synthesized by selective hydrogenation of 1Δ Testosterone acetate.

In this study was analyzed enzymatic activity of 5α reductase. Enzymatic activity was studied using human skin and prostate tissue homogenates incubated 1h at 37^0C with labelled tritium testosterone. As cofactor we used NADPH. After reaction stopping, testosterone metabolites were extracted with a mixture of cyclohexane/ethyl acetate. Product separation was realized using Celite chromatographic columns. As mobile phase we used a mixture of isooctane/toluene. Labelled testosterone used as substrate in enzymatic reaction was purified by column chromatography using previous system.

On collected fractions as result of chromatographic elution were determined enzymatic activities using a Packard liquid scintillation counter.

For metabolites identification were used testosterone, dihydrotestosterone, androstandione 3α and 3β androstandiols C-14 labelled as intern standards.

From radiochromatographic profiles were identified base peak of testosterone used as substrate, peaks of dihydrotestosterone, androstandione and also peaks of 3α and 3β androstandiols with very low intensity.

This study confirm the possibility of dihydrotestosterone and androstandione biosynthesis. Androstandiols can be also synthesised with low yields.

Biomathematical approach of ^{188}Re radiopharmaceuticals therapy characterization

Valeria Lungu[1], Dana Niculae[1], Gabriela Mihailescu[1], Sorin Baiculescu[2], Ileana Turcu[3], Leon Danaila[4]

[1] "Horia Hulubei" Institute for Physics and Nuclear Engineering, Bucharest, Romania
[2] "Stefan Odobleja" Academy of Cybernetics, Bucharest, Romania
[3] "Ana Aslan" National Institute of Gerontology and Geriatrics, Bucharest, Romania
[4] "Vlad Voiculescu" Institute for Cerebral-Vasculary Diseases, Bucharest

Acknowledgements

This work was partly supported by IAEA Vienna through Research Contract No. 10108.

VALERIA LUNGU

Horia Hulubei Institute for Physics and Nuclear Engineering, Bucharest, Romania

Strada Atomistilor, 407, Com. Magurele, Jud. Ilfov

P.O.B. MG 6, 76900, Romania

Tel : 0040 21 4042300/ 4518 ext

Fax: 0040 21 4574432 or 0040 21 4574440

Email : vlungu2000@yahoo.com

Summary

Purpose:In order to optimize radioimmunotherapy (RIT) as a cancer treatment modality, it is necessary to select the appropriate radionuclide and the biomolecule carrier. We have developed the radiolabeling with ^{188}Re (β emitter) of anti-CEA Mab for targeting CEA-producing tumors.

Material and Methods: Labeling was effectuated by the addition of $Na^{188}ReO_4$ *eluted from* $^{188}W-^{188}$Re generator to a preformulated biomolecule in SH prereduction form in the presence of a supplemental stannous ions. For the mathematical processing of the obtained results we used interpolation functions, as well as the different organs putted under investigation. Were used those interpolation functions for which the standard error is zero, correlation coefficient is the unit and the analytic expression emphasize generally exponential forms (the differential equations specific to the radioactive biodistribution have exponential integral curves as solutions).

Results:Radiochemical purity achieved was 92-96%. The resulted solutions have a pH value 5-7 and for intravenously uses only. The optimum filed of interpolation functions was determinate, comprising Hoerl, Modified Hoerl, Heart Capacity, Gaussian, Logistic, and Exponential type models. The optimum model existing in that field was also determined, in the condition in which the ratio between absolute error of the biodistribution surface/the mean surface of the optimum biodistribution is minimum.

Conclusion:The obtained optimum model has a predictive character, allowing the identification of the moment to which the maximum percent value for every other time point in the considered time interval $t_o - t_f$. This mathematical model can be used for every other pharmacokinetic paradigm.

References

[1] John E, Thakmur ML, DefluvioJ. Rhenium-186-Labeled Monoclonal Antibodies for Radioimmunotherapy, Preparation and Evaluation. J Nucl Med 1993; 34, 2: 260-267.

[2] Griffits GL, Goldenberg DM, Knapp FF. Direct Radiolabeling of Monoclonal Antibodies with Generator-produced Rhenium-188 for Radioimmunotherapy: Labeling and Animal Biodistribution Studies. Cancer Res 1991; 51: 4594-4602

[3] RhodesBA, Zamoro PO, Marek MI. Direct labeling of antibodies with Re-186, Diagn Oncol 1993; 3: 29 pp

[4] Deutsch E, et al. The chemistry of rhenium and technetium as related to the use of isotopes of these elements in therapeutic and diagnostic nuclear medicine. Nucl Med Biol 1986; 13: 465-477

[5] Griffits GL, Goldenberg DM. Technetium-99m, Rhenium-186 and Rhenium-188 Direct Labeled Antibodies. 4th Conference on Radioimmunodetection and Radioimmunotherapy of Cancer, Princeton, NJ, September, 1992

[6] Frank B, Visser GW, Strooner JW. High dose Rhenium-186 Labeling of Monoclonal Antibodies for Clinical Application, 6th Conference on Radioimmunodetection and Radioimmunotherapy of Cancer, Princeton, NJ, October, 1996

[7] Thakur ML, et al. Technetium99m-RC-160. A somatostatin analog. J Nucl Med 1994; 35: 259.

[8] Thakur ML, et al. Vapreotide labelled with Tc-99m for imaging tumours: preparation and preliminary evaluation. Int J Oncol 1996; 9: 445-451

[9] Zamora PO, Marek MJ, Knapp FF Jr. Preparation of 188Re-RC-160 Somatostatin Analog: a Peptide for Local/Regional Radiotherapy. Appl Radiat Isot 1997; 48: 305-309

[10] Varnum GM, et al. Rhenium labelled somatostatin analog RC-160: H - NMR and computer modelling conformational analysis, J Biol Chem 1994; 269: 12583-12588.

[11] Leucuta SE, Pop RD. - *Farmacocinetica* (Pharmacokinetics), Edit.Dacia, Cluj-Napoca, 1981

[12] *Sisteme de Inteligenta Artificiala* (Artificial Intelligence Systems), Edit.Academiei Romane, Bucuresti,1991

[13] Postelnicu T, Tautu P, - *Metode Matematice in Medicina si Biologie* (Mathematical methods in Medicine and Biology), Edit. Tehnica, Bucuresti,1971

[14] Nicu MD, Oprita N. – *Biotehnologie* (Biotechnology), Edit.Didactica si Pedagogica, Bucuresti,1979

[15] Zamfirescu M, Sajin G, Rusu I, Sajin M, Kovacs E. - *Efecte Biologice ale Radiatiilor Electromagnetice de Radiofrecventa si Microunde* (Biological effects of Electromagnetic, Radiofrequency and Microwave Radiations), Edit.Medicala, Bucuresti, 2000

Production and chemical separation of 48-V radioisotope

Z. Szucs[2], D. Dudu[1], C. Cimpeanu[1], A. Luca[1], E. Duta[1], M. Sahagia[1]

[1] National Institute for Physics and Nuclear Engineering " Horia Hulubei", Bucharest, Romania
[2] Institute of Nuclear Research of the Hungarian Academy of Sciences

The positron emitter ^{48}V isotope ($T_{1/2}$=16d, γ-lines: 511 keV(100%), 983,5(100%), 1312(97,6%) deserves interest in several fields of science. This is available for the transmitting scanning in the validation process of PET-camera by its positron emission, can be used for as an industrial monitor isotope by its γ-photons having high energy and intensity and is also suitable for biological study since it is the only radioisotope of the biological trace element, of V, which can be a radiotracer by its longer half-life.

The ^{48}V was produced by $^{nat}Ti(d,xn)^{48}V$ nuclear reaction in the U-120 cyclotron with activity of 6 mCi. The energy of irradiating beam was 13 MeV, its intensity was 5 μA, and the metallic Ti target dimension was 16x11x2 mm. For target cooling the circulated water in back side was used. After 3 cooling days only the ^{48}V and some ^{46}Sc ($T_{1/2}$=84d) produced by the side nuclear reaction, $^{48}Ti(d,\alpha)^{46}Sc$ were found in the target. For the preparation of source of ^{48}V, the Ti target was dissolved in HF and in sulfuric acid too. The ionexchanging separation was developed for both dissolving methods:

The dissolution of the chemically resistant Ti target is so violent in concentrated (3,5 % m/m) HF, that it is necessary to carry out in polyethylene tube because of avoiding of the splash of the dissolved target. An anion exchanging column, Dowex 1-8 (size 100-200 mesh, length 12 cm, ID 10 mm, treated 1 day earlier, prepared fresh) was used for separation in HF media. The reduced ionic form of Ti bond to resin, therefore the dissolved target was saturated with sulfure-dioxid produced in Kipp-equipment by the above chemical reaction:

$$Na_2SO_3 + 2\ HCl \rightarrow 2\ NaCl + H_2SO_3$$

The treated solution was diluted to concentration of 2 mol/l of HF and the same concentration of the HF was used as an eluent for separation. Flow rate of the elution was 1 ml/min. The eluate was colled fractionally.The fractions were measured by γ-spectrometry, which detected only ^{48}V.The advantages of this method are the easy dissolution of the target and the quick, complete separation of ^{48}V.The disadvantage are the avoiding glassware, all lab-equipments must be produced of HF-resistant plastic material and the final product difficult to use due to the aggressive HF media.

The sulfuric acid with concentration of 6 mol/l can also dissolve the target, however it is much more difficult than by the HF.It needs heating under reflux for 6 hours.During the dissolution was forming the solid salt of Ti in high amount.Only 50 % of the stohiometric necessary amount of sulfuric acid for fully dissolution was used because of avoid of dissolution of the part of the target, in which the nuclear reaction wasn't produced.After the dissolution the liquid and solid faze was separed and solid salts was dissolved by 0,01 mol/l sulfuric acid.This soft acidic circumstance is necessary for effective separation on the Amberlit CG-50 column.The higher oxidation stage and the peroxid-complex of Ti is guaranty for remaining of Ti on the cationexchange column.Therefore 1 % H_2O_2 in 0,01 mol/l nitric acid was added to the sample.The orange color is demonstrated the successful chemical reaction.For ionexchange separation this solution was used.The elution was carried out by 1 % H_2O_2 in 0,01 mol/l nitric acid as an eluent.The radio-

chromatogram was determined by the same method which was mentioned in the case of the separation in HF media.The chemical yield of the separation was more 95 %. The radionuclide impurity of ^{46}Sc was less 0,02 % determined by γ-spectrometry.The chemical purity of ^{48}V was 99,8 % in according to Ti determied by VIS-spectrophotometry using the absorbance of peroxid complex of Ti in 420 nm approximately.The advantages of this method are the softer chemical circumstances and the easy to use final product.The disadvantages are the long dissolution time, the several made by hand steps and the less separation ratio compared with the sepoaration in HF media.For application of any methods in production of ^{48}V with high amount of radioactivity would be necessary some modificatiopns to fit the method for work in shielded box by manipulators.

1. Annual Report of Institute of Nuclear Research of the Hungarian Academy of Sciences Debrecen, Hungary , nr.2001, martie 2002

Obtaining of high specific activity ^{186}Re, ^{188}Re perrhenates to be used for biomolecule labelling

C. Cimpeanu[1], M. Sahagia[1]

[1] Institute for Physics and Nuclear Engineering , POB MG-6, Bucharest, Romania

^{186}Re and ^{188}Re, two strong beta and weak gamma emitters having short half-lives, are intensely studied as promising radionuclides for radiotherapy. Their use for biomolecule labeling is mainly due to their similar behavior with ^{99m}Tc. This paper presents the irradiation operations in a 14 MW TRIGA SSR Reactor, the chemical processing for obtaining of high activity perrhenate solutions and the final characterization of the products.

Journal of Radioanalytical and Nuclear Chemistry, vol.252, nr.3, 2002

^{188}Re(Sn)HEDP - a therapeutic radiopharmaceutical: preparation and biodistribution studies

Dana Niculae[1], Valeria Lungu[1], Gabriela Mihailescu[1], Corneliu Podina[2], Mariana Purice[3]

[1] "Horia Hulubei" National Institute for Physics and Nuclear Engineering, Radiopharmaceutical Department, str Atomistilor 407, Bucuresti-Magurele

[2] University of Bucharest, Bd. Elisabeta 4-12, Bucuresti

[3] "C. I. Parhon" Institute of Endocrinology, Bd. Aviatorilor 34-36, sector 1, 79660 Bucuresti

^{188}Re(Sn)HEDP is a palliation agent for osseous metastases radiotherapy; the breast, prostate or thyroid cancers generally metastasize to the skeleton with severe bone pain. The aim of this study is a HEDP kit formulation for ^{188}Re labeling with, establish of a fast, reproducible and accurate labeling technique, as well as the in vivo biological testing by biodistribution studies of ^{188}Re(Sn)HEDP obtained by different labeling techniques. Preclinical (animal) studies are required to determine the biological distribution and the route and extent of excretion of the radiopharmaceutical.

The results concerning labeled compound biodistribution show a good specific accumulation of ^{188}Re(Sn)HEDP in bone, the radiation dose percent to gram of investigated organ ratio is a labeling technique function. The best results were obtained for the labeling in the conditions of an inert reaction atmosphere, acid pH (0.5 - 1), using carrier added labeling technique and incubation temperature 100 $^{\circ}$ C.

Key-words: biodistribution, HEDP, radiotherapy, ^{188}Re.

Waste Management and Site Restauration

Polyacrylic hydrogels, matrics for tritium liquide wastes storage

Cristian Postolache[1], Lidia Matei[1], Corneliu C. Ponta[1]

[1] National Institute of Research and Development for Physics and Nuclear Engineering "Horia Hulubei", Magurele, Bucharest, Romania, e-mail cristianpostolache@yahoo.com

Due to its high capacity for water absorption, polyacrylic acid obtained by radioinduced polymerization of acrylic acid water solution, represent an interesting alternative to HTO storage. Because changes in polymer network were determined by the presence of β radiation emitted by tritium, radiolytical and self-radiolytical studies are required for this application. As tritium is a radioisotope with medium half-life (12 years), simulation of radiolytical processes resulted during the storage period up to the quasitotal disintegration of radionuclide is necessary. Radiometric studies using specific labelled compounds with tritium were performed. The variation of gel/sol ratio with absorbed dose, absorbed dose rate and swelling degrees were analyzed. Sol and gel fractions were determinated by radiometric methods using polyacrylic hydrogels labelled with T at main chains of the polymer. Simulation of radiolytical processes was realized using γ radiation field emitted by a irradiation source of ^{60}Co which ensures a maximum of absorbed dose rate of 3 kGy/h. Self-radiolytical effects were investigated using labelled PAA in HTO with great radioactive concentration (37-185 GBq/mL). Influence of radioprotectors was analyzed too, but the most important parameters in radiolysis and self-radiolysis of the hydrogel system are detected to be the swelling degree. The experiments suggest as optimum for HTO storage as tritium liquid wastes a 1:30 PAA:HTO swelling degree at a radioactive concentration of HTO in the range 18.5-37 MBq/mL.

Some considerations on the radioactive waste assay system

L. Dinescu[1], I. Vata[1], R. Macrin[1], I.L. Cazan[1], Gh. Caragheorgheopol[1], C. Razdolescu[1]

[1] National Institute of Research and Development for Physics and Nuclear Engineering "Horia-Hulubei", IFIN-HH, P.O.Box MG - 6, RO - 76900 Bucharest, Romania

The movement and storage of containers of radioactive waste requires a characterization of radionuclides content, to verify the conformance with transportation and waste acceptance requirements. Since a low level of detection is desired, the gamma spectroscopy is often the only viable method for the content assay. This method is based on the gamma spectrum analysis and requires a suitable efficiency calibration for bulk containers.

The present study is focused on the efficiency calibration of the gamma spectroscopy system for a drum waste assay, constructed in IFIN-HH. In order to minimize the effect of non-homogeneities (matrix density, radioactive source distribution, etc) and to obtain a complete covering of the surface of the drum, the system is provided with an electromechanical device, which assures the simultaneously rotation and horizontal translation of the drum. A double translation (forward and backward) is performed to obtain the best possible accuracy, independent of the distribution of radioactive material in the drum. A lead collimated Ortec HPGe detector of 20% relative efficiency connected to 8192 channels MCA was used.

The radioactive waste is generally conditioned in 220l stainless steel containers. For the efficiency calibration we used a similar drum filled with Portland cement and a linear source of ^{152}Eu $\Lambda = 91.02 \pm 4.55$ MBq) produced by the radionuclide metrology group from the radioisotope department, IFIN-HH. The calibration drum is provided with 7 hollow tubes of 20 mm diameter, placed at different distances from the center of the drum. The linear calibration source was introduced successively in the 7 tubes and the gamma spectra were collected, while the drum was rotated and simultaneously translated. Using ASPERA 8k software (developed by IFIN-HH) the gamma spectra were analyzed and the average values of the net peak area for each of the selected energies (121.8 keV, 344.2 keV, 778.9 keV, 1112 keV and 1408 keV) and for each radial source position were obtained. These values were integrated over the drum volume and the total response of the detector was obtained. The detection efficiency was calculated for each of selected energies. The calibration curves for several values of

the cylinder radius, considering an approximately uniformly distributed source are shown in fig. 7

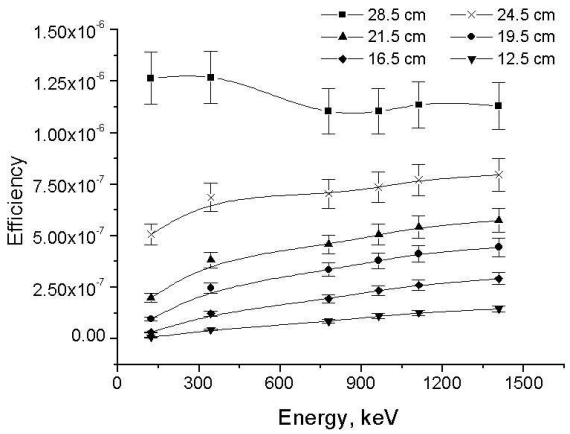

Figure 1: The dependence $\varepsilon = f(E)$ for six waste cylinders having different radiuses, inside the drum.

The minimum detectable activity (MDA) for the given geometry - a collimated HPGe (20% relative efficiency), a 220l cement filled drum and 10 min. measuring time is approximately 45 Bq/kg for ^{137}Cs and ^{60}Co. These values of MDA are considered as detection limits of the system. By increasing the measuring time, smaller values for MDA could be obtained.

The total measurement uncertainty ranges from - 70% to + 40% including the worst cases where the total activity is concentrated in one point located in center-bottom of the drum, for gamma ray energy less then 500 keV.

References

[1] l. Dinescu, I. Vata, I.L. Cazan, R. Macrin, Gh. Caragheorgheopol, Gh. Rotarescu, Nucl. Instr.&Methods / A, 487(3), 661-666 (2002)

Standardisation

Standardization of ^{65}Zn by the 4πPC-γ efficiency extrapolation method

M. Sahagia[1], C. Ivan[1], E.L. Grigorescu[1], M. Capogni[2], P.De Felice[2], A. Fazio[2]

[1] National Institute of R&D for Physics and Nuclear Engineering "Horia Hulubei", IFIN-HH, POB MG-6, RO -76900, Bucharest, Romania

[2] E.N.E.A., Istituto Nazionale di Metrologia delle Radiazioni Ionizzanti, C. R. Casaccia, POB 2400, I-00100 Rome A.D., Italy

Abstract

The paper presents the results obtained in the standardization of ^{65}Zn by using the 4πPC-γ coincidence installation of the Istituto di Metrologia delle Radiazioni Ionizzanti (INMRI), C.R.Casaccia, ENEA, Italy, by the efficiency extrapolation method. The basic relations existing between 4πPC efficiencies, coincidence equations, as well as the experimental results obtained in various conditions are presented. On the 4πPC channel, two sets of measurements were carried out: detection of the radiations from (K+L) electron capture-β^+, and from K electron capture-β^+; on the gamma channel, the measurements were made by assuring linearity extrapolation conditions, by measuring the 1115.6 keV quanta alone, and by approximate accomplishment of linearity condition.

The obtained values of activity were compared with the value determined by using a calibrated CENTRONIC IG11/20A ionization chamber.

Standardization of tritiated water and ^{204}Tl by TDCR liquid scintillation counting

Anamaria Cristina Razdolescu[1], Ph. Cassette[2]

[1] National Institute of R&D for Physics and Nuclear Engineering "Horia Hulubei"- IFIN-HH, Atomistilor str. 407, POB MG-6, Bucharest, Romania

[2] Laboratoire National Henri Becquerel- CEA/DIMRI-Saclay, France

Abstract

The TDCR method (Triple to Double Coincidence Ratio) was used to standardize tritiated water and a solution of ^{204}Tl with a combined uncertainty of 1-2%. The vial with liquid scintillator, in which the sample to be measured was dissolved, is optically coupled with 3 photomultipliers. The electronic module MAC-3 assures the selection of double and triple coincidences count rates, D and T, from the three counting channels. It contains the gating circuits necessary to obtain the effective time value and the extended dead time circuit. Specific computer programs, were used to calculate the free parameter value, the efficiency of D and so, the value of the activity. The optimal value of the Birks ionisation-quenching parameter, kB, was evaluated by changing the detection efficiency with grey filters. Three types of liquid scintillators, namely InstaGel, PPO+POPOP+Triton in toluene and Ultima Gold were employed. ^{204}Tl was measured in the frame of an international comparison organized by BIPM. For tritiated water a comparison was made with LNHB-Saclay; the relative difference between the obtained values for the massic activity was of only 0.2%.

Standardization of ^{68}(Ge+Ga)

E.L. Grigorescu[1], C.D. Negut[1], A. Luca[1], Anamaria Cristina Razdolescu[1], Mioara Tanase[2]

[1] National Institute of R&D for Physics and Nuclear Engineering "Horia Hulubei" - IFIN-HH, Atomistilor str. 407, POB MG-6, Bucharest, Romania
[2] CS ISPAT SIDEX, Galati, Romania

The radionuclide ^{68}Ga is mainly a positron emitter (89.2%), with a half life of 67.7 min. It is used in nuclear medicine, being chemically extracted from the mixture ^{68}(Ge+Ga); its precursor, ^{68}Ge, disintegrates 100% by electron-capture, with a half life of 271d.

A 4πbeta-gamma coincidence method was used for standardization, with a 4π proportional beta detector and a NaI(Tl) gamma detector. The capture radiations were not registered using foil absorbtion and a high beta threshold. Using supplementary foils for positron absorbtion, an extrapolation graph was obtained, with a slope of - 4,4%. Care was taken to compensate for the loss of ^{68}Ge, during the preparation of solid sources for measurement. A combined uncertainty of 1.1% was estimated.

Appendix

Publications

In Journals

Adam Gh., Adam S., Papp E.
Self-validating Gauss–Kronrod quadrature
Romanian Journal of Physics vol. 46, No. 5-6 (2001)

Adam Gh., Adam S.
Discrete group symmetry in the fast Chebyshev transform
Romanian Journal of Physics vol. 48, No. 5-6, (2003); The First Romanian National Conference of Theoretical Physics, Bucharest, 13-16 Sept. 2002; (extended abstract available at http://www.theory.nipne.ro/ctp2002/abstracts/a19.html*), (contribution available at* http://www.theory.nipne.ro/ctp2002/proced/proced.html*)*

Adam Gh., Adam S.
Enhancing reliability of interpolatory quadrature rules
Romanian Journal of Physics vol. 47, No. 1-2, 273–288 (2002)

Adam Gh., Adam S.
Increasing reliability of Gauss–Kronrod quadrature by Erastotenes' sieve method
Computer Physics Communications vol. 135 (no. 3), 261–277 (2001)

Adam Gh., Adam S.
Reply to the "Comment on reliable operations on oscillatory functions"
Computer Physics Communications, vol. 134, No. 2, 269–272 (2001)

Adam Gh., Adam S.
Robust automatic adaptive quadrature
Romanian Journal of Physics vol. 47, No. 3-4, 337–352 (2002)

Adam S.
Exchange and spin-fluctuation pairing in the two-band Hubbard model – Application to cuprates
New Trends in Superconductivity vol. 67, 29–38 (2002)

Papp E., Adam Gh., Micu C.
Using the transfer matrix approach to the derivation of exact energies to the Harper equation
Bul. St. UNBM/Fizica, vol. 1, 9–13 (2001)

Papp E., Micu C., Adam Gh.
The description of electrons on two-dimensional triangular lattices threa-ded by a transversal and homogeneous magnetic field
Physics Journal UNBM, vol. 1, 7–11 (2001)

M. C. Abreu, .., C. Alexa, V. Boldea, S. Dita et al., [NA38/NA50 Collaboration]
Enhancement Of Intermediate Mass Dimuons In Nucleus Nucleus Collisions At The CERN SPS,
Nucl. Phys. A **698**, *539 (2002).*

M. C. Abreu, .., C. Alexa, V. Boldea, S. Dita et al., [NA50 Collaboration]
Charmonia Suppression In P A Collisions At 450-GeV/C: New Results From NA50,
Nucl. Phys. A **698**, *543 (2002).*

M. C. Abreu, .., C. Alexa, V. Boldea, S. Dita et al., [NA50 Collaboration]
NA50 Results On Pb Pb Interactions At 158-GeV Per Nucleon,
Nucl. Phys. A **681**, *157 (2001).*

M. C. Abreu, .., C. Alexa, V. Boldea, S. Dita et al., [NA50 Collaboration]
Phi And Rho + Omega Vector-Mesons Produced In Lead Induced Collisions,
J. Phys. G **28**, *1809 (2002).*

M. C. Abreu, .., C. Alexa, V. Boldea, S. Dita et al., [NA50 Collaboration]
Production Of The Phi Vector-Meson In Heavy-Ion Collisions,
J. Phys. G **27**, *405 (2001).*

M. C. Abreu, .., C. Alexa, V. Boldea, S. Dita et al., [NA50 Collaboration]
Pseudorapidity distributions of charged particles as a function of centrality in Pb Pb collisions at 158-GeV and 40-GeV per nucleon incident energy,
Phys. Lett. B **530**, *33 (2002).*

M. C. Abreu, .., C. Alexa, V. Boldea, S. Dita et al., [NA50 Collaboration]
Recent Results On J / Psi From Experiment NA50,
Nucl. Phys. A **698**, *127 (2002).*

M. C. Abreu, .., C. Alexa, V. Boldea, S. Dita et al., [NA50 Collaboration]
Results From The Na50 Experiment On J / Psi Suppression In Pb Pb Collisions At The Cern SPS,
Nucl. Phys. Proc. Suppl. **92**, *43 (2001).*

M. C. Abreu, .., C. Alexa, V. Boldea, S. Dita et al., [NA50 Collaboration]
Results On Open Charm From NA50,
J. Phys. G **27**, *677 (2001).*

M. C. Abreu, .., C. Alexa, V. Boldea, S. Dita et al., [NA50 Collaboration]

Scaling of charged particle multiplicity in Pb Pb collisions at SPS energies,
Phys. Lett. B **530**, *43 (2002).*

M. C. Abreu, .., C. Alexa, V. Boldea, S. Dita et al., [NA50 Collaboration]
The dependence of the anomalous J/psi suppression on the number of participant nucleons,
*Phys. Lett. B***521**, *195 (2001).*

M. C. Abreu, .., C. Alexa, V. Boldea, S. Dita et al., [NA50 Collaboration]
Transverse Flow In Heavy Ion Interactions At The Cern SPS,
Nucl. Phys. Proc. Suppl. **92**, *55 (2001).*

T.Antoni and KASCADE collaboration
A non-parametric approach to infer the energy spectrum and the mass composition
Astropart.Phys.16 (2002) 245-263

T.Antoni and KASCADE collaboration:
Muon density measurements with the KASCADE central detector
Astropart.Phys.16 (2002) 373-386

S. Berceanu
The coherent states: old geometrical methods in new quantum clothes
Rom. Jour. Phys. **47**. *Nos 3-4, 353-358 (2002)*

P. Amaral, .., V. Boldea, S. Dita, D. Pantea et al. [ATLAS Collaboration],
Hadron energy reconstruction for the ATLAS calorimetry in the framework of the non-parametrical method,
Nucl. Instrum. Meth. A **480**, *508 (2002)*

P. Amaral, .., V. Boldea, S. Dita, D. Pantea et al. [ATLAS TileCal Collaboration],
A Precise Measurement Of 180-GeV Muon Energy Losses In Iron,
Eur. Phys. J. C **20**, *487 (2001).*

G. Beer, .., A. M. Bragadireanu, C. Curceanu, T. Ponta, D. L. Sirghi et al.
A New Method To Obtain A Precise Value Of The Mass Of The Charged Kaon,
Phys. Lett. B **535**, *52 (2002).*

I.M.Brancus, H.Rebel, M.Duma, A.F.Badea, C.Aiftimiei, J.Oehlschlager
Muon arrival time distributions of simulated extensive air showers in view of mass discrimination
Acta Phys.Polonica B, 33 (2002) 323-329

I. Caprini, L. Micu, C. Bourrely
Quark hadron duality, factorization and strong phases in $B_0 \to \pi^+\pi^-$ decay
*Eur.Phys. J.C***21**, *145-153 (2001).*

A. Ramani, B. Grammaticos, A.S. Cârstea, Y. Ohta
On the autonomous limit of discrete Painleve equation
Physica A **305**, *437 (2002)*

A.S. Cârstea, A. Ramani, B. Grammaticos
Linearisable supersimetric equations
Chaos, Solitons and Fractals, **14***(1), 155-158 (2002)*

B. Grammaticos, T. Tamizhmani, A.S. Cârstea
A bilinear approach to the discrete Painleve I equations
J. Phys. Soc. Japan, **71**, *443 (2002)*

V. Cercasov, A. Pantelică, M. Sălăgean, G. Caniglia, A. Scarlat
Comparative study of the suitability of three lichen species to trace-element air monitoring
Environmental Pollution **119/1**, *129-139 (2002)*

C.Ciortea, D.E.Dumitriu, S.E.Enescu, A.Enulescu, D.Flueraşu, I.Piticu and Z.S.Szilagyi
Inner shell vacancy production and mean charge states of MeV/u Fe, Co, Ni and Cu ions in Au and Bi solid targets
Nucl. Instr. and Meth. in Phys. Res. **B 193** *(2002) 109 -*

I.I.Cotăescu and M. Vişinescu
Dynamical algebra and Dirac quantum modes in the Taub-NUT background
Class.Quantum Grav. **18**, *3383 (2001)*

I.I.Cotăescu and M. Vişinescu
Hierarchy of Dirac, Pauli and Klein-Gordon conserved operators in Taub-NUT background
Journ. Math. Phys. **43**, *2978 (2002)*

I.I.Cotăescu and M. Vişinescu
Non-existence of f-symbols in generalized Taub-NUT spacetimes
J.Phys. A: Math.Gen. **34**, *6459 (2001)*

I.I.Cotăescu and M. Vişinescu
Runge-Lenz operator for Dirac field in Taub-NUT background
Phys.Lett. B **502**, *229 (2001)*

I.I.Cotăescu and M. Vişinescu
The Dirac field in Taub-NUT background
Int.J.Mod.Phys. A **16**, *1743 (2001)*

L.-C. Crasovan, B. A. Malomed, D. Mihalache
Stable vortex solitons in the two-dimensional Ginzburg-Landau equation
Physical Review E **63**, *016605 (2001)*

L.-C. Crasovan, G. Molina-Terriza, J. P. Torres, L. Torner, V. M. Perez-Garcia, D. Mihalache
Globally-linked vortex clusters in trapped wave fields
Physical Review E **66**, *036612 (2002)*

L.-C. Crasovan, B. A. Malomed, D. Mihalache
Erupting, flat-top, and composite spiral solitons in the two-dimensional Ginzburg-Landau equation
Physics Letters A **289**, *59 (2001)*

L.-C. Crasovan, B. A. Malomed, D. Mihalache
Spinning solitons in cubic-quintic nonlinear media
Pramana Journal of Physics **57**, *1041 (2001)*

D.S. Delion, A. Insolia, R.J. Liotta

Anisotropic α-decay
Yadernaia Physika **65**, *685-689 (2002); Phys. Atomic Nuclei* **65**, *653-657 (2002)*

D.S. Delion, A. Săndulescu, S. Mişicu, F. Carstoiu, W. Greiner
Double fine structure in the binary cold fission
Journal of Physics **G28**, *289-306 (2002)*

D.S. Delion, A. Săndulescu, W. Greiner
Self-consistent description of the ternary cold fission: Tri-rotor mode
Journal of Physics **G28**, *2921-2938 (2002)*

D.S. Delion, A. Săndulescu
Towards a selfconsistent α-decay theory
Journal of Physics **G28**, *617-625(2002)*

D.S. Delion, G.G. Dussel, R.J. Liotta
Towards a microscopic description of an α-condensate in nuclei
Romanian Journal of Physics **47**, *97-106 (2002)*

D.S. Delion, J. Suhonen
Influence of the continuum on cluster-decay processes
Yadernaia Physika **65**, *653-659 (2002); Phys. Atomic Nuclei* **65**, *621-627 (2002)*

D.S. Delion, J. Suhonen
Microscopic structure of four body resonances
Romanian Journal of Physics **47**, *177-188 (2002)*

D.S. Delion, R.J. Liotta
Proton emission from highly deformed nuclei
Romanian Journal of Physics **47** *(2002) (in press)*

L. Dinescu, I. Vata, I. L. Cazan, R. Macrin, Gh. Caragheorgheopol, Gh. Rotarescu
On the efficiency calibration of a drum waste assay system
Nuclear Instruments & Methods in Physics Research A 487 (2002) 661-666

S.E.Enescu, I.Bibicu, M.N.Grecu, C.Ciortea, Al.Enulescu and A. Kluger
Rayleigh Scattering of Mössbauer Radiation on Rb_2ZnCl_4 around T_I
Rom.J.Phys. **46** *(9-10) (2001)*

C. Etrich, N.-C. Panoiu, D. Mihalache, F. Lederer
Limits for interchannel frequency separation in a soliton wavelength-division multiplexing system
Physical Review E **63**, *016609 (2001)*

D. Grecu, Anca Vişinescu
Modulational instability in some nonlinear one–dimensional lattices and soliton generation
Annals of the University of Craiova, **12**, *129-149 (2002)*

D. Grecu, Anca Vişinescu, A.S. Cârstea
Beyond nonlinear Schrödinger equation approximation for an anharmonic chain with harmonic long range interactions
Journal of Nonlinear Mathematical Physics **8** *139-144 (2001).*

D. Grecu, Anca Vişinescu
Soliton signature in the infrared spectra of nonlinear quasi-onedimensional molecular crystals
Studia Universitatis Babes-Bolyai" Special Issue, Proceedings PIM 164-169 (2001)

D. Grecu
Plasma oscillations in a layered electron gas (LEG) model revisited
Rom. Journ. Phys. **47** *(3-4), 437-445 (2002)*

Grigore D. R.
Gauge Invariance of the Quantum Electrodynamics in the Causal Approach to Renormalization Theory
Ann. Phys. (Leipzig) 10, 439-471 (2001)

Grigore D. R.
Scale Invariance in the Causal Approach to Renormalization Theory
Ann. Phys. (Leipzig) 10, 473-496 (2001)

Grigore D. R.
The Standard Model and its Generalisations in Epstein-Glaser Approach to Renormalisation Theory II: the Fermion Sector and the Axial Anomaly
Journ. Phys A 34, 5429-5462 (2001)

Grigore D. R.
The Structure of the Anomalies of Gauge Theories in the Causal Approach
Journ. Phys. A 35, 1665-1689 (2002)

Grigore D. R.
Wess-Zumino Model in the Causal Approach
European Phys. Journ. C 21 (Particles and Fields), 732-734 (2001)

R.Haeusler, A.F.Badea, H.Rebel, I.M.Brancus, J. Oehlschlager
Distortions of experimental muon arrival time distributions of extensive air showers by the observation conditions
Astropart.Phys.16 (2002) 421-426

D. B. Ion and M. L. Ion,
Evidences For Nonextensivity Conjugation In Hadronic Scattering Systems,
Phys. Lett. B **503**, *263 (2001).*

D. B. Ion and M. L. Ion,
New Nonextensive Quantum Entropy And Strong Evidences For Equilibrium Of Quantum Hadronic States,
Phys. Lett. B **519**, *63 (2001).*

D. B. Ion and M. L. Ion,
Optimality Entropy And Complexity In Quantum Scattering,
Chaos Solitons Fractals **13**, *547 (2002).*

Y. V. Kartasov, L.-C. Crasovan, D. Mihalache, L. Torner
Robust propagation of two-color soliton clusters supported by competing nonlinearities

Physical Review Letters **89**, *273902 (2002)*

B. A. Malomed, L.-C. Crasovan, D. Mihalache
Stability of vortex solitons in the cubic-quintic model
Physica D **161**, *187-201 (2002)*

I. V. Melnikov, D. Mihalache, N.-C. Panoiu, F. Ginovart, A. Zamudio Lara
Coherent amplification of dual-frequency optical solitons in a doped fiber
Optics Communications **191**, *133 (2001)*

Jan Louis, Andrei Micu
Heterotic String Theory With Background Fluxes
Nucl.Phys. **B626** *26-52, 2002*

Jan Louis, Andrei Micu
Type 2 Theories Compactified on Calabi-Yau Threefolds in the Presence of Background Fluxes
Nucl.Phys. **B635** *395-431, 2002*

D. Mihalache, D. Mazilu, I. Towers, B. A. Malomed, F. Lederer
Stable two-dimensional spinning solitons in a bimodal cubic-quintic model with four-wave mixing
Journal of Optics A: Pure and Applied Optics **4**, *615-623 (2002)*

D. Mihalache, D. Mazilu, L.-C. Crasovan, I. Towers, A. V. Buryak, B. A. Malomed, L. Torner, J. P. Torres, F. Lederer
Stable spinning solitons in three dimensions
Physical Review Letters **88**, *073902 (2002)*

D. Mihalache, D. Mazilu, L.-C. Crasovan, I. Towers, B. A. Malomed, A. V. Buryak, L. Torner, F. Lederer
Stable three-dimensional spinning optical solitons supported by competing quadratic and cubic nonlinearities
Physical Review E **66**, *016613 (2002)*

D. Mihalache, L.-C. Crasovan
Optical spatiotemporal solitons in quadratic media
Proc. SPIE **4430**, *451 (2001)*

D. Mihalache
Spinning optical spatiotemporal solitons in quadratic media
Acta Physica Polonica A **99**, *47 (2001)*

V.A. Moscalenko, P. Entel, M. Marinaro, D.F. Digor, D. Grecu
The cell representation of the three-band Hubbard model
Fiz. Eks. Ciastitz Atom. Iadra **33**(*4*), *964-1003 (2002)*

Agata Olariu, Ragnar Hellborg, Kristina Stenström, Goran Skog, Mikko Faarinen, Per Persson and Bengt Erlandsson
Dating of some Romanian fossil bones by combined nuclear methods
Journal of Radioanalytical and Nuclear Chemistry, Vol. 253 No.2 (2002) p.307-311

E. A. Ostrovskaya, Y. S. Kivshar, D. Mihalache, L.-C. Crasovan
Multichannel soliton transmission and pulse shepherding in bit-parallel-wavelength optical fiber links
IEEE Journal of Selected Topics in Quantum Electronics **8**, *591-596 (2002)*

N.-C. Panoiu, D. Mihalache, C. Etrich, F. Lederer
Influence of inter-channel frequency separation on the transmission capacity of a soliton based WDM system
Proc. SPIE **4271**, *366 (2001)*

N.-C. Panoiu, I. V. Melnikov, D. Mihalache, C. Etrich, F. Lederer
Soliton generation from a multi-frequency optical signal
Journal of Optics B: Quantum and Semiclassical Optics **4**, *R53-R68 (2002)*

N.-C. Panoiu, I. V. Melnikov, D. Mihalache, C. Etrich, F. Lederer
Multiwavelength pulse transmission in an optical fibre-amplifier system
Quantum Electronics **32**, *1009-1016 (2002)*

J. M. Link, .., D. Pantea et al. [FOCUS Collaboration]
A high statistics measurement of the Lambda/c+ lifetime,
Phys. Rev. Lett. **88**, *161801 (2002)*

J. M. Link, .., D. Pantea et al. [FOCUS Collaboration]
A measurement of branching ratios of D+ and D/s+ hadronic decays to four-body final states containing a K(S),
Phys. Rev. Lett. **87**, *162001 (2001)*

J. M. Link, .., D. Pantea et al. [FOCUS Collaboration]
A new measurement of the Xi/c+ lifetime,
Phys. Lett. B **523**, *53 (2001)*

J. M. Link, .., D. Pantea et al. [FOCUS Collaboration]
A new measurement of the Xi/c0 lifetime,
Phys. Lett. B **541**, *211 (2002)*

J. M. Link, .., D. Pantea et al. [FOCUS Collaboration]
Cerenkov particle identification in FOCUS,
Nucl. Instrum. Meth. A **484**, *270 (2002)*

J. M. Link, .., D. Pantea et al. [FOCUS Collaboration]
Evidence for new interference phenomena in the decay D+ → K- pi+ mu+ nu,
Phys. Lett. B **535**, *43 (2002)*

J. M. Link, .., D. Pantea et al. [FOCUS Collaboration]
Measurement of natural widths of Sigma/c0 and Sigma/c++ baryons,

Phys. Lett. B **525**, *205 (2002)*

J. M. Link, .., D. Pantea et al. [FOCUS Collaboration]
Measurement of the relative branching ratio BR(Xi/c+ → p+ K- pi+)/BR(Xi/c+ → Xi- pi+ pi+),
Phys. Lett. B **512**, *277 (2001)*

J. M. Link, .., D. Pantea et al. [FOCUS Collaboration]
Measurements of relative branching ratios of Lambda/c+ decays into states containing Sigma,
Phys. Lett. B **540**, *25 (2002)*

J. M. Link, .., D. Pantea et al. [FOCUS Collaboration]
New measurements of the D0 and D+ lifetimes,
Phys. Lett. B **537**, *192 (2002)*

J. M. Link, .., D. Pantea et al. [FOCUS Collaboration]
New measurements of the Gamma(D+ → anti-K*0 mu+ nu)/Gamma(D+ → K- pi+ pi+) and Gamma(D/s+ → Phi mu+ nu)/Gamma(D/s+ → Phi pi+) branching ratios,
Phys. Lett. B 541, *243 (2002)*

J. M. Link, .., D. Pantea et al. [FOCUS Collaboration]
Reconstruction of Vees, kinks, Xi-'s, and Omega-'s in the FOCUS spectrometer,
Nucl. Instrum. Meth. A **484**, *174 (2002)*

J. M. Link, .., D. Pantea et al. [FOCUS Collaboration]
Search for CP violation in the decays D+ → K(S) pi+ and D+ → K(S) K+,
Phys. Rev. Lett. **88**, *041602 (2002)*

J. M. Link, .., D. Pantea et al. [FOCUS Collaboration]
Measurement of the D+ and D/s+ decays into K+ K- K+,
Phys. Lett. B **541**, *227 (2002)*

J. M. Link, .., D. Pantea et al. [FOCUS Collaboration]
New measurements of the D+ → anti-K*0 mu+ nu form factor ratios,
Phys. Lett. B **544**, *89 (2002)*

J. M. Link, .., D. Pantea et al. [FOCUS Collaboration]
Observation of a 1750-MeV/c**2 enhancement in the diffractive photoproduction of K+ K-,
Phys. Lett. B **545**, *50 (2002)*

(DIRAC Collaboration) A.M. Rodriguez, ..., Gh. Caragheorgheopol, S. Constantinescu, M. Iliescu, M. Pentia, C. Petrascu, T. Ponta, D. Pop, et al.
The DIRAC experiment at CERN: current status and future perspectives
πN Newslett. 16: 352-354, 2002

DIRAC Collaboration: A. Lanaro, ... M. Pentia, Gh. Caragheorgheopol, S. Constantinescu, C. Petrascu (Curceanu), M. Iliescu, T. Ponta, D. Pop, et al.
A determination of the S-wave pion-pion scattering lengths from the measurement of the lifetime of pionium
Proc. Int. Conf. on High Energy Physics [ICHEP 2000], 27 July - 2 August 2000, Osaka [Japan], Eds. C.S. Lim, Taku Yamanoka, Vol.I, 359-362, World Scientific, 2001

DIRAC Collaboration: F. Gomez, ..., M. Pentia, Gh. Caragheorgheopol, S. Constantinescu, C. Petrascu (Curceanu), M. Iliescu, T. Ponta, D. Pop, et al. (79 autori)
DIRAC experiment at CERN
Nucl.Phys.B 96: 256-266, 2001

DIRAC Collaboration: J. Schacher, ... M. Pentia, Gh. Caragheorgheopol, S. Constantinescu, C. Petrascu (Curceanu), M. Iliescu, T. Ponta, D. Pop, et al.
Experimental status of pionium at CERN
Proc. Int. Conf. Chiral Dynamics 2000: Theory and Experiment, 17-22 July 2000, Newport News [Virginia, USA], Springer Verlag, 2001

STAR Collaboration: K.H. Ackermann, ..., M. Pentia, et al.
Elliptic flow in Au + Au collisions at $\sqrt{s_{NN}}$ = 130 GeV
Phys.Rev.Lett. 86:402-407, 2001

J.F. Gomez, .., T. Ponta et al. [DIRAC Collaboration]
Dirac Experiment
Nucl. Phys. Proc. Suppl. **96**, *259 (2001).*

E.A.Preoteasa, C.Ciortea, B.Constantinescu, Daniela Flueraşu, Sanda-Elena Enescu, D. Pantelică , F.Negoiţă, Elena Preoteasa
Analysis of composites for restorative dentistry by PIXE, XRF and ERDA
Nucl. Instr. and Meth. in Phys. Res. **B 189** *(2002) 426 - 430*

L. Torner, S. Carrasco, J. P. Torres, L.-C. Crasovan, D. Mihalache
Tandem light bullets
Optics Communications **199**, *277 (2001)*

J. P. Torres, S. L. Palacios, L. Torner, L.-C. Crasovan, D. Mihalache, I. Biaggio
Method for generating solitons sustained by competing nonlinearities by use of optical rectification
Optics Letters **27**, *1631-1633 (2002)*

I. Towers, A. V. Buryak, R. A. Sammut, B. A. Malomed, L.-C.Crasovan, D. Mihalache
Stability of spinning solitons of the cubic-quintic nonlinear Schrödinger equation
Physics Letters A **288**, *292 (2001)*

Anca Vişinescu, D. Grecu
Randomness effects on modulational instability of a discrete self-trapping equation
Roumanian Journal of Physics **48** *nr. 4-5 (2003); Proceedings of the First National Conference on Theoretical Physics, editors D. Grecu, Anca Vişinescu http://www.theory.nipne.ro/ctp2002/proceedings*

Anca Vişinescu, D. Grecu
Solitonic model for energy transport in quasi-1-D biological systems
Roumanian Journal of Physics **47** *509-518 (2002).*

M. Vişinescu
Fermions in Taub-NUT background
Int. Journ. Mod. Phys. **A17**, *1049 (2002)*

M. Vişinescu
Spinning particles and Dirac operators in Taub-NUT background
Rom. Journ. Phys. **47**, *519 (2002)*

M. Vişinescu
Spinning particles, Dirac-type operators on curved spaces and the role of Killing-Yano tensors
Annals of the Univ. Craiova **12**, *40 (2002)*

Books and Chapter in Books

S. Berceanu
Coherent states, phases and symplectic areas of geodesic triangles, in *Coherent States, Quantization and Gravity*, Edited by M. Schlichenmaier, A. Strasburger, S. Twareque Ali, A. Odjziewicz
Warsaw University Press, Warsaw 2001, pp. 129-137

M. Vişinescu
Generalized Taub-NUT metrics and Killing-Yano tensors

Proceedings of the NATO Advanced Research Workshop "Noncommutative Structures in Mathematics and Physics", Kiev (2000), Kluwer Academic Publisher, Dordrecht (2001)

Preprints

Adam Gh., Adam S., Plakida N.M.
Reliability conditions on quadrature algorithms
Preprint JINR Dubna, E-17-2002-205, 20pp.; extended version to be published in Computer Physics Communications, 2003;
http://arXiv.org/abs/cs.NA/0303004
and at the Elsevier site :
http://www.mathpreprints.com/math/Preprint/adamg/20030415/1.

Plakida N.M., Anton L., Adam S., Adam Gh.
Exchange and spin-fluctuation superconducting pairing in the Hubbard model in the strong correlation limit
Preprint JINR Dubna, E-17-2001-59, 30pp.

I.Caprini, J. Fischer
Analytic continuation and perturbative expansions in QCD
hep-ph/0110344

V. M .Karnaukhov, V. I. Moroz, C. Coca
About the common features of the possible exotic states K(1630), N(3520), Sigma(3170) observed experimentally
JINR-E1-2001-185, Sep 2001. 5pp.

I.I.Cotăescu and M. Vişinescu
Dirac operators on Taub-NUT space: Relationship and discrete transformations
hep-th/0202034, to appear in Gen. Rel. Grav. (2003)

I.I.Cotăescu and M. Vişinescu
Hierarchy of Dirac, Pauli and Klein-Gordon conserved operators in Taub-NUT background
hep-th/0107205, to appear in J.Math.Phys. (2002)

Grigore D. R., Scharf G.
A Supersymmetric Extension of Quantum Gauge Theory
hep-th/0204105, to appear in Annalen der Physik

Grigore D. R., Scharf G.
The Quantum Supersymmetric Vector Multiplet and Some Problems in Non-Abelian Supergauge Theory
hep-th/0212026

Grigore D. R.
Ward Identities and Renormalization of General Gauge Theories
hep-th/0108083

D.B. Ion and E.K. Sarkisyan
Dual Coherent Particle Emission as Generalized Cerenkov–like Effect in High Energy Particle Collisions

e-Print Archive: hep-ph/0209039
V.M Karnaukhov, C. Coca, V. I. Moroz
About the common features of the possible exotic states K(1630), N(3520), Σ(3170) observed experimentally"
Communication of JINR E1 2001-85
M. Pentia, S. Constantinescu
Uncertainties induced by multiple scattering in upstream detectors of the DIRAC setup
DIRAC Note 01-04, CERN, 25 Oct. 2001
A. N. Aleev, .., T. Ponta, T. Preda et al. [EXCHARM Collaboration]
Inclusive production of antihyperons in nC intarections
JINR-D1-2001-283, Dec 2001. 20pp.
A. N. Aleev, .., T. Ponta, T. Preda et al. [EXCHARM Collaboration]
Inclusive production of hyperons in nC interactions
JINR-D1-2001-98, May 2001. 18pp.
Anca Vişinescu, D. Grecu
Statistical approach of the modulational instability of a discrete self-trapping equation
arXiv:nlin.SI/0212043

International Conferences

Adam Gh., Adam S.
Efficient automatic and reliable division strategy in automatic adaptive quadrature
Invited talk at The 2-nd International Colloquium "Mathematics in Engineering and Numerical Physics", April 22-27, 2002, Bucharest

Adam Gh., Adam S.
Reliability criteria for local quadrature rules
Invited talk at The 12-th National Conference of the Romanian Physical Society "Trends in Physics", Târgu Mureş, 26-28 Sept. 2002

Adam Gh., Scutaru H., Ixaru L., Adam S., Rizea M., Ştefănescu E., Mihalache D., Isar A., Mazilu D., Craşovan L.
Dynamics of dissipative systems and the computational physics
CERES Programme Annual Scientific Session, Bucharest, December 2–3, 2002

F. Prino et al., .., C. Alexa, V. Boldea, S. Dita et al., [NA50 Collaboration]
J / Psi Production in Proton Nucleus and Nucleus Nucleus Interactions at the CERN SPS
30^{th} *International Workshop on Gross Properties of Nuclei and Nuclear Excitation: Hirschegg 2002: Ultrarelativistic Heavy Ion Collisions, Hirschegg, Austria, 13-19 Jan 2002.*
*Published in *Hirschegg 2002, Ultrarelativistic heavy-ion collisions* 254-263*

M.C. Abreu et al., .., C. Alexa, V. Boldea, S. Dita et al., [NA50 Collaboration]
New Results on Nuclear Dependence of J / Psi and Psi-prime Production
37^{th} *Rencontres de Moriond on QCD and Hadronic Interactions, Les Arcs, France, 16-23 Mar 2002.*
e-Print Archive: hep-ex/0207014 450-GeV PA Collisions
M.C. Abreu et al., .., C. Alexa, V. Boldea, S. Dita et al., [NA50 Collaboration]
Searchng for QGP: the J / Psi Probe in the NA50/CERN Experiment
7^{th} *Conference on Intersections Between Particle and Nuclear Physics (CIPANP 2000), Quebec City, Quebec, Canada, 22-28 May 2000.*
*Published in AIP Conf.Proc.549:341-345, 2002 Also in *Quebec City 2000, Intersections of particle and nuclear physics* 341-345*
M.C. Abreu, .., C. Alexa, V. Boldea, S. Dita et al., [NA50 Collaboration]
Centrality Behaviour of J / Psi Production in NA50
31st International Symposium on Multiparticle Dynamics (ISMD 2001), Datong, China, 1-7 Sep 2001.
*Published in *Datong 2001, Multiparticle dynamics* 127-131*
e-Print Archive: hep-ph/0111429
R. Arnaldi, .., C. Alexa, V. Boldea, S. Dita et al., [NA50 Collaboration]
The Onset of the Anomalous J / Psi Suppression in Pb-Pb Collisions at the CERN SPS
36^{th} *Rencontres de Moriond on QCD and Hadronic Interactions, Les Arcs, France, 17-24 Mar 2001.*
e-Print Archive: hep-ex/0106079
S. Beole, .., C. Alexa, V. Boldea, S. Dita et al., [NA50 Collaboration]
Latest Results from NA50 on J / Psi Suppression in Pb Pb Collisions at 158 GeV/c
International Nuclear Physics Conference (INPC 2001): Nuclear Physics and the 21st Century, Berkeley, California, 30 Jul - 3 Aug 2001.
*Published in *Berkeley 2001, Nuclear physics in the 21st century* 561-565*

T.Antoni, A.Bercuci, H.J.Mathes, S.Zagromski and KASCADE collaboration: Untersuchungen der Myon Componentene ausgedehnter Luftschauer mit den Streamer
Tube Detektoren im Zentraldetektor des KASCADE-Experiments
Physikertagung gemeinsam mit der Fruhjahrstagung der DPG, Leipzig, 18-22 Marz, 2002, Verhandlungen der Deutschen Physikalischen Gesellschaft, R.6, Bd.37 (2002) T 101.7

A.F.Badea and KASCADE collaboration:
Sensitivity and consistence studies of muon arrival time distribution measured by KASCADE
12-th International Symp.of Very High Energy Cosmic Interactions (ISVHECRI) CERN, Geneve, Switzerland, July 15-20, 2002

A.F.Badea, R.Ulrich and KASCADE collaboration:
Reconstruction of shower observables at the KASCADE Grande Experiment
Physikertagung gemeinsam mit der Fruhjahrstagung der DPG, Leiztig, 18-22 Marz, 2002, Verhandlungen der Deutschen Physikalischen Gesellschaft, R.6, Bd.37 (2002) T 401.5

D.L. Balabanski, M. Danchev, V.N. Gourev, T. Badica, I. V. Popescu, A. Olariu, O. Guguianu, I. Stefanescu
Studies of trace elements in glaciers at the Livingston Island, Antarctica
International Conference on Applications of High Precision Atomic and Nuclear Methods, 2-6 September, 2002, Neptun, Romania, 2-6 September, 2002, Neptun, Romania

S. Berceanu, A. Gheorghe
Realization of Lie algebras by first-order differential operators with holomorphic polynomial coefficients on Kähler coherent state orbits
talk by S. Berceanu at the Sophus Lie seminary, Humbold University, Berlin 6-8 December (2001)

S. Berceanu and A. Gheorghe
Differential operators on orbits of coherent states
Oral communication by S. Berceanu at the First National Conference on Theoretical Physics, September 13-16, 2002, Magurele Bucharest, Romania;
http://www.theory.nipne.ro/ctp2002/proced/proced.html
also arXiv: math. DG/0211054 v 1 4 Nov. 2002, 10 p; to appear

S. Berceanu, A. Gheorghe
Linear Hamiltonians on homogeneous Kähler manifolds of coherent states
talk by S. Berceanu at "The fifth international workshop on differential geometry and its applications", Timisoara - ROMANIA, September 18-22, 2001, to appear

S. Berceanu
The coherent states: old geometrical methods in new quantum clothes. A revisit
1st Annual Communication Session of the Theoretical Physics Department, January, 24-25 2002 In memoriam Aretin Corcioivei

S. Berceanu
Asupra continuitatii scolii de geometrie de la Kazan
Comunicare orala la Academia Romana cu ocazia sesiunii de comunicari a sectiei de stiinte matematice a Academiei Romane, Bicentenar-ului Janos Bolyay: Geometriile neeuclidiene, ieri si azi, 13 decembrie 2002

S. Berceanu
On the geometrical significance of the phase of the scalar product of coherent states
"XXth Workshop on Geometric Methods in Physics, Algebraic and Geometric Foundations of Quantum Systems" Bialowieza, Poland, July 1 – July 7, 2001

A.Bercuci and KASCADE collaboration:
The measurements of muons with the KASCADE Central Detector
18-th European Cosmic Rays Symp. (ECRS), Moscow, Russia, July 8-12 (2002)

I.M.Brancus, J.Wentz, B.Mitrica, M.Petcu, H.Rebel, H.Bozdog, H.J.Mathes, A.Bercuci, A.Aiftimiei, M.Duma and G.Toma
Experimental studies of the East-West effect of the muon charge ratio at energies relevant to atmospheric neutrino anomaly
16-th Int.Conf.on Particles and Nuclei (PANIC02) Osaka, Japan, Sept.30- Oct.04.2002

I.M.Brancus, J.Wentz, B.Mitrica, B.Vulpescu, M.Petcu, H.Rebel, H.Bozdog, H.J.Mathes, A.F.Badea, A.Bercuci, A.Aiftimiei, M.Duma, G.Toma and A.Meli
Measurements of the East-West effect of the muon charge ratio at energies relevant to atmospheric neutrino anomaly
12-th International Symp.of Very High Energy Cosmic Interactions (ISVHECRI) CERN, Geneve, Switzerland, July 15-20, 2002

C.Buttner and KASCADE collaboration:
Muon production heights determined in the KASCADE experiment
12-th International Symp.of Very High Energy Cosmic Interactions (ISVHECRI) CERN, Geneve, Switzerland, July 15-20, 2002

C.Buttner, K.Daumiller, P.Doll, K-H.Kampert, D.Martello, R.Obenland, J.Zabierowski and KASCADE collaboration:
Myonproduktionshohen und Myonlateralverteilungen bestimmt mit dem Myon spurdetektor des KASCADE Experiment
Physikertagung gemeinsam mit der Fruhjahrstagung der DPG, Leiztig, 18-22 Marz, 2002, Verhandlungen

der Deutschen Physikalischen Gesellschaft, R.6, Bd.37 (2002) T. 401.6

V. Cercasov, A. Pantelică
On air pollution investigation in six Romanian cities through lichen transplants used as bioaccumulators and analysed by EDXRFA and INAA
International Conferece on Urban Air Pollution, Bioindication and Environmental Awareness (EuroBionet2002), University of Hohenheim, Stuttgart, Germany, 5-6 Nov., 2002

C.Ciortea, D.Dumitriu, D.Flueraşu, I.Piticu, A.Enulescu, S.Z.Szilagyi, S.E.Enescu, M.M. Gugiu and T.A. Dumitrescu
Inner-shell Vacancy Production and Multiple Ionization Effects in .1-1.75 MeV/u Mn, Fe Co, Ni, Cu + Au, Bi Collisions
National Physics Conference, September 26-29, 2002, Tg. Mures, Romania (oral presentation)

D. S. Delion, A. Săndulescu, S. Mişicu, W. Greiner
Coupled channels description of cold fission processes
Proceedigs of the "International Conference on Modern Sub-Nuclear and laboratory Experiment University of Athens, Georgia, USA, September 11-13, 2002 (in press)

D. S. Delion, A. Săndulescu, S. Mişicu, W. Greiner
The anisotropy in cold ternary fission
Proceedigs of the WE-Heraeus Seminar "Symposium on Nuclear Clusters: from Light Exotic to Super heavy Nuclei" Rauischholzhausen, Germany, August 5-9, 2002 (in press)

D. S. Delion, A. Săndulescu, S. Mişicu, W. Greiner
Theory of binary and ternary cold fission
Proceedigs of the "Third International Conference on Fission and Neutron rich Nuclei" Sanibel Island, Florida, USA, November 3-9, 2002 (in press)

D.S. Delion, Insolia, R.J. Liotta
Anisotropic α-decay in deformed nuclei
Proceedigs of the CRIS-2002 Conference "Exotic Clustering", Catania, Italy, June, 10-14, 2002 Eds. S. Costa, A. Insolia, C. Tuve (American Institute of Physics, New York, 2002) p.12-19

S. Dobrescu, L. Schachter
RECRIS-Romanian ECR ion source: performances and experimental developments
The 9th International Conference on Ion Sources ICIS'01, Sept. 2001, Oakland, California, USA

S.E.Enescu, I.Bibicu, A.Kluger, V.Zoran, A.D.Stoica and V.Tripadus
Nuclear Method for Materials Investigations: the Rayleigh Scattering of Mössbauer Radiation
Energetica Nucleară - Prezent şi viitor, 30 de ani de activitate în domeniul energeticii nucleare la Institutul de Cercetări Nucleare Piteşti, iulie 2001

S.E.Enescu, I.Bibicu, A.Kluger
A Study of the Pyrolytic Graphite by Rayleigh Scattering of Mssbauer Radiation
5th Seeheim Workshop on Mssbauer Spectroscopy, May 21-26, 2002, Seeheim, Germany

M. Falcitelli, S. Ianuş, A. M. Pastore and M. Vişinescu
Some applications of Riemannian submersions in physics
Talk at the First National Romanian Conference on Theoretical Physics, Bucharest, Romania, September 13-16, 2002; to appear in Proceedings

A.Gentils, L.Thomé, J.Jagielski, S.E.Enescu, F.Garrido, M.Beauvy, G.Blaise
High Temperature Behavoiur of Fission Product Analogs Implanted into Nuclear Ceramics
IV International Symposium "Ion Implantation and other Applications of Ions and Electrons", Kazimierz Dolny, Poland, June 10-13, 2002

D. Grecu, Anca Vişinescu
Bound state of two solitons in a Davydov model. Evolution in higher order approximation
Conferinta Nationala de Fizica, Iasi, Oct. 2001

D. Grecu, Anca Vişinescu
Influence of third order dispersion on the bound state of two solitons of the NLS equation
Conferinta Nationala de Fizica, Tg. Mures, sept. 2002

D. Grecu, Anca Vişinescu
Modulational instability in some nonlinear one–dimensional lattices and soliton generation
The 3-rd International Spring School and Workshop on Quantum Field Theory and Hamiltonian Systems, Calimanesti, May 6-12, 2002

D. Grecu, Anca Vişinescu
Statistical approach of the modulational instability of the discrete self-trapping equation
Conferinta Nationala de Fizica, Tg. Mures, sept. 2002

M.Hambasch, J.R.Horandel and KASCADE collaboration:
Untersuchung der Ankunfstverteilung von Hadronen in Luftshowern.
Physikertagung gemeinsam mit der Fruhjahrstagung der DPG, Leiztig, 18-22 Marz, 2002, Verhandlungen der Deutschen Physikalischen Gesellschaft, R.6, Bd.37 (2002)T 101.1

A.Haungs and KASCADE collaboration:
KASCADE: a unique tool for high energy cosmic rays measurements
21-sr Symp.on Relativistic Astrophysics, Firenze, Italy, Dec.9-13, (2002)

A.Haungs and KASCADE collaboration:
Muon density spectra as probe of the muon component at the air shower simulations.

12-th International Symp.of Very High Energy Cosmic Interactions (ISVHECRI) CERN, Geneve, Switzerland, July 15-20, 2002

J.R.Horandel and KASCADE collaboration:
Hadrons in extensive air showers.Recent results of KASCADE hadron calorimeter
18-th European Cosmic Rays Symp. (ECRS), Moscow, Russia, July 8-12 (2002

J.R.Horandel and KASCADE collaboration:
Inconsistencies in EAS simulaitons-longitudinal vs. lateral development
12-th International Symp.of Very High Energy Cosmic Interactions (ISVHECRI) CERN, Geneve, Switzerland, July 15-20, 2002

J.R.Horandel and KASCADE collaboration:
Interactions with high transverse momentum in EAS
12-th International Symp.of Very High Energy Cosmic Interactions (ISVHECRI) CERN, Geneve, Switzerland, July 15-20, 2002

J.R.Horandel and KASCADE collaboration:
Measurement of the energy spectrum of unaccompanied hadrons at the sea level
12-th International Symp.of Very High Energy Cosmic Interactions (ISVHECRI) CERN, Geneve, Switzerland, July 15-20, 2002

J.R.Horandel and KASCADE collaboration:
Test of high energy hadronic interaction models with the KASCADE hadron calorimeter. Particle physics with EAS detectors.
12-th International Symp.of Very High Energy Cosmic Interactions (ISVHECRI) CERN, Geneve, Switzerland, July 15-20, 2002

K.H.Kampert and KASCADE collaboration:
The physics of the knee in the cosmic-ray spectrum. Recent results from KASCADE
Physikertagung gemeinsam mit der Fruhjahrstagung der DPG, Leiztig, 18-22 Marz, 2002, Verhandlungen der Deutschen Physikalischen Gesellschaft, R.6, Bd.37 (2002)HK 4.1

K.H.Kampert and KASCADE collaboration:
KASCADE-Grande: Measurements of cosmic rays in the energy range from 10^{16}- 10^{18} eV.
12-th International Symp.of Very High Energy Cosmic Interactions (ISVHECRI) CERN, Geneve, Switzerland, July 15-20, 2002

K.H.Kampert and KASCADE collaboration:
The knee in the cosmic ray spectrum.Reent results from KASCADE.
18-th Int.Workshop on Weak Interactions and Neutrinos (WIN) Christchurch, New Zeeleand, Jan.21-26, 2002

V.M Karnaukhov, C. Coca, V. I. Moroz
Processes with a possible formation of exotic states
International Seminar on High Energy Physics Problems, SHEPP XV, *Dubna 2001; Proceedings, vol II page 150*

A.Kluger, S.E.Enescu, I.Bibicu, C.Ciortea, and A.Enulescu
Data acquisition system for Rayleigh scattering of Mössbauer radiation
National Physics Conference, September 26-29, 2002, Tg. Mures, Romania

G.Maier, K.H.Kampert, H.Schieler, H.Ulrich, J.Van Buren and KASCADE collaboration:
Suche nach siderischer Anisotropie der kosmischen Strahlung mit dem KASCADE-Experiment
Physikertagung gemeinsam mit der Fruhjahrstagung der DPG, Leiztig, 18-22 Marz, 2002, Verhandlungen der Deutschen Physikalischen Gesellschaft, R.6, Bd.37 (2002)T 201.7

J.Milke and KASCADE collaboration:
Test of hadronic interaction models with the KASCADE hadron calorimeter
12-th International Symp.of Very High Energy Cosmic Interactions (ISVHECRI) CERN, Geneve, Switzerland, July 15-20, 2002

R.Obenland, C.Buttner, K.Daumiller, P.Doll, K-H.Kampert, D.Martello, J.Zabierowski and KASCADE collaboration:
Ausflosung des Myonspurdetektors von KASCADE
Physikertagung gemeinsam mit der Fruhjahrstagung der DPG, Leiztig, 18-22 Marz, 2002, Verhandlungen der Deutschen Physikalischen Gesellschaft, R.6, Bd.37 (2002) T.208.4

Agata Olariu, Ragnar Hellborg, Kristina Stenström, Bengt Erlandsson, Mikko Faarinen, Per Persson
Dating of Some Fossil Romanian Bones by Accelerator Mass Spectrometry
International Conference on Applications of High Precision Atomic and Nuclear Methods, 2-6 September, 2002, Neptun, Romania

C. Riccardi, .., D. Pantea et al. [FOCUS Collaboration]
Results on Charm Mixing and CP violatipn from FOCUS
International Conference on CP violation, Pisa, Italy, 12-17 June, 2001

G. Boca, .., D. Pantea et al. [FOCUS Collaboration]
New Results on Charm Decays and Lifetimes from Fermilab Experiment FOCUS
International Conference on HEP, Budapest, Hungary, 12-18 July, 2001

R. K. Kutschke, .., D. Pantea et al. [FOCUS Collaboration]
Charmed Hadron Spectroscopy at FOCUS
Frontiers in Contemporary Physics II - Nashville, TN 5-10 March, 2001

S. Bianco, .., D. Pantea et al. [FOCUS Collaboration]

Spectroscopy Results from FOCUS
International Conference on HEP, Budapest, Hungary, 12-18 July, 2001
A. Pantelică, V. Cercasov, E. Steinnes, H.Th. Wolterbeek
Use of nuclear and atomic techniques in air pollution studies by transplant lichen exposure, bulk deposition, and airborne particulate matter collection in România
International Conference of Applications and High precision Atomic & Nuclear Methods (HIPAN2002), Neptun, România, 2-6 Sept., 2002, http://www.nipne.ro/Cenex/cex_eur.htm
(DIRAC Collaboration) J. Saborido, ..., Gh. Caragheorgheopol, S. Constantinescu, M. Iliescu, M. Pentia, C. Petrascu, T. Ponta, D. Pop, et al.
Di-meson lifetime measurement with DIRAC
MESON 2002 Workshop, May 2002, Cracow [Poland].
(DIRAC Collaboration) L. Afanasyev, ..., Gh. Caragheorgheopol, S. Constantinescu, M. Iliescu, M. Pentia, C. Petrascu, T. Ponta, D. Pop, et al.
Measurement of $\pi^+\pi^-$ atom lifetime at DIRAC
ICHEP 2002 Conference, 24-31 July 2002, Amsterdam [USA].
(DIRAC Collaboration) V. Yazkov, ... , Gh. Caragheorgheopol, S. Constantinescu, M. Iliescu, M. Pentia, C. Petrascu, T. Ponta, D. Pop, et al.
Experimental investigation of $\pi^+\pi^-$ atoms
The 5th Conference Quark Confinement and the Hadron Spectrum, 10-14 September 2002, Gargnano, Garda Lake [Italy].
DIRAC Collaboration: A. Lanaro, ..., M. Pentia, Gh. Caragheorgheopol, S. Constantinescu, C. Petrascu (Curceanu), M. Iliescu, T. Ponta, D. Pop, et al.
πK atom: observation and lifetime measurement with DIRAC
Proc. Int. Workshop on Hadronic Atoms [HadAtom01], 11-12 October 2001, Bern [Switzerland], Eds. J. Gasser, A. Rusetsky and J. Schacher, BUHE-2001-07, 2001
DIRAC Collaboration: A.M Rodriguez Fernandez, ..., M. Pentia, Gh. Caragheorgheopol, S. Constantinescu, C. Petrascu (Curceanu), M. Iliescu, T. Ponta, D. Pop, et al.
The DIRAC experiment at CERN: current status and future perspectives
9th International Symposium on Meson-Nucleon Physics and the Structure of the Nucleon, 26-31 July 2001, Washington DC [USA], 2001
DIRAC Collaboration: C. Santamarina, ..., M. Pentia, Gh. Caragheorgheopol, S. Constantinescu, C. Petrascu (Curceanu), M. Iliescu, T. Ponta, D. Pop, et al.
DIRAC (PS-212) experiment at CERN
Proc. Int. Workshop on Hadronic Atoms [HadAtom01], 11-12 October 2001, Bern [Switzerland], Eds. J. Gasser, A. Rusetsky and J. Schacher, BUHE-2001-07, 2001
DIRAC Collaboration: P. Kokkas, ..., M. Pentia, Gh. Caragheorgheopol, S. Constantinescu, C. Petrascu (Curceanu), M. Iliescu, T. Ponta, D. Pop, et al.
Dimeson lifetime measurement with DIRAC at CERN
Proc. Int. Workshop on Chiral Fluctuations in Hadronic Matter, 26-28 September 2001, INP Orsay [France], 2001
A.M. Rodriguez Fernandez, .., T. Ponta et al. [DIRAC Collaboration]
The DIRAC Experment at CERN: Current Status and Future Perspectives
9^{th} *International Symposium on Meson - Nucleon Physics and the Structure of the Nucleon (MENU 2001), Washington, District of Columbia, 26-31 Jul 2001.*
Published in PiN Newslett.16:352-354, 2002
L. Afanasev, .., T. Ponta et al. [DIRAC Collaboration]
Detection of Atoms Consisting of pi+ and pi- Mesons at PS CERN
9^{th} *International Conference on Hadron Spectroscopy (Hadron 2001), Protvino, Russia, 25 Aug - 1 Sep 2001.*
Published in AIP Conf.Proc.619:745-748, 2002
*Also in *Protvino 2001, Hadron spectroscopy* 745-748*
E.A.Preoteasa, C.Ciortea, B.Constantinescu, Daniela Flueraşu, Sanda-Elena Enescu, D.Pantelică, F.Negoiţă and Elena Preoteasa
Analysis of composites for restorative dentistry by PIXE, XRF and ERDA
g^{th} *International Conference on PIXE and its Applications (PIXE2001) June 8-12, 2001, Guelph, Canada*
R.A. Ionescu, H. Wolter
Equal-time hierarchies for one-particle Green functions
Strong Non-equilibrium Matter, Workshop on Quantum Transport in Relativistic Heavy Ion Physics of the European Graduate School Copenhagen-Giessen "Complex Systems of Hadrons and Nuclei", November 2001, Giessen, Germany
M.Roth and KASCADE collaboration:
Determination of primary energy and mass in the PeV region by Bayes unfolding technique
12-th International Symp.of Very High Energy Cosmic Interactions (ISVHECRI) CERN, Geneve, Switzerland, July 15-20, 2002
M.Roth and KASCADE collaboration:
Eine nichtparametrische Entfaltung zur Bestimmung der elementspektren der geladenen kosmischen strahlung im PeV Bereich

Physikertagung gemeinsam mit der Fruhjahrstagung der DPG, Leiztig, 18-22 Marz, 2002, Verhandlungen der Deutschen Physikalischen Gesellschaft, R.6, Bd.37 (2002) T 201.6

L. Schachter, S. Dobrescu, G. Rodrigues, A. Drentje
Enhanced highly charged ion production using a metal-dielectric liner in the KVI 14 GHZ ECR ion source
The 9th International Conference on Ion Sources ICIS'01, Sept. 2001, Oakland, California, USA

H.Schieller and KASCADE collaboration and LOPES collaboration:
KASCADE Extensive Air Schauer Experimen
SPIE Astronomical Telescopes and Instrumentation Hitton Waikoloa, Hawaii, USA, Aug.22-28, 2002

J. Scholz, A.Haungs, M.Roth and KASCADE collaboration:
Untersuchung von Luftschauern an der Treiggerschwelle von KASCADE
Physikertagung gemeinsam mit der Fruhjahrstagung der DPG, Leiztig, 18-22 Marz, 2002, Verhandlungen der Deutschen Physikalischen Gesellschaft, R.6, Bd.37 (2002) T 101.6

Kristina Stenström, Ragnar Hellborg, Mikko Faarinen and Per Persson, Göran Skog, Agata Olariu, Silviu Olariu, Dan Cutoiu
Radioecological applications of 14C measurements at the Lund Accelerator Mass Spectrometry (AMS) Facility
International Conference on Applications of High Precision Atomic and Nuclear Methods, 2-6 September, 2002, Neptun, Romania

L.Thomé, A.Gentils, S.E.Enescu, J.Jagielski, F.Garrido
On the Use of Ion Beams for the Selection of Nuclear Waste Matrices
International Conference on Application of High Precision Atomic&Nuclear Methods (HIPAN2002), September 2-6, 2002, Neptun, Black Sea Coast, Romania

H.Ulrich and KASCADE collaboration:
Energy spectra of cosmic rays in the knee region
12-th International Symp.of Very High Energy Cosmic Interactions (ISVHECRI) CERN, Geneve, Switzerland, July 15-20, 2002

H.Ulrich, R.Glasstetter, K.H.Kampert, G.Maier and KASCADE collaboration:
Bestimmung primaerer Energiespektren einzelner Massengruppen der kosmischen Strahlung in Bereich des Knies.
Physikertagung gemeinsam mit der Fruhjahrstagung der DPG, Leiztig, 18-22 Marz, 2002, Verhandlungen der Deutschen Physikalischen Gesellschaft, R.6, Bd.37 (2002)T 201.3

J. Van Buren, K. H. Kampert, G.Maier, H.J.Mayer, H.Schieler, H.Ulrich and KASCADE collaboration:
Bestimmung des Energiespektrums des kosmischen Strahlung in Bereich des Knies mit Hilfe von Schauergroessenspektren
Physikertagung gemeinsam mit der Fruhjahrstagung der DPG, Leiztig, 18-22 Marz, 2002, Verhandlungen der Deutschen Physikalischen Gesellschaft, R.6, Bd.37 (2002)T 201.4

M. Vişinescu
Fermions in Taub-NUT background
Invited talk at the Fifth Workshop on "Quantum Field Theory under the Influence of External Conditions", Leipzig (2001), to be published in Int.J.Mod.Phys. A (2002)

M. Vişinescu
Fermions in Taub-Newman-Unti-Tamburino background
Invited lecture at the International Workshop "Quantum Gravity and Superstings", JINR-Dubna, Russia, July 11-18, 2002

M. Vişinescu
Spinning particles, Dirac-type operators on curved spaces and the role of Killing-Yano tensors
Invited lecture at the Spring School and Workshop on "QFT and Hamiltonian Systems", Calimanesti, Romania, May 6-12, 2002; to appear in Proceedings

Scientific Exchanges

Foreign Visitors

Dimiter L. Balabanski
Faculty of Physics, University of Sofia, BG-1164 Sofia, Bulgaria
Cercasov V.
University of Hohenheim, Institute of Physics, Stuttgart, Germany, 21-30 Aug., 2002, Summaries, pp. 45
Ragnar Hellborg
Lund University, Department of Physics, Division of Nuclear Physics, Box 118, SE-221 00 Lund, Sweden
V.M Karnaukhov
JINR, Dubna, Russia
R. Kristic
CERN, Geneva, Switzerland.
A. Schopper
CERN, Geneva, Switzerland.

Visits Abroad

I. Caprini
CERN, Geneva, Switzerland.
I. Caprini
Center of Theoretical Physics, Marseille, France.
I. Caprini
ICTP, Trieste, Italy.
I. Caprini
Institute of Theoretical Physics, University of Berne, Switzerland.
C. Coca
CERN, Geneva, Switzerland.
C. Coca
University of Cambridge, Cambridge, United Kingdom.
C. Coca
University of Rio de Janeiro -UFRJ, Rio de Janeiro, Brasil.
S. Dobrescu
Frankfurt/Main, Germany, Institut für Kernphysik der J. W. Goethe Universität, oct.-nov. 2001, working stage in the frame of WP15 IDRANAP
S.E.Enescu
Orsay, France, Centre de Spectrométrie Nucléaire et de Spectrométrie de Masse, jan.-june and oct.-nov.2002, working stages
S.E.Enescu
Orsay, France, Centre de Spectrométrie Nucléaire et de Spectrométrie de Masse, sept.-dec. 2001, working stage
Grigore D. R.
Institute of Theoretical Physics, Zürich University, Switzerland
M. Orlandea
CERN, Geneva, Switzerland.
Pantelică A.
University of Hohenheim, Institute of Physics and Meteorology, Stuttgart, Germany, 20-25 Feb., 2002
Pantelică A.
University of Technology, Interfaculty Reactor Institute, Delft, Olanda, 25 Feb.- 19 March, 2002
Mircea Pentia
CERN
R.A. Ionescu
Sektion Physik, Universität München, Germany
L. Shachter
Frankfurt/Main, Germany, Institut für Kernphysik der J. W. Goethe Universität, oct.-nov. 2001, working stage in the frame of WP15 IDRANAP

Seminars Abroad

Adam Gh., Adam S.
Reliability conditions on quadrature algorithms
General Laboratory Seminar, JINR-Dubna, Russia, September, 03, 2002

S. Berceanu
Holomorphic differential operators with polynomial coefficients on Kähler coherent state orbits
seminary at the Universite Libre de Bruxelles, December 4, 2001; also at Lille University, December 11, 2001

I. Caprini
Analytic continuation and perturbative expansions in QCD
ICTP, Trieste, Italy.

I. Caprini
Analytic continuation and perturbative expansions in QCD
Institute of Theoretical Physics, University of Berne, Switzerland.

I. Caprini
Dispersion relations and final state interactions in $B \to \pi\pi$ and $K \to \pi\pi$ decays
Center of Theoretical Physics, Marseille, France.

M. Pentia
DIRAC 2002 - Data Taking Quality Analysis
CERN, 30 Oct. 2002

Anca Vişinescu
Randomness effects on modulational instability of a discrete self-trapping equation
University of Lecce, Dept. Theor. Phys., Lecce, Italy, Oct. 17, 2002

Anca Vişinescu
Statistical approach of the modulational instability of the discrete self-trapping equation
University of Bari, Depart. of Math., Bari, Italy, Oct. 11, 2002

M. Vişinescu
Dirac-type operators on curved spaces
Department of Mathematics, Univ. Bari, Italy, October 11, 2002

M. Vişinescu
Fermions on curved spaces
Department of Mathematics, Univ. Bari, Italy, October 9, 2002

M. Vişinescu
Spinning particles and Killing tensors
Department of Physics, Univ. Lecce, Italy, October 17, 2002

Directorate

Dr. Emilian Drăgulescu – General Director
Dr. Florin D. Buzatu – Scientific Director
Dr. Petru M. Racolţa – Technical Director
Ec. Alexandru Popescu – Finance Director

Research Staff

Nuclear Physics Department
Bucurescu Dorel, Haţeganu Cornel, Poenariu Dorin, Calboreanu Alexandru, Buta Apostol, Borcea Cătălin, Iordăchescu Alexandru, Ionescu Bujor Manuela, Drăgulescu Emilian, Corcalciuc Valentin, Petrovici Alexandrina, Petrovici Mihai, Avrigeanu Marilena, Zamfir Nicolae, Olariu Silviu, Cutoiu Dan, Schachter Leon, Avrigeanu Vlad Gabriel, Pădureanu Ion, Ivaşcu Marin, Popescu Ion, Căta Danil Gheorghe, Petraşcu Marius, Bădica Teodor, Isbăşescu Alina, David Ioana, Berceanu Ionela, Brâncuş Ileana, Simion Victor, Enulescu Alexandru, Ciortea Constantin, Pentia Mircea, Pop Amalia, Pârlog Marian, Iacob Victor Eugen, Gherghescu Radu, Ion Mihail, Mirea Mihail Doloris, Ur .Călin Alexandru, Piticu Ion, Păpureanu Vladimir, Duma Marin, Pantelică Dan, Flueraşu Daniela, Tarta Petru Dorinel, Petrache Costel, Petraşcu Horia, Legrand Iosif Charles, Căta Danil Irina, Bordeanu Cristina, Nica N.Ninel, Enescu G.Sanda Elena, Scîntee N.Nicolae, Szilagyi Szabolcs Zoltan, Ionescu M. Remus Amilcar, Rădulescu Aurel, Răduţă Adriana Rodica, Răduţă Alexandru Horia, Olariu Agata, Mărginean Nicolae Marius, Sabaiduc Vasile, Petris D.Mariana, Andronic N.Anton, Dumitriu M. Dana Elena, Stroe Lucian, Negoiţă Florin, Vaman Georgeta, Vulpescu Bogdan, Stoicea Gabriel, Aranghel Dorina, Glodariu Tudor, Badea Aurelian Florin, Radu Florin, Mărginean Raluca Maria, Aiftimiei Doina, Bastea T.Sorin, Popescu I.Răzvan, Drafta George, Tabacaru Gabriel, Toader Cristian Florentin, Albu Mihaela, Stetcu Ionel, Borcan Cristina, Stefanescu Irina, Dobrescu Bogdan, Bercuci Alexandru, Stefan Gheorghe Iulian, Gugiu Marin Marius, Ionescu Paul, Olariu Albert, Radu Aimee Theodora, Oros D.Ana Maria, Popa Gabriela, Negret Alexandru, Colci Madalina, Mihăilescu Liviu Cristian, Suliman Gabriel, Preda Mitică, Mitrică Bogdan, Toma Gabriel, Buta Adina-Mihaela.

Theoretical Physics Department
Grecu Dan, Vişinescu Mihai, Ixaru Liviu, Rădescu Eugen, Răduţă Apolodor, Diţă Petre, Micu Liliana, Angelescu Nicolae, Scutaru Horia, Caprini Irinel, Stratan Gheorghe, Berceanu Stefan, Grama Nicolae, Adam Gheorghe, Mihalache Dumitru, Apostol Marian, Stoica Sabin, Silişteanu Ion, Grigore Radu Dan, Delion Doru Sabin, Stefănescu Eliade, Ceauşescu N.Valentin, Cîrstoiu Florin Cornel, Buzatu Florin Dorian, Vişinescu Anca, Adam Sanda, Gheorghe I.Alex Cezar, Bundaru Mircea, Rizea Mărgărit, Mazilu Dumitru, Isar Aurelian, Săndulescu Nicolai, Ursu Ioan, Baran Virgil, Mişicu Şerban Dragoş, Despa Florin, Bîrsan Vasile Victor, Bulboacă Iosif, Cârstea Adrian Stefan, Craşovan Lucian Cornel, Horoi Mihai, Costin Ovidiu, Baboiu Daniel Marian, Panoiu Nicolae Coriolan, Schiaua Claudiu Cornel, Cune Liviu Cristian, Manoliu I.Mihaela, Doloc A.Lida, Firica Radu Gabriel, Moldoveanu Florin, Vaman Diana, Paraoanu Gheorghe Sorin, Mihut Izabela Ramona, Acatrinei Ciprian Sorin, Răduţă Cristian, Pacearescu Larisa, Ispas Simona Giorgiana, Bora Florin, Negoiţă Gianina Alina.

Particle Physics Department
Ion B.Dumitru, Ponta Titus, Diţă Sanda, Boldea Venera, Coca Cornelia, Pantea Dan, Cotorobai Florin Valeriu, Petraşcu Cătălina Oana, Rosca Aura, Alexa R.Călin, Preda Titi, Iliescu Mihail, Popescu Sorina, Groza Radu Liviu, Bragadireanu Alexandru, Kusko Cristian, Anghel Dragos Victor, Sirghi Diana Laura, Micu Andrei, Orlandea Marius Ciprian, Sandru Adriana Ileana, Rusu Vadim.

Life and Environmental Physics Department
Galeriu Dan, Mateescu Gheorghe, Dorobanţu Ion, Vamanu Vasile Dan, Berinde Alexandru, Petcu Ileana, Mocanu Nicolae, Sandru Elena, Stângă Doru, Mărgineanu Romul Mircea, Slavnicu Stelian Dan, Ceaus Mihai, Gheorghiu Adriana, Preoteasa Eugen, Călin Marian Romeo, Puşcalău Mirela Angela, Radu Mihai, Stochioiu Ana, Moiseev Tamara, Dumitru Radu Octavian, Moisoi Nicoleta, Gheorghiu Dorina, Acasandrei Valentin Teodor, Apostoaei Andrei Iulian, Savu Iulia Diana, Manciu Felicia Speranţa, Breban Domnica Cristina, Turcanu Catrinel Octavia, Niculae Carmen Georgeta, Acasandrei Maria Adriana, Corol Delia Irina, Melintescu Mirela Anca, Albu Nicolae Marius, Mihai Felicia, Rădulescu Ileana, Haranguş Livia, Vamanu Bogdan Ioan, Iordan Andreea Luminita, Olteanu Carmen Ileana, Creţu Mirela Ileana, Mitrică Ionel.

Informatics and Communications
Zamfirescu Ion, Constantinescu Serban, Manu Valentin, Cărbunaru Octavian, Dima Mihai Octavian, Apostu Ana-Maria, Păuna Eduard Dănuţ.

Applied Nuclear Physics Department
Constantinescu Olimpiu, Caprini Mihai, Ciobanu Mircea, Tripăduş Vasile, Caragheorgheopol Gheorghe, Rusu Alexandru, Cătănescu Vasile, Pantelică Ana, Racolţa Petru Mihail, Bădescu Elisabeta, Petcu Mirel Adrian, Măgureanu Constantin, Constantinescu Bogdan, Cruceru Ilie, Cincu Manuela, Stan Sion Cătălin, Constantin Florin, Gârlea Cristina, Bartoş Daniel, Niculescu Mihaela Liliana, Lupu Mihaela, Nicolescu George, Mihai Nelu, Vasilescu Angela, Rădulescu Mihaela, Crăciun Liviu, Ioan Petre, Crânganu Elena, Enăchescu Mihaela, Todor A. Aurel Dorin, Ilaş Dănuţ, Ivan P.Adrian, Arsenescu N.Remus, Bugoi Roxana

Nicoleta, Radu Alina, Rusu Claudiu, Dănilă Bogdan, Militaru Otilia, Ianculescu M. Cristian, Alexandreanu Bogdan, Udrea Serban Alexandru, Minca Mariana, Popescu Lucia-Ana, Muresan Ofelia, Serban Alin Titus, Dogaru Marius Stefan, Manea Ioana, Petre Alexandru Bogdan, Nicorescu Carmen, Cucoaneş Andi Sebastian, Voiculescu Dana, Zaharia Petre.

Nuclear and Vacuum Engineering Department
Daniş Ana, Popescu Corneliu, Drăguşin Mitică, Duţă Viorel, Popa Victor, Mateescu Gheorghe, Giolu Gheorghe, Pătrăşcu Sanda, Lucaciu Adriana, Guţă Tudor Dragoş, Popescu Aurora, Lungu Claudiu Teodor, Pop Dan, Mureşan Raluca Anca, Tuca Carmen Alexandra, Borca Camelia Nicoleta, Timiş Cozmin Nicolae, Ilie Theodor, Boicu Alin, Mustaţă Carmen Georgeta, Crăciun Marian Virgil.

TANDEM Accelerator Group
Dobrescu Serban, Dumitru Gabriel, Dima Răzvan.

Cyclotron Group
Ivanov Eugen, Vâţă Ion, Dudu Dorin, Ploştinaru Dan, Catană Dumitru, Rusen I.Ion, Lixandru George Cristian, Pop Adrian.

Radioactive Waste Plant
Dinescu Lucreţia, Rotărescu Gheorghe, Ene Daniela, Dragolici Felicia Nicoleta, Iancu Dumitru, Rotaru Păstoriţa Rodica, Cazan Ioan Lucian, Nicu Mihaela Daniela, Ionaşcu Laura Florina, Mihai Cosmin, Matei Daniela, Stoica Paul, Haralambie Magdalena.

National Radioactive Waste Repository
Păunica Iosif.

Nuclear Reactor Group
Zorliu Adrian, Mincu Gh.Ion, Dragolici Cristian, Petran Corneliu, Isbăşescu Mihai.

IRASM – Technological Irradiations
Ponta Corneliu, Moise Ioan Valentin, Georgescu Rodica Maria, Bratu Eugen, Negut Constantin Daniel, Postelnicu Mihaela.

Radioisotope Research and Production Department
Sahagia Maria, Negoiţă Nicolae, Borza Virginia, Postolache Cristian, Lungu Valeria, Fugaru Viorel, Ivan Constantin, Simion Corina Anca, Chiper Diana, Luca Aurelian, Grigorescu Leon, Manea I.Simona Eugenia, Neacşu V.Elena, Cîmpeanu Cătălina, Razdolescu L.Ana-Maria, Mihăilescu Gabriela, Barna Cătălina Mihaela, Niculae (Mihancea) Dana, Petraşcu Anca Maria, Duţă Elena, Matei Lidia.

Design, Development, and Technological Transfer Department
Serbina Leonardo, Alecu Ana, Rădulescu Laura, Udup Emil.

Radioprotection
Floare Gabriel, Frujinoiu Cătălin, Preda Mihaela, Ciort Codruţa Adriana, Jitea Rose Marie, Virgolici Marian, Achim Alexandru.

Standards, Metrology and Quality Certification
Bercea Sorin, Purghel Lidia, Macrin Rodica, Iancso Georgeta, Celarel Aurelia, Iliescu Elena, Hurezeanu Dorina, Iancu Rodica, Cenusa Z.Constantin, Costin Aurelia Monica.

"HORIA HULUBEI" NATIONAL INSTITUTE OF PHYSICS AND NUCLEAR ENGINEERING

INTERNAL ORGANIZATION

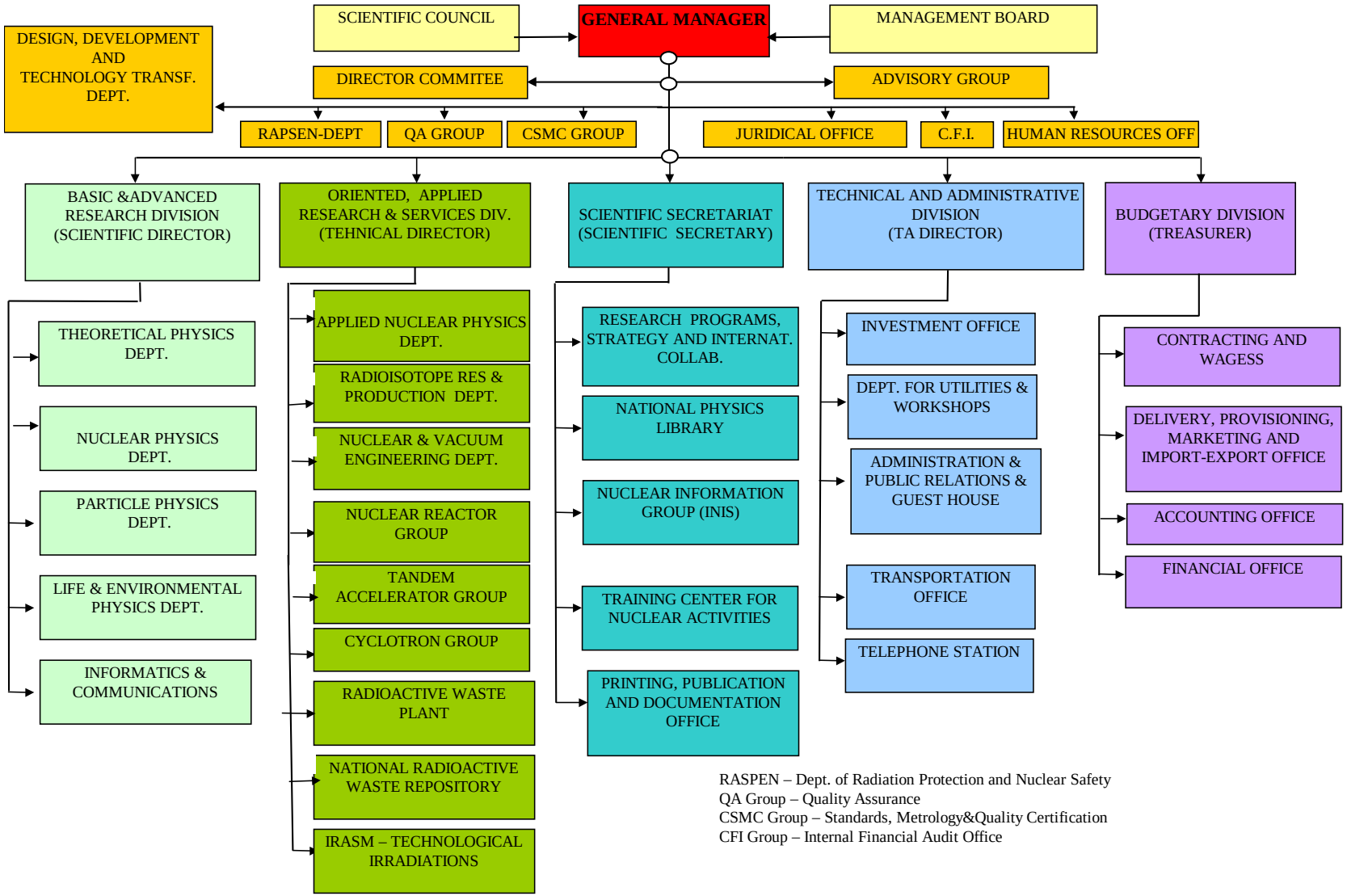

RASPEN – Dept. of Radiation Protection and Nuclear Safety
QA Group – Quality Assurance
CSMC Group – Standards, Metrology&Quality Certification
CFI Group – Internal Financial Audit Office

Author Index